Visualizing chromosomal rearrangements caused by replication fork stalling in a single cell

A thesis Submitted to the University of Sussex for the degree of Doctor of Philosophy

Chieh-Ju Lee

January 2014

Declaration

I hereby declare that this thesis has not been and will not be submitted in whole or in part to another University for the award of any other degree.

Signature:

Chieh-Ju Lee

Acknowledgements

I would like to thank Professor Tony Carr for the opportunity to have a PhD position in his lab and for his continuous support. Many thanks for the suggestions and support from Professor Tony Carr, Dr. Eva Hoffmann and Dr. Jo Murray. I would like to thank Dr. Yari Fontebasso, Dr. Alexander Lorenz, Dr.Takashi Morishita, Dr. Stephanie Schalbetter, Dr. Takeshi Sakuno, Dr. Ken'Ichi Mizuno and Dr. Ellen Tsang for strains and plasmids and Dr. Izumi Miyabe for the method of PFG electrophoresis. Many thanks to Dr. Ken'Ichi Mizuno for helpful discussion and technical advice in this study.

UNIVERSITY OF SUSSEX

Chieh-Ju Lee

A thesis submitted for the degree of Doctor of Philosophy

Visualizing chromosomal rearrangements caused by replication fork stalling in a single cell

SUMMARY

Aberrant chromosome structures can promote tumors in the early stages of carcinogenesis and lead to tumor cells becoming resistant to chemotherapy, for example by changing in drug metabolism. Dicentric (containing two centromeres) and acentric (containing no centromeres) chromosomes are two abnormal chromosome structures that consider as precursors of a variety of gross chromosomal rearrangements (GCRs) generated by subsequent recombination events [1-7]. However, the mechanism of the dicentric and acentric palindromic chromosome formation and their subsequent metabolism is difficult to directly visualise. The previous results from our lab shows that replication forks stalled at a specific replication termination sequence (RTS1) can result in the formation of the dicentric and acentric palindromic chromosomes in the fission yeast *Schizosaccharomyces pombe* [48-52]. However, the formation of acentric and dicentric chromosomes results in a significant viability loss, due to instability and miss-segregation of the chromosomes in the yeast cells. Thus, their fate is difficult or impossible to follow. To resolve this problem, a non-essential mini-chromosome (Ch^{16}) was developed as a novel model system in this project. The behaviour of rearranged chromosome in *vivo* and their subsequent fate have been visualised by integrating the lac operator (*lacO*) and tetracycline operator (*tetO*) arrays with auxotrophic makers, adjacent to the *RTS1* locus on Ch^{16}. The results reveal imbalanced segregation of a dicentric chromosome and subsequently undergoes a breakage event. An acentric chromosome appears to be decoupled or lost rapidly from the nucleus.

Table of Contents

Abbreviation

Ade	adenine
Arg	arginine
ATM	Ataxia telangiectasia mutated protein
ATR	Ataxia telangiectasia and Rad3-related protein
BFB cycle	breakage–fusion–bridge cycle
BIR	break-induced replication
BSA	albumin from bovine serum
CFSs	common fragile sites
Ch^{16}	mini-chromosome
CEN3	centromere 3
CRs	chromosomal rearrangements
CSE	citrate-phosphate buffer
DIC filter	differential interference contrast filter
DNA-PKcs	DNA protein kinase
DSBs	double-strand break
DSBR	double-strand break repair
E. coli	*Escherichia coli*
EDTA	ethylenediaminetetraacetic acid
EMM2	Edinburgh minimal media
EtBr	ethidium bromide
FoSTeS	fork stalling and template switching
Gm	gentamycin
GFP	green fluorescent protein
His	histidine
HJ intermediate	Holliday Junctions intermediate
Hph	hygromycin
HR	homologous recombination
HU	hydroxyurea
KAc	potassium acetate
Kan	kanamycin
KOD polymerase	DNA polymerase from *Thermococcus kodakaraensis* (KOD)
lacO	lac operator
LB	Luria-Bertani media
LCRs	low-copy repeats
Leu	leucine

LMT agarose	low melting temperature agarose
LiOAc	lithium acetate
LOH	loss of heterozygosity
MMBIR	microhomology-mediated BIR
MMEJ	microhomology-mediated end joining
MMR	DNA mismatch repair
NaCl	sodium chloride
NAHR	non-allelic homologous recombination
NaOH	sodium hydroxide
Nat	nourseothricin
nmt41promptor	thiamine-repressible promoter
NHEJ	non-homologous end joining
ORF	open reading frame
PEG	polyethylene glycol
PFGE	Pulsed Field Gel Electrophoresis
RMCE	Cre recombinase-mediated cassette exchange
PMD	Pelizaeus-Merzbacher disease
Pol filter	bright-field polarizing filter
RFLA	restriction fragment length analysis
RFBs	DNA replication fork barriers
RFSs	rare fragile sites
RPA	replication protein A
RTS1	replication termination sequence
S. pombe	*Schizosaccharomyces pombe*
SDSA	synthesis-dependent strand annealing
SDS	sodium dodecyl sulfate
SSA	single-strand annealing
2-D gels	two-dimensional agarose gels
tdTomato	tomato red fluorescent protein
tetO	tetracycline operator
Ura	uracil
YE	liquid yeast extract media
YEA	Yeast extract agar
YNBA	Yeast nitrogen base agar

CHAPTER 1

INTRODUCTION

1.1 Reasons to Study Chromosomal Rearrangements

Chromosomal rearrangements (CRs) broadly signify genetic changes. They vary from single base pair (bp) changes to megabase size cytogenetic alterations leading to genomic instability [1-3] (Table 1). Each type of rearrangement is important in pathology and evolution. Such genomic instability is the hallmark of cancer and it is also strongly associated with the susceptibility to cancer in many human disorders [4-6]. Chromosomal rearrangements often occur as a result of DNA replication dysfunction [7-12]. Normally, impediments to replication fork movements are rescued by error-free mechanisms [13]. Nonetheless, genomic rearrangements can arise when error-free fork recovery fails. How failure of these mechanisms results in CR can be a complex problem. CR may occur directly from either a double-strand break (DSBs) formation [14-17] or DSBs-independent faulty template switching [18-20]. This thesis mainly focuses on chromosomal rearrangements which are mediated by a template-switch via inappropriate ectopic homologous recombination events without a DSB intermediate. How subsequent outcomes of such events may occur are also presented in this work.

1.1.1 Characteristics of chromosomal rearrangements

Chromosomal rearrangements can cause a variety of structural DNA changes ranging from small scale alterations [21,22] like base pair changes, insertions or deletions, to

larger scale changes such as chromosomal translocations, segmental duplications, whole chromosome loss or duplication and large palindromic chromosome formation (i.e. acentric and dicentric chromosomes *etc.* [23]) (Table 1). Studies in mammalian cells show high complexity; the mechanisms underlying genomic instability are generally investigated by revealing the breakpoints at the sequence level. The breakpoints junctions are surrounded by clustered mutations, additions of nucleotides, deletions and duplications and are thought to derive from processes involving multiple DNA repair mechanisms. Recent sequencing studies have revealed several striking phenomena driven by complex genomic rearrangements, such as chromothripsis [5, 24] (Table1), where the chromosome develops at least three breakpoints via exchange of genetic material associated with multiple rearrangements events. Chromothripsis can be involved in structural chromosomal alterations, where previously separated genetic regions became juxtaposed.

Table 1. The type of genomic variations.

Variation	Rearrangement type	Size range
Single base-pair changes	Point mutations, single nucleotide polymorphisms	1 bp
Small-scale insertions/deletions	Short size of sequence is added/deleted	1-50 bp (majority in < 10 bp)
Fine-scale structural alteration	Deletions, duplications, tandem repeats, inversions	50 bp to 5 kb
Intermediate-scale structural alteration	Deletions, duplications, tandem repeats, inversions	5kb to 50 kb
Large-scale structural alteration	Deletions, duplications, large tandem repeats, inversions	50 kb to 5 Mb
Chromosomal variation	Large cytogenetically visible deletions, duplications, translocation, inversions, palindromic chromosome formation and aneuploidy	<5 Mb to entire chromosomes
Other	Chromothripsis	Multi-event CR in localised regions of single chromosomes or chromosome arms

Although each type of rearrangement provides a significant driving force in evolution and contributes to biological diversity, much of this genomic variation is disadvantageous and is relevant to various diseases. In humans, such pathological conditions associated with CRs are not restricted only to different cancer types but also caused a number of genomic disorders [1-7]. Cancer is a somatic disease, arising from one single cell in the body. CRs can inactivate tumour suppressors and confer oncogene expression regulating phenotypes such as accelerated cell growth or altered cell proliferation and increased drug resistance, thus contributing to cancer proneness. Hence, CRs are thought to provide a significant role during early carcinogenesis. A genomic disorder is defined as a disease in which all of the cells in the patient's body contained the rearrangements [7-12]. The clinical phenotype of genomic disorders is a consequence of aberrant dosage of genes (due to a gain or a loss within the regional genomic architecture) that result from CRs. Many genome disorders occur by non-allelic homologous recombination (NAHR) between region specific low-copy repeats (LCRs) (please refer to additional discussions below) in meiosis during gametogenesis in the parent [8-12]. There are some very rare patients who are mosaic (i.e. half of the cells are normal, while the other half having chromosomal rearrangements), and it is thought this might be a mitotic event in the first division following the fertilization stage [7-8].

In human pathological diseases associated with CRs, which can be a result of the perturbation in the biological balance of the normal state at any genetic locus and the accumulation of the group of pathological conditions. For instance, amplification of the oncogene ERBB2 (also termed HER2) is known to be prevalent in breast cancer patients with an increased disease recurrence and a poor prognosis [25]. These alterations in the regions of variable DNA copy number also amend the expression

levels of genes, thus allowing the resulting transcription levels to be higher or lower than those maintained by transcription of the original copy number. Thereby, a high level of ERBB2 can over-activate downstream signalling pathways and accelerate tumour progression by the promotion of cell growth. Some additional copies of other genes that result from CRs might offer redundancy which regulates new or modified functions or expression patterns [26]. Overall, CRs can be thought to be a cause of genomic reassembly with high frequencies of mutagenesis and high levels of genetic instability, which are often observed in cancer and other pathological disorders.

1.1.2 Replication failures and chromosomal rearrangements

During each cell division, the DNA must be accurately replicated and precisely segregated. These critical steps can sometimes be inhibited by DNA replication fork barriers (RFBs) such as DNA impairment or DNA-protein complex [9]. While not formally a replication fork barrier, the depletion of the dNTPs pool can fail to support normal replication and block or interfere with the progression of the replication forks [27, 28]. When the cells respond to such replication stress, this may lead to genomic rearrangements and may provide an adaptation to environmental changes, which can be disadvantageous to cell viability. Genomic instability associated with CRs can be induced by the failure of DNA replication, which subsequently undergoes imperfect, aberrant or unscheduled DNA reparation (See section 1.1.3 for more on reparation pathways). DNA replication perturbations rescued by accurate reparation do not result in structural changes of the DNA. For instance, a damaged sequence can utilize homologous sequence at the same chromosomal position in the sister chromatid or the homologous chromosome to overcome DNA replication obstacles. However, unscheduled repair mechanisms might use homologous or microhomologous

sequences in the ectopic chromosomal template and can potentially change the genomic structures, leading to aberrant rearrangements [29]. Research designated to identify CRs and their intermediates from both yeast and cultured human cells [30] suggests that experimentally increased replication stress causes problems that would manifest in genetic instability, resulting in genome variations and high mutagenesis. In the yeast model, chronic replication stress can trigger CRs and result in clustered mutations for 100s of kb. In cultured human cells, agents that perturb normal replication and cause replication stress – like aphidicolin and hydroxyurea – are persuasive inducers of CRs [31]. Aphidicolin, a specific inhibitor of replicative DNA polymerases, can disturb DNA replication and induce copy number variations at the chromosomal fragile sites throughout the genome. Likewise, hydroxyurea can result in insufficient activation of the nucleotide biosynthesis pathways via inhibition of the enzyme ribonucleotide reductase, causing nucleotide pool depletion and failure in maintaining normal DNA replication.

Moreover, in humans, some of the chromosomal fragile sites could act as a common indicator for replication-associated problems [32, 33]. Fragile sites can allow visualisation of the replication errors at the cellular level. Chromosomal fragile sites are defined as specific regions that preferentially exhibit visible gaps or breaks on the metaphase chromosomes in conditions where replication stress is accumulated (Figure 1-1). Thus, fragile sites are considered to be a hallmark of stalled forks that can become prone to genetic rearrangements. According to their respective frequencies, fragile sites are classified into rare (RFSs) and common (CFSs) categories. Up to 120 fragile sites have been described in the human genome. Rare fragile sites exist in less than 5% of the population, and are often composed of nucleotide repeat expansion mutations, which are prone to be associated with secondary DNA structure formation

(i.e. hairpins or non-B DNA structures). Hence they are often susceptible to block replication forks resulting in spontaneous breakage. Common fragile sites are a normal part of the human genome and most CFSs are typically stable under normal replicative conditions. Recent work has proposed that CFSs are the regions that contain lower origin density or difficult to replicate sequences and are particularly larger than 500 kb of genes [32]. CFSs thus are likely to initiate proper replication. However, due to inefficient origin firing, they are more likely to subsequently form breakages due to the incomplete replication. These observations suggest therefore that replication failures are a primary cause for genetic instability during early cancer development and can underlie genomic alterations.

Figure 1-1. Schematics of a chromosomal fragile site inducing chromosome rearrangements. When DNA replication perturbation happens at a chromosomal fragile site, chromosome rearrangements may occur and lead to genomic instability such as deletions, inversions, translocations, palindromic chromosomal intermediates (i.e. acentric and dicentric chromosomes). Here described in the case of chromosomal rearrangement that forms acentric and dicentric chromosome may occur via two possible mechanisms: one is when chromosomal fragile sites are prone to brake. The broken-end chromatids may rejoin together to form acentric and dicentric chromosomes; alternatively, when forks stall at chromosomal fragile sites, chromosome rearrangements can also result from faulty template switching mechanisms fusion using homologous or non-allelic sequence to form the acentric and dicentric chromosomes which is break event-independent. An example of chromosomal fragile sites present in human. *Immunofluorescence staining of Human metaphase chromosomes with breaks at FRA3B site counterstained with DAPI [32]. Yellow arrowheads indicate broken FRA3B fragile site expression due to inefficient origin firing; white arrowheads indicate an intact FRA3B.

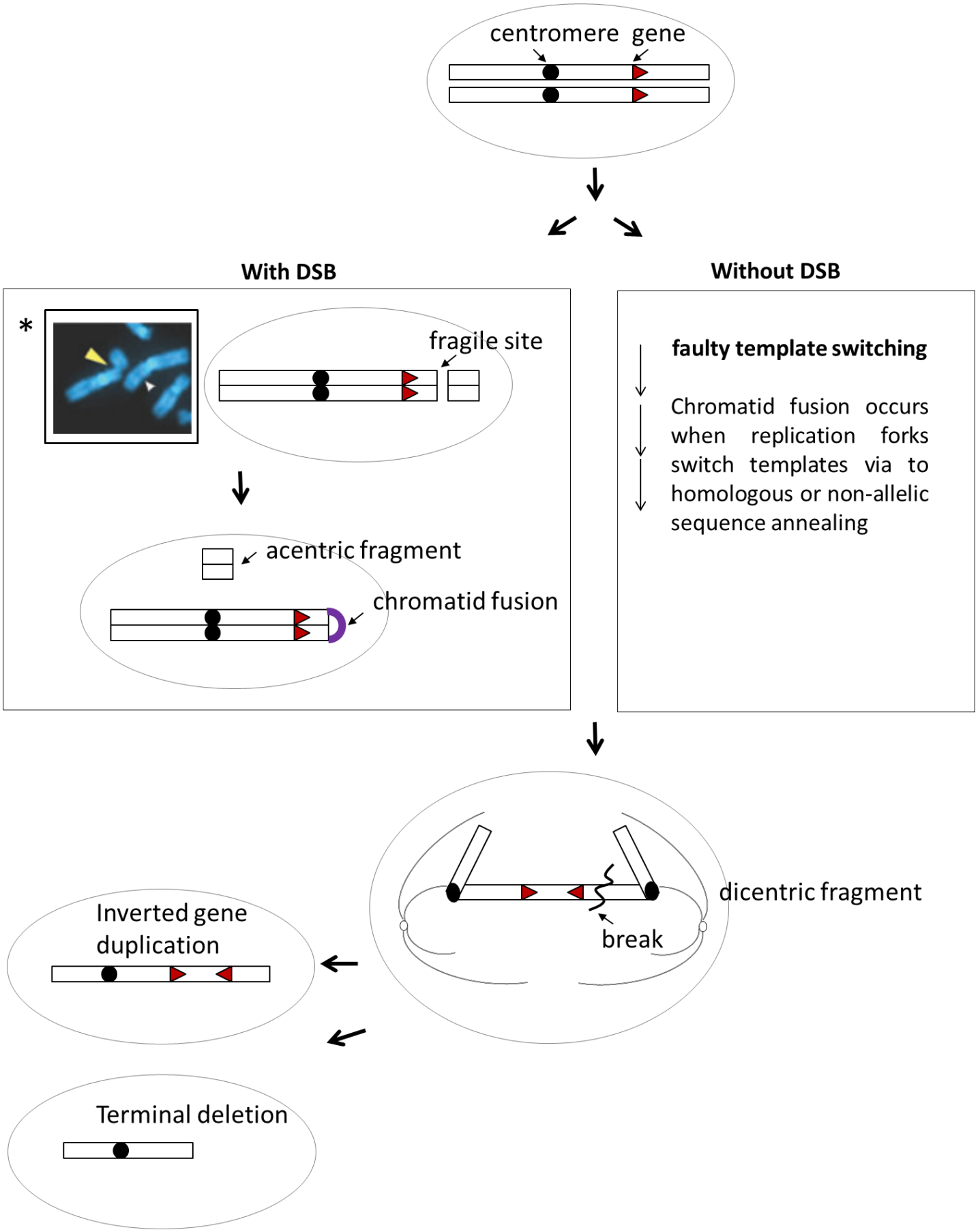
centromere gene
With DSB
Without DSB
*
fragile site
acentric fragment
chromatid fusion
faulty template switching
Chromatid fusion occurs when replication forks switch templates via to homologous or non-allelic sequence annealing
dicentric fragment
break
Inverted gene duplication
Terminal deletion

1.1.3 Palindromic chromosomal intermediates: a common outcome of chromosomal rearrangements

Sequencing studies based on clinical syndromes associated with a particular miss-regulated gene have facilitated the research of chromosomal rearrangements. Nevertheless, sequencing of a cell line or a patient generally provides only a snapshot of the stable outcome of a series of transient events. Therefore, the transient events that led to the stable rearrangement are usually only implied from the final structure. These events generally implicate the initial formation of the dicentric and acentric palindromic chromosomes (a dicentric chromosome has two centromeres, whereas an acentric has no centromere) [35-37]. Both acentric and dicentric chromosomes are extremely unstable and their production is proposed to be characteristic of cancer development. The amplification of oncogenes is the most common issue that has been connected to acentric and dicentric chromosomal generation. Acentric and dicentric chromosomes are also proposed to contribute to cancer initialization. They might form a platform for tumor cells to become resistant to chemotherapy, for example by altering drug metabolism [38].

The potential mechanism of the dicentric chromosomes to generate CRs may involve a sequence of events. Once the unstable dicentric chromosome structures are generated, a series of events may eventually result in their stabilisation; however, often at the expense of further rearrangements [39-41]. Dicentric chromosomes can misalign on the mitotic spindle due to the two centromeres (Figure1-1, 1-7B). Thus, a single DNA molecule can be pulled towards both daughter cells, forming a bridge of DNA. Such events can result in the random breakage of the dicentric chromosome (usually between the two centromeres). The breakage that generates large inverted duplications and repeated cycles can cause amplification of the inverted repeat.

Following DNA replication, the two sister chromatids, which do not have a telomere, can fuse, resulting in another dicentric chromosome, which again can form a bridge of DNA when miss-segregated. This cycle will continue until being stabilised by other mechanisms (such as via the addition of a telomere). This is known to be the breakage–fusion–bridge cycle (BFB) and the resulting rearrangements are often inverted duplications, deletions or translocations (Figure1-1, 1-7B). Acentric chromosomes have no centromeres and are likely to be the precursors for specific extra chromosomal elements, including ‘‘double minutes’’ which, at least in yeast models, can accumulate in response to the selection for gene amplification [42-44]. Figure1-2 shows a flow chart of the generation of acentric and dicentric chromosomes as an example that illustrates the link between the DNA replication stress and the rearrangement events leading to genomic instability. When impaired DNA replication is present, chromosomal rearrangements occur, which subsequently generate unstable intermediate genomic products (such as acentric and dicentric chromosomes). These intermediates, then in turn, promote tumour cell development

1.1.4 DSBs and the failure of fork recovery

The sequence of events that may cause chromosomal rearrangements can be described as follows: when cells replicate their DNA, the replication forks encounter some problems and consequently, fork stalling occurs, which might result in fork collapse. When error-free fork recovery fails, the newly-synthesised strands in the collapsed fork may anneal to other sequences in the genome leading to genome rearrangements [45]. It is speculated in this review that this event may arise from either DSBs generation dependent (Figure1-1, left panel) or independent pathways (Figure1-1, right panel).

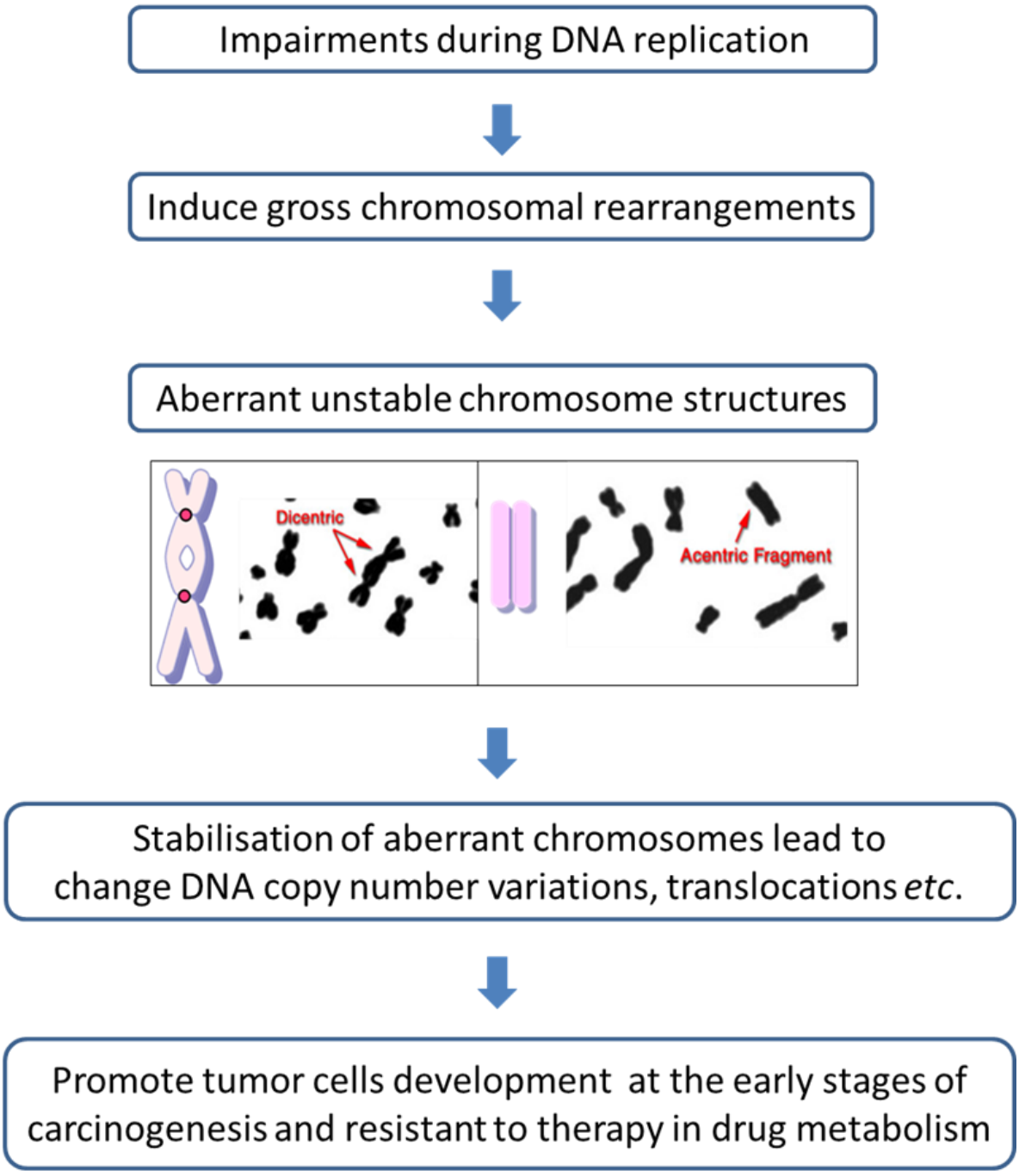

Figure1-2. Flow chart showing the process initiated by perturbations of DNA replication and followed by inducing gross chromosomal rearrangements to generate aberrant chromosomes structures (such as acentric and dicentric chromosomes). The chromosomal structure alterations will undergo further rearrangements to change DNA copy numbers. These alterations include gene duplications, deletions, inversions or translocations and support tumor cell development. * The figures of the dicentric and acentric chromosomes are provided form the following website: http://www.mun.ca/biology/scarr/Dicentric_chromosomes.html.

Reviewing the literature seeking for similar observations on genome rearrangements has been revealed that genomic instability can be initiated by DSBs. DSBs is a common proceeding cause of CRs. There are two major pathways to repair DSBs [15, 29 and 46]: non-homologous end joining (NHEJ) and homologous recombination (HR). DSBs can be accurately rescued by each of these pathways. However, DSBs are also toxic DNA lesion that may undergo CRs if NHEJ is incorrect rejoining or ectopic homologous template is used via HR. As Lambert *et al*. described [19], "Recombination is a 'double-edged sword,' preventing cell death when the replisome disassembles at the expense of genetic stability". HR events can lead to simple and complex chromosomal aberrations, characterized by sequences of breakpoint junction in the genome [14]. The observation of resulting genotypes associated with genomic rearrangements might be difficult to explain by a single recombination event (such as NAHR or NHEJ). Hence, the complex CRs have been proposed to generate unstable chromosomal intermediates. For example, a dicentric chromosome is proposed to be the common intermediate product during breakage-fusion-bridge (BFB) cycles that involve multiple repetitive HR events. Sometimes, dicentric chromosomes might be formed by fusions of sister chromatids where the telomeres are lost through NHEJ. NHEJ mediated repair of the breakage of the chromosome by rejoining the free ends at two different loci produces a new, rearranged chromosome [13].

Recently, several lines of evidence emerged to support an alternative view suggesting that CRs may also be derived from the various related or individual events without a DSB intermediate; CRs may arise from faulty template switching during HR at stalled forks (Figure1-1, right panel and section) [19-20, 47-53]. Here, this work reports and discusses two systems in yeast to study faulty template switching. These yeast genetic systems use an inverted repeat to induce chromosomal rearrangement and as a

consequence, giant chromosome is generated (resulting from inverted repeat fusion via a faulty template switching) [48-50]. Inverted repeat fusion has been reported in bacteria as well [54]. Inverted repeats are common in many eukaryotic genomes; for instance, human genome contains a number of repetitive DNA repeats such as Alu elements, which represents ~10% of the genome and low copy repeats (LCRs) (~5%). These repeats are usually separated by other sequences [56]. Fusion of inverted repeats has been reported in cancer-prone human diseases such as the Pelizaeus-Merzbacher disease (PMD) [52-92]. Hence, inverted repeat fusion has a significant relevance in the disruption of chromosomal stability.

Two yeast systems showed rearrangements that involved inverted repeats. This suggests that during DNA replication, errors can occur nearby inverted repeats and the inverted repeats can fuse to form dicentric or acentric chromosomes. A genome instability-induced system has been designed in *Saccharomyces cerevisiae* possessing aberrant genomic architecture (for example, instability of a dicentric chromosome) [48]. This system was reported to contain a highly unstable genetic region that appears to contribute to genome instability during DNA replication. By the following rearrangements (likely to involve BFB cycle), a dicentric chromosome is prone to induce CRs. The authors suggest that fusion events occur by a DSB-independent, replication-based pathway. In our group, we have used a series of genetic systems that contained a known natural RFBs-replication termination sequence (RTS1) in fission yeast *Schizosaccharomyces pombe* [19, 49-50, 55-60]. RTS1 is a ~850 bp DNA sequence originally located near the mating type locus and is associated with several proteins (i.e. Rtf1 and Rtf2) to ensure unidirectional replication during mating type switching [59]. The progression of the replication fork can be paused in a controllable manner in this system (see details in section 1.4.3). When stalled DNA replication

forks are present, HR attempts to repair the damage. However, homologue regions of the repeats can be used by HR instead of the allelic regions and the attempt to repair the damage will result in CRs. These genetic systems were proven to efficiently undergo multiple recombination events. They also enabled the visualisation of the chromosomal rearranged products (including instability of acentric and dicentric chromosomes; gene inversion and translocation), eventually leading to specific CRs. These data led us to the development of two template exchange models by which chromosomal rearrangements may arise from non-allelic homologous recombination (NAHR) and U-turn (see details in section 1.4). No DSBs were detected in these models during the rearrangement processes [49-50]. However, as our model contained the replication fork stalling site on chromosome III of *S. pombe,* rearrangements resulted in essential genetic alterations, thus a significant loss of cell viability made it difficult to follow the subsequent recombination events.

1.1.5 Aims of this work

This thesis is an extension of our previous study described above. However, to overcome the loss of viability in the previous systems I placed the experimental construct on an extra, nonessential mini-chromosome. This system provides a mean to directly visualise the chromosome rearrangements and follow the fate of the rearranged chromosomes. My findings showed that this system overcame the limitation of our previous model. In the following sections, I would like to illustrate the current scope of the replication fork biology and cellular responses to encountering a DNA replication lesion. These responses are likely to coordinate fundamental DNA repair mechanisms or to activate DNA checkpoint pathways. I will discuss more detail about our current research in this chapter. Moreover, I divided all my results into three chapters: in Chapter 3, I will present the detail of how I

constructed the experimental yeast strain which contains the mini-chromosome to achieve the aim of this thesis; Chapter 4 reports the information about the behaviour of mini-chromosome while chromosome arrangement occurring; Chapter 5 focuses on the fate of rearranged chromosomes. In Chapter 6, I draw the discussion and summarise the conclusions of my study. The final chapter shows the relevant references for this project. Notably, the materials and methods for my experiments are documented in Chapter 2.

1.2 Replication fork biology

Replication errors are known to contribute significantly to genome rearrangements driven by either DSBs or template exchange events [14-17, 18-20, 61]. Thereby, molecular studies of fork biology provide early and vital clues on the links between replication errors and genome instability. During DNA replication, replication forks might be arrested by obstacles, resulting in a temporary stalled fork. A stalled fork is normally rescued by error-free regulatory and repair mechanisms described below. But if the stalled fork fails to recover, the newly-synthesised strands may restart at other ectopic sequences in the genome, leading to chromosomal rearrangements. Understanding this failure of the replication fork recovery may be crucial to identifying how genome rearrangements can occur. Fork biology however still exhibits some uncertainties caused by a lack of a direct evidence to define fork-stalling *in vivo* or *in vitro* systems. Here, I present more details on the definitions in fork biology and discuss five prospective models on the fate of stalled forks. Stalled forks might either undergo error-free fork recovery or collapse and genome rearrangements can arise when the recovery mechanisms fail (Figure 1-3).

1.2.1 Progression of DNA replication

In order to inherit biological information, all living organisms must duplicate their genetic material to provide one identical copy to each of the daughter cells prior to the next cell division. The process is referred to as semiconservative replication and takes place with each strand of the original unwinding duplex DNA molecule serving as the template. A sequence of events produces the complementary strand to obtain two identical copies of the molecule. DNA replication occurs within the S-phase of the cell cycle and begins at particular sequences in a genome called origins. Bacteria only have a single circular chromosome and typically one single replication origin [62]. Most eukaryotes contain long linear double-stranded DNA molecules with multiple replication origins on each chromosome that usually initiate at distinct firing times [63-64]. Once the origin is activated, two replication forks proceed from this point and progress independently and bi-directionally. The replication fork is a branch configuration in which the two parental strands are separated. The replisome is a multiprotein complex that is associated with the occurrence of the separation event [65]. It consists of the major proteins of DNA synthesis, including 1. Pre-replication complex proteins such as the mini-chromosome maintenance complex (MCM), 2. Other helicases required for the unwinding of the original strands, 3. Replication elongation factors, including DNA polymerases (i.e. polymerase-α, polymerase-ε and polymerase-δ etc.), 4. Polymerase accessory factors such as the clamp loader replication factor C (RFC) and the clamp proliferating cell nuclear antigen (PCNA), and 5. Other regulatory factors, for example a fork protection complex involving the DNA replication checkpoint mediator (Mrc1), the topoisomerase 1-associated factor 1 (Tof1) and the chromosome segregation in meiosis protein 3 (Csm3) [63, 66].

Figure 1-3. The model of replication fork biology.

The model describes the process of stalled fork, collapsed fork, fork restart or failure as it encounters at the replication fork barrier (RFB). In the presence of *DNA damage*, stalled fork can activate checkpoint pathways to stabilise the replication complex (RC) and to remove the lesion and resume replication. However, if the checkpoint dysfunctions or in the absence of RFB removal RC disassociates from the fork resulting in collapsed fork. Cells have evolved multiple mechanisms to respond to collapsed forks and resume new strand synthesis. But if the restarted fork uses inappropriate DNA template for template switching or DSBs repair mechanisms a fork failure will occur and lead to ectopic chromosomal rearrangements.

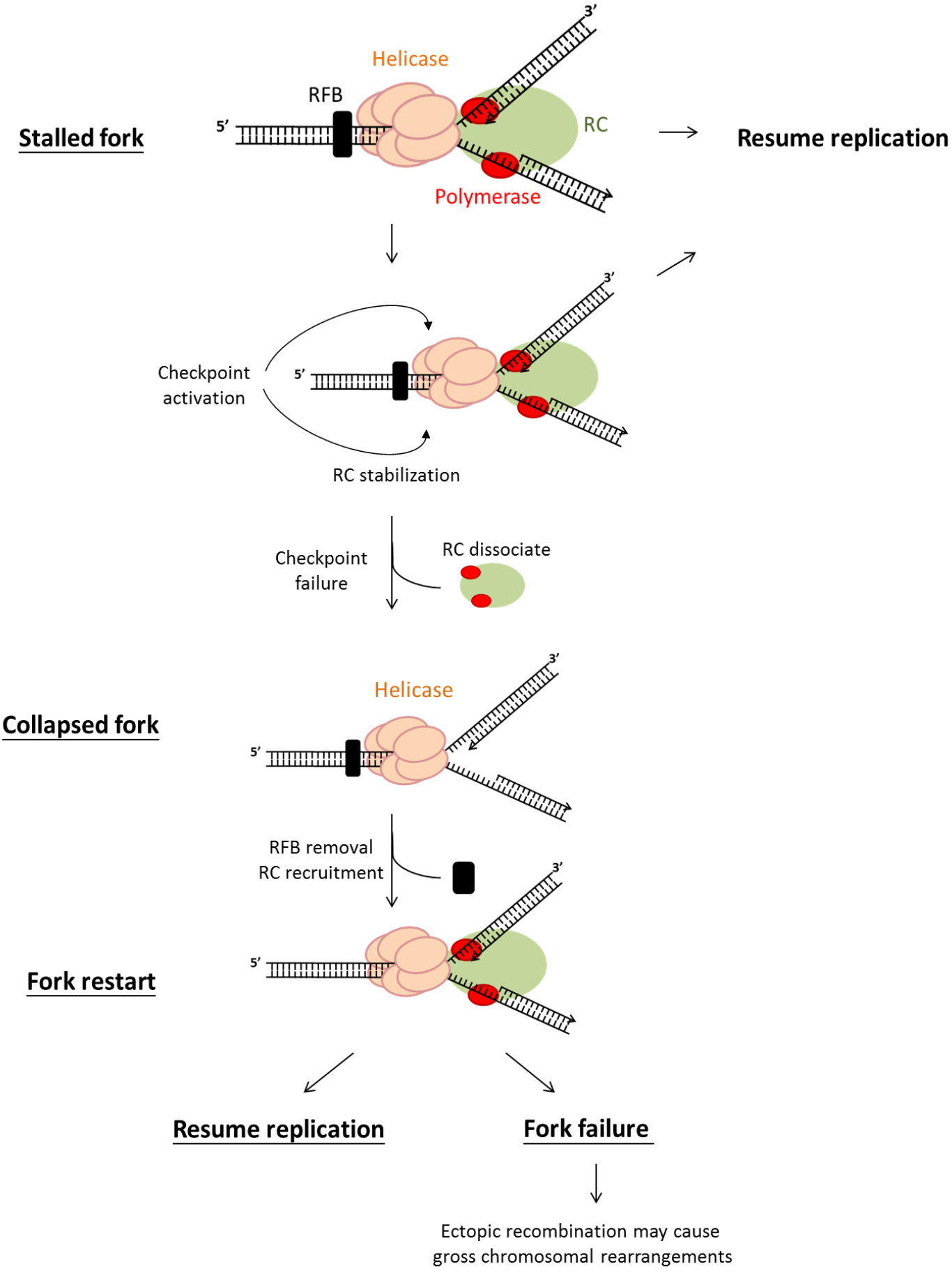
Stalled fork
Helicase
RFB
5′
3′
RC
Polymerase
Resume replication
Checkpoint
activation
RC stabilization
Checkpoint
failure
RC dissociate
Collapsed fork
Helicase
RFB removal
RC recruitment
Fork restart
Resume replication
Fork failure
Ectopic recombination may cause
gross chromosomal rearrangements

1.2.2 Stalled forks

A “stalled fork” is present when the replisome progression is arrested by a temporarily physical barrier at the DNA Y structures (Figure 1-3) [60, 67]. Stalling can be induced by a wide variety of obstacles such as DNA damage (e.g. produced by, exposure to ionizing radiation, ultraviolet light or chemicals), unusual DNA sequences (e.g., secondary structures like G-quadruplex DNA), replication converging with transcription (e.g., at tRNA genes) or tightly occupied by nonhistone DNA binding proteins (e.g., at centromeres, origins of replication during chromosome duplication) [28]. Nucleotide depletion leads to failure to support normal replication and thus impeded progressing fork movements [9]. Consequences of a stalled fork can be less deleterious. Cellular responses and proofreading mechanisms can offer near perfect fidelity for DNA replication. Resumption of DNA replication can be facilitated by DNA helicases or DNA repair proteins via repairing the damage site or removing a blocking protein. When a replication fork is stalled, DNA helicase can continue to unwind and separate the parental strands presenting single stranded DNA. These exposed ssDNA strands can be accurately repaired by HR-dependent repair [69] and cause the activation of the checkpoint response or likely other mechanisms. A stalled fork can be protected by the intra-S phase checkpoint pathway [69-73], including the checkpoint protein kinases Tel1/ATM [74-75], Mec1/Rad3/ATR [74, 76-77], Rad53/Cds1 and Chk1 [78] (Section 1.3.4 for more detail) to stabilise replisome association and resume new DNA synthesis without further intervention. Moreover, in eukaryotic cells, a stalled fork can also be rescued by a neighbouring converging fork from adjacent origins and thus complete replication [29]. As bacterial cells contain only a single origin on the whole chromosome, they appear to remove or bypass the blocking lesion preferentially by using homologous recombination to restart the fork as rescue by an oncoming converging fork is not possible [68].

1.2.3 Collapsed forks and restart

Not all stalled forks can be successfully stabilised [60]. A "collapsed fork" is defined as a fork where some components of replisome are disassociated from the replication fork (Figure 1-3). Thus, a collapsed fork is thought to be more deleterious than a stalled fork. A collapsed fork may be susceptible to insufficient activation of the intra-S phase checkpoint which is required for rebuilding replisome and resumption, requires more than 100 bp of ssDNA production. For instance, interstrand cross-linking (ICLs) agents block DNA replication without ssDNA generation [79]. It will result in collapsed forks where the intra-S phase checkpoint pathway fails to be activated.

Very little is understood on collapsed fork structures and on which replisome proteins are present or absent [65]. Attempts to restart a variety of DNA structures may result from processing of a collapsed fork, see in Figure 1.4 [45, 80]. (1) A "chicken foot" structure. The branch migration leads to a regressed fork structure, which can be degraded directly by resection of nucleases (such as Dna2 and Exo1) that allows a lesion repair or bypass [81,82], or a regressed fork can be involved in strand invasion, and possibly formation of a Holliday structure that is subsequently resolved [83-88]. (2) Gap formation behind the fork. When restarting DNA synthesis the replisome may be recruited upstream or downstream of a collapsed site resulting in ssDNA gaps that can be repaired by error-prone translesion synthesis (TLS) or error-free homologous recombination (HR) using the sister chromatids as templates [60, 89]. (3) DSBs at a fork. When a DSB occurs, it is repaired mainly by accurate HR, NHEJ and MMEJ mechanisms (Section1.3.2 for more detail). (4) Hemicatenanes. A hemicatenane is a topological intertwining configuration in which one strand of a duplex is coiled around one strand of another duplex that may be mediated by Rad51 and Rad52.

Resolution of the hemicatenane is most probably aided by the helicase Sgs1 and topoisomerase Top3 [48, 90]. (5) A "closed fork". The ligation of newly-synthesised leading and lagging strands give rise to closed forks at close inverted repeats. This structure can generate large regions of single strand DNA structures [53]. A collapsed fork can be perfectly restarted by several repair mechanisms. But they also potentially become a substrate for deleterious recombination events. Failure to anneal to the correct templates or improper repair processing can contribute to genome rearrangements. Although a fork failure rarely happens because it can be prevented by several pathways, if forks use the incorrect DNA template then it allows fork recovery, but at a high frequency of genomic errors (Figure 1-3).

1.2.4 The studies on replication fork biology

An effective way to study DNA structures is by two-dimensional agarose gels (2-D gels), which can distinguish various molecular species of DNA since they have different conformations and electrophoretic mobility [91]. 2-D gels can provide significant information where forks stall, and combined with biochemical techniques it can identify potential structures. For example, one X-structure identified in 2-D gels is probably a Holliday structure when it can be resolved by nucleases (e.g. RuvC). However X structures can also indicate the presence of a hemicatenane rather than a Holliday structure when it cannot be resolved by RuvC. Description of specific fork structures outlined above still appears to be a major technical challenge and is far from complete.

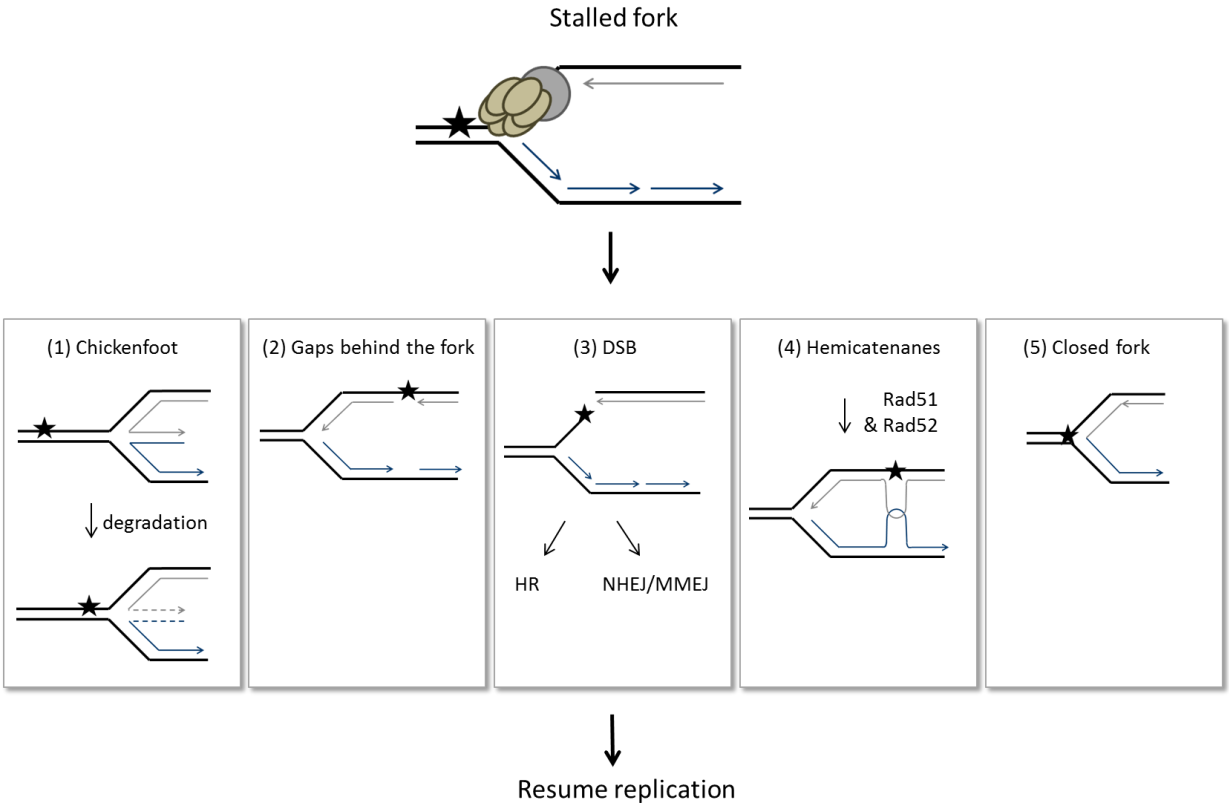

Figure 1-4. The models of structures generated after fork arrested at a lesion.

(1) Chickenfoot structures. The reversal of the fork forms a chickenfoot structure, which can be degraded by nuclease or undergo template switch reaction. (2) Gaps behind the fork. Fork progression slows down and ssDNA gaps accumulate behind the fork. (3) DSBs at a fork. The stalled fork may suffer a DSB. The DSBs can be repaired by HR, NHEJ and MMEJ mechanisms. (4) Hemicatenanes. Rad51 and Rad 52 promote template switch mechanism to form hemicataenes. (5) A closed fork. The newly-synthesised leading and lagging strands fused at closely inverted repeats. Star indicates a replication obstacle.

1.3 DNA repair mechanisms and other cellular responses for maintenance of genome integrity

The DNA repair mechanisms are vital for the maintenance of genomic integrity in all organisms. Failure to correct DNA damaged lesions is not confined to cause genetic disorders and passing these heredity traits to offspring can influence its life span and contribute to evolutional disadvantage. The processes of DNA repair mechanisms at collapsed forks essentially occur by two general pathways: homologous recombination (HR) and non-homologous repair (Table2.). The obvious distinctions between these is that HR requires extensive identity of DNA sequence (about 50 bp in *E. coli* and more than 300 bp in mammalian cells), whereas non-homologous repair mechanisms only need microhomology (about 5-25 bp DNA sequence) or no homology at all [13, 92-93]. Here, I discuss several major homology and non-homology based DNA repair mechanisms for the understanding how these can avoid the generation of genome variations or lead to genome instability when these mechanisms fail (Table 2.).

1.3.1 Homologous recombination repair

HR can underlie several DNA repair mechanisms and it uses a similar or identical sequence to repair the damaged site. HR is also responsible for ordered segregation of chromosomes and forming new combinations of linked alleles at meiosis. During mitosis and meiosis as well as in DNA repair, HR involves the same basic steps; after a single-strand or double-strand break or when replication forks collapse/break, 5' ends of the break are cut back to leave an overhanging 3' tail - "resection". Following resection, the overhanging 3' end of the broken DNA molecule "invades" toward a similar or equivalent DNA molecular template [15].

Table 2. DNA repair mechanism

■ Homologous recombination repair

Mechanism	DSB	Process	Breakpoint feature
Double-strand break repair (DSBR)	Two-ended break	HR-based template invasion between forks	Homology
Synthesis-dependent strand annealing (SDSA)	Two-ended break	HR-based template invasion between forks	Homology
Single-strand annealing (SSA)	Two-ended break	HR-based template invasion between forks	Homology
Break-induced replication (BIR)	One-ended break	HR-based template invasion between forks	Homology

■ Non-homologous repair

Mechanism		DSB	Process	Breakpoint feature
Non-replicative	Non-homologous and microhomology-mediated end joining (NHEJ & MMEJ)	One-ended break	Directly joined two broken-ends	Homology not required or microhomology needed (5–25bp)
	Breakage–fusion–bridge cycle (BFB cycle)	>1 break	Multiple NHEJ	Homology not required or microhomology needed (5–25bp)
Replicative	Replication slippage or template switching	Not required	Replication slippage within forks	Microhomology
	Fork stalling and template switching (FoSTeS)	Not required	Template switching between forks	Microhomology
	Microhomology-mediated BIR (MMBIR)	One-ended break	Template switching between forks	Microhomology

The process of invasion requires the 3' end overhang exposed single-stranded DNA to be bound by replication protein A (RPA) [69]. Mediator proteins (such are Rad52, Rad55/57 in eukaryotes) then replace RPA with RecA/Rad51. With the help of this strand exchange protein (RecA in prokaryotes, its orthologous in eukaryotes is Rad51 in DSBs repair and Dmc1 in meiosis) the nucleoprotein filament is formed [68]. This nucleoprotein filament mediates searching for homologous duplex partner of the 3' overhang. After finding a region of homology, the invasion strand replaces part of the sequence of the homologous duplex strand, forming a displacement loop (D-loop). This D-loop presents a mobile cross-shaped configuration connected between two DNA molecules that is composed of the invading 3' overhang strand and a sister chromatid in mitosis or a homologous chromosome in meiosis. An intermediate crossover structure known as a Holliday junction forms after branch migration across the homologous chromosomal template which extends the length of heteroduplex DNA [83-90]. These junctions are subsequently disassembled (SDSA, see below) or either resolved or dissolved by an endonuclease (like Mus81–Eme1 in fission yeast and human) or dissolvase (Top3/RecQ helicase) respectively [94]. This allows the separation of either non-crossover or crossover recombinant products depending on the orientation of the resolution [95].

Non-crossover event involves that acceptor sequence will be transferred an allelic copy from the donor, while the allelic sequence of the donor retains its identity. However, during crossover by the reciprocal breakage of two DNA molecules a precise exchange occurs between the acceptor and donor partner. To understand more detail about homologous recombination I describe the HR dependent mechanisms of DNA break repair in the situations where two double stranded ends occur as well as those where only one is present. Besides the two most common models on how

homologous recombination repairs double-strand breaks in DNA (the double-strand break repair (DSBR) pathway and the synthesis-dependent strand annealing (SDSA) pathway) (Figure 1-5) an alternative model for double-strand breaks repair is the single-strand annealing (SSA) pathway that occurs in the absent of a homologous template (Figure 1-6A). An additional model of homologous recombination based repair is initialized from one-ended break repair achieved by the break-induced replication (BIR) pathway. This occurs especially when the replisome runs into a nick or a broken replication fork is otherwise generated (Figure 1-6B).

1.3.1.1 Double-strand break repair (DSBR)

DSBR and SDSA pathways are similar in their first resection steps (Figure 1-5) [15]. One unique feature of DSBR is to form an intermediate with two Holliday junctions. In DSBR, after resection the ssDNA 3' overhanging end invades the sister chromatid or homologous chromosome and facilitates the generation of the first Holliday junction. The second 3' overhang, which occurs at the same break site without being involved in strand invasion, is captured to form the second Holliday junctions. These double Holliday junctions are resolved subsequently by endonucleases and repair the gap, becoming ligated to form either non-crossover or crossover products.

1.3.1.2 Synthesis-dependent strand annealing (SDSA)

In SDSA [15], the extending part of the invading 3' strand along the recipient DNA duplex can be separated from the template by a helicase (Figure 1-5). This invading 3' strand with partial newly-synthesised DNA anneals back with the other 3' overhang that locates at the original break site in the damaged chromosome by complementary base pairing. The break repair is completed by gap resealing and ligation. Consequently, HR via the SDSA pathway only results in non-crossover products.

Figure 1-5. Mechanisms of double-strand break repair (DSBR) and synthesis-dependent strand annealing (SDSA).

Each line shows a single nucleotide chain: the broken DNA molecules are shown as red lines; homologue or sister molecules are shown in blue lines. In DSBR 5' ends of a DSB are resected to leave 3' overhanging tails, followed by 3' ends invasion into homologous sequence forming a D loop. The 3' end then primes a new DNA synthesis (dotted green line), which can past the position of the original break. In the left pathway, the second end is integrated into the D-loop, which forms a double Holliday junction; the junctions are resolved by an endonuclease. This event will generate non-crossover or crossover products, depending on the resolution in the same or different orientations at the two junctions, respectively. SDSA initiates the same way as DSBR. However, after the extension step the invading end with the newly-synthesised DNA will part from the template by a helicase. The invading end may encounter the second end from original DSBs, and anneals with it again using complementary base pairing (dotted arrow). Thus, the second end restarts DNA synthesis and gets ligated.

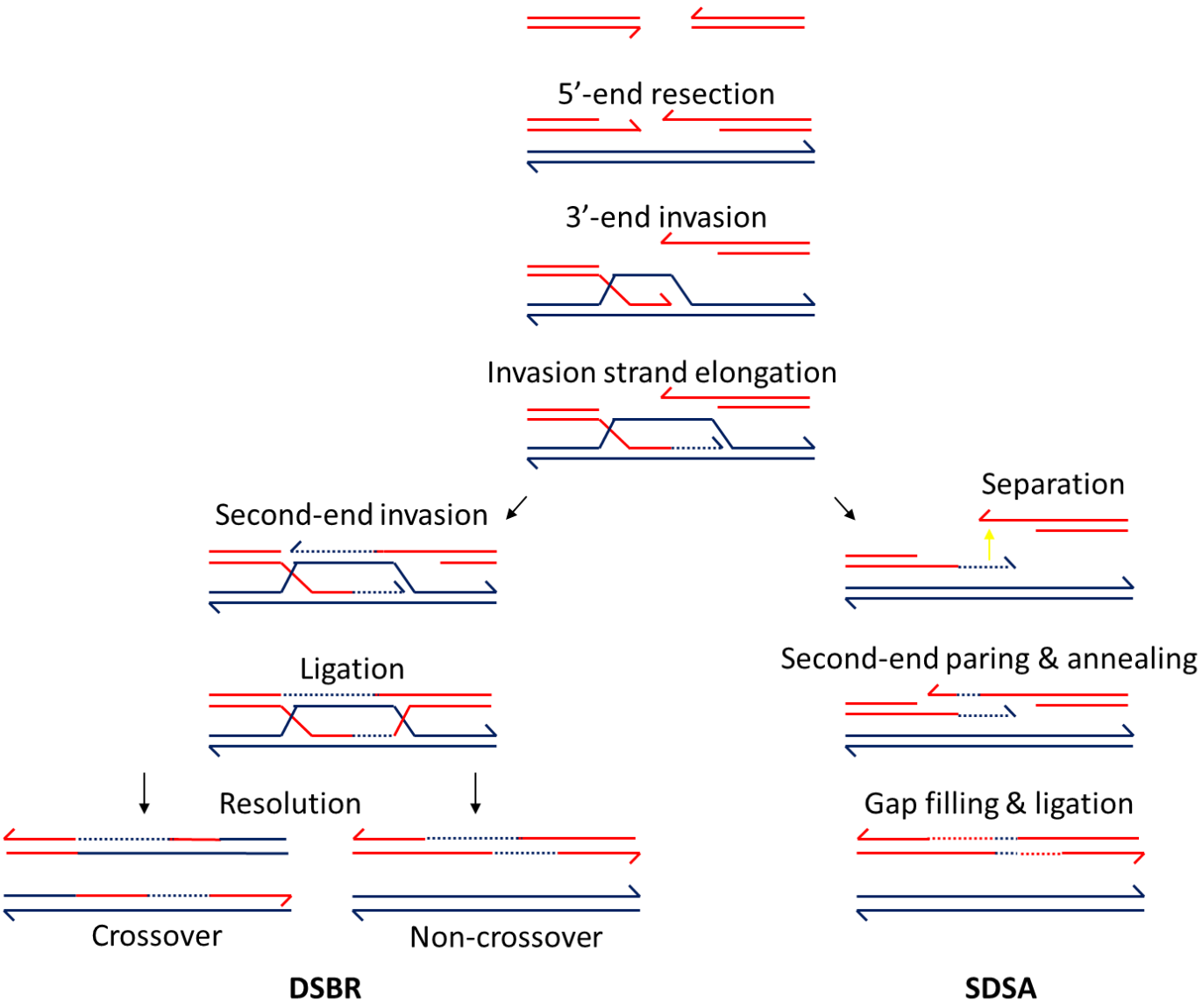
5’-end resection
3’-end invasion
Invasion strand elongation
Second-end invasion
Separation
Ligation
Second-end paring & annealing
Resolution
Gap filling & ligation
Crossover
Non-crossover
DSBR
SDSA

1.3.1.3 Single-strand annealing (SSA)

The SSA pathway of homologous recombination repairs double-strand breaks flanked by direct repeat sequences (Figure 1-6A). SSA pathway differs from DSBR or SDSA pathways in that it does not require a separate DNA molecule as a template, [15, 96-97]. The SSA pathway only occurs at a single DNA duplex and uses the homologous sequences (after their resection) to directly ligate with each other on either side of the break without the requirement of a homologous partner. The process of SSA does not have the invasion step and thus does not require strand exchange proteins-RecA/Rad51. However, the annealing protein-Rad52 has a necessary role in the alignment of each of the repeat sequences and enables them to anneal. After completed annealing the single-stranded gaps are filled in by new DNA synthesis and flap the non-complementary tails. The flapping regions are clipped off by a set of nucleases, such as Rad1/Rad10. Repair by this mode results in the loss of DNA sequence between the repeats: one of the repeats and all the intervening DNA sequences. The SSA pathway is thought to result in high mutagenesis rate with the outcome of genetic material deletions.

1.3.1.4 Break-induced replication (BIR)

During DNA replication, replication forks sometimes encounter a nick leading to a broken fork where only one DSBs end is presented (Figure 1-6B). These broken forks can be repaired by BIR. BIR presents some similar properties to SDSA [98]. Both pathways show an invasion of the 3' tail into a homologue DNA duplex and extend DNA synthesis forming a D-loop. While in SDSA the new 3' extended tail anneals back with the second end of the DSBs in BIR model the extended 3' end fails to find a complementary second end so it reinvades to form a D-loop again, extending further.

Figure 1-6. Mechanisms of single-strand annealing (SSA) and break-induced replication (BIR). (*A*) In SSA 5'-end resection does not lead to invasion of homologous sequence. If there are complementary single-stranded sequences (shown by the filled red squares) on either side of DSBs, these can anneal with each other. Removal of flaps, gap filling and ligation, results in the deletion of the sequence between the repeats and one of the repeats. (*B*) The BIR pathway begins at one-ended DSBs derived from broken replication forks caused by a nick in a template strand (Black arrowhead). BIR can be viewed as a modification of SDSA. However, in BIR, the extended 3'end fails to find a complementary second end of the DSBs. This forces the 3' end to reinvade into the homologous template, and extends further. This process of invasion, extension and separation might be repeated several times until a more stable replication fork is formed. The fork can now complete the replication until the end of the molecule. Each line shows a single nucleotide chain: broken DNA molecules are presented as red lines; homologue or sister molecules are drawn in blue lines.

A.

SSA

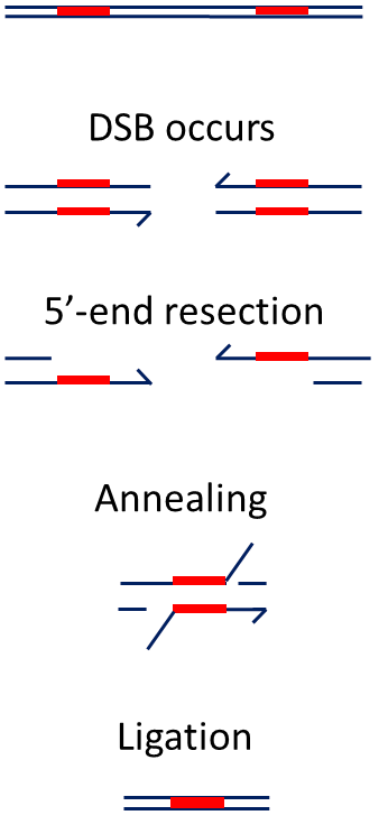
DSB occurs
5’-end resection
Annealing
Ligation

B.

BIR

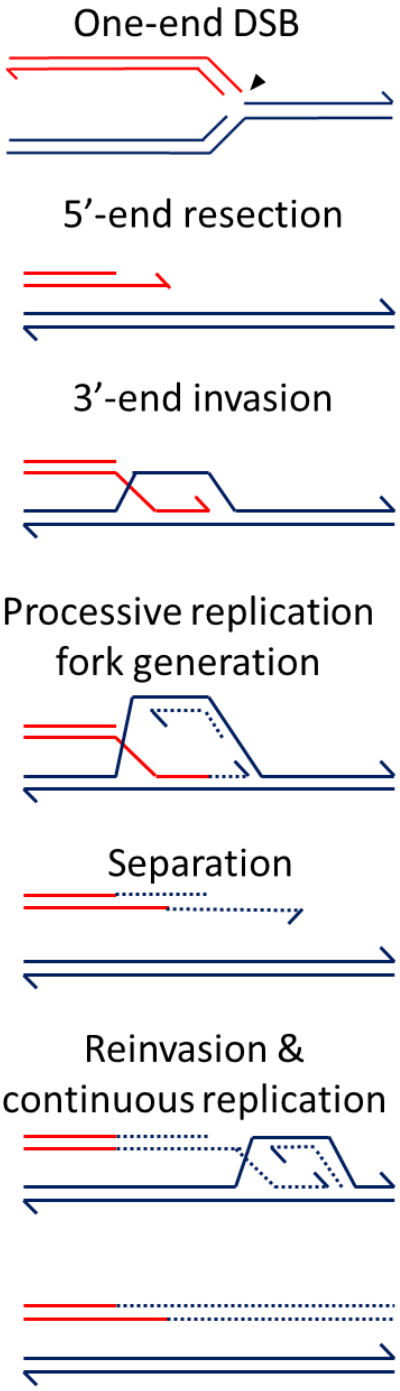
One-end DSB
5’-end resection
3’-end invasion
Processive replication
fork generation
Separation
Reinvasion &
continuous replication

The process of invasion, extension and separation might be repeated several times until the formation of a more proceeding replication fork. Finally, the fork completes replication to the end of the molecule and allows copying the donor template to the damaged end of the chromosome.

1.3.2 Non-homologous repair

In contrast to homologous recombination, which requires a homologous sequence to guide the repair, the mechanisms of non-homologous recombination typically utilize very limited microhomology or no homology to repair a DNA damaged molecule. The DNA repair mechanisms of non-homologous recombination are classified into replicative and non-replicative non-homologous mechanisms. In the next sections, I will explain the mechanisms that do not use HR to repair a damaged molecule.

Non-replicative non-homologous repair

1.3.2.1 Non-homologous and microhomology-mediated end joining (NHEJ & MMEJ)

In the process of non-homologous end joining (NHEJ), two DNA ends are directly joined (Figure 1-7A) without the need of homologous sequence [15, 46]. The first event of the NHEJ system in eukaryote is the recruitment of a heterodimer Ku protein consisting of Ku70 and Ku80, which form a complex with catalytic subunit of DNA protein kinase (DNA-PKcs), promoting bridging of the double-strand breaks ends. When the two overhangs are rejoined in the correct positions, NHEJ repairs the damage accurately. Nevertheless, inappropriate NHEJ can cause loss of nucleotides resulting in small scale (1–4bp) deletions of the DNA sequence at or nearby the junction. When NHEJ pathway is unavailable, double-strand breaks can be repaired by an alternative error-prone pathway called microhomology-mediated end joining (MMEJ) (Figure 1-7A). MMEJ needs 5–25bp microhomologous sequences which are

often presented in the single-stranded overhangs on either side of the break, annealing broken strands and execute Ku protein and DNA-PK independent repair mechanism. The MMEJ pathway is prone to alignment of the strands with mismatched ends that are exposed a 5-25bp of complementary sequences. By removing overhanging nucleotides (flaps on the aligned strand) and insertion of missing nucleotides MMEJ ligates the DNA strands without proofreading and it results in deletions of genetic material.

1.3.2.2 Breakage–fusion–bridge cycle (BFB cycle)

The occurrence of a DSB can cause a chromosome to lose its telomere which might induce breakage–fusion–bridge (BFB) cycle. BFB is initialized by the generation of a dicentric chromosome (Figure 1-7B) [39-41]. After replication, two sister chromatids are duplicated without the telomeres. DNA repair systems are recruited to the free ends of the two sister chromatids and fuse them to form a dicentric chromosome. In some cases a translocation event in inverted orientation between two chromosomes can also create a dicentric chromosome. To restore stability of the genome a dicentric chromosome must undergo further rearrangements. During the anaphase the two centromeres of the dicentric chromosome are pulled to separate nuclei as a result of the anaphase bridge formation, causing a random breakage on the dicentric chromosome. The break will lead to new ends that lack telomeres. After replication, these new ends will fuse and form a new dicentric chromosome, and a cycle is established. The cycle can cease by telomere addition or other mechanisms that stabilises the chromosome [99]. It is believed that the physical properties of a dicentric chromosome and its further process of the breakage–fusion–bridge cycle is linked to the amplification of large inverted duplications in human cancer cells.

Figure 1-7 Mechanisms of non-homologous and microhomology-mediated end joining (NHEJ & MMEJ) and breakage–fusion–bridge cycle (BFB cycle).

(*A*) Each line shows a single nucleotide chain: two different broken DNA molecules are drawn in different colour; red lines and blue lines perform two different chromosomes. NHEJ is referred to directly ligate broke ends without the requirement of a homologous template. MMEJ only requires short homologous DNA sequences, called microhomologies. These microhomologies are often present in single-stranded overhangs on the ends of breaks. (*B*) BFB cycle. A DSB can occur in a chromosome, causing it to lose a telomere. After replication, both sister chromatids lack telomeres. Each line shows a single nucleotide chain: sister chromatids are drawn in red and blue. These two ends are thought to fuse and form a dicentric chromosome. At the anaphase, the two centromeres of the dicentric chromosome are pulled apart, forming a bridge. Eventually, a random breakage occurs. The chromosome is duplicated again and if it has an unprotected end after replication the two sister chromosomes can fuse again to generate a new a dicentric chromosome (green arrow). The broken end chromosome can be repeated to fuse and rejoin until stable products form by for example a new telomere addition. This cycle leads to the formation of a large inverted duplication. Amplification and deletion of the large sequences can occur by random breakage. Centromeres are indicated by a blue or red circle; telomeres by a brown block.

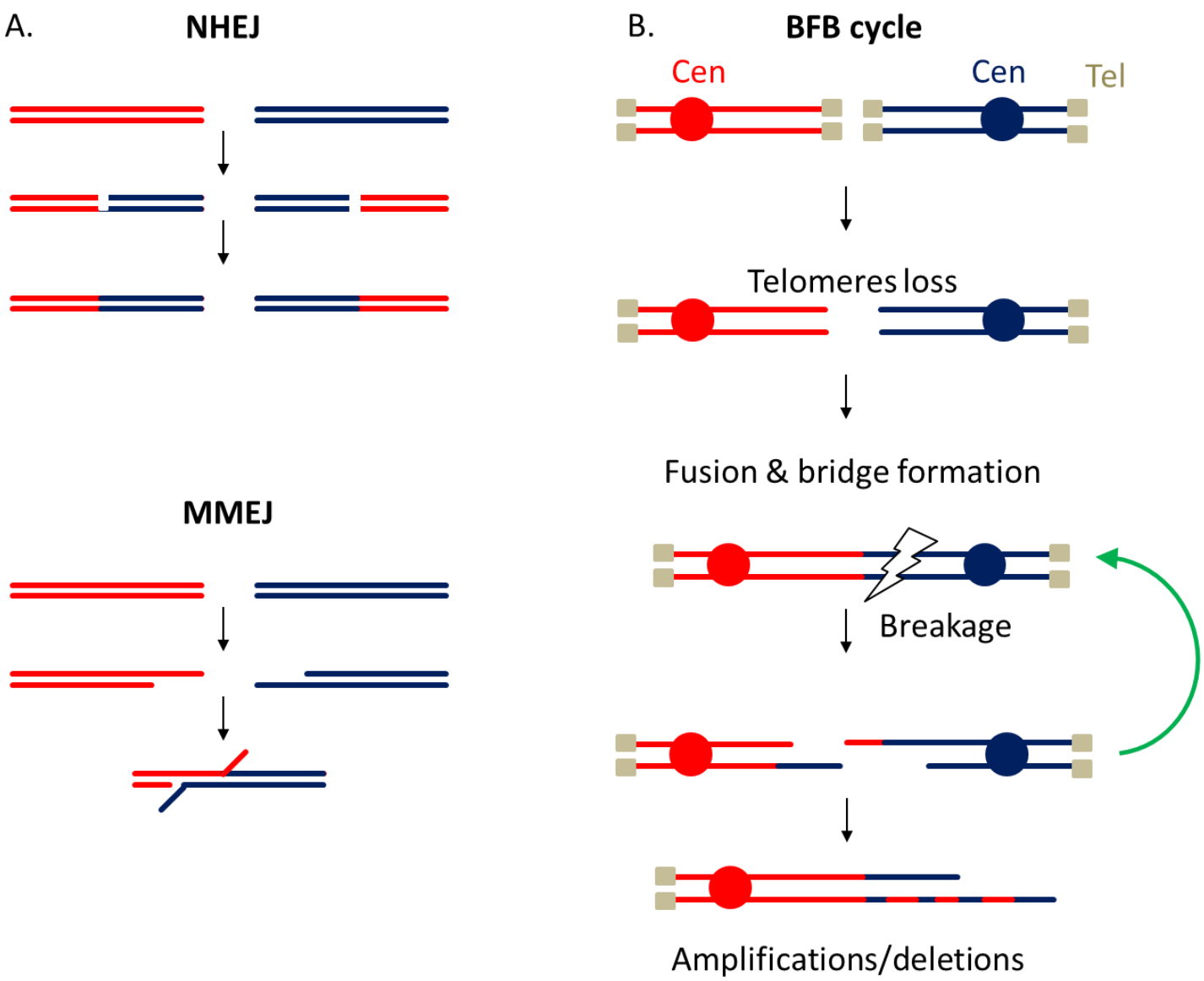
A.
NHEJ
MMEJ
B.
BFB cycle
Cen
Cen
Tel
Telomeres loss
Fusion & bridge formation
Breakage
Amplifications/deletions

Replicative non-homologous repair

1.3.2.3 Replication slippage or template switching

Replication slippage occurs during DNA replication along short repetitive (direct repeat) sequences (Figure 1-8A) [18, 100]. A slippage event is often found at the site of replication, for instance, at Okazaki fragments where a single strand is exposed in the lagging-strand template. During the replication process, the replisome can encounter a direct repeat which is prone to form a secondary structure (like a hairpin configuration) in the template. This structure might lead to the temporary arrest of the replication fork. The newly-synthesised strand can detach from the template and pair with another adjacent repeat in the same template strand. After replication resumption, it produces a deletion of DNA repeat sequence. In some cases, the newly-synthesised strand backtracks and duplicates the region that was previously replicated, leading to incorporate an insertion.

1.3.2.4 Fork stalling and template switching (FoSTeS)

When replication forks encounter the regions or areas that are difficult to replicate (e.g. low-copy repeats or a nick), forks are prone to be arrested and lead to a switch to another fork to bypass the DNA lesion or to resume replication. In the FoSTeS model (Figure 1-8B) [101], once replication fork stalls the newly-synthesised 3' end switches to another active replication fork as a new template via microhomology (4–15bp). Due to the process of great complexity, FoSTeS pathway has been recently proposed to explain the complex genomic rearrangements [101].

Figure 1-8. Mechanisms of replication slippage, fork stalling and template switching (FoSTeS) and microhomology-mediated BIR (MMBIR).

(*A*) Replication slippage. Each line shows a single nucleotide chain: the DNA molecule in leading-strand replication are shown as red lines; lagging-strand replication as blue lines. Lagging-strand template exposes a length of a single strand during replication. The 3' primer end of newly-synthesised DNA strand can "jump" to another sequence which shows a short length of homology on the exposed template. This move might occur if formation of secondary structures such as a loop formation in the lagging-strand template results in the failure of replication of this part of the template. As shown, this event produces a deletion. (*B*) FoSTeS. Each line represents a single DNA strand. Three different sequence regions are shown in blue, red and green blocks. When block in the progress of the replication fork occurs, the 3' primer end may detach from its template, and might then misalign on a single-stranded template sequence on another active replication fork that shares microhomology. As shown here, it will produce a deletion of the sequence between the two replication forks. (*C*) MMBIR. Each line represents a single DNA strand. When a replication fork collapses, the 5' end of the broken molecule will be resected from the break, exposing a 3' overhanging tail (red). When RecA or Rad51 recruitment that would allow invasion of homologous duplex fails, the 3' overhanging end can anneal to any exposed ssDNA of another template (blue) with which shares microhomology with it. The broken end extends (blue dotted arrow), followed by separation of the template again resulting in a 3' tail. It can anneal to another single-stranded microhomology sequence. In the example shown in the figure it anneals back to the original (red) molecule that can continue to the end of the chromosome. The resulting molecule contains short sequences from other genomic locations.

A. **Replication slippage**

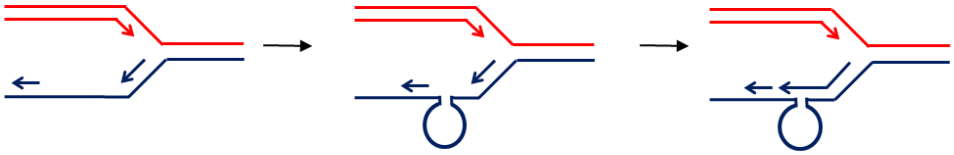

B. **FoSTeS**

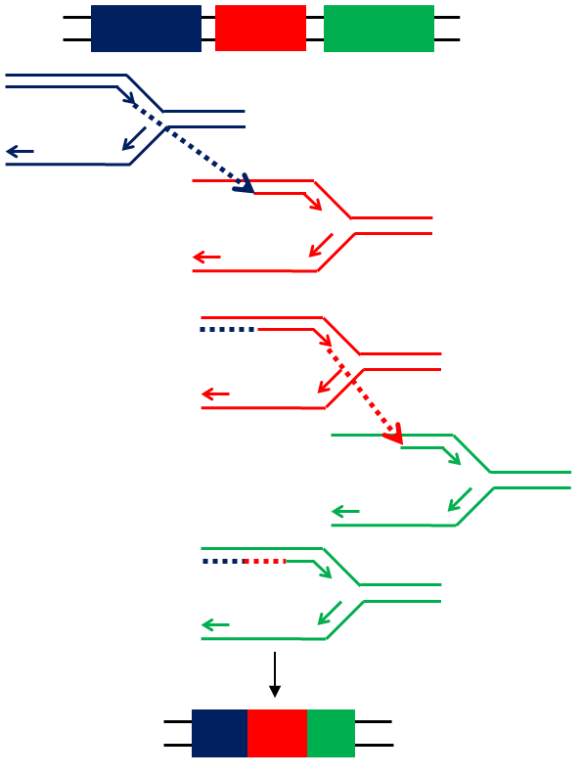

C. **MMBIR**

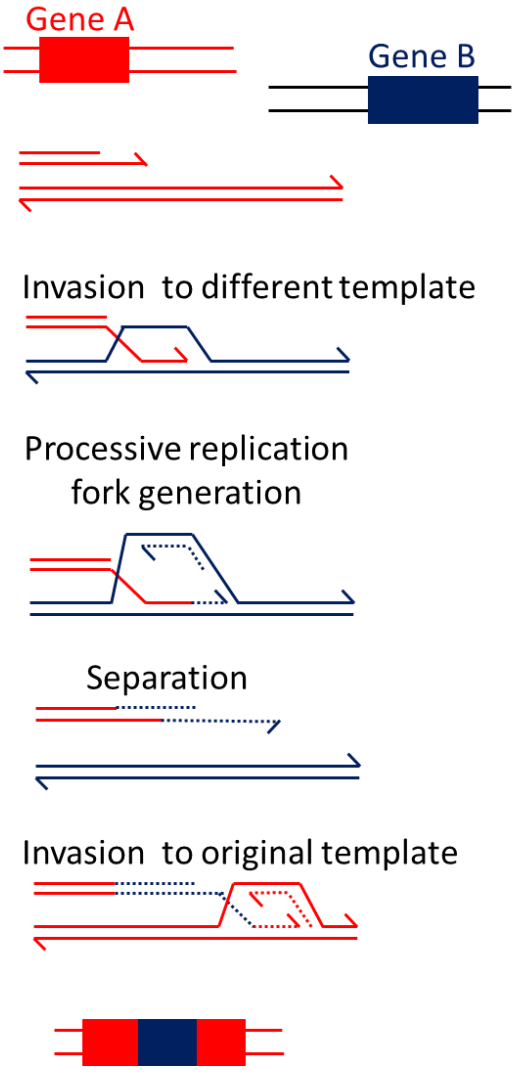

1.3.2.5 Microhomology-mediated BIR (MMBIR)

MMBIR is based on the modification of BIR mechanism for one-end double stranded break repair (Figure 1-8C) [15, 101]. The distinctions between them is that BIR is RecA/Rad51-dependent because it includes an invading 3' end into a homologous repair partner. Thus, BIR is known to be limited when RecA/Rad51 is down regulated. By contrast, the annealing event of the MMBIR model requires only microhomology sequence to complete DNA repair and thus is a RecA/Rad51-independent pathway. MMBIR is regarded as a substitute pathway instead of BIR when RecA/Rad51 is insufficient.

1.3.3 Genetic instability due to unscheduled DNA repair mechanisms via non-allelic homologous recombination

The mechanisms of DNA repair via homologous recombination can use similar or identical sequences to repair damaged sequence. If a damaged region is repaired using homologous sequence in the same chromosomal position of the sister chromatid or the homologous chromosome, the repair is error-free without any changes in DNA structure. However, in some occasions, the improper repair might utilize homologous sequences in different genomic/non-allelic positions. The process is termed non-allelic homologous recombination (NAHR) (Figure 1-9) [15]. NAHR is a form of homologous recombination that occurs between two non-allelic homologous sequences. NAHR mostly occurs within low copy number repeats (LCR) where sequences bear >95% identity homologous elements through the human genome. These events are responsible for a wide range of disorders. Misalignment of LCRs during NAHR is an important mechanism underlying CRs. NAHR is responsible for translocations, deletions, inversions and loss of heterozygosity (LOH). NAHR causes crossing over in a recombination repair event using a direct ectopic repeat on the same

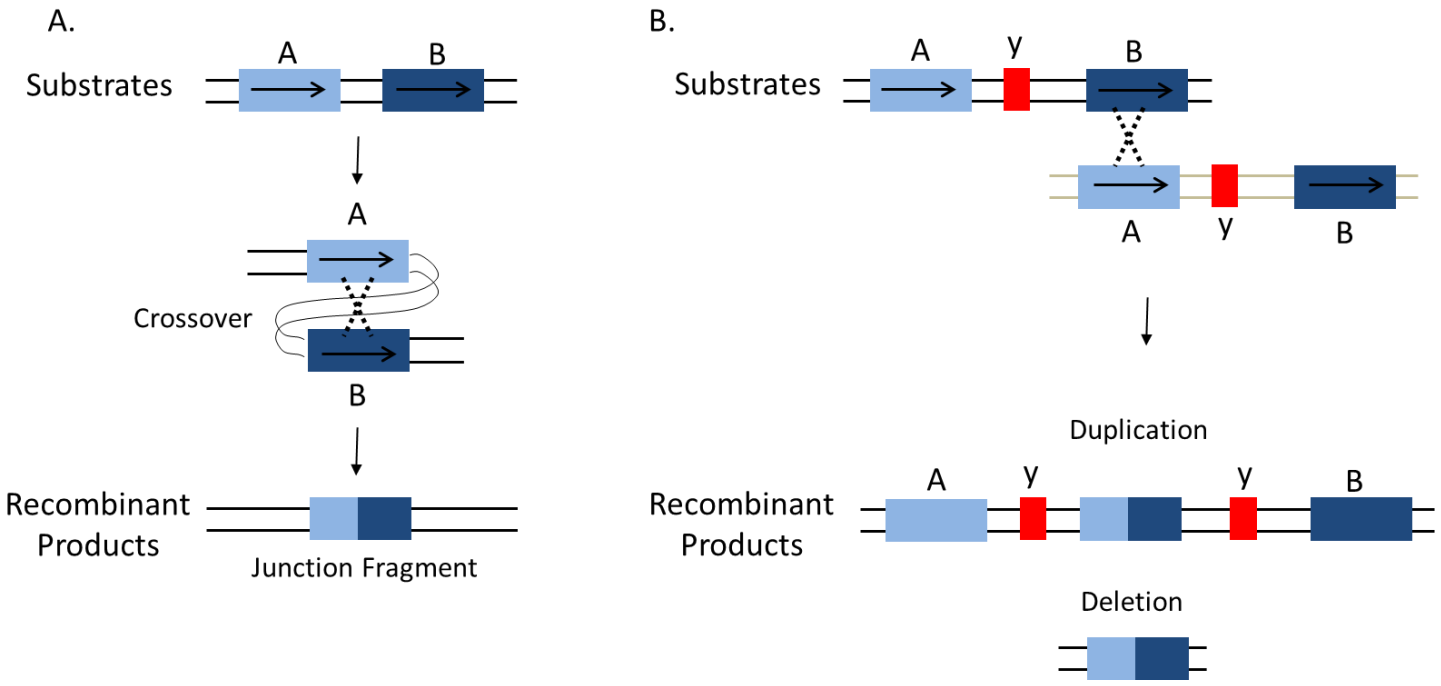

Figure 1-9. Generation of either duplication or deletion rearrangement by NAHR.

Each line represents a single DNA strand. The substrates and products of recombination are shown. NAHR can utilize two non-allelic homologous sequences (block A and B) as substrates for recombination on the same (*A*) or sister, homologous chromosome (*B*). (*A*) The high homology region are depicted as blue rectangles with different shades of blue, Block A and B misalign in direct orientation (shown by arrows), and subsequently cross over. The end result with the deletion of the sequence between the two blocks is shown as a two-tone blue junction fragment. (*B*) NAHR can also occur by unequal crossing over if a recombination event uses a direct repeat as homology on sister, homologous chromosome (or occurs between two lengths of DNA that have high homology sequence, but are not allele). A crossover outcome leads to products that are reciprocally duplicated and deleted for the sequence between the repeats (y, red block).

chromosomal template (Figure 1-9A). It can lead to reciprocally duplicated or deleted genes within these repeats (Figure 1-9B). A crossing over between different chromatids carrying the same alleles can result in heterozygosity from extensive translocations. Altogether, when non-allelic homologous recombination occurs between different highly similar sequences during meiosis, this event might give rise to genetic disorders since it causes the loss or increase of the genetic martial. In mitotic (somatic) cells NAHR can cause rearrangements of various types which are common in cancer. Thereby, while homologous recombination is a vital basis of DNA repair mechanisms, it is also regarded as hazardous when unscheduled DNA repair mechanisms are executed by NAHR.

1.3.4 Other cellular responses in the maintenance of genome integrity

Chromosomal structural changes can be induced by an incorrect choice of homologue partner leading to rearrangements. Cells prevent such changes by avoiding the faulty recombination events through several different regulatory pathways. First, at the chromosomal level, cohesins play a vital role for the accurate reparation of DNA. Cohesin is a protein complex that holds sister or homologous chromatids together and regulates their separation during mitosis or meiosis, respectively [102]. Cohesin is cleaved at the time of anaphase onset (in mitosis) and meiosis II (in meiosis) and is then dissociated from the chromatids. While the cohesins still bind the two chromatids together, they are, nevertheless, assembled at DSBs keeping the two ends of a single DSB together. This facilitates the accurate damage reparation using a sister/homologue chromatid as the preferred partner. Cohesin also provides a physical structural barrier to restrict the opportunity for the utilization of either the intrachromosomal or interchromosomal templates through NAHR, which are susceptible to genetic instability.

Secondly, at the DNA level, there is another reparation pathway to avoid DNA mismatch pairing: DNA mismatch repair (MMR), which can be a barrier to homologous recombination (i.e. recombination between nearly identical sequences) [103-105]. MMR excises the wrongly incorporated or damaged (e.g. miss-incorporation of bases, erroneous insertion, and deletion) and replaces them with the correct nucleotide during DNA replication and recombination, as well as repairs some forms of DNA damaged bases (e.g. removal of UV induced damaged bases-thymine dimers are repaired by NER). The removal process involves a few or up to thousands of base pairs of the newly-synthesised DNA strand. Such reparation reduces the chance of arrested forks, thus reduces the likelihood of an incorrect restart.

1.3.4.2 Checkpoint activation in response to DNA damage and replication stress

In order to maintain the integrity of the genome, cells also utilize surveillance and checkpoint signalling pathways to react to the replication perturbations (e.g. ssDNA or DSBs) [70-72]. The replication checkpoints are the prime defence barriers against replication fork instability. The procession of checkpoint signalling pathways aid the pausing of replication forks temporarily and ensures that the DNA replication resumes/restarts at the normal level. The replication checkpoints are activated through intertwined networks of sensors, mediators and effector to detect, transmit and amplify the damage or replication stress signal. The DNA damage is detected by the checkpoint sensors, following activation of the mediators and phosphorylation of effector kinases. The effector kinases transmit the signals to their downstream target proteins leading to cellular responses (e.g. cell cycle arrest, apoptosis, inhibition of origin firing, stabilisation of replisome associated with DNA and regulation of DNA

repair). There are two key checkpoint sensors to initiate the intra-S phase checkpoint [106]: Ataxia telangiectasia mutated protein (ATM) [74-75], and Ataxia telangiectasia and Rad3-related protein (ATR) [74, 76-77] (Table 3). They are implicated to play a role in different disturbed replication situations. The ATM pathway responds mainly when a replication fork encounters a DSB. Whilst ATR pathway detects stalled RFs where exposed ssDNA regions, the progression of ATR pathway can inhibit fork reversal. For the ATM pathway, the MRN mediator complex, composed of Mre11, Rad50 and Nbs1, are recruited at the DSBs. These recruited proteins can activate ATM and this is thought to arrest the fork before the DSBs, thus preventing further progression of recombination structure generation. In contrast, ATR pathway is activated by the exposed ssDNA regions when the replisome dissociates from the DNA. Once ssDNA–RPA is formed at the collapsed replication forks, two checkpoint mediator proteins requites: ATR-interacting protein (ATRIP) and checkpoint clamp loader Rad17. Rad17 loads the proliferating cell nuclear antigen (PCNA)-like checkpoint clamp Rad9–Rad1–Hus1 (9-1-1complex) [78]. The 9-1-1 complex is then further phosphorylated by ATR and amplifies signals for checkpoint activation. Following ATM and ATR activation, they then trigger the recruitment and activation of mediator proteins to the site of the DNA damage through the phosphorylation of the effector checkpoint kinases Chk2 and Chk1. Finally, the activation of the effector kinases promotes the checkpoint response through the phosphorylation of targets protein for different, specific processes (including cell cycle arrest, DNA repair procession, and etc.). When checkpoint pathways do not act properly, aberrant structures, such as collapsed and regressed forks will be accumulated. These intermediates are likely substrates for the chromosomal rearrangements by the inappropriate or unscheduled DNA reparation.

Table 3. Checkpoint activation in response to replication perturbation.

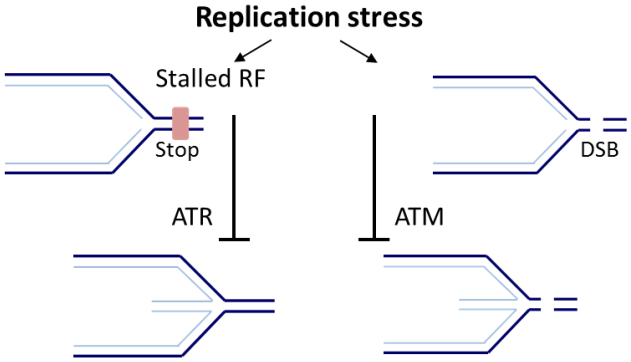

	Humans		*S. pombe*		*S. cerevisiae*	
Sensor	ATR-ATRIP 9-1-1	ATM-MRN	Rad3-Rad26 9-1-1	Tel1-MRN	Mec1-Ddc2 Rad17–Mec3–Ddc1	Tel1-MRX
Mediator	TopBP1		Rad4		Dpb11	
	Claspin		Mrc1	Crb2	Mrc1	Rad9
Effector	Chk1	Chk2	Cds1	Chk1	Rad53	Chk1

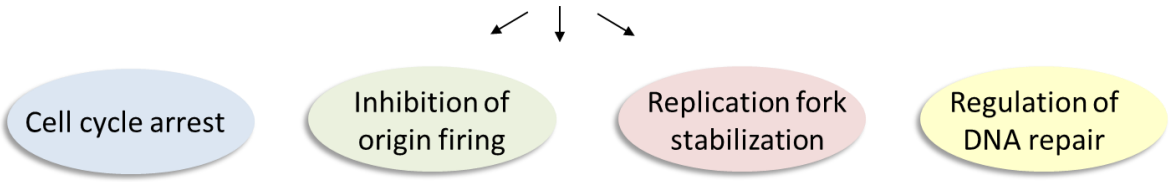

An overview of checkpoint signalling. During replication stress, damage is recognized by the checkpoint sensors and through activation of mediators transmit the signal to effector kinases by phosphorylation events, eventually generate full checkpoint response. The main factors involved in the DNA damage and replication checkpoints in humans, *S. pombe* and *S. cerevisiae* are shown.

1.4 Replication fork barriers (RFB)

The replication fork barriers are obstacles to the movement of replication forks and have been known to cause chromosomal rearrangements observed in model organisms. In human cells and yeasts, chromosomal fragile sites are commonly implicated in natural RFBs mechanisms. Fragile sites are often viewed as loci which are naturally difficult to replicate. These specific chromosomal regions are likely to pause the normal process of chromosome replication and become sensitive to breakage, leading to potential genetic rearrangements under replication stress [11, 32-34]. Furthermore, Szilard *et al.* (2010) exploited yeast histone H2A. Indeed, the presence of the phosphorylated form of H2A (γ-H2A) - is a well-known DNA damage marker. Distribution of phosphorylated γ-H2A was enriched specifically at the natural RFBs in unstressed wild-type yeast cells [114]. Consequently, according to the available evidence of replication inhibition at impediments, RFBs have been more and more discussed in connection with genome stability. The main known RFBs can be classified into three groups: exogenous, genetic, and intrinsic. Exogenous RFBs interfere with DNA replication by either damaging the DNA template (e.g., UV light, gamma irradiation) or depleting the deoxynucleoside triphosphate (dNTP) pools for DNA synthesis (e.g. hydroxyurea) [28, 31].

Chemically induced RFBs often cause damage to the DNA bases, which can occur randomly throughout the genome blocking the replication fork in passing through the impediment on the template. The lack of all or some of the dNTPs slows down the speed of DNA replication and inhibits the replication progression. Genetic RFBs are usually driven by mutations in genes that involve the accuracy of DNA replication and the speed of DNA synthesis (for instance, mutations in the components of the

replisome apparatus and mutations of ribonucleotide diphosphate reductase, or better known as the rate limiting enzyme in dNTP synthesis). The final category is the intrinsic RFBs (iRFBs), which are usually associated with specific chromosomal features. Intrinsic RFBs include: non-histone DNA-protein binding complexes (e.g., centromeres and dormant origins), which are special loci tightly bound by non-histone proteins with an influence over the fork progression; transcriptional units (e.g., tRNA genes and ribosomal DNA), which are often involved in replication–transcription clashes; DNA sequences that are susceptible to form non-canonical structures and a range of novel poor-characterized regions (e.g. some fragile sites can form DNA secondary structures and replication slow zones that are prone to rearrangement while perturbing fork progression) [28, 60]. Hence, the cause of replication impediments can be either designed or accidental. Different forms of RFBs arrest replication forks in distinct ways. RFBs are thus themselves highly variable.

In prokaryotes, RFBs can regulate normal replication termination. The position of directional replication termination site in *E. coli* genome is called "Ter" site. Ter sequence is bound by the Tus protein to curb replicative helicase activity, forming a polar stalled fork [60]. When replication is initiated from a single origin, *oriC*, replication forks travel each half of the circular chromosome in a bidirectional manner and terminate at the Ter sequence. This avoids the genetic instability caused by replication forks clashing with transcription. However, a study revealed that Ter sites in *E. coli* plasmids were deletion hotspots, suggesting that genomic instability could be caused by protein mediated replication arrest. The study also showed that Ter sites were hotspots for homologous recombination repair behind the collapsed replication forks that eventually lead to deletions. The Ter site appears not only to regulate normal DNA replication termination but also to generate aberrant recombination

products once it is positioned elsewhere in the genome. In eukaryotes, stalled forks promote the activity of DNA helicases or specific DNA repair proteins that remove the obstacle from the site of incorporation, allowing replication to resume.

Experiments in eukaryotic cells also indicate that arrested forks are prone to inappropriate recombination [28, 58 and 115]. In order to ensure the accurate completion of replication and to maintain genomic stability, cells have developed over time multilevel control mechanisms to respond to the different types of arrests. Generally, obstacles to replication fork progression destabilise the replisome, block replicative helicases and disturb polymerase fidelity. Cells protect themselves from the consequences of RFBs using several general strategies. First, expression of RFB activity can be prevented, for example, by repairing DNA damage or removing DNA-protein interactions using specialized helicases. If RFBs are present, activation of the intra-S phase checkpoint will attempt to maintain the replisome in a 'stalled' fork conformation. Sometimes, in the case of replisome failure (a collapsed fork), the fork DNA will be protected to allow rebuilding of the replisome to restart DNA replication.

1.4.1 Chromosomal rearrangements caused by inverted fusions in fission yeast

To understand how DNA replication stress contributes to chromosome rearrangements, the Rtf1-RTS1 fork-stalling system was developed in our laboratory using the fission yeast, *Schizosaccharomyces pombe*, as an experimental model (see Figure 1-10A and description below). *RTS1* sequence is a natural polar RFB near the mat locus in *S. pombe*. During mating type switching in *S. pombe*, *RTS1* sequence can block forks from the centromere side of the mat locus DNA replication [56]. By

exploiting the replication termination sequence (*RTS1*) established on the chromosome III of *S. pombe* genome (Figure 1-10B), a replication fork can be arrested under a controllable manner, efficiently leading to chromosome rearrangements [19, 49-50, 55-60].

1.4.2 *Schizosaccharomyces pombe* characteristics

The fission yeast *Schizosaccharomyces pombe* provides an excellent model system for studying genetic alterations [107-109]. *S. pombe* is a rod-shaped yeast that grows by elongation and divides by medial fission. They measure approximately 3 to 4 micrometres in diameter and 7 to 14 micrometres in length. *S. pombe* contains its genome distributed in three chromosomes, ranging in size from 3.5 to 5.7 megabases. *S. pombe* is distantly related to the budding yeast *Saccharomyces cerevisiae*. Evolutionarily, these two yeasts are as diverged from each other as from mammals. *S. pombe* cells presented the vegetative growth as haploids and can also be grown as diploids as a transient stage during sexual differentiation. The mitotic division cycle occurs quite rapidly with a generation time around 2 to 4 hours. The mitotic cell cycle of *S. pombe* cells is characterised by its predominant G_2 phase, followed by M (Mitosis), G_1 and S (DNA replication), where the G_1 phase is very short in duration. Under nutritional starvation, *S. pombe* cells will arrest mitosis in the G1 phase. Two haploid cells from different mating types then conjugate to form a transient diploid, or zygote followed by the production of four spores (tetrad) packaged into an ascus through the meiotic cycle. The ability to undergo sexual differentiation which allows *S. pombe* cells to exchange, or recombine genetic information, makes fission yeast a useful genetic model system.

1.4.3 The Rtf1-RTS1 fork-stalling system

The Rtf1-RTS1 fork-stalling system has been established *in vivo* and provides an opportunity to understand the link between the replication fork blockage and chromosomal rearrangements (Figure 1-10A) [19]. *RTS1* sequences are a form of programmed RFBs that have evolved for specific purposes. In nature, programmed RFBs are generally direction-dependent and facilitate a polar arrest of fork coming from one direction and allow unblocked passage of forks coming from the opposite direction [28, 57-58]. The Rtf1-RTS1 fork-stalling system is based on a ~850bp replication termination sequence (*RTS1*) that is required as a polar replication fork barrier near the *mat* locus and blocks fork coming from the centromere side during *S. pombe* mating type switching [56]. Genetic screens identified that *RTS1* sequences associate with several proteins to pause the replication fork progression; Four genes have been shown to interact with the *RTS1* sequences, *swi1*, *swi3*, *rtf1*, and *rtf2* [59, 116]. *Swi1* and *swi3* are components of the replisome and activate the S-phase checkpoint pathway for the stabilisation of stalled forks. Rtf1, a Myb-like DNA binding protein and Rtf2, a PCNA interacting protein are transcription termination factors that interfere with the replicative helicase. Two distinct cell-types (h^+ or h^-) express distinct sexual markers in fission yeast. Mating type switching from one sexual type to another occurs near the mating type locus, *mat1*. An imprint at the *mat1* locus of *S. pombe* initiates the replication-coupled recombination mechanism required for the mating-type switching. The formation of the imprint involves a lagging-strand-induced replication pause at *mat1* and depends on unidirectional fork progression ensured by the RTS system. This imprint is maintained until the next cell cycle when the leading-strand replication complex is arrested at the imprint. The resolution of the stalled fork in the leading-strand requires HR-based process which

allows the recombination between *mat1* and one of the silent donor cassettes *mat2P* or *mat3M*, leading to the mating-type switching [56].

We have used the natural properties of *RTS1* sequences as a barrier that blocks replication fork movement in one direction for the development of the Rtf1-RTS1 fork-stalling system. As described above at programmed RFBs, a polar fork arrest is caused by Rtf1, a non-histone protein, binding to the RTS1 sequence. In our laboratory, a series of fork-arrest-induced assays have been established, here, our discussion focuses mainly on the inverted repeat (*RuraR*) and the palindrome (*RuiuR*) system [49, 50]. In the inverted repeat *RuraR* assay, an *ura4* marker is introduced flanked by two inverted *RTS1* sequences (Figure 1-10B). Palindromes are a type of inverted repeat sequences separated by a few base pairs. Palindrome *RuiuR* assay contains two *ura4*$^+$ marker genes in inverted orientation with a 14bp DNA sequence spacer between them and flanked by *RTS1* inverted repeats (Figure 1-10B). Both constructs have been established separately on chromosome III of *S. pombe* and was confirmed to generate acentric and dicentric chromosomes by chromosomal rearrangements. By controlling the expression of the *rtf1*$^+$ gene, the progressing forks can be artificially inhibited by Rtf1 binding to the RTS1 sequences. To regulate the expression of *rtf1*$^+$ genes, an inducible thiamine-repressible promoter *nmt41* was introduced to replace the *rtf1*$^+$ gene promoter. The expression of Rtf1 protein is detected after 12 hours of thiamine removal and reaches a peak at around 16 hours. Fork arrest within either *RuraR* or *RuiuR* was predicted. Indeed, when *rtf1*$^+$ was expressed, more than 94% of the forks stopped at the outer part of each RTS1 barriers of *RuraR* or *RuiuR* assays and the recovery of the arrested forks were mediated by a DSB-independent mechanism and involved the recruitment of repair proteins at the RTS1 site (see details below). Subsequent fork-arrest based rearrangement events

occurred at high frequencies (~15–25%), allowing further molecular analysis. This Rtf1-RTS1 fork-stalling system also provided a direct evidence that fork failure leads to genome rearrangements.

Figure 1-10. (*A*) Schematics of the Rtf1-RTS1 fork-stalling system. A replication fork is stalled initially by the *RTS1* sequence bound by the inducible Rtf1 protein, which leads to fork collapse. Restart of the fork can lead to chromosomal rearrangements and generate acentric and dicentric chromosomes. *RTS1* sequence is shown as the blue square; white triangle indicates the orientation for replication fork stalling. (*B*) Inverted repeat (*RuraR*) and palindrome (*RuiuR*) assay. We used the Rtf1-RTS1 fork-stalling system to initiate recombination events. *RuraR* and *RuiuR* assays are based on development of the Rtf1-RTS1 fork-stalling system established on ChrIII in *Schizosaccharomyces pombe*. *RuraR* assay is one single *ura4* gene flanked by *RTS1* inverted repeats, while *RuiuR* assay contains two *ura4* genes in inverted orientation with 14bp DNA sequence spacer flanked by *RTS1* inverted repeats. Blue squares *RTS1* sequence; white triangle indicates the orientation for stalling a replication fork and the orientation of *ura4* gene. (*C*) Spot test to check cell viability. Cells suffer viability loss and miss-segregation due to *RuraR* and *RuiuR* construct established on the essential chromosome III of *S. pombe*. Cells containing *RuraR* and *RuiuR* assay on ChrIII lost viability after replication fork arrest ("pause on" growth). Cells that underwent miss-segregation in mitosis showed the presence of lagging chromosomes visualised by DAPI and Calcofluor stain.

A. The Rtf1-RTS1 fork-stalling system

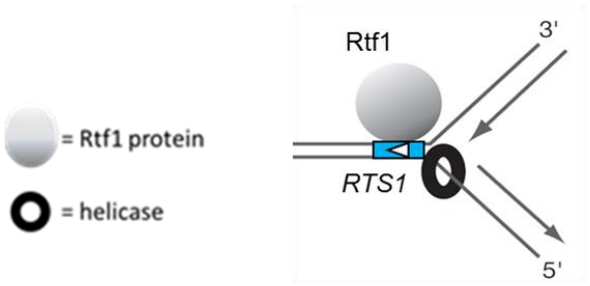

B. Previous model : chromosome III of *S. pombe*

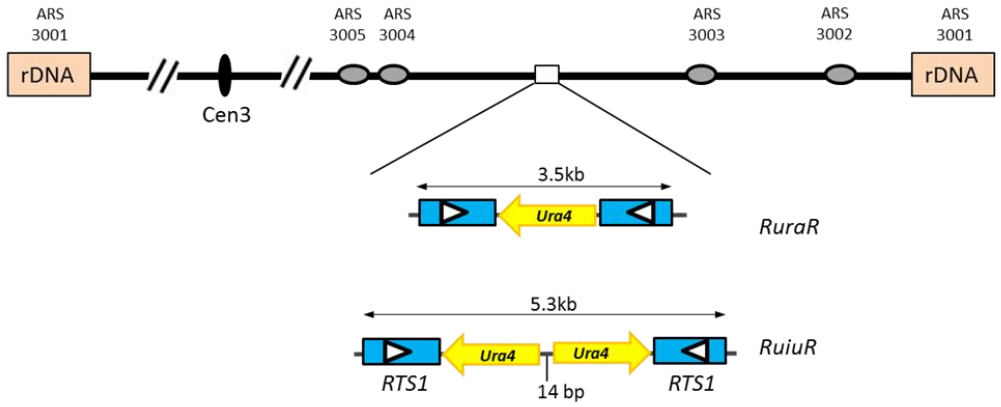

C.

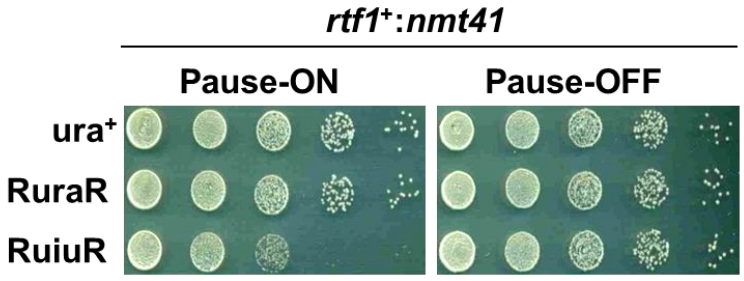

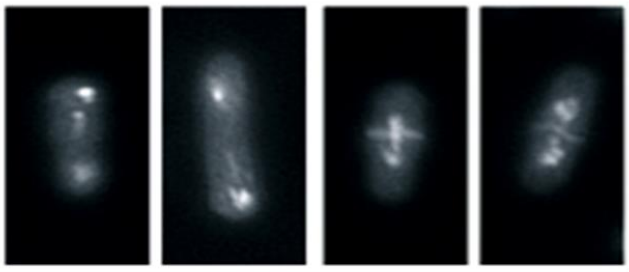

DAPI for DNA-staining; Calcofluor for staining septum

	% aberrant in mitosis
Pause-ON	18
Pause-OFF	0

Mizuno et al.

1.4.4 Observations on chromosomal rearrangements from our previous model on chromosome III

To investigate recombination events and the mechanisms of acentric and dicentric chromosomes formation, we exploited the inverted repeat (*RuraR*) and palindrome (*RuiuR*) assay (Figure 1-10B). Previous findings have determined that HR plays a major role in the restart of collapsed forks. *Rad22*^{RAD52} mutants fail to survive upon the *rtf1*$^{+}$ expression, indicating that Rad22 ^{RAD52} needs to be recruited to the RTS1 barrier and that HR is required to rescue replication perturbation for cell survival [19]. Moreover, the observation that recombination proteins Rhp51^{Rad51} and Rad22^{Rad52} foci accumulated at the *RTS1* sites in *RuraR*-induced fork stalling further supports the association between HR and genome instability. With intact HR system, more cells remained viable. It suggests that arrested forks were efficiently rescued by the recruitment of recombination proteins behind the site of fork collapse. However, some cells that generated chromosomal rearrangement products were invaluable. These products can be studied by molecular analysis. Hence, exploiting yeast synthetic constructs allowed us to identify two HR protein-dependent restart mechanisms via template exchange, resulting in chromosomal rearrangement events. One is the non-allelic homologous recombination (NAHR) model (Figure 1-12) and the other is the HR-dependent U-turn model (Figure 1-13) [49, 50]. More detailed explanations for these two models are presented below.

1.4.4.1 Non-allelic homologous recombination (NAHR) model

HR-dependent replication template exchange model has been revealed originally from the *RuraR* assay (Figure 1-10B, *RuraR*) [19, 49]. The fork was confirmed to arrest at *RuraR* loci, which led directly to chromosomal rearrangements. After the fork is collapsed nearby a *cen*-proximal RTS1 locus, a nascent strand 3’ end is coated by

Rhp51^{Rad51} forming a nucleofilament. This strand attempted to exchange template by annealing to homologous *RTS1* repeats (Figure 1-12, i-v). This inappropriate template exchange lead to the formation of a D loop intermediate followed by the partial completion of the *RuraR* locus replication. Arrival of the second replication fork to the RTS1 barrier, from the *tel*-proximal side, led to a second faulty template exchange. This exchange then enabled the complete replication of the DNA and resulted in the formation of a transient HJ intermediate between RTS1 inverted repeats. Finally, the resolution of HJ intermediate could generate acentric and dicentric chromosomes (Figure 1-12, vi-vii). With native two-dimensional gel electrophoresis analysis (2-D gels), two additional signals were detected; one was 8–10 kb migrated to the apex of the Y arc and the other was around 10 kb migrated to the X spike. These X structures suggested HJs-like structures containing a fully replicated *RuraR* locus were a result of the physical exchanges between the close RTS1 repeats. Both signals were absent in the *rad22* deletion cells, suggesting that they are recombination intermediates produced during the replication fork restart. These analyses provided a significant physical evidence for the replication template exchange between RTS1 repeats caused by fork arrest at a RTS1 site. Non-allelic homologous recombination (NAHR) is one pathway likely to be involved in fork arrest recovery.

Rhp51^{Rad51} forming a nucleofilament. This strand attempted to exchange template by annealing to homologous *RTS1* repeats (Figure 1-12, i-v). This inappropriate template exchange lead to the formation of a D loop intermediate followed by partial completion of the *RuraR* locus replication. Arrival of the second replication fork to the RTS1 barrier, from the *tel*-proximal side, lead to a second faulty template exchange. This exchange then enabled the complete replication of the DNA and resulted in the formation of a transient HJ intermediate between RTS1 inverted

repeats. Finally, resolution of HJ intermediate could generate acentric and dicentric chromosomes (Figure 1-12, vi-vii). By native two-dimensional gel electrophoresis analysis (2-D gels), two additional signals were detected; one was 8–10 kb and migrated at the apex of the Y arc and another was around 10 kb and migrated on the X spike. This X structures suggested HJs-like structures containing a fully replicated *RuraR* locus resulted from physical exchanges between the close RTS1 repeats. Both signals were absent in *rad22* deletion cells, showing that they are recombination intermediates produced during the replication fork restart. These analyses provided a significant physical evidence for the replication template exchange between RTS1 repeats caused by fork arrest at a RTS1 site. Non-allelic homologous recombination (NAHR) is one pathway likely to be involved in fork arrest recovery.

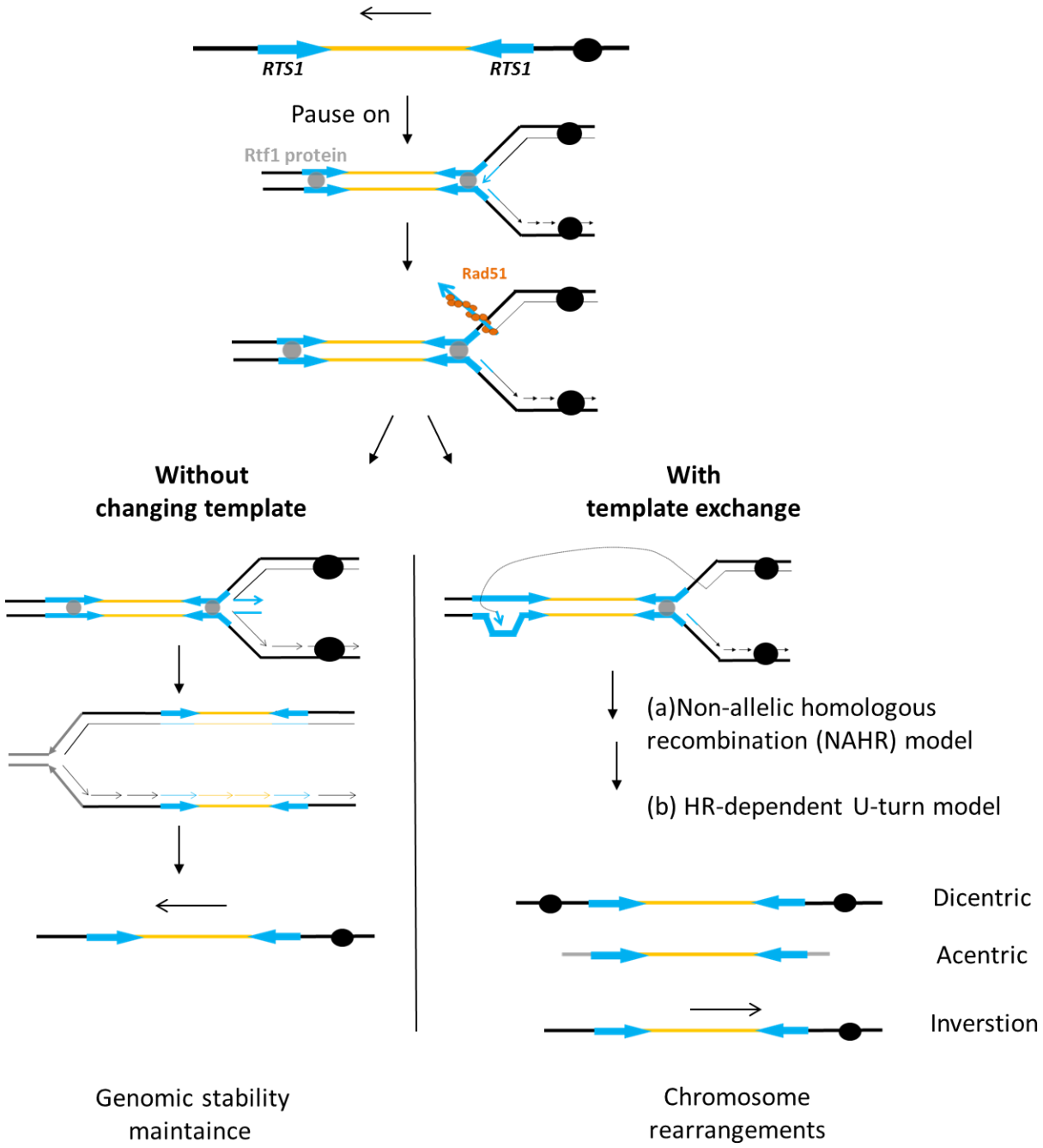

Figure 1-11. The model of inverted repeat (RuraR) and palindrome (RuiuR) assay generating acentric and dicentric chromosomes.

In RuraR or RuiuR assay (the direction of blue arrow is indicated the polarity of the *RTS1* barrier; yellow is *ura4* gene), replication fork pauses nearby *RTS1* to induce chromosomal rearrangements. The rearrangement promotes acentric and dicentric chromosome formation.

Figure 1-12. Non-allelic homologous recombination (NAHR) model.

When Rtf1 protein is expressed and bound to RTS1 sites, over 94% of the forks stop at the RTS barriers. Collapsed forks recruit homologous recombination (HR) proteins (such as Rad51) and generate single-stranded DNA behind the site of fork arrest. The forks undergo a faulty template switch and form transient Holliday Junctions (HJ)-like recombination intermediate structures. This faulty replication template exchange mechanism leads to acentric and dicentric chromosome formation.

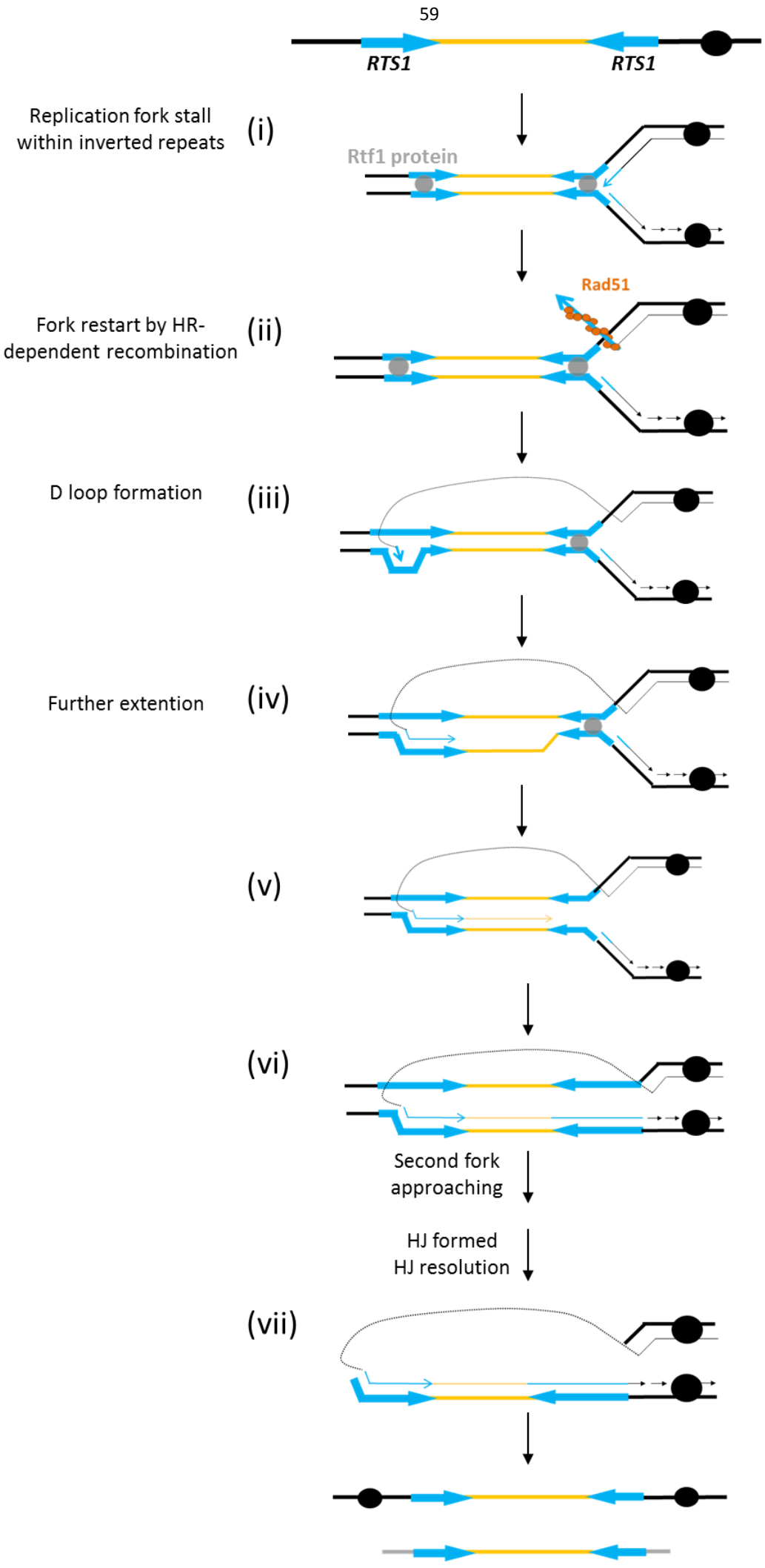
RTS1
RTS1
Replication fork stall within inverted repeats
(i)
Rtf1 protein
Rad51
Fork restart by HR-dependent recombination
(ii)
D loop formation
(iii)
Further extention
(iv)
(v)
(vi)
Second fork approaching
HJ formed
HJ resolution
(vii)

1.4.4.2 HR-dependent U-turn model

The U-turn model has been discovered from the *RuiuR* assay (Figure 1-10B, *RuiuR*) [50, 52]. Fork restart nearby *RuiuR* locus occurred at the expense of an extremely high frequency (~15–25%) of inappropriate recombination compared to the *RuraR* assay (~2%). Our results indicated that the fork resumed by a replication template exchange mechanism using the homologous inverted repeats of the RTS1 sequence. Remarkably, a more detailed analysis revealed that a single RTS1 sequence derivative is still capable of generating acentric and dicentric chromosomes after arrangements. Thereby, Mizuno et al. suggested that besides the replication template exchange mechanism, there was an alternative pathway, the U-turn mechanism. However, it is still uncertain as to how a coordinated restart fork is regulated by the U-turn formation. A model of the U-turn mechanism has been proposed where the fork restarts in the reversed orientation (U-turn) (Figure 1-13). The concept of the U-turn model is relatively simple; after regression, the fork travels to the nearby palindrome centre, the newly-synthesised strand from the leading strand becomes detached and generates a nascent 3'-end (Figure 1-13B, i). This single strand is proposed to be annealed to its complementary loci in the lagging strand to form a "closed" Y structure intermediate (Figure 1-13B, ii) [53]. Subsequently, the closed Y-structure-like intermediate ligates to the adjacent Okazaki fragment and completes the replication with the formation of a dicentric chromosome (Figure 1-13B, iii). Note that in this model, there is no requirement for DSBs formation.

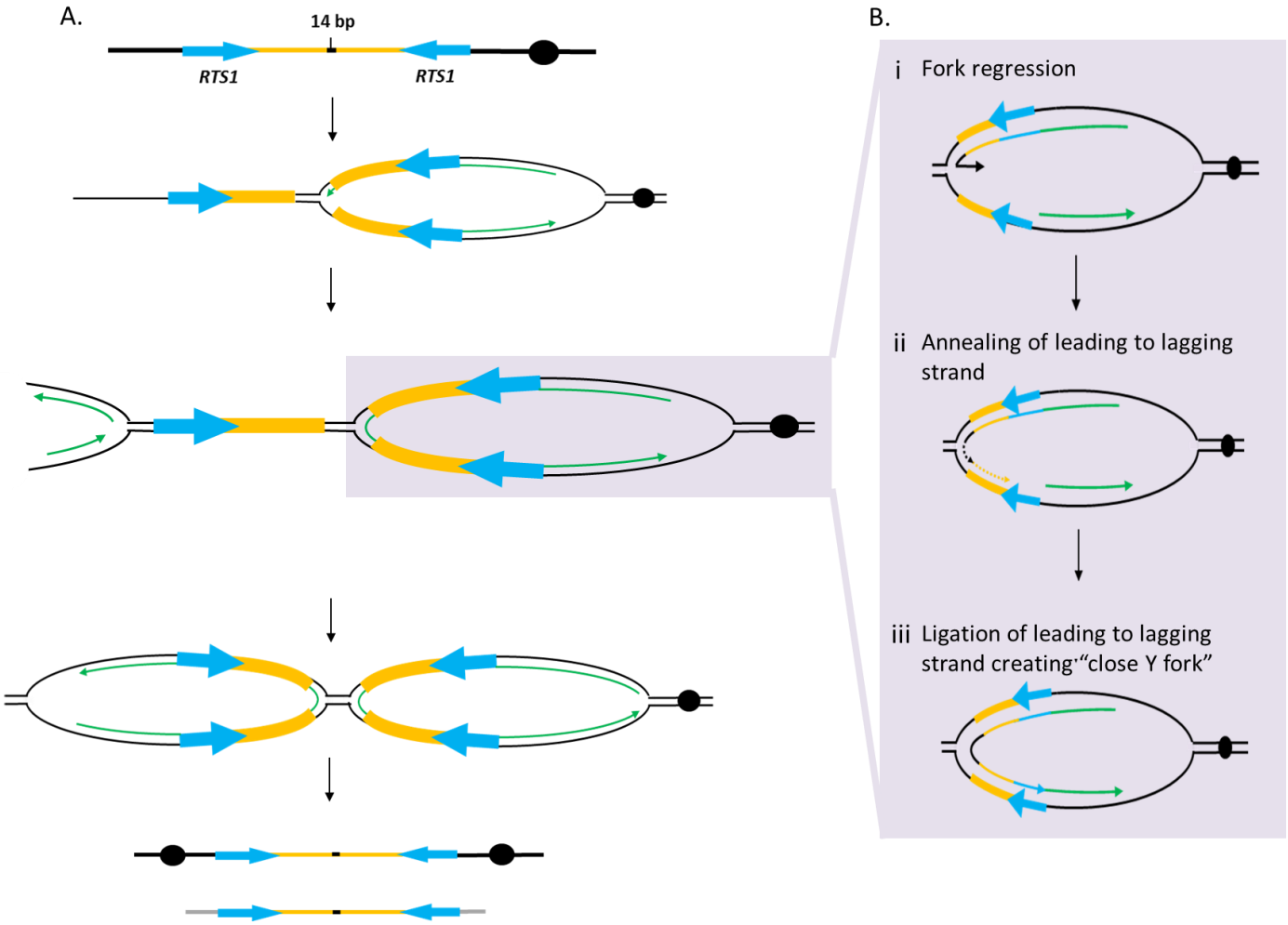

Figure 1-13. HR-dependent U-turn model.

(A) A U-turn model for RTS1- fork stalling. Failure of fork restart leads to a "closed" Y structure intermediate. Finally, the ectopic recombination events generate acentric and dicentric chromosomes. (B) Details of the mechanism that leads to a "closed" Y structure intermediate. During fork regression, the newly-synthesised strand from the leading strand becomes detached and generate a nascent 3'-end. This single-strand can anneals to the lagging strand template at a close homologous sequence to form a "closed" Y structure.

1.4.4.3 Fork arrest induces chromosomal rearrangements

To sum up the aforementioned studies, the *RuraR* and *RuiuR* assays have allowed us to identify chromosomal rearrangement initialized via two HR-dependent models, namely the NAHR and U-turn models. Interestingly, DSBs were not detected as intermediates, and these processes are distinct from fork stalling and template switching (FoSTeS), which is HR independent, and specially driven by microhomologous sequences. The HR proteins aid the pairing of the nascent strand to either a correct or faulty template during its invasion behind the collapsed fork. As a result of the faulty template exchange, high frequencies (15–25%) of acentric and dicentric chromosomes were observed in our fork-arrested systems. This result provides direct evidence supporting fork arrest leading to chromosome rearrangement events. Formation of these isochromosomes also indicates that forks restart is possible by using homologous sequence of the ectopic RTS1 on the same chromosome. However fork restart also occurs at a lower frequency using an RTS1 sequence on a different chromosome (Originally, RTS1 sequence is located nearby the *mat1* locus of chromosome II) [19]. This suggests that the strand dissociated from the collapsed fork can be annealed to any homologous sequence and is only regulated by the proximity of the two RTS1 sequences. Figure 1-14 shows a simplified illustration of these two models. Both models require HR-dependent template exchange using non-allelic homologous sequence at the expense of inappropriate chromosome rearrangements. Once HR proteins restart the fork with incorrect template, acentric and dicentric chromosome formation can cause the loss of cell viability [49].

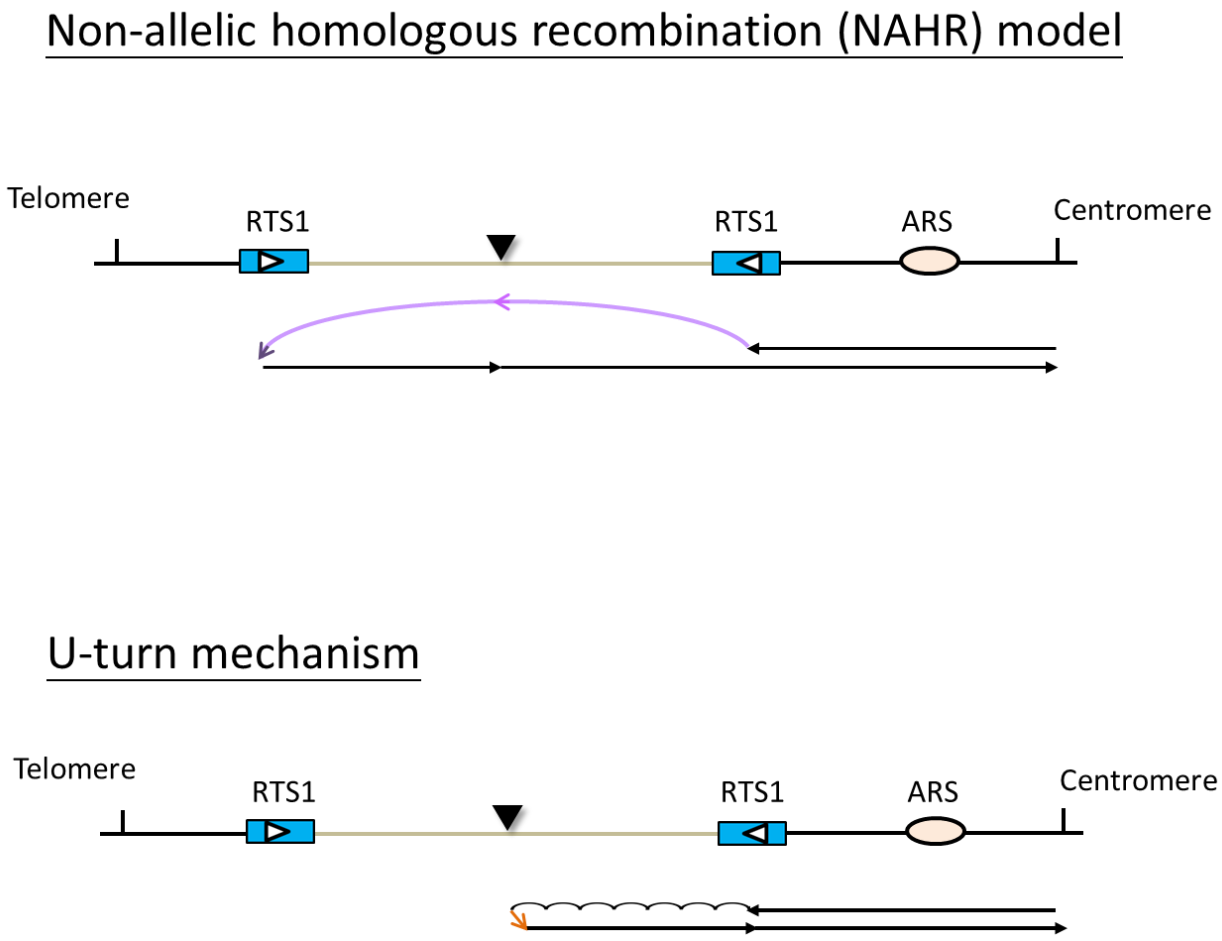

Figure 1-14. Two mechanisms involved in chromosomal rearrangements.

We determined that forks restart by homologous recombination behind collapsed sites. The recombination-replication mechanisms via non-allelic homologous recombination and U-turn models.

1.4.4.4 Checkpoint function on arrested replication fork

DNA damage checkpoints are not required for cell viability in response to these fork-arrest induced processes. Checkpoint-deficiency in cells (i.e. the absence of $Rad3^{ATR}$ or $Cds1^{Chk2}$) did not affect cell viability during fork stalling [49, 50]. Collapsed forks can form at RTS1 even in the presence of physiological checkpoint apparatus. *RTS1* sequence naturally exists nearby the *mat1* locus where it is important for mating-type switching. Thus, RTS1 barriers are programmed replication barriers, which have evolved for a specific purpose. Hence, the fork fate at RTS1 barrier, without checkpoint activation, might be independent of the normal fork stabilisation machinery. Generally, the replication checkpoint can protect stalled forks from replisome disassembling. In the presence of an intact checkpoint system, recombination foci ($Rhp51^{Rad51}$ and $Rad22^{Rad52}$) still appear rapidly at the *RTS1* locus [19], suggesting that replication forks are not stabilised when the forks are stalled and that the replisome disassembles rapidly. This is in contrary to the requirement of the replication checkpoint for cell viability in response to hydroxyurea (HU) treatment. HU is known to cause DNA damage during replication by the depletion of dNTPs, consequently leading to fork stalling. Recombination foci arising from HU induced replication forks disassemble only if the checkpoint is dysfunctional (which cause the replisome to dissociate from the site of nucleotide incorporation) [117]. Under HU treatment, approximately 300 bp of ssDNA is generated during the DNA repair processing (followed by RPA protein coating), which can efficiently activate ATR^{Rad3}-dependent checkpoints. It is still unclear as to why the checkpoint functions did not impact cell viability in our fork stalling system. This might be due to cells having different responses to different forms of RFB.

1.4.4.5 Recovery of arrested replication forks by error-prone homologous recombination

By using a fork-arrest based assay in fission yeast, we have demonstrated that the recovery of collapsed forks by homologous recombination was error-prone [50, 51]. When the fork encounters problems (in a leading-strand error), arrested replication fork can restart at a downstream site (~1,000 nucleotides), leaving a gap in the newly-synthesised daughter strand [20]. Usually, the gap is filled by error-free post replication pathway using the other newly replicated DNA daughter molecule as a template. Gaps can also be filled by an error-prone faulty template switch mechanism as described previously, stalled nascent strands may anneal to an incorrect template sequence on the lagging strand [18-19, 48-50]. Subsequently, the resolution of the intermediate by unknown endonucleases and repair synthesis that fuses to generate acentric and dicentric chromosomes [49]. Additionally, when the replisome has been rebuilt from the fork collapse, fork progression is restarted [13], nascent strands may undergo intra-template switching leading to error-prone repair via replication slippage. Intra-molecular template switching mechanisms occurring in the nascent strands were disassociated from the template and misalign with the template again between short tandem repeats (micro-homology). This causes a loop formation, either in the nascent strand or within the template, leading to small insertions/duplications or deletion events, separately. Another possible reason for the inaccuracy of restarting DNA synthesis is that one or more components of the replisome complex are missing during the restart event. This still, however, remains to be determined.

1.4.4.6 Recombination is required for cell viability

HR proteins are determined as required for cell viability and the formation of rearrangements. Genetic analyses of recombination functions experimentally

identified a major role for HR by using the *RuraR* or *RuiuR* induced fork stalling systems. Our results have revealed that HR mutants displayed slow growth and loss of viability, supported by the observation that genomic instability was increased in HR-defective cells (deletion of *rad52*, *rad51*, *rad59*, *rad52* and *rad1*) [49]. HR mutants generally fail to restart fork progression and thus are also unable to form acentric and dicentric chromosomes as rearrangements are generated by a template exchange during the restart event. This suggests that without HR, if two converging forks are arrested on the outer boundary of the *RTS1* repeats, cells cannot resume replication, and would die because of the incomplete genome duplication. In the presence of HR function, cells usually can restart normal replication without the consequences or can restart at the expense of fork failure/floundering and generate fusion products. We speculate that if HR finds the correct template for the nascent strand at a collapsed fork, cells can survive. However, if the choice of the template is incorrect, acentric and dicentric chromosomes are formed and cells lose their viability. Based on our assay of the previous data and also some recent studies, altogether these have led us to proposing the four models for the outcomes of the fork-arrest: 1. Cells remain viable from replication restart event via HR protein-dependent mechanism that leads to an unchanged chromosome III. 2. Replication restart fails. Such cells are then expected to lose viability as a result of the incomplete replication. 3. Cells can restart replication. The synthesis of DNA is, however, error-prone after the fork recovery. 4. Restarted replication occurs on an inappropriate template. Cells are not viable because the HR-dependent rearrangements between the *RTS1* repeats form acentric and dicentric chromosomes. Due to the fact that cells are no longer viable after an extremely high frequencies of rearrangements, very little is known about the consequences of acentric and dicentric chromosomes formation and how they undergo further rearrangements. This leads us to the development of a novel experimental

model on the extra mini-chromosome in this work. The data generated from this system is described in details below.

1.4.5 A novel model: fork-arrest system on the mini-chromosome

We were particularly interested in how the replication failure can result in genome alterations. A better understanding of these processes can provide useful insights to the cause of the various genomic disorders. Using *RuiuR* assays established on chromosome III of *S. pombe*, we reported that the recovery of impeded replication forks by homologous recombination was characterised by high levels of genetic instability and high frequencies of chromosomal rearrangements. Observation of a significant cell viability loss caused by the genome instability and miss-segregation of the acentric and dicentric chromosomes made it difficult to investigate further the downstream processes. To overcome such limitation of the previous experimental model, we have established a novel system to follow the fate of the rearranged chromosomes using the non-essential extra mini-chromosome (Ch^{16}). To achieve this aim the ~ 4.5 kb (120 repeat) lac operator (*lacO*) and ~ 10 kb (256 repeat) tetracycline operator (*tetO*) repeats were integrated onto the right arm of the mini-chromosome (Figure 1-15) [119-120]. Placing the replication fork barrier between the *lacO* and *tetO* repeats can provide an opportunity to understand the mechanism of *RTS1* induced chromosome rearrangements and follow the fate of the rearranged chromosomes. The nourseothricin (*Nat*) resistant gene was inserted on the left arm of the mini-chromosome, serving as a selection marker to ensure the presence of the mini-chromosome. The modified mini-chromosome system is named as Ch^{16}-NRUH. Figure 1-15 shows the strategy of the modified mini-chromosome system that was used in this thesis. GFP-tagged *lacI* gene (The lacI/GFP binds to the *lacO* repeats) and tdTomato-tagged *TetR* gene (The TetR/tdTomato binds to the *tetO* repeats) were

integrated onto the chromosome II (Figure 1-16) [120]. In this modified mini-chromosome system, by integrating the *tetO* and *lacO* arrays onto the mini-chromosome on either side of *RuiuR* loci, we were able to visualise the rearrangement events *in vivo*, directly within a single cell. The data collected using this system is presented in the following chapters.

1.4.5.1 The mini-chromosome system

The non-essential mini-chromosome (Ch^{16}) was modified in order to explore the mechanisms of the dicentric and acentric palindromic chromosome formation and their subsequent fate. The mini-chromosome was obtained by generating an aneuploidy disomic extra chromosome from of chromosome III of *S. pombe* by γ-irradiation [110-113]. The advantages of the mini-chromosome include: mitotic stability, conserved copy number and relatively small size that makes it separable from the three regular chromosomes by a Pulsed Field Gel Electrophoresis (PFGE) electrophoresis [121]. The mini-chromosome has ~500 kb DNA sequence deleted, i.e. most sequence of chromosome III, and lacks nucleolar rDNA while retaining the pericentric region and an intact centromere 3 (CEN3) region. The fission yeast strains that were used in this thesis contained a single copy of the mini-chromosome with auxotrophic markers *ade6-m216* together with *ade6-m210* on chromosome III, resulting in an ade^+ phenotype through heteroallelic complementation.

On the minimal media supplemented with a low concentration of adenine (10 mg/l) colonies which contain the mini-chromosome can be distinguished from the colonies that do not based on the differences in their colours; ade^+ strains form white colonies indicating that they contain both *ade6* alleles, and ade^- strains form pink colony suggesting the loss of either *ade6-m216* or *ade6-m210* makers. In general, aneuploids

are highly unstable in *S. pombe*. However, our system appeared to be stable in maintaining the extra chromosome in the haploid genome because of its small size. The mini-chromosome was stably maintained in *S. pombe* with a loss at only $1x10^{-4}$ frequency. Furthermore, the mini-chromosome exhibited similar activities as natural chromosomes during replication and cell segregation in either mitosis or meiosis [110]. A single copy of the mini-chromosome was faithfully segregated and passed to each daughter cells with high fidelity compared to two of the mini-chromosome copies that were lost, one of them at around tenfold higher in frequency. Although the mini-chromosome has certain partial sequence homology of the chromosome III, the single mini-chromosomes in zygotes were segregated independently during meiosis. Moreover, it is intriguing that no recombination occurred between the homologous sequences of mini-chromosome and chromosome III, indicated by the tetrad and random spore analyses of the mini-chromosome. Altogether, these data showed that the mini-chromosomes segregate faithfully and independently. Consequently, a single copy mini-chromosome of *S. pombe* was used for subsequent experiments.

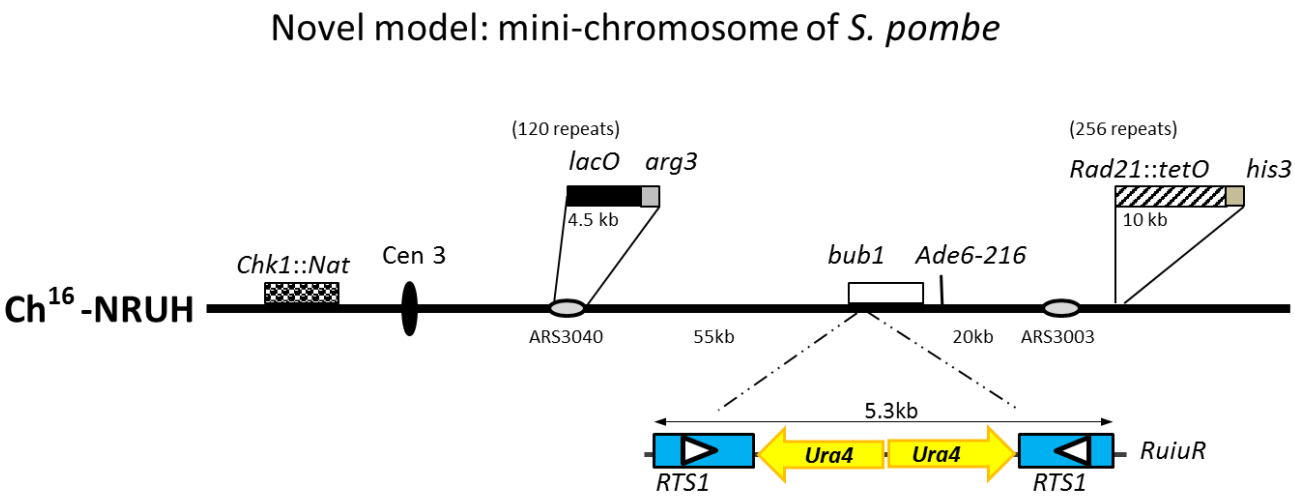

Figure 1-15. The modified mini-chromosome system.

The modified mini-chromosome system is named as Ch^{16}-NRUH. The lac operator (*lacO*) repeats-*arg3*$^{+}$ and tetracycline operator (*tetO*) repeats-*his3*$^{+}$ were inserted on the right arm of the mini-chromosome, either side of the *RuiuR* loci. Nourseothricin (*Nat*) resistant gene was placed at *chk1* locus on the left arm of the mini-chromosome as a selection marker to follow the presence of the mini-chromosome. The *lacO* repeats-*arg3*$^{+}$ replaced *ars* (3040) sequence and *tetO* repeats-*his3*$^{+}$ replaced the *rad21* locus. The *RuiuR* system was integrated at the upstream part of the *bub1*gene.

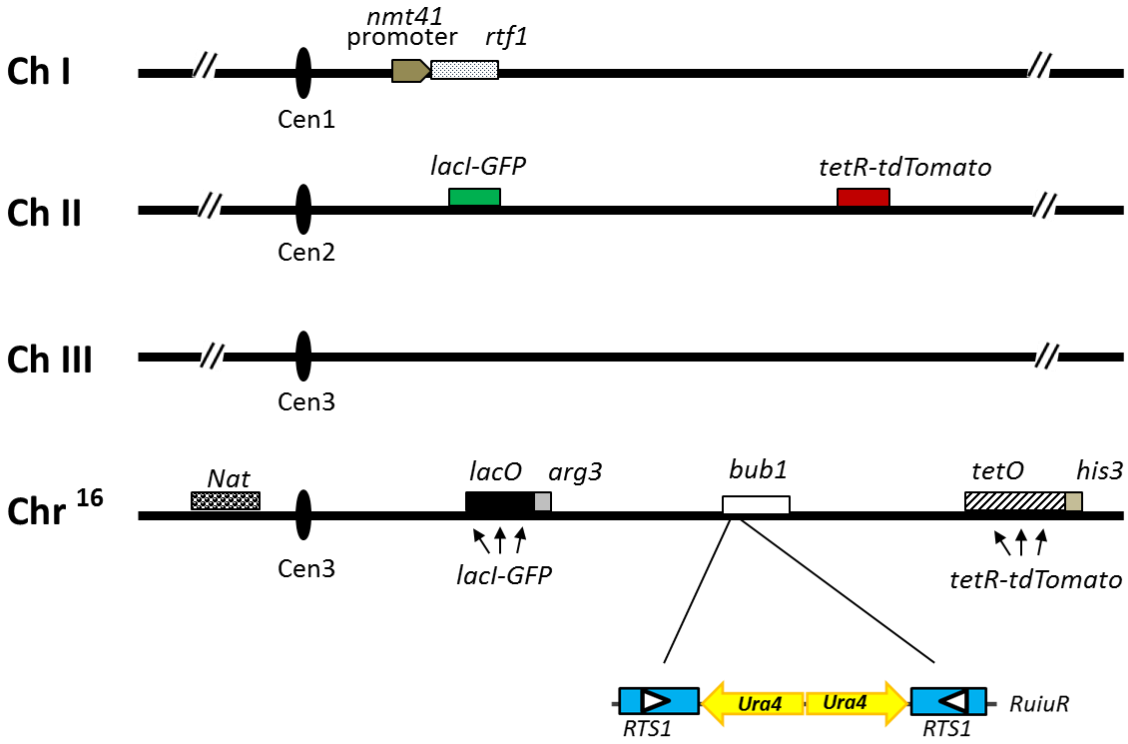

Figure 1-16. The system to monitor chromosomal rearrangements in *S. pombe*.

RuiuR construct was placed on *bub1* gene loci of mini-chromosome to induce replication forks stalling regulated by nmt41 promoter through controlling Rtf1 protein (placed on chromosome I). To directly visualise the chromosomal rearrangements, the *lacO* and *tetO* repeats located on the either side of the *RuiuR* loci can be bound by the LacI-GFP and TetR-tdTomato fluorescent protein. The *lacI-GFP* and *tetR-tdTomato* genes were integrated on chromosome II.

1.4.5.2 Tetracycline operator (tetO) and lac operator (lacO) arrays

In order to visualise the positions of the dicentric and acentric chromosomes in a single cell and to analyse their fate *in vivo*, the use of tetracycline operator (*tetO*) and lac operator (*lacO*) arrays have proven to be a powerful assay [119-120]. Labelling the mini-chromosome with two *tetO* and *lacO* repeats at specific loci enabled the investigation of chromosome distribution and behaviour in growing cells. Here, the two different fluorescent tags, the *lac*O/LacI-GFP (green fluorescent protein) and the *tet*O/TetR-tdTomato (tomato red fluorescent protein) were used [122-123, 126]. The green fluorescent protein (GFP, absorption and emission spectra with maxima at 529 and 569 nm, respectively) of the jellyfish *Aequorea Victoria* have been purified and revolutionized in the early 1960s [124]. The tdTomato (absorption and emission spectra with maxima at 554 and 581 nm, respectively) is a derivative of dsRed from the mushroom coral *Discosoma striata*. This intramolecular tandem dimer is a very bright variation [125]. Although the GFP and tdTomato fluorescence protein have slightly overlapping spectra, they are still able to produce clean spectral separation using the appropriate filter sets.

1.5 Objectives

1.5.1 Establishing the modified mini-chromosome system in *S. pombe*

Visualizing the chromosomal rearrangement events directly *in vivo* using the mini-chromosome system is expected to work. The mini-chromosome provides a working platform to monitor the fate of acentric and dicentric chromosomes without significant cell viability loss. Previous results in our laboratory have already proven that the *RuiuR* assays established on chromosome III of *S. pombe* can initialize chromosomal rearrangement events. Here, a mini-chromosome system, containing the

repeat arrays of *lacO* and *tetO* on either side of the inducible fork barriers – *RuiuR* is used. Exogenous lacI/GFP protein (The lacI proteins bind the *lacO* sequences) and tetR/tdTomato protein (The tetR proteins bind the *tetO* sequences) visualised specific genomic regions on Ch^{16} labelled with two different fluorescent colours. As a result, according to the distribution of two different colours of the fluorescent proteins, it is possible to trace the fate of the mini-chromosome in real-time. During construction of the experimental model, I integrated nourseothricin (*Nat*) resistance gene and enabled easy cassette exchange for further experiments with kanamycin *(Kan)* resistance gene flanked by loxP and loxM3 sites into alternative arms of the mini-chromosome as the selective markers. The tetracycline operator (*tetO*) and lac operator (*lacO)* arrays were set at either side of the fork arrest loci on the mini-chromosome. Such *tetO* repeats were placed adjacent to a $his3^{+}$ gene at the *rad21* locus and the *lacO* repeats with an $arg3^{+}$ gene situated at the autonomously replicating sequence *ars* (3040) (as described in Chapter 3). In parallel, I have constructed another strain that contained *lacI* gene fused with *gfp* gene and *tetR* gene tagged with *tdTomato* gene on chromosome II (the construct was a gift obtained from Dr. Takeshi Sakuno). In this strain, thiamine-repressible promoter *(nmt41promptor)* was replaced with *rtf1*promoter to control Rtf1 protein expression on chromosome I. Eventually, after crossing these two strains, the experimental strain was obtained with the following target genes: 1. *nmt41* promoter is nearby $rtf1^{+}$gene on chromosome I. 2. The *lacI*/*gfp* gene and *tetR*/*tdTomato* gene are located on chromosome II. 3. Nat^{R} gene is inserted on the right arm of mini-chromosome. 4. The *tetO* repeats with a $his3^{+}$ gene replaced at the *rad21* locus. 5. The *lacO* repeats with an $arg3^{+}$ gene replaced *ars* (3040) (Figure 1-15). (*RuiuR* assays were provided by Dr. Ken'Ichi Mizuno).

1.5.2 Direct visualisation of chromosomal rearrangements in a single cell

The strategy is relatively simple in concept: after the rearrangements occur, a mini-chromosome forms acentric and dicentric chromosomes. Telomere proximal signal tethered with tetR/tdTomato protein shows acentric chromosomes as well as the telomere proximal side of the parental mini-chromosome. As dicentric chromosomes contain the centromere proximal signal, dicentric and parental chromosomes are both labelled with the lacI/GFP protein at the centromere proximal side (Figure 1-17). Thus, while parental chromosomes signal both at centromere (GFP) and telomere (tdTomato) proximal regions, acentric chromosomes show signal only at the telemetric region (tdTomato) while the dicentric chromosomes signal only at the centromere proximal (GFP) region. In our assay, when fork stalling was not induced ("pause off" growth), the *lacO* and the *tetO* repeats were always located at the same chromosome, even during cell division (Figure 1-18 A). The signals of tetR/tdTomato and lacI/GFP displayed co-localization within the nucleus. In contrary, when rearrangements occurred ("pause on" growth), the *lacO* and the *tetO* repeats did not always exist on the same chromosome due to the formation of acentric and dicentric chromosomes. Two different colours of fluorescent proteins were separated on the acentric (indicated by the *tetO*/tetR-tdTomato) and dicentric (shown by the *lacO*/ lacI/GFP) chromosomes (Figure 1-18 B). Therefore, this system was exploited in a way to distinguish the acentric and dicentric chromosomes by following the movement of the two tdTomato dots (located on the acentric chromosomes) and the two GFP foci (presented on the dicentric chromosomes). We expected that when the fork-arrest induced rearrangements occurred during the S phase in *S. pome*, it will lead to a generation of isochromosomal products. Such chromosomal intermediates exhibited delocalised signals of the tetR/tdTomato and the lacI/GFP within nucleus. Due to the

unusual architecture of the acentric and dicentric chromosomes, they can cause segregation problems in the M phase (classified into the metaphase, anaphase and telophase). In fact, during each cell division, bi-oriented chromosomes are aligned along the equator of the cell by a bipolar spindle oriented to the centromeres, which are then required to ensure accurate chromosome segregation. An acentric chromosome does not have centromeres and as a consequence that the spindle fails to attach or miss-attaches to it. This causes the random distribution or dislocation of the acentric chromosome within the nucleus. A dicentric chromosome on the other hand has two centromeres, and its unstable conformation can lead to further rearrangements (such as BFB cycle) with a strong relevance to genome instability. By following the tdTomato and the GFP patterns, the miss-segregation phenomenon can be revealed in a single cell and contribute to the better understanding of how cells respond to aberrant genetic materials. Notably, the analysis of the properties of rearranged chromosomes *in* vivo mentioned above was monitored by a DeltaVision deconvolution light microscope system.

1.5.3 Monitor the fate of the rearranged palindrome chromosomes

Giant palindromes, such as the acentric and dicentric chromosomes, have been proposed to be the precursors for oncogene amplification and have been observed commonly in cancer cells. These chromosome intermediates are prone to undergo further rearrangements, which can ultimately result in gene amplifications, deletions and translocations. During the anaphase, each aligned chromosome is bound by spindle poles towards the opposite sides of a cell. However, when a dicentric chromosome is formed, cells encounter problems in chromosome separation leading to miss-segregation because of the dicentric chromosome containing two centromeres. Figure 1-19 shows the potential fates of the dicentric chromosomes during a cell

division. A dicentric chromosome can be pulled towards the same direction and stay intact located in one of the daughter cells. A dicentric chromosome can also be attached from the opposite sides by spindle poles and exposed to tension during spindle pole separation leading to random breakage. The random breakage causes an unequal distribution of genetic material in the daughter cells. The products may be stabilised by new telomere formation or other pathways. After duplication of a broken-end chromosome, the resulting two chromosomes lacking their telomeres can fuse with each other, generating a new dicentric chromosome and undergoing a next breakage–fusion–bridge (BFB) cycle until stabilised products are produced (e.g. by telomere addition, inactivation or deletion of one of centromeres) [39-41]. Generally, such further rearrangement event eventually results in gaining or losing some genetic material. However, how these unstable chromosomes undergo further rearrangements is still elusive. My construct – through a number of different markers established on the non-essential mini-chromosome – provides an apparatus to follow the fate of the mini-chromosome after the acentric and dicentric chromosome formation (Figure 1-17). Using the non-essential mini-chromosome, I attempted to determine the subsequent outcome of a dicentric chromosome through several lines of data in various ways including measuring the frequency of marker loss and following the loci of the markers on the rearranged chromosomes. These data offer significant information in understanding the subsequent metabolism of an acentric and a dicentric chromosome generation.

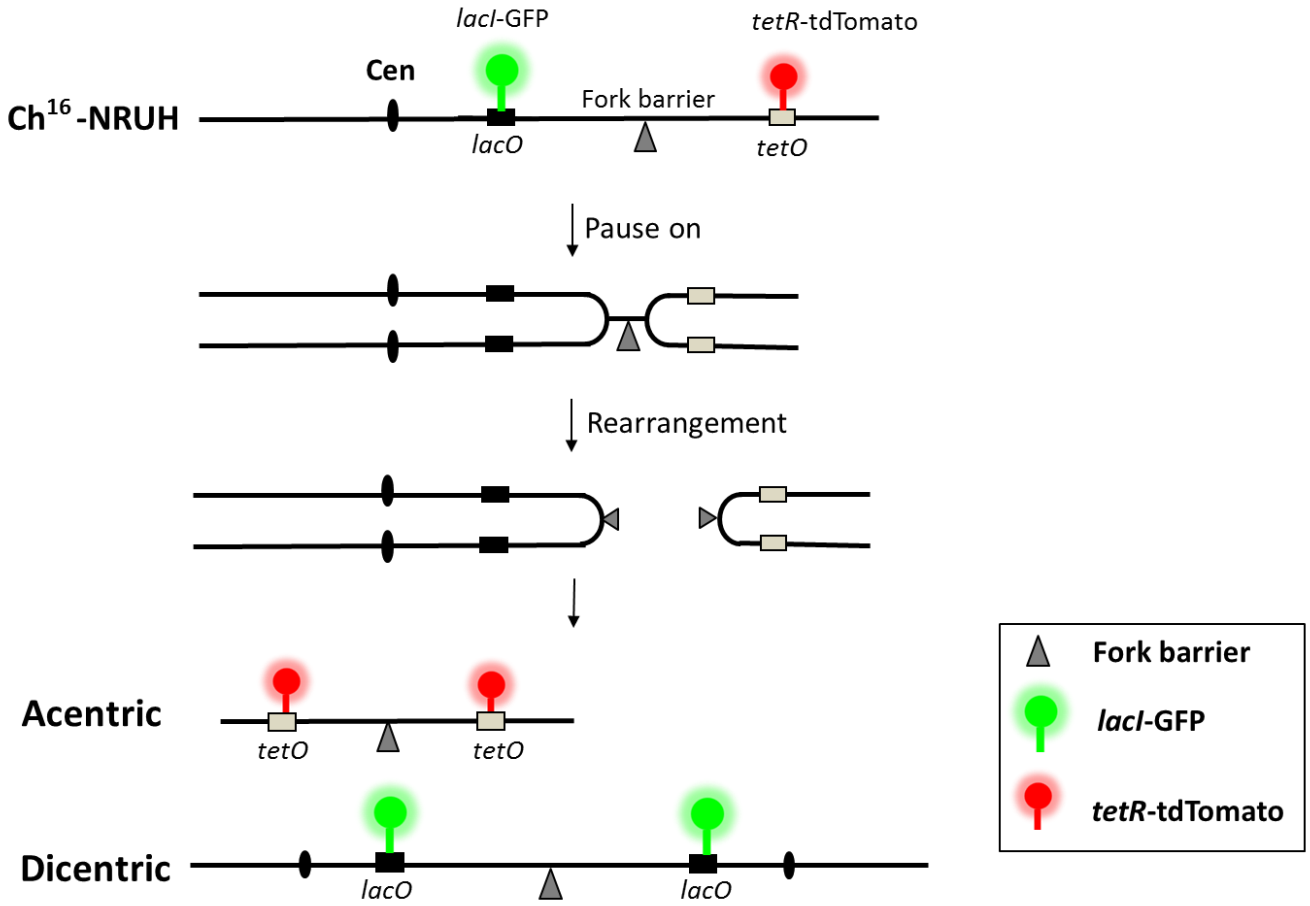

Figure 1-17. Schematics of the visualisation of the chromosomal rearrangements in the mini-chromosome system (Ch^{16}-NRUH).

The *lacO* and *tetO* repeats are bound by the lacI-GFP and tetR-tdTomato fluorescent protein. After generating the acentric and dicentric chromosomes ("pause on" growth), the tetR-tdTomato fluorescent protein can show the locations of parental mini-chromosome and acentric chromosomes; the lacI-GFP fluorescent protein can indicate the position of the parental mini-chromosome and dicentric chromosomes in a single cell.

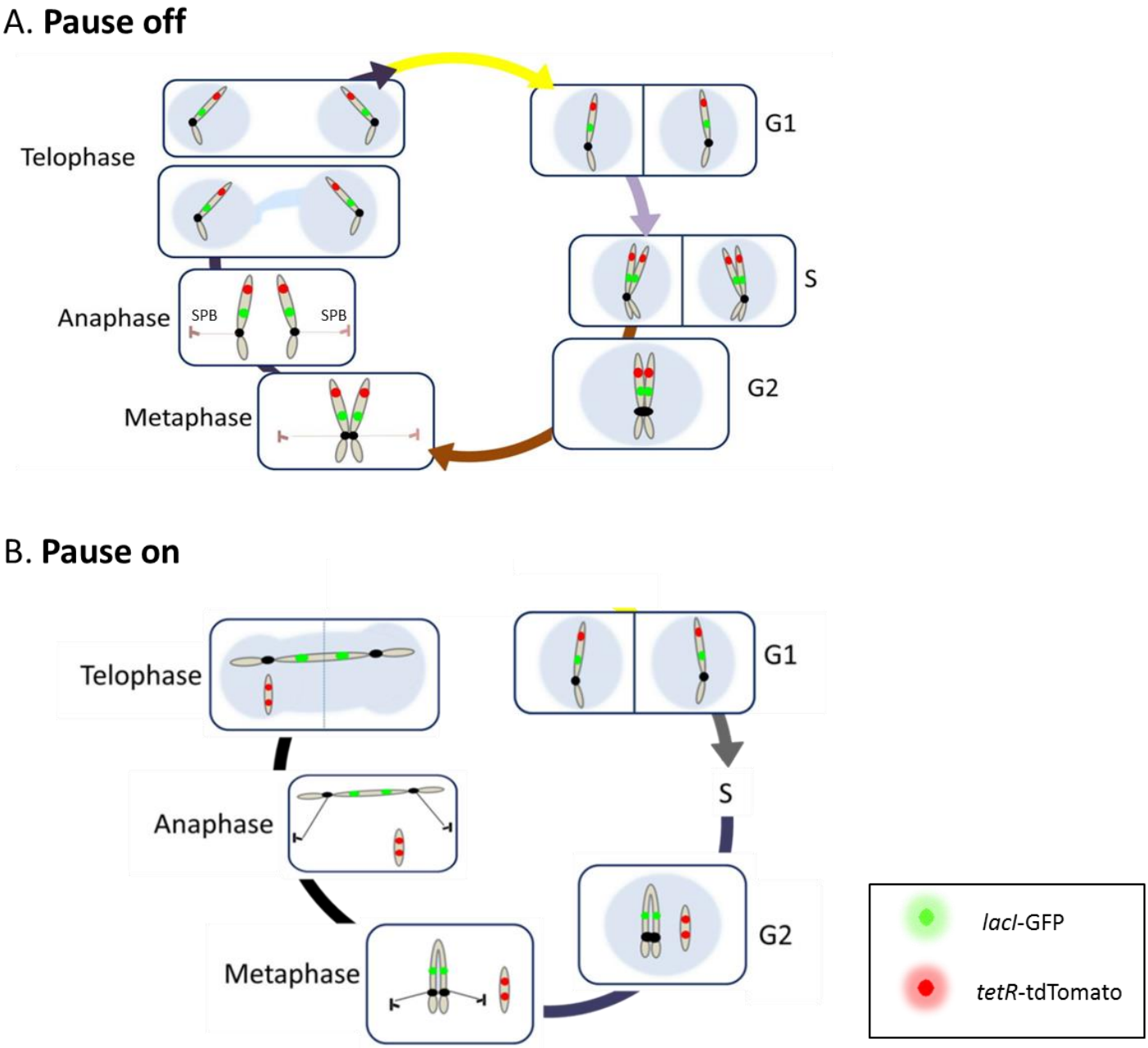

Figure 1-18. Visualisation of the chromosomal rearrangements through the cell cycle in *S. pombe*.

To visualise the chromosomal rearrangements, the *lacO*/lacI-GFP and *tetO*/tetR-tdTomato systems were used on the Ch^{16}-NRUH, on either side of the inducible fork barriers loci. (*A*) In replication during the pause off growth, no chromosomal rearrangements occurred, the lacI-GFP and tetR-tdTomato spots co-localised on the parental mini-chromosome in mitosis. (*B*) During "pause on" growth, the Ch^{16}-NRUH split into the acentric and dicentric chromosomes and the lacI-GFP and tetR-tdTomato dots separated as the acentric and dicentric chromosomes formed, respectively.

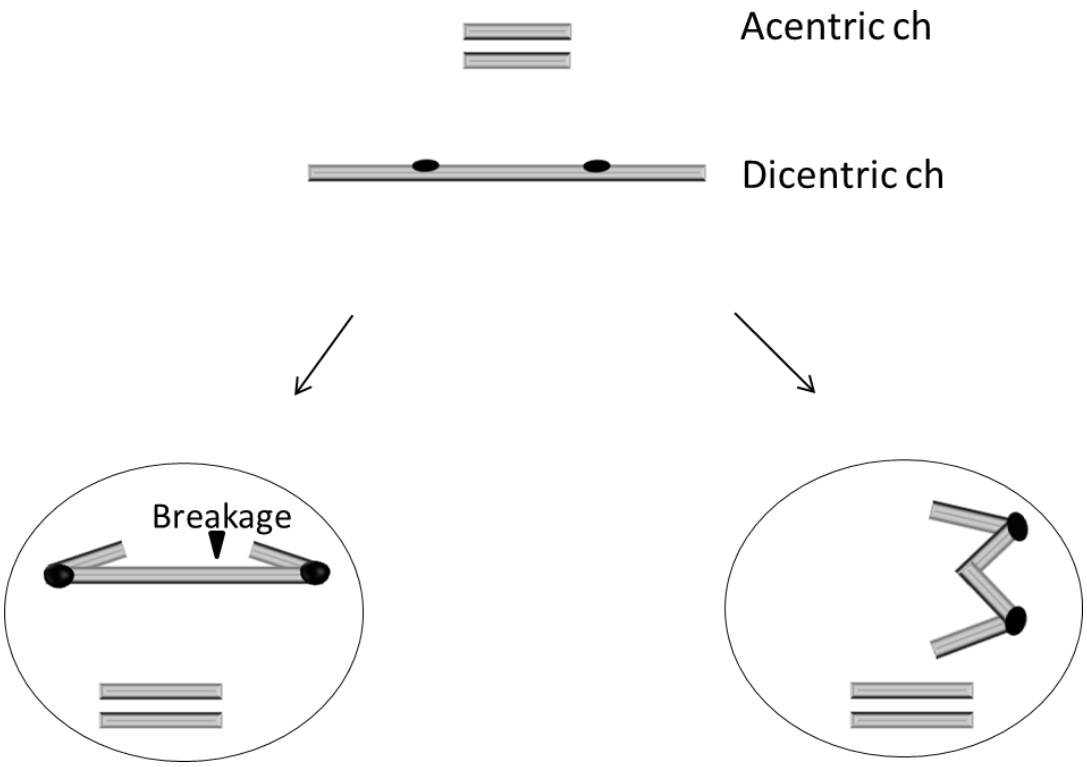

Figure 1-19. The fates of the dicentric chromosomes as formed.

After the dicentric chromosomes are formed, cells encounter some problems leading to miss-segregation in the anaphase due to the two centromeres on the dicentric chromosome. The dicentric chromosomes can be pulled towards the same direction (might a random breakage occur afterward) or – if attached by opposite spindle poles – towards both sides of cells. This movement exhibits tension on the dicentric chromosome leading to a random breakage.

CHAPTER 2

MATERIALS AND METHODS

2.1 Materials

Unless stated otherwise all chemicals used in this project were purchased from Sigma-Aldrich (Dorset, UK) and Fisher Scientific (Leicestershire, UK).

2.1.1 Media

Liquid yeast extract (YE): 0.5 % yeast extract, 3 % glucose, 100 μg /ml arginine, leucine, uracil and histidine and 200 μg /ml adenine.

Yeast extract agar (YEA): YE with 2.5 % agar

Yeast nitrogen base agar (YNBA): 0.5 % yeast extract, 3 % glucose, 2.5 % agar, 1.25 % ammonium sulphate, 2 mM NaOH supplemented with appropriate amino acids (at a final concentration of 100 μg /ml). Nourseothricin or kanamycin resistant strains were selected on YNBA plates supplemented with 100 μg/ml nourseothricin (*Nat*, Werner BioAgents, clonNAT, 51000) or 200 μg/ml kanamycin (geneticin disulphite-G418, Melford, catalogue no. G0175) respectively.

Table1. Reagents for EMM2 media

10000x Trace elements	
5.0g/l	H_3BO_3
4.0g/l	$MnSO_4$
4.0g/l	$ZnSO_4 \times 7H_2O$
2.0g/l	$FeCl_3 \times 6H_2O$
1.5g/l	Na_2MoO_4
1.0g/l	KI
0.4g/l	$CuSO_4 \times 5H_2O$
10.0g/l	Citric acid
1000x Vitamins for EMM2 media	
1.0g/l	Pantothenic acid
10.0g/l	Nicotinic acid
10.0g/l	Inositol
0.01g/l	d-Biotin

Edinburgh minimal media (EMM2): 3.1 g/l potassium hydrogen phthalate, 1 g/l KCl, 1.1 g/l $MgCl_2.6H_2O$, 10 mg/l Na_2SO_4, 13 mg/l $CaCl_2.2H_2O$, 5 g/l NH_4Cl, 1.4 g Na_2HPO_4, 5 g/l glucose , vitamins and trace elements (Table 1) supplemented with the appropriate amino acids (at a final concentration of 100 μg/ml).

Luria-Bertani (LB, Fisher Bioreagent, catalogue no. BP14262): 0.5 % yeast extract, 1 % tryptone, 1 % NaCl. Ampicillin or kanamycin A resistant strains were selected on LB agar plates supplemented with 100 μg/ml ampicillin sodium salt (Sigma, catalogue no. A9518) or 100 μg/ml kanamycin monosulfate (Kanamycin A, Melford, catalogue no. K0126) respectively.

2.1.2 List of strains

Table 2. The strains are used in this thesis

Strain	Mating type	Genotype
CJ01	h^+	*ade6-m210, arg3-D4, his3-D1, leu1-32, ura4-D18, chr16, ade6-m216*
CJ06	h^+	*ade6-m210, arg3-D4, his3-D1, leu1-32, ura4-D18, chr16, ade6-m216, chk1::natMX6*
CJ07	h^+	*ade6-m210, arg3-D4, his3-D1, leu1-32, ura4-D18, chr16, ade6-m216, chk1::natMX6*
CJ08	h^+	*ade6-m210, arg3-D4, his3-D1, leu1-32, ura4-D18, chr16, ade6-m216, chk1::natMX6*
CJ09	h^+	*ade6-m210, arg3-D4, his3-D1, leu1-32, ura4-D18, chr16, ade6-m216, chk1::natMX6*
CJ13	h^+	*ade6-m210, arg3-D4, his3-D1, leu1-32, ura4-D18, chr16, ade6-m216, chk1::natMX6, bub1::loxP-kanMX6-loxM3*
CJ17	h^+	*ade6-m210, arg3-D4, his3-D1, leu1-32, ura4-D18, chr16, ade6-m216, chk1::natMX6, bub1::loxP-kanMX6-loxM3*
CJ18	h^+	*ade6-m210, arg3-D4, his3-D1, leu1-32, ura4-D18, chr16, ade6-m216, chk1::natMX6, bub1::loxP-kanMX6-loxM3*
CJ24	h^+	*ade6-m210, arg3-D4, his3-D1, leu1-32, ura4-D18, chr16, ade6-m216, chk1::natMX6, bub1::loxP-kanMX6-loxM3*
CJ40	h^+	*ade6-704, his7$^+$<<Pdis1-GFP-lacI-NLS, z::hph^R<<Padh31:tetR-Tomato, arg3-D4, his3-D1, leu1, ura4-D18*
CJ41	h^-	*ade6-704, arg3-D4, leu1-32, ura4-D18, chr16, ade6-m216, chk1::natMX6, bub1::loxP-kanMX6-loxM3*
CJ42	h^+	*ade6-704, arg3-D4, leu1-32, ura4-D18, chr16, ade6-m216, chk1::natMX6, bub1::loxP-kanMX6-loxM3, rad21::9kbtetO-his3$^+$*
CJ53	h^-	*rtf1:Pnmt41:rtf1$^+$:sup3.5, his7$^+$<<Pdis1-GFP-lacI-NLS, z::hph^R<<Padh31:tetR-Tomato, ade6-704, arg3-D4, his3-D1, leu1-32, ura4-D18*
CJ56	h^-	*rtf1:Pnmt41:rtf1Δ:sup3.5, his7$^+$<<Pdis1-GFP-lacI-NLS, z::hph^R<<Padh31:tetR-Tomato, ade6-704, arg3-D4, his3-D1, leu1-32, ura4-D18*
CJ69	h^-	*rtf1:Pnmt41:rtf1Δ:sup3.5, his7$^+$<<Pdis1-GFP-lacI-NLS, z::hph^R<<Padh31:tetR-Tomato, ade6-704, leu1-32, ura4-D18, chr16, ade6-m216, chk1::natMX6, bub1::loxP-kanMX6-loxM3, rad21:: 9kb tetO-his3$^+$, ARS:: 4.5kb lacO-arg3$^+$*
CJ73	h^-	*rtf1:Pnmt41:rtf1$^+$:sup3.5, his7$^+$<<Pdis1-GFP-lacI-NLS, z::hph^R<<Padh31:tetR-Tomato, ade6-704, leu1-32, ura4-D18, chr16, ade6-m216, chk1::natMX6, bub1::loxP-kanMX6-loxM3, rad21:: 9kb tetO-his3$^+$, ARS:: 4.5kb lacO-arg3$^+$*
CJ90	h^-	*rtf1:Pnmt41:rtf1$^+$:sup3.5, his7$^+$<<Pdis1-GFP-lacI-NLS, z::hph^R<<Padh31:tetR-Tomato, ade6-704, leu1-32, chr16, ade6-m216, chk1::natMX6, bub1::loxP-RuiuR-loxM3, rad21:: 9kb tetO-his3$^+$, ARS:: 4.5kb lacO-arg3$^+$*
CJ126	h^-	*rtf1:Pnmt41:rtf1Δ:sup3.5, his7$^+$<<Pdis1-GFP-lacI-NLS, z::hph^R<<Padh31:tetR-Tomato, ade6-704, leu1-32, chr16, ade6-m216, chk1::natMX6, bub1::loxP-RuiuR-loxM3, rad21:: 9kb tetO-his3$^+$, ARS:: 4.5kb lacO-arg3$^+$*

2.1.3 List of oligonucleotides

Table 3.

A. Primers used in PCR amplification for cloning (written 5′–3′)	
tetO F	GGGGTCGACACGAATTCGGATCCCTCGAGGCTAGCAGGG
tetO R	CCCCGTCGACAGGGAGCTTACTTCCTCTCTATCACTGATA
Rad21up_F	GGG GAGCTCGCGGCCGCCAAGGTTGTAATCGGAGTTTTCCGT
Rad21up_R	TAAGTGCAATAGTAAAGAAAACGTTGAAAGGTCGACAAAAAGAGGGGAATCAAAA
His 3_F	TTTTGATTCCCCTCTTTTTGTCGACCTTTCAACGTTTTCTTTACTATTGCACTTA
His 3_R	TAGTAAACCCGTATCATCGCATTGGGTACCTCTATGCAAAGCTAACGAATCTTTAATTCT
His 3 up 500bp_R	AACAGTAAACAGGGAGTACTTCATTGCTTTCCAAG
Rad21down_F	AGAATTAAAGATTCGTTAGCTTTGCATAGAGGTACCCAATGCGATGATACGGGTTTACTA
Rad21down_R	CCCCTGCAGGCGGCCGCATTTCTTTATCTTCGTTTATCTCAA
LacO F	GGG GAGCTCTTGGCGGAGATACTCTAGCAGGTCAACGAG
LacO R	CCCCCCGGGGCTTAGATCTGTCGACTCTAGAGATATTTG
Rgf1_F	GGGGAATTCGCGGCCGCGGGAGCCGGCGAGAACTGTAAGTAC
Rgf1_R	TTTCGACCTTGTAATATTTTTTTTATTTACCCCGGGGAGCTCGAACAGGAGAGCCGTAAGGATAAT
Arg3_F	ATTATCCTTACGGCTCTCCTGTTCGAGCTCCCCGGGGTAAATAAAAAAAATATTACAAGGTCGAAA
Arg3_R	ATGAAAATACTGCAAAACTGATGAGGTACCAGAGGATAGCATTAAGCGGGTAATAATTTT
Arg3 up 500bp R	TTTCAATTGCAAACTGAATAATTCTTCTCGACTAA
Rgf1_F	GGGGAATTCGCGGCCGCGGGAGCCGGCGAGAACTGTAAGTAC
Rgf1_R	TTTCGACCTTGTAATATTTTTTTTATTTACCCCGGGGAGCTCGAACAGGAGAGCCGTAAGGATAAT
SPCC645_F	AAAATTATTACCCGCTTAATGCTATCCTCTGGTACCTCATCAGTTTTGCAGTATTTTCAT
SPCC645_R	CCCCTGCAGGCGGCCGCATTTGCCCTTATTTGTGGATTGTT

B. Primers used in PCR amplification for yeast integration (written 5′–3′)	
Nat^R integration_F	GACTGTAAATAATACACATGCCAAAATTTGCAACATATGCTTGTGTTATATTATAATCTTCTTTCCCTT TACACCAAAGACGGATCCCCGGGTTAATTAA
Nat^R integration_R	TTGAAAATAAATTCACAACGAAGTCAAACAACAGGTTTCTTTTACAAACGAACTGGCACGACCTT TCAAAAGATGTGCAAGAATTCGAGCTCGTTTAAAC
Kan^R integration_F	ATGTCCGATTGGCGGCTTACAGAAAATGTACTTGACCAAAACATACCTGAAACTAAACCCAGGGA GTCCAAGACTCGCCT
Kan^R integration_R	GACATTATCGAAGAATTGGATGACCCCGTGGATGTTTGGTATCGCTGCATCGAATGGCTCTTGGAA ACAAGATTTTTGGG
Sup3-5 nmt-rtf1$^+$ integration_F	TCCCTTGCTATACTGATTACCTTTTGTCAATGTTTTTTTCTTAATATTTCTTCAGACAAGTGAACATTA TTATGCCAATAGCACCAAGGACGTCCCTATC
Sup3-5 nmt-rtf1$^+$ integration_R	AGTTGATCATCGACAAAGAGCTCTTCATTGTCCTCTGTATCCGGTCTGCAACTTAAATTGTTTTTTC CTTGCATGATTTAACAAAGCGACTATAAGTCAG
Sup3-5 nmt-rtf1$^\Delta$ integration_F	TCCCTTGCTATACTGATTACCTTTTGTCAATGTTTTTTTCTTAATATTTCTTCAGACAAGTGAACATTATTATGCCA ATAGCACCAAGGACGTCCCTATC
Sup3-5 nmt-rtf1$^\Delta$ integration_R	TTCTCTCAATGAATACACAAAAAATTTAAATCTATGACTTTGAGGAAGTAGTTAAAATAAATTTGTTCATGTAGG ATTTAACAAAGCGACTATAAGTC

C. Primers used in the amplification of DNA for probing Southern blots (written 5'–3')	
Probe A_F	CTGCCCAGATGCGAAGTTA
Probe A_R	CAAATTTGCCCAAGTATCAGAC
Probe B_F	ATTGGCGATACTTCACTGGA
Probe B_R	CATTTTCGCATTTAACTCAACC
Probe C_F	TGACCCCGTGGATGTTTGGTATCGC
Probe C_R	CGTTGCATTCTAATGAGCAAAGAAC
Probe D_F	ACGCCGCGCCCCTGTAGAGAAA
Probe D_R	GCCGGGGATCGCAGTGGTGAGTA
Probe E_F	GGGAAAAGTCAAGAATCAAGGTT
Probe E_R	GACTCGTATGCCAGAAGAAGGTT
Probe F_F	TGAAAAGAAATCGCTATGGAGTGT
Probe F_R	GATTTGCCCTTATTTGTGGATTG
Probe his_F	ATTAAAGACTCACATTGCTACACA
Probe his_R	TGAGGATAAAATTTGCAT
Probe Gm_F	GCAGTCGCCCTAAAACAAA
Probe Gm_R	TGGGTCGATATCAAAGTGC
Probe arg_F	TGTCCTGTTATTAATGGTCTTTGT
Probe arg_R	GTTTGCACATTCCCCAGAT
Probe Km_F	CGCAGACCGATACCAGGAT
Probe Km_R	GACATTATCGCGAGCCCATTTA
Probe ura_F	AGGATCGCAAATTCGCAGACA
Probe ura_R	TCGCTACCGCAGTTTACAATCAC
Probe Cen_F	TCCCATCTTGCGACCCTTTCTA
Probe Cen_R	CCTGCTCGTCTTCCCTTCTCAAT
Probe Tel_F	TTAGAATGCAACGTTGGAAAGAGG
Probe Tel_R	TCGGGAAAGAAGCAGCAGTGT
Probe X_F	GAAACCGACCTCTCCTGACGAA
Probe X_R	GTTGATCCACCGCACTCTTTGA

2.2 Methods: *E. coli* techniques

2.2.1 Molecular cloning techniques

Restriction digestions were carried out using restriction enzymes with appropriate restriction buffer at specific temperature and reaction time according to the manufacturer's instructions (New England Biolabs, NEB). Digested vector (100 ng) and insert DNA were mixed in various molar ratio (1:2 to 1:4 depending on the size of the fragments) and incubated with T4 DNA ligase (New England Biolabs, catalogue no. M0202S) at 16 ℃ overnight.

2.2.2 *E. coli* transformation

E. coli DH5 alpha cells were defrosted on ice, 2 µl of ligation mixture was added and incubated for 30 minutes on ice followed by 90 seconds heat-shock at 42 ℃. Cells were cooled down on ice for 2 minutes, 1ml LB was added and cells were allowed to recover on 37 ℃ for 1 hour. Aliquots of the transformation were plated on LB plates supplemented with ampicilin (100 µg /ml) or other appropriate antibiotic and incubated overnight at 36 ℃.

2.2.3 Plasmid extraction from *E. coli*

5 ml *E. coli* culture was grown overnight at 36 ℃ in LB supplemented with ampicillin (100 µg/ml). After centrifugation at 13,000 rpm for 1 minute at room temperature cells were resuspended in 200 µl of buffer P1 (50 mM Tris-HCl pH 8.0, 10 mM EDTA, 100 µg/ml RNaseA). 300 µl of buffer P2 (200 mM NaOH, 1% (w/v) SDS) was added and incubated at room temperature for 5 minutes. 300 µl of buffer P3 (3M KAc pH 5.5) was added and incubated on ice for 10 minutes. After centrifugation at 13,000rpm for 10 minutes at room temperature the supernatant was

transferred into a sterile tube and mixed with 1 volume of isopropanol to precipitate DNA. The pellet was washed with 500 µl of 70% Ethanol and resuspended in 20 µl of distilled water containing 0.5 mg/ml RNaseA for further applications.

2.2.4 Fusion PCR

The KOD Hot Start DNA polymerase (Novagen, catalogue no. 424762T) was used for fusion PCR. The reaction mix contained 100 ng of each DNA fragments including the overlap region for fusion, 0.2 mM dNTPs (dATP, dTTP, dCTP, dGTP, Roche, catalogue no. 11814362001), 0.2 µM of each primer, 1x KOD reaction buffer, 1-6 mM $MgSO_4$ and 0.02 U/µl KOD polymerase. The PCR cycling conditions were as follows: 95 ℃ for 3 minutes initial denaturation, followed by 30 cycles of 95 ℃ for 30 seconds denaturation of DNA template, 55~60 ℃ for 30 seconds primer annealing and 68 or 72 ℃ for 30–40 seconds extension. A final extension step was performed at 72 ℃ for 10 minutes. Primers used for fusion PCR are listed in Table 3.

2.3 Methods: yeast techniques

2.3.1 Gene disruption

An antibiotic cassette was amplified with primers of ~100 bp (20 bp homology to the cassette and 80 bp homology to the desired chromosomal locus) as listed in Table 3 B. The pFA6a-natMX6 plasmid was used to generate Nat^R gene integration cassette, while the pFA6a-kanMX6 plasmid was used to produce Kan^R gene integration cassette (both plasmids were obtained from Tony Carr's lab). In order to regulate the Rtf1 protein expression, *nmt41* promoter combined with *sup3-5* gene that was as a selection marker, were used to either replace the *rtf1* promoter or delete *rtf1* gene. The pGEM-NTAP plasmid (provided by Dr. Ellen Tsang) contains a *sup3-5* gene and

nmt41 promoter was used to amplify integration cassette for targeted locus, the amplified primers listed in the Table3 B. The PCR product was purified and transformed into *S. pombe* cells as described below. The auxotrophic marker was cloned into pUC19 plasmid flanked by 500 bp homology to the targeted locus (see details in Chapter 3).

2.3.2 *S. pombe* transformation

Yeast cells were grown in 100 ml YEL at 30℃ for 16-18 hours (up to $1x10^7$ cells/ ml), 1×10^8 cells were transferred in a sterile 50 ml polypropylene tube and harvested by centrifuging at 3,500 rpm for 3 minutes at room temperature. Cells were washed with 50 ml distilled water, followed by washing with 10 ml of LiOAc-TE (0.1 M LiAc, 0.01 M Tris-HCl, 0.001M EDTA, pH 7.5). The pellet was resuspended in 0.3 ml of LiOAc-TE buffer, and incubated at 30 °C for 1 hour. 50 μg of carrier DNA (10 mg/ml Invitrogen Salmon Sperm DNA, catalogue no. VX15632011) and 5 μl of the integrating DNA (1 μg DNA / 5 μl TE) were added into 100 μl of cell suspension and incubated at 30 ℃ for 30 minutes. 700 μl of 40 % PEG/LiAc-TE (2 g Polyethylene glycol resolved in 5 ml LiOAc-TE buffer) was added and incubated at 30 ℃ for 1 hour. 43 μl of 100 % DMSO were added and cells were heat-shocked at 42 ℃ for 5 minutes and washed with 1ml distilled water. Cells were resuspended in 100 μl water and spread on plates with proper nutritional supplement and incubated at 30 ℃ for 3-4 days. For integration of antibiotic markers, cells were first spread on YEA plates and grown for 24 hours at 30 ℃. When the colonies are formed, they are checked using the replica plated on selected plates which contain the relevant drugs (100 μg/ml NAT or 100 μg/ml G-418), following to incubation at 30 ℃ for 3~4 days.

2.3.3 *S. pombe* crossing and random spore analysis

Fresh h^- and h^+ strains were mixed together on an ELN plate in a drop of distilled water and incubated at 25 ℃ for 2 days. The sporulation efficiency was tested by checking for the presence of asci under the light microscope. Cells were transferred by an inoculation loop into 98 µl of distilled water. 2 µl of a 1:10 dilution of *Helix pomatia* Juice was added and placed on a rotating wheel overnight at room temperature. Spores were counted using a Haemocytometer and 1,000 of spores were plated on YEA and incubated for 3~4 days at 30 ℃.

2.3.4 Chromosome loss assay

S. pombe cells were collected from 10 ml YE grown at 30 ℃ for 16-18 hours and harvested by centrifuging at 3,500 rpm for 1 minute at room temperature. The cells were washed with 1ml distilled water, transferred to 1.5 ml sterile microcentrifuge tube and collected by centrifugation. The pellet was resuspended in 100 µl sterile water and spread on YNBA with 10 mg/ml adenine. After incubation at 30 ℃ for 48 hours, pink colonies (proposed to have lost the mini-chromosome) were re-streaked and grown at 30 ℃ for 48 hours to form single colonies. Five colonies of each pink strain were then patched on YNBA containing 10 mg/ml adenine and grown at 30 ℃ for 24 hours. The colonies were subsequently replicated on YNBA with Nat (100 g/ml clonNAT, Werner BioAgents, catalogue no. 51000) and incubated at 30 ℃ for 72 hours to establish the *Nat* resistance gene cassette lost concomitantly with the mini-chromosome.

2.3.5 Spot test for cell viability

S. pombe cells were grown in EMM2 media with thiamine supplement (15 µM)

(“pause off” growth) or without thiamine supplement (“pause on” growth) at 30 ℃ for 24 hours. A series of dilutions ($1x10^7$ to $1x10^3$ cells/ ml) was made and 10 µl of each dilution was spotted on YNBA with the appropriate amino acids with or without thiamine supplement and incubated at 30 ℃ for 3–4 days.

2.3.6 Cre/lox site-specific recombinase-mediated cassette exchange (RMCE)

An efficient method for gene replacement using Cre recombinase-mediated cassette exchange (RMCE) was described previously [127]. To create the base strain the kanMX6 cassette flanked by loxP and loxM3 (loxP-*kan*^{R}-loxM3 cassette) was amplified from pAW8-kanMX6 plasmid. The primers used for the amplification contained ~80 bp of homology to the genomic target locus at a 5’ end and 20 bp homology to pAW8-kanMX6 on the 3’ end. The primers used for this amplification step are listed in Table 3B. This PCR product was inserted to replace 200 bp of the upstream part of the *bub1* gene on the mini-chromosome using standard transformation techniques based on homologous recombination. 100 µg/ml geneticin disulphate (*Kan*, G418, Melford, catalogue no. G0175) was added to the YEA plates for selection of G418 resistant cells. Integration was checked by PCR and subsequently confirmed by sequencing. For gene replacement using the RMCE method, a fork-arrest system– *RuiuR* – was cloned into the pAW8 plasmid flanked by loxP and loxM3 sites [49 and 70] resulting in pAW8-RuiuR plasmid. The pAW8-RuiuR also contains the *LEU2*$^+$ marker of *Saccharomyces cerevisiae* that can complement *S. pombe leu1-32* mutants as well as the Cre recombinase that enables recombination exchange event (seen in Chapter 3). After pAW8-RuiuR was transformed into the base strain transformants were selected for the presence of the plasmid (leu$^+$) on YNBA without Leu supplement enabling these cells to recombine

with the target sequence on the mini-chromosome. Single colonies were transferred into rich YE media and grown overnight (30 ℃) then 1,000 cells were plated onto YEA plates. Lack of selective pressure in rich media allows cells to lose the plasmid. The final construct was expected to show Kan^S, Leu^-, Ura^+ phenotype. Hence, after colony formation plates were replica plated onto YNBA without Leu to check the absence of pAW8-RuiuR, on YEA plates with G418 for the absence of the *kan* resistant gene and onto YNBA without Ura plates for the presence of *RuiuR* system.

2.3.7 Conformation of gene integration

2.3.7.1 Chromosomal DNA preparation

To confirm integration on the genotypic level genomic DNA was isolated from *S. pombe* transformants. Cells were grown in 10 ml YE at 30 ℃ for 12~16 hours and harvested by centrifugation at 3,500 rpm for 5 minute at room temperature. The pellet was resuspended in 1 ml buffer SP1 (1.2 M sorbitol, 50 mM citric acid, 50 mM Na_2HPO_4, 40 mM EDTA pH 5.6) containing 1 mg/ml Zymolyase T20 (Seikagaku, AmsBiotechnology, catalogue no. 120491- 1) to create spheroplasts. Cells were incubated at 37 ℃ water bath for 15-30 minutes and checked for the presence of spheroplasts using light microscope by adding 5 % SDS. When 90 % of the cells formed spheroplasts they were harvested by centrifugation at 3,500 rpm for 5 minute at room temperature and resuspended in 450 µl 5xTE (0.05 M Tris-HCl, 0.005 M EDTA pH 7.5). To lyse the cells 50 µl of 10 % SDS was then added followed by 5 minutes incubation at room temperature. To remove proteins and other contaminants from the cell lysate, 150 µl of 5 M KAc was added and the mixture was incubated for 10 minutes on ice. The precipitate was removed by centrifugation at 13,000 rpm for 10 minute at 4℃ and the supernatant was transferred to a new eppendorf tube. The DNA was recovered by adding 1 volume of room-temperature isopropanol followed

by incubation on ice for 10 minutes. After centrifugation (13,000 rpm for 10 minute at 4 ℃) the DNA pellet was washed with 500 µl room-temperature 70 % ethanol and dried using a speed vacuum dryer. The dried DNA pellet that was suspended in 250 µl 1xTE containing 5 µl of 10 mg/ml RibonucleaseA and incubated at 37 ℃ for 20 minutes. This preparation was used for PCR analysis. However, for other downstream applications such as restriction fragment length analysis by a Southern blot hybridization higher DNA yield and purity could be achieved through processing the following steps. 2 µl of 10 % SDS and 20 µl of 5 mg/ml Proteinase K (Sigma, catalogue no. P2308) were added and incubated at 55 ℃ for 1 hour. For efficient removal of proteins and other contaminants the DNA solution was extracted twice by Phenol chloroform extraction; 500 µl of Phenol: chloroform: isoamyl alcohol (mixture 25:24:1, Sigma, catalogue no. 77617) was added and the solution was gently mixed by vortex. After centrifugation (1,500 rpm for 5 minute at room temperature) the transparent aqueous upper phase containing the DNA was transferred to a new eppendorf tube. 1/10 volume of potassium acetate was firstly added to neutralize the sodium hydroxide from the previous step in the pH range 3.8-5.8 and also helped to form insoluble precipitate of DNA upon a high salt concentration environment. Subsequent treatment with 1 volume isopropanol was added to the supernatant to precipitate the DNA out of solution. The mixture was incubated on ice for 10 minutes and centrifuged at 13,000 rpm for 15 minute at 4 ℃. DNA pellet was washed with 500 µl 70 % ethanol followed by centrifuging at 13,000 rpm for 15 minute at 4 ℃. Finally, the pellet was resuspended in 30 µl 1xTE and incubated at 37 ℃ for 20 minutes to help solubilisation.

2.3.7.2 Yeast colony PCR

A loop-full of fresh yeast cells were suspended in 50 µl distilled water and heated to

95 ℃ for 5 minutes in a PCR machine (Biometra T3 Thermocycler). Cell lysis was span down by using a Minifuge. 25 µl of upper supernatant from cell lysis was mixed with 25 µl of reaction mixture containing final concentrations of 1x Taq Buffer, 2.5 mM $MgCl_2$, 0.2 mM of nucleotide (dATP, dTTP, dCTP, dGTP, Roche, catalogue no. 11814362001), 0.2 µM primers, 0.025 U Taq DNA polymerase (Thermo Fisher Scientific, catalogue no. AB-0192/B).

2.3.7.3 Restriction fragment length analysis (RFLA) using a Southern blot hybridization

5 µg of yeast genomic DNA was digested with appropriate restriction enzymes in a total volume of 200 µl and incubated overnight at temperatures according to the manufacturer's instructions. Restriction enzymes and buffers were purchased from New England Biolabs. To stop the reaction, DNA was precipitated as described before. The precipitated DNA was dried using a speed vacuum dryer and subsequently resuspended DNA in 30 µl distilled water by incubation at 37 ℃ water bath for 20 minutes. The DNA was separated by gel electrophoresis on 1 % agarose gel at constant 50V for around 24 hours in a Bio-Rad SubCell GT gel apparatus with 1x TAE buffer (40 mmol/l Tris, 40 mmol/l acetate, 2.0 mmol/l EDTA, and pH 8.0). The agarose gel was incubated in depuration solution (0.25 M hydrochloric acid) for 30 minutes, then placed in denaturation solution (1.5 M NaCl, 0.5 M NaOH) for 30 minutes and finally soaked in neutralization buffer (1 M Tris pH 8.0 and 1.5 M NaCl) for 30 minutes. The DNA was transferred onto a GeneScreen Hybridization Transfer Membrane (Perkin Elmer, catalogue no. NEF983001PK) either by capillary transfer overnight with 10x SSC (3 M NaCl, 300 mM Sodium citrate) or by Amersham Biosciences Vacugene XL apparatus overnight with 20x SSC. After drying the membranes, the transferred DNA was UV cross-linked to the nylon membrane at 254

nm using a Stratalinker (1200 J/m2) (Stratagene Cloning Systems, La Jolla, California, USA).

For the preparation of the radioactive probe, 47 µl distilled water containing 150 ng/µl of the DNA template was boiled for 5 minutes and subsequently cooled down on ice. The template DNA solution was added to the labelling reaction tube (GE Healthcare, Ready-To-Go DNA Labelling Beads (dCTP, catalogue no. 27-9240-01) with 3 µl ^{32}P-dCTP (EasyTides, Deoxycytidine, 5'-triphosphate, [alpha-32P]-50mM Tricine (pH 7.6), green, Perkin Elmer, catalogue no. NEG513Z). The DNA labelling reaction was processed at 37 °C for 15 minutes and was purified using G-50 Microspin columns (Illustra Microspin G-50 columns, catalogue no. GZ27533002). This probe can hybridise with its complementary DNA sequence and thus form a double-stranded DNA molecule. Hybridization buffer consisted of SSC, 1x Denhardt's reagent, 1% Sarcosyl (Sigma, catalogue no. 61747). For pre-hybridisation membranes without the probe were pre-warmed in hybridization buffer containing 0.1 % BSA in a roller tube and incubated for 30 minutes at 65 °C with gentle rotation. The membrane was hybridised with radioactively labelled DNA probe in hybridization buffer containing 100 µg/ml Salmon sperm DNA (Invitrogen, catalogue no. VX15632011) at 65 °C overnight with gentle rotation. To remove the non-specifically bound probe prior to detection the following series of washes were performed: the membrane was firstly washed twice with wash buffer I (2x SSC, 1% SDS, pre-warmed to 65 °C) in a roller tube for 15 minutes at 65 °C with gentle rotation; subsequently the membrane was washed twice with 500 ml wash buffer II (0.1x SSC, 0.01 % SDS, pre-warmed to 42 °C) for 15 minutes at room temperature under agitation. After air-drying the membrane the location of the probe was detected by directly exposing the membrane to a storage phosphor screen (Fuji BAS-MS Imaging Plate) using a FujiFilm

FLA-5100 Fluorescent Image Analyser or Molecular Dynamics Storm 840 phosphorimager apparatus. The software AIDA Image analyzer v4.27 was used to determine the position and intensity of the radioactive probe. The primers for preparing probes are listed in Table 1.

2.3.7.4 Pulsed field gel electrophoresis (PFGE)

To prepare agarose embedded yeast chromosomal DNA 3×10^8 *S. pombe* cells were collected from 10 ml YEL (grown at 30 ℃ for 12 hours), washed with 1 ml distilled water and collected by centrifuging at 3,500 rpm for 5 minute at 4 ℃. The pellet was suspended and incubated in 2 ml CSE (20 mM citrate-phosphate buffer, 50 mM EDTA at pH5.6 containing 0.9 M sorbitol) with lyticase (1 mg/ml, Sigma, catalogue no. L2524) at 37 ℃ for 15-30 minutes to generate spheroplasts. Cells were placed in 37 ℃ water bath for 15-30 minutes and presence of the spheroplasts was checked for by light microscope after adding 5 % SDS. After production of 90 % spheroplasts, cells were harvested by centrifuging at 3,500 rpm for 5 minute at 4 ℃. In parallel, 0.8 % (w/v) agarose was prepared by dissolving 0.8 g of agarose in 100 ml TSE (0.125 M EDTA, pH 7.5, 0.9 M sorbitol). The spheroplasts were resuspended in 100 µl of TSE and incubated in 37 ℃ water bath for 3 minutes the 133 µl of 0.8 % (w/v) agarose was added and the mixture was quickly placed into the plug mould. The gel plugs were solidified completely on ice for 5 minutes. Sliced gel plugs were first incubated in lysis buffer I (10 ml of 0.25 M EDTA, 0.05 M Tris-HC1, pH 7.5, 1 % SDS) at 50 ℃ for 1.5 hours then transferred into lysis buffer II (5 ml of 0.5 M EDTA, 0.05 M Tris-HCl, pH 9.5 containing 20 mg/ ml proteinase K) and incubated at 55 ℃ for 48 hours. Two conditions of electrophoresis for separating various sizes of chromosomes were used: 1.0 % of pulsed-field certified agarose (Bio-Rad) gel is useful in separating DNA molecules up to 2 Mb in size. The plugs were equilibrated in 0.5x

TBE buffer (45 mmol/l Tris, 45 mmol/l borate, 1.0 mmol/l EDTA, pH 8.3). 0.8 % agarose concentrations was used for separations of higher molecular weight DNA – 3 to 6 Mb. These plugs were equilibrated in 1x TAE buffer (40 mmol/l Tris, 40 mmol/l acetate, 2.0 mmol/l EDTA, and pH 8.0). The plugs were placed on each tooth of the comb, fixed with agarose and 150 ml 0.8 % or 1 % (w/v) agarose solution was poured into the mould. When gel was cooled to room temperature the casting the gel and the platform were slide in the electrophoresis cell. For separation of DNA molecules up to 2 Mb, the gels were electrophoresed in 0.5x TBE buffer and run for 24 hours at 6 V/cm with a 50 to 90 second switch time ramp at an angle of 120°. The buffer was recirculated at 14 ℃ in a CHEF-DR II system (Bio-Rad). For separation of 3 to 6 Mb DNA molecules, the gels were electrophoresed in 1x TAE buffer and the run time was 48 hours at 2 V/cm with 1,800 seconds switch time ramp at an angle of 100° with recirculation at 14 ℃.

2.3.8 Methods for studying fork-arrest induced chromosomal rearrangement at the *RTS1* barrier and synchronization of yeast strains using a lactose gradient

It has been previously reported from our laboratory that a fork-arrest system can stall replication at a non-histone protein/DNA complex – the *RTS1* barrier [49]. The yeast strain harbouring modified Ch^{16} that contains the fork-arrest system- *RuiuR* (see details in Chapter 3) was grown in YE media (where *nmt41* promoter was repressed) at 30 ℃ overnight and washed twice with distilled water to remove the remaining YE media. Induction of the transcript from RTF1 by thiamine supplement through the *nmt41* promoter took around 14 to 16 hours. $1.6x10^6$ cells were grown in 10 mL of EMM2 containing appropriate supplements in the presence (“pause off” growth) or absence (“pause on” growth) of thiamine at 30 ℃ for 16 hours. To accumulate cells in

the G_2 phase for imaging, a serial gradient of lactose concentrations were prepared as shown in Table 4, and l.5 ml of each diluents were added into a 15 ml Falcon tube in sequential order (from bottom layer 30 % to top layer 7 % (w/v) lactose concentrations). The induced cells (~1.5x 10^8 cells, OD_{600}= ~0.5) were placed on the top of the gradient and spun at 1,000 rpm at room temperature for 8 minutes. 400 µl of the top layer cells were collected as the G_2 phase cells and used for downstream applications.

Table 4. Preparation for lactose gradient

Adding order	30% Lactose (ml)	7% Lactose (ml)
1	10	0
2	8.75	1.25
3	7.5	2.5
4	6.25	3.75
5	5	5
6	3.75	6.25
7	2.5	7.5
8	1.25	8.75
9	0	10
10	1.5x 10^8 cells in 1 ml media	

2.3.9 Clone selection assay to determine rates of rearranged chromosome formation and mini-chromosome loss after rearrangement

The yeast strain containing modified Ch^{16} (Ch^{16}-NRUH *nmt-rtf1*$^+$, the strain CJ90, see detail in Figure 4-1B) was grown in YE at 30 ℃ overnight. To induce chromosomal rearrangement, cells were re-inoculated and grown in 10 ml EMM2 in the presence (“pause off” growth) or absence (“pause on” growth) of thiamine at 30 ℃ for 16 hours. Aliquots of 300 cells were spread on YEA plate and incubated for 2–3 days on 30 ℃.

To confirm the phenotype after colonies were formed cells were replica plated to YEA supplemented with Nat, YNBA containing Ura and YNBA containing His and Arg (all plates were supplemented by 30 mM thiamine, "pause off" growth). After incubation for 4–5 days at 30 ℃ the colonies were counted to determine the number of colonies with different phenotypes. The cells harbouring a Ch^{16}-NRUH were identified as the Nat^R Arg^+ Ura^+ His^+ phenotype. The rate of cells losing the full-length Ch^{16} was obtained from the number of the Nat^s Arg^- Ura^- His^- cells divided by Nat^R Arg^+ Ura^+ His^+ cells. The strain containing a dicentric chromosome showed the Nat^R Arg^+ Ura^+ His^- phenotype. The rate for cells that indicated the presence of a dicentric chromosome was obtained from the number of the Nat^R arg^+ ura^+ his^- divided by Nat^R arg^+ ura^+ his^+ cells. When a random breakage event occurred on a dicentric chromosome during cell division we observed three forms of chromosomes resulting in the Nat^R Arg^+ Ura^+ His^- (Type I phenotype of clone) or the Nat^R Arg^+ Ura^- His^- (Type II phenotype of clone) or the Nat^R Arg^- Ura^- His^- (isochromosome) phenotypes. The rate of each type of rearranged chromosome formation was calculated by the number of colonies divided by Nat^R Arg^+ Ura^+ His^+ cells. To determine the further rearrangement on the monocentric chromosomes derived from a dicentric ones, Nat^R Arg^+ Ura^+ His^- cells were cultured in the YE media at 30 ℃ for 24 hours, then 300 cells were spread on YEA. After colony formation, plates were replicated onto YEA supplemented with Nat, YNBA with Ura and YNBA with His and Arg (all plates contained 30 mM thiamine, "pause off" growth). A portion of cells were continuously cultured in YE media at 30 ℃ in the presence of thiamine ("pause off" growth) for 24 hours again and the procedure mentioned above was repeated for a period of 15 days. The rates of rearranged chromosome formation resulted from each number of different phenotype colonies divided by Nat^R Arg^+ Ura^+ His^+ cells.

2.4 Microscopy

To monitor the rearranged chromosomes 4.5 kb of *lacO* and 10 kb of *tetO* arrays were integrated to either side of the fork arrest site on the non-essential mini-chromosome (named as Ch^{16}-NRUH). Centromere proximal dots were marked with a *lacO*/LacI-GFP placed at ~110 kb from CEN3 at one side and ~55 kb from RTS1 barrier at the other side (Figure 3-13 A). To visualise the *lacO* elements, the LacI–GFP was expressed under the control of the fission yeast *Dis1* promoter. Telomere proximal spots were labelled with a *tet*O/TetR-tdTomato placed ~27 kb from RTS1 barrier. The TetR-tdTomato was expressed under the regulation of the *adh31* linked to *tet*O repeats. Following the localization of the fluorescently labelled the GFP and tdTomato fusion proteins enabled the dynamic analysis of chromosome rearrangements and movements.

2.4.1 Visualisation of fixed fission yeast cells

Induction of chromosomal rearrangement and synchronization of yeast strains using a lactose gradient were carried out as described above. Isolated G_2 cells were cultured in minimal media either with or without thiamine supplement. Aliquots were collected at regular time intervals (5 minutes), then 1/100 volume of 10 % sodium azide (Sigma-Aldrich, catalogue no. Aldrich-438456) and 1/10 volume of 0.5 M EDTA were added followed by incubation on ice for 5 minutes to stop cell growth. 1 volume of 10 μg/ml Hoechst 33342 stain (Invitrogen, catalogue no. H21492) was used to stain DNA at room temperature for 5 minutes. The cells were harvested by centrifugation at 1,500 rpm for 1 minute at room temperature. To fix the cell, the pellet was resuspended in 100 % pre-cooled methanol and centrifuged immediately at 1,000 rpm for 30 seconds at room temperature. Subsequent treatment with 100 % pre-cooled

acetone was added to resuspended cell pellet, centrifuged immediately at 1,000 rpm for 30 seconds at room temperature and aspirated supernatant. Cells were resuspended with the remaining acetone, spread onto the surface of a microscope slide and mounted with 1.2 % of LMT (low melting temperature) agarose/Tris-acetate (0.1M Tris adjusted to pH 8.5 with acetic acid). Coverslips were applied and sealed with nail polish and cells were observed at room temperature using a DeltaVision deconvolution light microscope Core system. Two-colour imaging, excitation and emission of the fluorescent proteins were performed using a dual-band filter set of FITC-TRITC for the GFP (FITC 470/560 filters for excitation/ emission) and the tdTomato (TRITC 550/620 filters for excitation/ emission) fluorescence. The images for showing Hoechest dye staining to visualise the nucleus using DAPI filters (DAPI 350/460 filters for excitation/ emission). The GFP fluorescence images were acquired with an exposure setting of 0.5 s, whereas tdTomato fluorescence images were obtained with an exposure setting of 0.2 s. A single bright-field polarizing (Pol) image was collected at 0.2 s exposure time. The images for showing Hoechest dye staining was acquired at 0.01 s exposure time. Five z-axis images for all data points were acquired at a step size of 0.4 μm through the cell, deconvolved (the deconvolved parameters shown in Table 5) and projected into a single reconstruction image with the use of softWoRx software. Following are the conditions used for camera: Model is CoolSNAP_HQ2 / HQ2-ICX285, gain is 1.00 X, speed is 10000 KHz and temp setting is at -25 ℃.

Table 5. Optical parameters used for deconvolution of fixed imaging experimental point	
Size (X, Y, Z)	512, 512, 5
Size (W, T)	4, 1
Sequence	W -> Z -> T
Pixel Size (dX, dY, dZ)	0.065, 0.065, 0.400
Wavelengths (nm)	-50.00, 525.00, 605.00, 455.00
Min, Max, Mean (w=-50.0 nm)	149.00, 285.00, 202.85
Min, Max, Mean (w=525.0 nm)	102.00, 232.00, 571.63
Min, Max, Mean (w=605.0 nm)	107.00, 1205.00, 657.19
Min, Max, Mean (w=455.0 nm)	94.00, 271.00, 513.23
Rotation Angles (alpha, beta, gamma)	0.00, 0.00, 0.00
Extended Header Size (bytes)	4096
Extended Header Type	4

2.4.2 Time-lapse imaging of living fission yeast cells

For live cell imaging synchronous G_2 phase cells were continuously grown in minimal media either with or without thiamine supplement on 30 ℃ in Lab-Tek chambers (Thermo Scientific, catalogue no. 154526) wells (1.3x 10^5 cells/well) that had been coated with 1 mg/ml Concanavalin A-rhodamine (ConA) (Sigma-Aldrich, catalogue no. C5275) for 1 hour. Chambers were pre-equilibrated for 20 min and filmed on a DeltaVision Personal DV deconvolution light microscope system equipped with a temperature controller (30 ℃). Images were recorded at up to twenty pre-programmed positions with 90 s intervals for a period of 30 min to 2 hours (mitosis). Time-lapse acquisitions of optical Z-series of ten frames were separated by a step size of 0.4 μm for each pre-programmed position. A dual-band filter set of

Table 6. Optical parameters used for deconvolution of live cell imaging experimental point	
Size (X, Y, Z)	512, 512, 10
Size (W, T)	3, 32
Sequence	W -> Z -> T
Pixel Size (dX, dY, dZ)	0.129, 0.129, 0.400
Wavelengths (nm)	-50.00, 528.00, 617.00
Min, Max, Mean (w=-50.0 nm)	1216.00, 1720.00, 1268.58
Min, Max, Mean (w=528.0 nm)	1282.00, 2013.00, 432842.69
Min, Max, Mean (w=617.0 nm)	1205.00, 1454.00, 400394.31
Rotation Angles (alpha, beta, gamma)	0.00, 0.00, 0.00
Extended Header Size (bytes)	294912
Extended Header Type	4

FITC-TRITC was used for the GFP and tdTomato fluorescence proteins. We also used transmitted polarizing filters (differential interference contrast, DIC) for transmitted light images controlled by the softWoRx software. Exposure time was set at 50 ms for GFP, tdTomato and DIC channels. Following are the conditions used for camera: Model is Cascade2_1K EMCCD / E2V CCD-201, gain is 4.00 X, speed is 10000 KHz and temp setting is at -55 ℃. The images were deconvolved (the deconvolved parameters shown in Table 6) and projected into a single reconstruction image with the use of the softWoRx software.

2.4.3 Image presentation

All image analysis was accomplished by the softWoRx software. Images were deconvolved (the deconvolved parameters shown in Table 5 and 6) and subsequently used to project all data points for an entire collected sequence of stacks from starting and ending Z section using the softWoRx image analysis software. The ImageJ macro tool was used to determine the positions between marker arrays (http://rsbweb.nih.gov/ij/macros/tools/). All collected data was processed by Adobe Photoshop 9 and exported into Microsoft Excel and Microsoft PowerPoint for the analysis of the localizations.

CHAPTER 3

ESTABLISHMENT OF MINI-CHROMOSOME SYSTEM

3.1 Introduction

The aim of the project was to directly visualise the formation of the dicentric and acentric palindromic chromosomes and their fate using the *lacO*/LacI-GFP and *tetO*/TetR-Tomato integrated on either side of a fork arrest site on the non-essential mini-chromosome. Previous studies from our laboratory used a fork-arrest system – either *RuraR* or *RuiuR* – present on the essential chromosome III. To control replication fork arrest the thiamine-repressible promoter (*nmt41*) was inserted upstream of *rtf1*$^{+}$ gene to regulate the *rtf1* transcription and thus Rtf1 protein levels. It was demonstrated that the *RuraR* and *RuiuR* systems induced replication fork stalling when the Rtf1 protein was bound to *RTS1*. Subsequently the stalling fork can lead to a recombination event and form chromosomal rearrangements. Conversely, in the absence of the Rtf1 protein, replication forks can pass through *RTS1* sequence and replicate it normally. A limitation of the original systems was that Rtf1 protein induced chromosome III rearrangements which rapidly caused the loss of cell viability. It was thus difficult to understand the mechanism and events beyond the first cell cycle. Hence, we changed the location of the experimental construct to the non-essential mini-chromosome. This allowed me to directly monitor chromosome behaviour *in vivo* by following the movement of the GFP and tdTomato foci without (or very slight) viability loss.

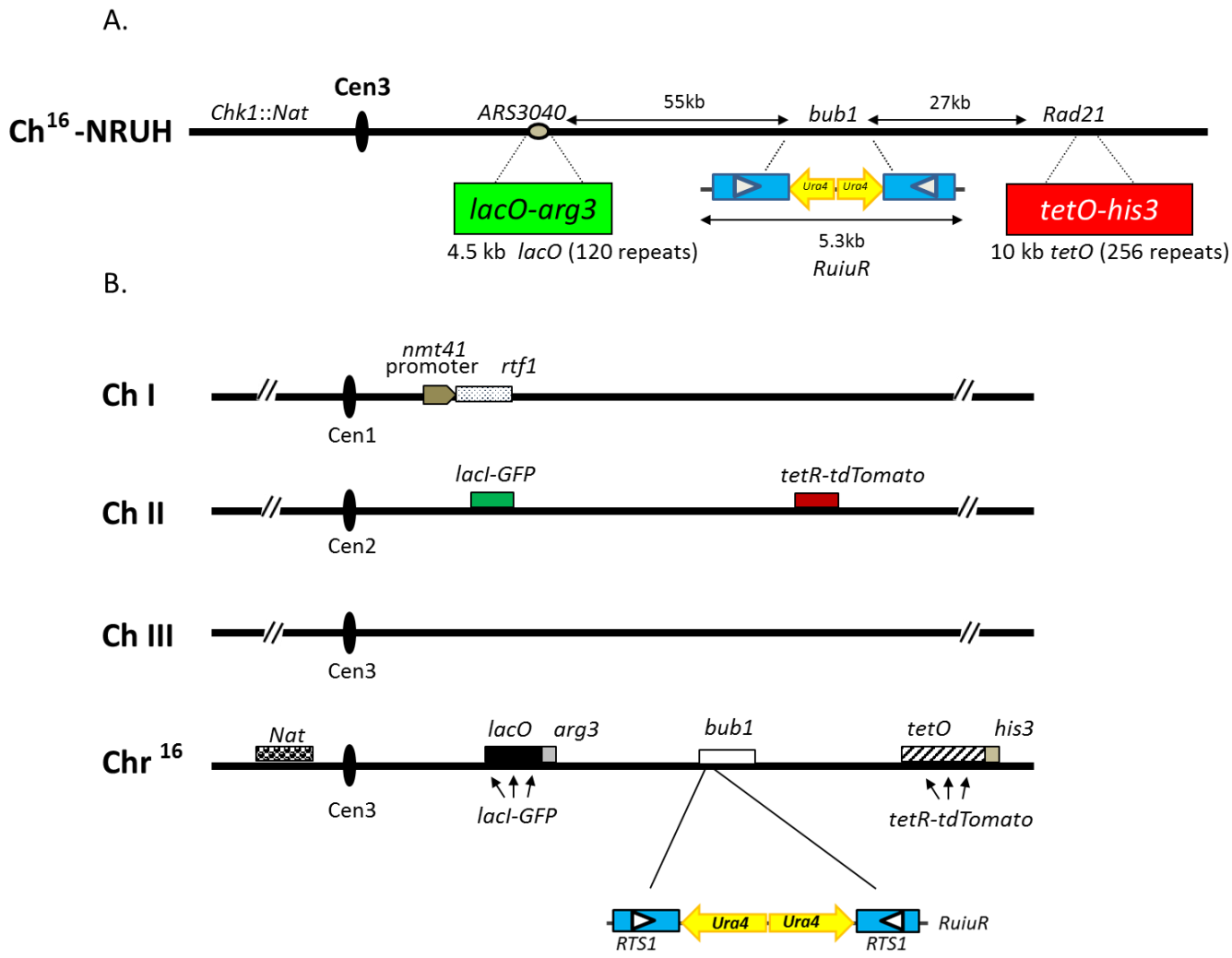

Figure 3-1. Model of the constructs on the mini-chromosome in the experimental *S. pombe* strain. (*A*) Schematic representation of the mini-chromosome construct (Ch^{16}-NRUH). The *Nourseothricin* (*Nat*) gene was introduced into the *chk1* locus as the selectable marker. The 4.5 kb *lacO* repeats with the *arg3*$^{+}$ gene is located at ARS (3040) and the 9 kb *tetO* repeats with *his3*$^{+}$ gene replaced *rad21*. The fork arrest system (*RuiuR*) was inserted to replace the upstream part of the *bub1* gene. (*B*) Schematic of the desired yeast construct for the following experiments. To regulate *rtf1*$^{+}$ expression the original *rtf1* promoter on chromosome I was replaced by *nmt41*. The *lacI-gfp* and *tetR-tdtomato* were established on chromosome II.

3.2 Establishment of the mini-chromosome system

The experimental yeast model is proposed to contain all the following genes: 1. A *nourseothricin* (*Nat*) resistance gene is used either as a selectable marker for either the presence of intact Ch^{16} or rearranged form products while chromosomal rearrangements occurring; 2. Fluorescently marked chromosomal loci. Tetracycline operator (*tetO*) repeats and lactose operator (*lacO*) repeats; 3. A fork-arrest system. *RuiuR* sequence on the Ch^{16}-NRUH (Figure 3-1 A); 4. The *lacI-gfp* and *tetR-tomato* fusion genes on chromosome II; 5. The *nmt41* promoter replacing the *rtf1* promoter on chromosome I to enable regulation of the replication fork stalling in a controllable manner on the mini-chromosome (Figure 3-1B). To save time, I established two *S. pombe* construct strains in parallel (stain I and II) and these strains were crossed to generate the final experimental yeast construct (Figure 3-2).

To construct strain I: I inserted *nourseothricin* (*Nat*) and *kanamycin* (*Kan*) resistance genes into either arms of the mini-chromosome as the selectable markers. We used the flexibility of the Cre/lox system and introduced a "base strain (named as Ch^{16}-NRUH)" locus which contains Kan^R gene flanked by incompatible loxP/loxM sites. This allowed us to subsequently replace this locus with any DNA sequence we wish by the Cre/lox site-specific recombinase-mediated cassette exchange (RMCE) [127] (see details below). In this project we replaced it with a fork-arrest system (*RuiuR*). However, our previous studies showed that the fork-arrest system may slightly induce chromosomal rearrangements due to spontaneous cruciform extrusion and hence we decided to integrate the fork-arrest system using RMCE method at the last step. To obtain the two fluorescently targeted genetic regions, the *tetO* repeats with an auxotrophic a $his3^+$ gene marker were inserted at the *rad21* locus and the

lacO repeats with an *arg3*$^{+}$ gene marker were integrated at the autonomously replicating sequence-*ars* sequences (3040) (Figure 3-1 A).

Strain II is proposed to bear the *nmt41* promoter instead of *rtf1*promoter in order to control Rtf1 expression and also contains a system for visualizing the chromosomal behaviour via the expression of the fusion proteins LacI-GFP and TetR-tdTomato from the chromosome II of *S. pombe*. The yeast strain which encompasses fusion genes of *lacI-gfp* and *tetR-tdTomato* on chromosome II has previously been established and was provided by Dr. Takeshi Sakuno. Using this strain, I replaced the *rtf1*promoter with *nmt41* promoter on chromosome I, generating the final strain II. After these genetic integrations, strain I and II were crossed to produce the "base strain (named as Ch^{16}-NRKH)" (Figure 3-2). In the final step, a RMCE method was carried out and recombination occurred between the lox sites, allowing the loxP-*Kan*^{R}-loxM cassette of the base strain (Ch^{16}-NRKH) to be exchanged by the loxP-*RuiuR*-loxM cassette (located on the donor plasmid), generating the stain containing Ch^{16}-NRUH (Figure 3-2).

Figure 3-2. Schematic representation of the *S. pombe* constructs.

Strain I contained the following genes on Ch[16]: *nourseothricin* (*Nat*) resistance gene, *kanamycin* (*Kan*) resistance gene flanked by loxP/loxM3 sites (P: loxP site and M3: loxM3), the *tetO* repeats with a *his3*$^{+}$ gene and the *lacO* repeats with an *arg3*$^{+}$ gene. Strain II contained the *nmt41* promoter which replaced *rtf1* promoter on chromosome I, the *lacI-gfp* and *tetR-tdtomato* fusion genes located on chromosome II. After crossing strains I with II and selecting for the appropriate construct, the loxP- *Kan* ^{R}-loxM3 was replaced by the fork arrest system (*RuiuR*) using Cre recombinase-mediated cassette exchange. Note that all genes on the mini-chromosome were non-essential as they were also present on Chromosome III.

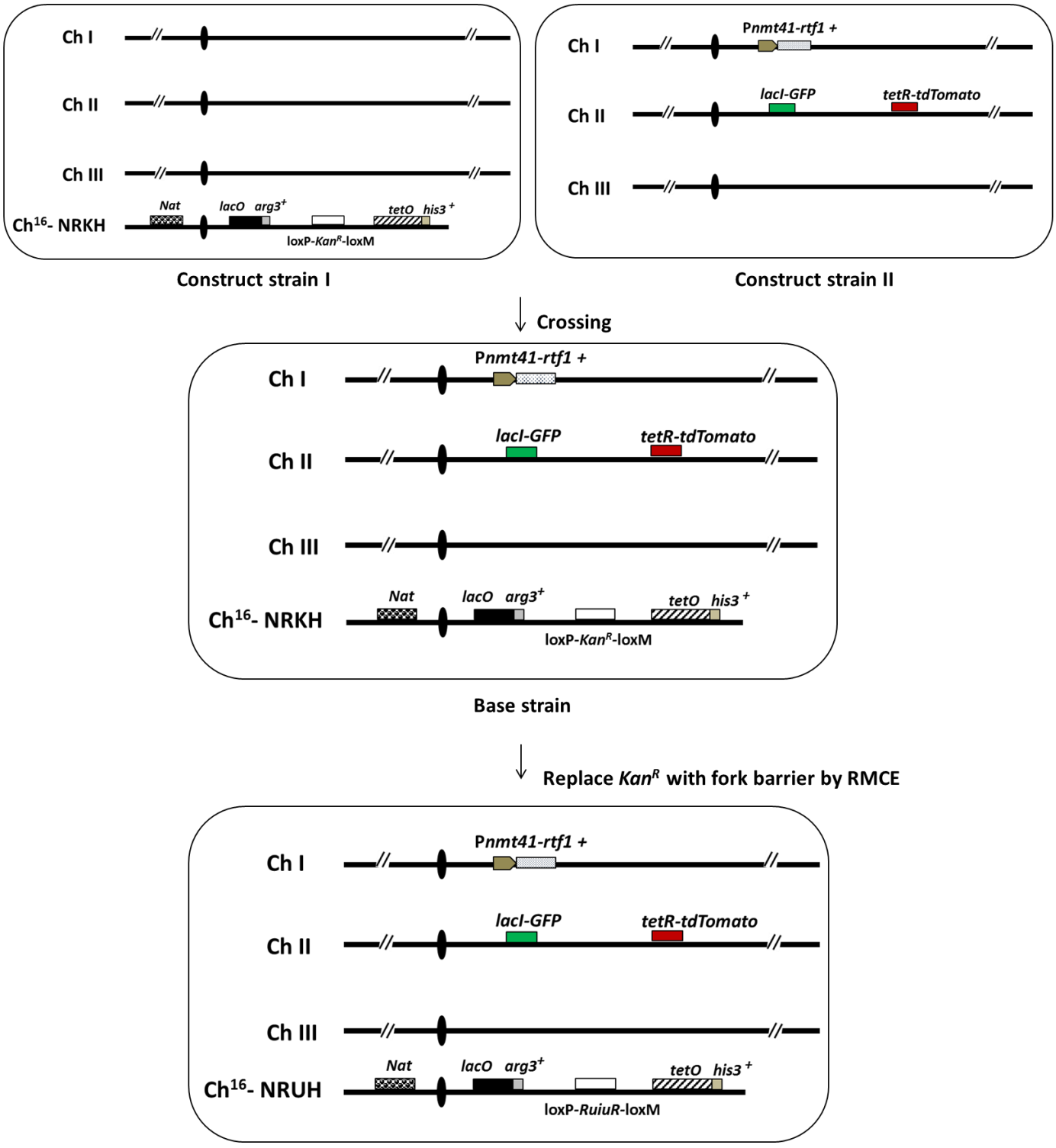
Ch I
Ch II
Ch III
Ch16- NRKH
Nat
lacO arg3+
tetO his3+
loxP-KanR-loxM
Construct strain I
Pnmt41-rtf1 +
lacI-GFP
tetR-tdTomato
Construct strain II
Crossing
Base strain
Replace KanR with fork barrier by RMCE
Ch16- NRUH
loxP-RuiuR-loxM

3.2.1 Construction of strain I

3.2.1.1 Transformation of the nourseothricin gene into mini-chromosome of S. pombe

The *nourseothricin* (*Nat*) resistance gene was integrated as a selection marker for indicating the presence of the mini-chromosome. Nat^R gene was integrated into CJ01 (*ade6-m210, arg3-D4, his3-D1, leu1-32, ura4-D18, chr16, ade6-m216*). To verify the correct integration of a Nat^R gene at *chk1* locus locus on the mini-chromosome rather than on chromosome III we used chromosome loss assay, restriction fragment length analysis (RFLA) and pulsed field gel electrophoresis. For the chromosome loss assay nat^+ yeast cells were spread on YNBA containing 10 mg/ml adenine. White colonies contained both chromosome III (which had the *ade6-210* mutation) and the mini-chromosome (which had the *ade6-216* mutation) because of the inter-genetic complementation between *ade6-210* and *ade6-216* results in the ability to produce adenine. Pink colonies represented cells where the mini-chromosome has been lost: when the *ade6-216* allele was lost together with the mini-chromosome the cells were unable to produce adenine and a red coloured metabolic intermediate accumulated in the cytocole. The pink colonies were streaked to form single colonies. The five representative pink colonies for each strain were patched on YNBA containing 10 mg/ml Adenine. The five colonies were replicated on YNBA supplemented with Nat (Figure 3-3A and B). If Nat^R gene was inserted correctly into the mini-chromosome pink colonies could not grow on YNBA with Nat. These strains were collected for further experiments (Figure 3-3 C, red square).

Subsequently, the strains that have introduced the Nat^R gene on the mini-chromosome were confirmed to have site-specific integration by RFLA. In a control strain (C) without an integrated Nat^R gene after digestion with *Hinc*II or *Acc*I only one band was detectable at either 4.2 kb or 2.3 kb, respectively, with the probe A (targeting the

region upstream the integration place of the *Nat*^{R} gene cassette). If the *Nat*^{R} gene had replaced *chk1* loci, two bands should appear at 4.2 kb and 2.5kb for *Hinc*II and 4kb and 2.3 kb for *Acc*I digestion by the probe A. 8 colonies were tested for the presence of the mini-chromosome with *Nat*^{R} integration by RFLA (Figure 3-4B). Finally, five out of these strains were used to further verify the correct site-specific integration on the mini-chromosome using the pulsed field gel electrophoresis (PFGE) combined with a Southern blot hybridization. This demonstrated whether the *Nat*^{R} gene was located on the mini-chromosome. The agarose gel staining with Ethidium bromide (EtBr) shows the position of chromosome I, II, III and the mini-chromosome (Ch^{16}). Except for colony no.5, chromosome III and Ch^{16} can be detected using the probe A (Figure 3-4C, middle panel). Similarly, in sample 1 to 4, the probe B (probe recognizing the ORF of the *Nat*^{R} gene) hybridised to the mini-chromosome demonstrating that these colonies represent the desired strain (Figure 3-4C, right panel). These colonies were named CJ06, CJ07, CJ08 and CJ09 (*ade6-m210, arg3-D4, his3-D1, leu1-32, ura4-D18, chr16, ade6-m216, chk1::natMX6*), and CJ06 was used for the further experiments. The starting strain without *Nat*^{R} gene integration as control showed no signal detected by the probe B. The band present on colony no. 5 has been elusive and may be caused by chromosome translocation between chromosome III and Ch^{16}.

Figure 3-3. Integration of nourseothricin resistance gene into *S. pombe* construct strain I

(*A*) After transformation of *nourseothricin* (*Nat*^{R}) resistance gene into *S. pombe* it may be integrated on either chromosome III or Ch^{16} because they contain partial homologous sequence. (*B*) Integration of the *Nat*^{R} gene was confirmed by chromosome loss assay. After the *Nat*^{R} gene transformation, the yeast cells were cultured in liquid YE medium. Cells were then spread on YNBA supplemented with 10 mg/ml adenine. If the cells had lost their mini-chromosome and only contained *ade-210* allele on chromosome III, adenine synthesis was halted and during the process cells accumulated a red pigment as a metabolic intermediate. Pink colonies, which presumably had lost their mini-chromosome were firstly patched on YNBA with 10 mg/ml adenine. The phenotype was checked using replica plated on YNBA with 100 μg/ml Nat. (*C*). Enlarged picture of YNBA Nat plates with replica plated pink colonies. Top panel in red square shows the desired strain containing the *Nat*^{R} gene integration on Ch^{16} – i.e. cells that did not grow on YNBA with 100 μg/ml Nat without the mini-chromosome. However, if the *Nat*^{R} gene integrated on chromosome III cells were able to grow on YNBA with Nat even after the loss of Ch^{16} (ade$^-$ pink strains) as the bottom four panels shown.

A.

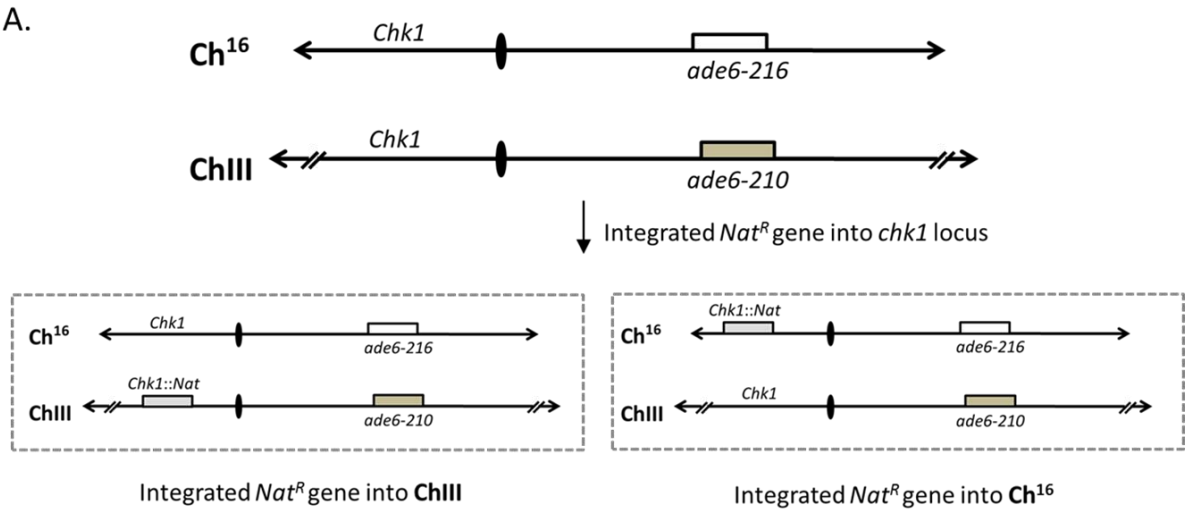

B.Chromosome Loss Assay

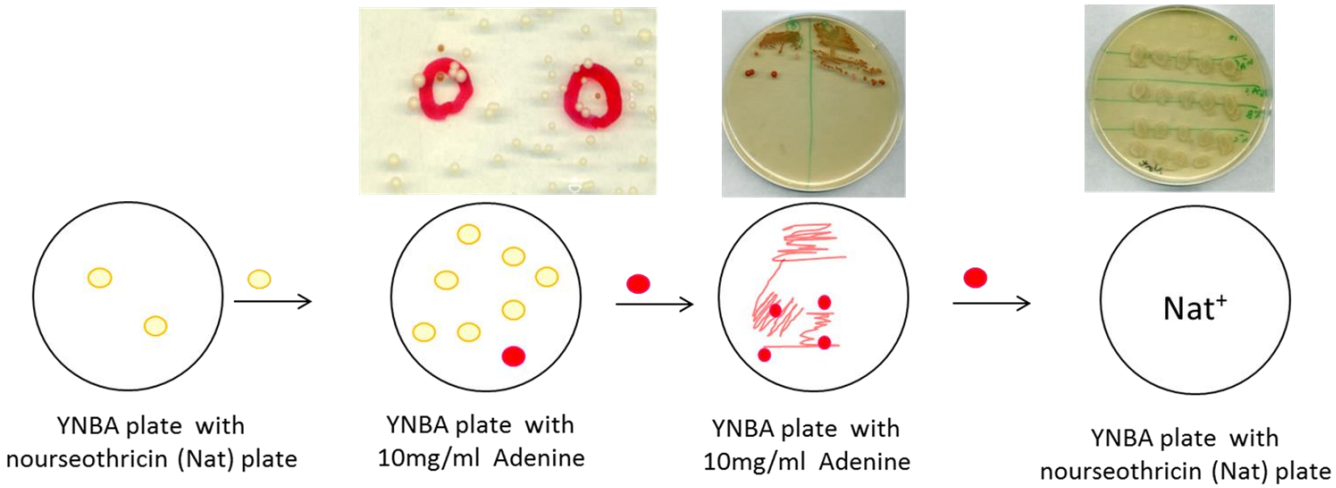

C.

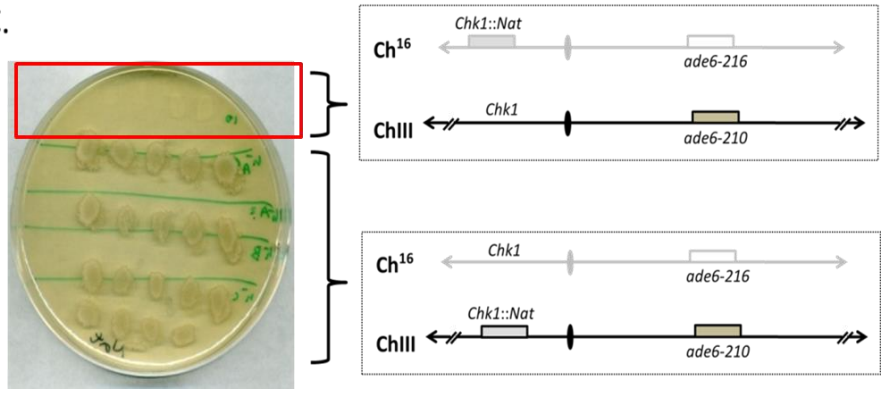

Figure 3-4. Integration of the Nourseothricin resistance gene into *S. pombe*.

(*A*). Positions of the probes used in a Southern blot hybridization are shown as filled blocks under Chromosome III and Ch^{16}. Fragment lengths after *Hinc*II and *Acc*I digestion at the *chk1*gene locus before and after replacement with Nat^R are shown. (*B*). Restriction Fragment Length Analysis (RFLA) combined with a Southern blot hybridization. If the Nat^R gene was integrated into the *chk1*gene locus a band at 2.5 kb for *Hinc*II and 4 kb for *Acc*I digestion was visible by the probe A (targeting the region outside of integrated the Nat^R gene cassette). M: DNA ladder marker. 1-8: strains tested for the Nat^R integration. C: Control; the strain CJ01 which was without the Nat^R gene integration. (*C*). Pulsed Field Gel Electrophoresis (PFGE). The agarose gel staining with EtBr (left panel) indicates the position of chromosome I, II, III and Ch^{16}. Except for no. 5, the probe A hybridised to both chromosome III and Ch^{16} (middle panel) in every colony. In colony no. 1 to 4 the mini-chromosome were detected by the probe B (probe targeting the ORF of the Nat^R gene) (right panel). C: Control; the strain CJ01 which was without the Nat^R gene integration.

A.

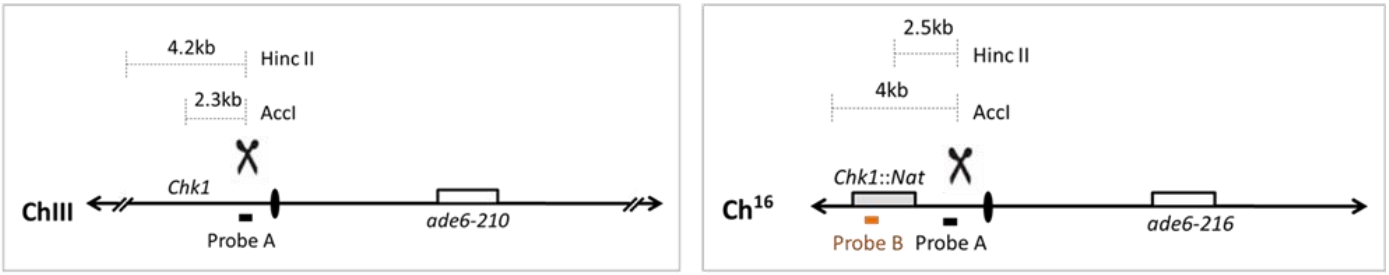

B.

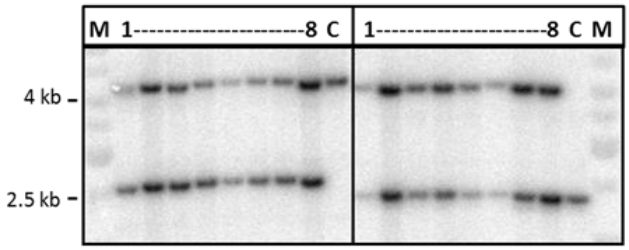

Expected fragment sizes (in kb)

	chk1	NAT
HincII	4.2	2.5
AccI	2.3	4

C.

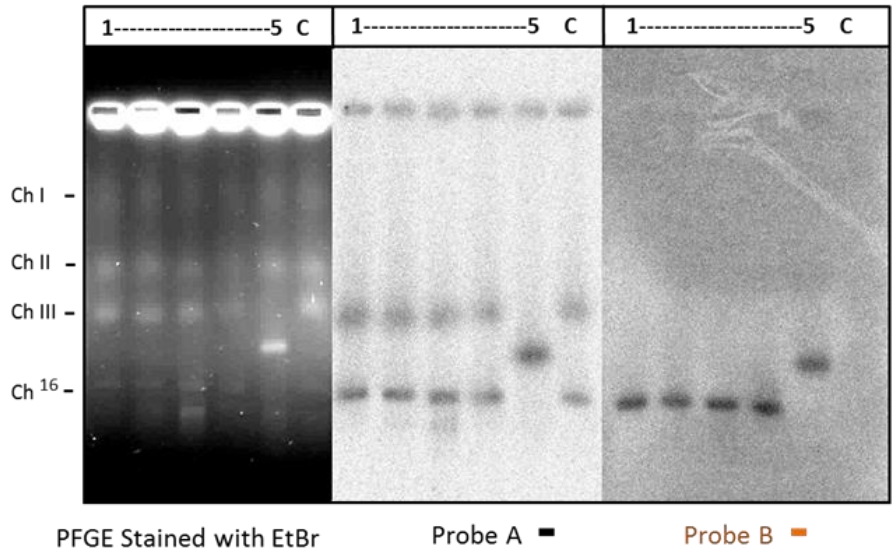

3.2.1.2 Integration of the Kanamycin (Kan^R, G418^R) gene into the mini-chromosome of S. pombe

The yeast strain CJ06 (*ade6-m210, arg3-D4, his3-D1, leu1-32, ura4-D18, chr16, ade6-m216, chk1::natMX6*) was used to integrate a *kanamycin* (*Kan^R, G418^R*) resistance gene to replace the upstream (200bp) part of *bub1* gene [128]. This had two functions, one is to make sure to obtain the right arms of mini-chromosome and the other is to provide the base construct to enable the induction of various replication stall systems later on, using a RMCE method (seen in section 3.3). The *Kan^R* gene flanked by loxP and loxM3 (termed loxP-*Kan^R*-loxM3 cassette) was amplified by PCR with flanking primers with homology designed to target the *bub1* loci, enabling homologous recombination to this site. Creating the base strain involved the replacement of the upstream part of *bub1* gene coding sequence with the loxP-*Kan^R*-loxM3 cassette. The loxP-*Kan^R*-loxM3 cassette integration on the mini-chromosome was identified using chromosome loss assay and verified by a RFLA and a pulsed field gel electrophoresis (PFGE). Firstly, yeast cells which have both resistance for Nat and Kan were chosen. To confirm that the *Nat^R* and *Kan^R* genes were located on Ch^{16} instead of chromosome III, a chromosome loss assay was used. In the desired strains, if the mini-chromosome was lost – indicated by pink colony formation - cells could not grow on YNBA with Nat and Kan. Ten colonies were collected for checking by a RFLA and a PFGE (Figure 3-5A to C). Subsequently, the strains that had introduced the *Nat^R* and *Kan^R* gene on the mini-chromosome were also tested by RFLA (Figure 3-5B). For the strain CJ06, which had only the *Nat^R* gene on its mini-chromosome, a single band was visible at 1 kb after *Ava*I digestion followed by probing with the probe C (targeting a region outside of *bub1* gene and has recognition site on both ChrIII and Chr16). When the *Kan^R* gene replaced the loci at *bub1* on the mini-chromosome a 1 kb and a 1.8 kb fragments were detected after

*Ava*I digestion by probing with the probe C. In parallel, the seven candidates were also tested by a PFGE combined with a Southern blot hybridization to prove that the *Nat*^{R} and *Kan*^{R} genes were located unerringly on the mini-chromosome (Figure 3-5C). Chromosome III and Ch^{16} of all candidates were detected using the probe A (Figure 3-5C, middle panel). As a control we used the strain without the *Kan*^{R} gene integration. No signal was shown using the probe D (probe targeting the ORF of the *Kan*^{R} gene) (Figure 3-5 C, right panel). Failure to integrate the *Kan*^{R} genes in candidates 1 and 2 resulted in no signal when hybridised by the probe D. Four candidate revealed that integration of the *Kan*^{R} genes occurred on chromosome III. In sample 3, 5, 6 and 7, the probe D was able to hybridise to the mini-chromosome. These strains were named as CJ13, CJ17, CJ18 and CJ24 (*ade6-m210, arg3-D4, his3-D1, leu1-32, ura4-D18, chr16, ade6-m216, chk1::natMX6, bub1::loxP-kanMX6-loxM3*) and which was used for further experiments.

Figure 3-5. Integration of the kanamycin resistance gene into the mini-chromosome of *S. pombe* (*A*). Positions of the probes used in a Southern blot hybridization are indicated as filled blocks on Chromosome III and Ch^{16}. DNA fragment lengths after *Ava*I digestion of the *bub1* gene locus and the *bub1* gene locus where the first 200 bps were replaced by the Kan^R gene are presented. (*B*). The Kan^R gene that was integrated at the *bub1* locus showed a band at 1.8kb with *Ava*I digestion and was detected by the probe C (probe flanking the region outside of bub1 gene). M: DNA ladder. C: Control, the strain CJ06 which is without the Kan^R gene integration. (*C*). Pulsed Field Gel Electrophoresis (PFGE). The agarose gel staining with EtBr indicates the position of chromosome I, II, III and Ch^{16} (left panel). In all tested colonies chromosome III and Ch^{16} were detected by the probe A (probe targeting the region outside of the Nat^R gene integration) (middle panel). In colonies no. 3, 5 to 7 the probe D (probe targeting the Kan^R gene) hybridised on the mini-chromosome (right panel). C: Control, the strain CJ06 which is without the Kan^R gene integration.

A.

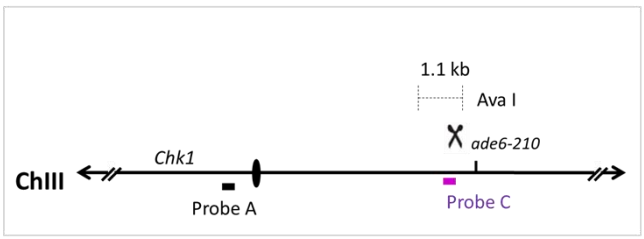

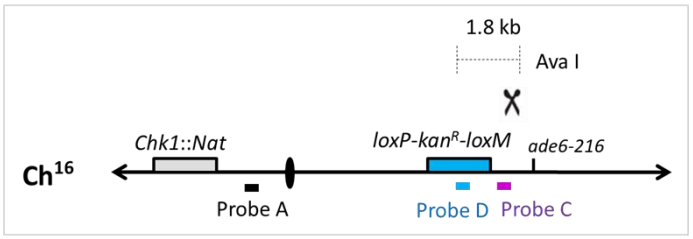

B.

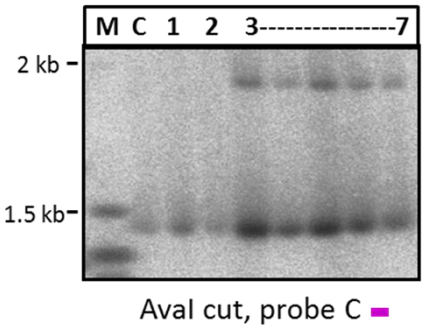

Expected fragment sizes (in kb)

	bub1	Kan
AvaI	1.1	1.8

C.

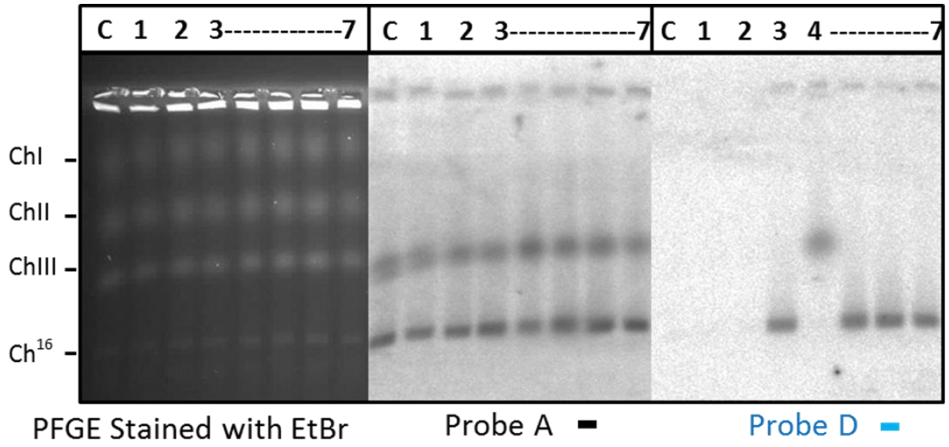

3.2.1.3 Integration of the tetO and lacO repeats into the mini-chromosome of S. pombe

1. Plasmid construction for the tetO and LacO Fragments

The *tetO* and *lacO* array have been developed as useful tools to visualise genomic changes microscopically. Here, 256 (around 9 kb) of *tetO* repeats and 120 (around 4.5 kb) of *lacO* repeats were used to fluorescently mark chromosomal loci on either side of the fork-arrest site on Ch[16]. Two specific vectors, pRHR and pRAS, were created based on pUC19 for subsequent the *tetO* and *lacO* repeat integration. During establishment of these vectors, a fusion fragment consisting of an auxotrophic marker gene flanked with homologues region sequences for the targeted locus was firstly established using PCR-based amplification (Figure 3-6). Subsequently, the fusion fragments of the *tetO* insertion from the pRHR plasmid were cloned into *Sal*I sites of pUC19. This contained the *his3*$^{+}$ marker flanked by upstream and downstream homologue sequences of *rad21*. For the *lacO* pRAS plasmid was used. This contained the *arg3*$^{+}$ marker flanked by upstream and downstream homologue sequence of *ars* (3040) cloned into *Sac*I sites of pUC19.

Originally, for fusion PCR, 60 bp overlapping regions between the marker and homologue region sequence containing specific restriction enzyme sites were designed. However, the fusion PCR was not successful. Thus, the overlapping region between the upstream homologous sequence and the marker gene was extended from 60 bp to 500 bp (Figure 3-6). Construction of the plasmid is summarized in three steps: (1) Amplification of four fragments including a. 500 bp upstream homologue sequence for *rad21;* b. 500 bp upstream part of *his3*$^{+}$; c. full-length *his3*$^{+}$ gene; and d. 500 bp downstream homologues sequence of *rad21* ; (2) A two-step fusion PCR. To combine the upstream homologues sequence with 500 bp upstream part of *his3*$^{+}$

maker a primary fusion PCR was used. Next, the resulting fragment from the primary fusion PCR, that contained upstream homologous sequence and 500 bp upstream part of *his3*$^{+}$ gene, was mixed together with the full-length *his3*$^{+}$ gene and the downstream homologue sequence and fused by the secondary fusion PCR; and (3) Cloning of the fused fragment into pUC19 vector. The resulting plasmid was named pRHR. The same protocol (with adding different template fragments) was used to construct the vector for the *lacO* repeats, named pRAS.

The 256 (around 9 kb) repeats of the *tetO* sequence was obtained from pLAU44 (provided by Dr. Takashi Morishita). There were 10 bp of different random sequences inserted between each and every *tetO* (19 bp) site (Figure 3-7A). It is expected that 10 bp spacers interspersed heterogeneously and thus reduced substantially the recombination and replication instability of the *tetO* sequence in *E. coli* and yeast [119]. The 9 kb *tetO* repeats also include a *gentamycin* resistance (*Gm*^{R}) antibiotic resistance marker positioned in the middle of the 9 kb *tetO* fragment. The 9 kb *tetO* fragment was obtained from pLAU44 after digesting with *Nhe*I and *Xba*I. The *tetO* fragment and the *Sal*I site of pRHR vector were modified by T4 DNA polymerase to convert them into blunt ends. Finally, the 9 kb *tetO* fragment was cloned into the modified *Sal*I site of pRHR vector (Figure 3-7B). The liner of *tetO* fragment was produced from pRHR-9kb tetO that was treated with *Not*I and subsequently transformed into *S. pombe*.

For 120 (around 4.5 kb) repeats of the *lacO* sequence, 10 bp of different random sequence was inserted between each and every *lacO* (21 bp) site to stabilise the lacO repeats [119] (provided by Dr. Takashi Morishita) (Figure 3-8A). The 4.5 kb *lacO* fragment, which also contained the *kanamycin* resistance (*Km*^{R}) antibiotic resistance

marker, was obtained from pLAU43 after firstly digesting with *Nhe*I and subsequently treated this fragment with T4 DNA polymerase to convert it into blunt ends. Finally, 4.5 kb *lacO* fragment was subcloned into *Sac*I site of pRAS vector (Figure 3-8B). The final liner *lacO* fragment was generated from pRAS-4.5kb lacO, using *Not*I digestion and subsequently transformed into *S. pombe*.

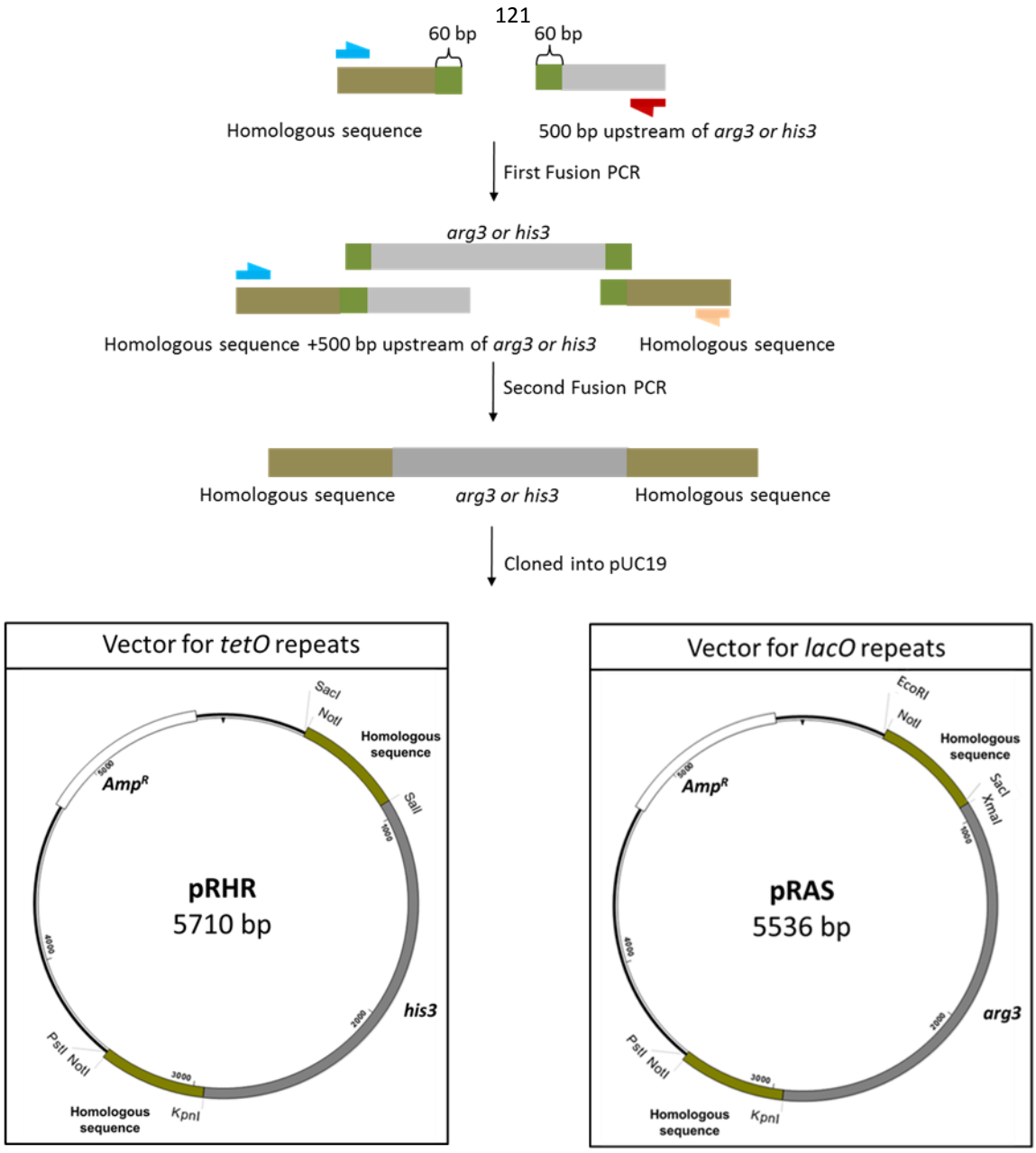

Figure 3-6. Plasmids created for the *tetO* and *lacO* fragments.

Construction of pRHR plasmid. The overlapping region between the upstream homologues sequence of *rad21* and the *his3*$^{+}$ gene was extended from 60 bp to 500 bp by the first fusion PCR. The second fusion PCR generated a fused fragment that contained *his3*$^{+}$ gene flanked by homologues sequence of *rad21* and this was then subcloned it into the *Sal*I sites of pUC19. The new vector for the *tetO* was named pRHR. The construction of pRAS for the *lacO* insertion: pRAS was created with the same method to produce a fused fragment that contain *arg3*$^{+}$ gene flanked by homologues sequence of *ars (3040)* and subsequently it was cloned into the *Sac*I sites of pUC19.

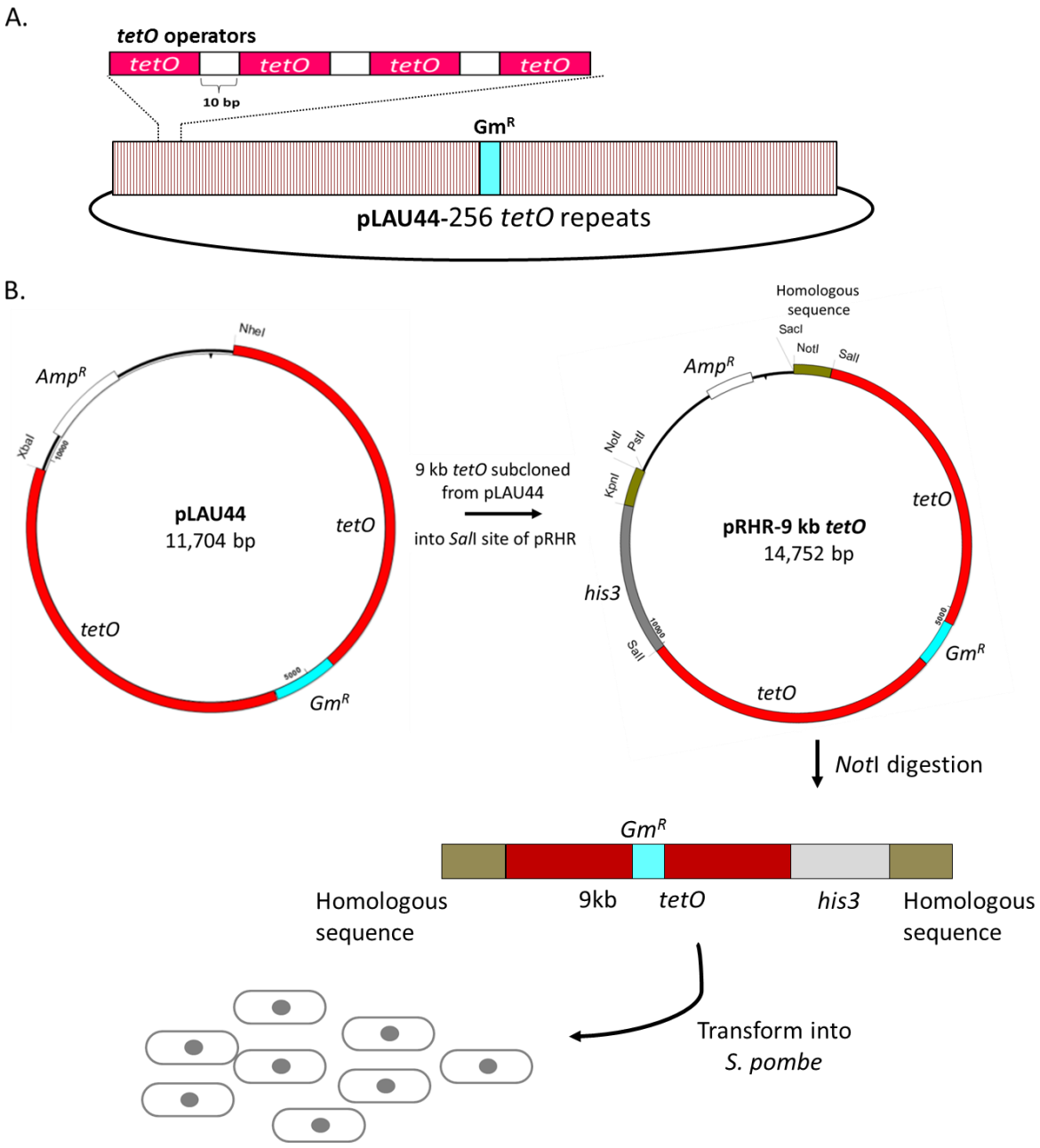

Figure 3-7. Schematics of the construction of the *tetO* repeats for transformation.

(*A*) The plasmid, pLAU44 contains the 256x (9 kb) repeats of *tetO* sequence with 10 bp of different random sequence inserted between each and every *tetO* (19 bp). (*B*). The 9 kb *tetO* fragment including the *gentamycin* resistance (Gm^R) antibiotic resistance marker positioned in the middle of the 9 kb *tetO* fragment was produced from pLAU44 after digesting with *Nhe*I and *Xba*I. Afterwards, the 9 kb *tetO* fragment and the *sal*I digested pRHR vector were modified by T4 DNA polymerase to convert the restriction ends into blunt ends. The final liner *tetO* fragment was then cloned into pRHR. The resulting plasmid – pRHR-9kb tetO – was used to generate the final *tetO* fragment by digestion with *Not*I. This fragment was subsequently transformed into *S. pombe.*

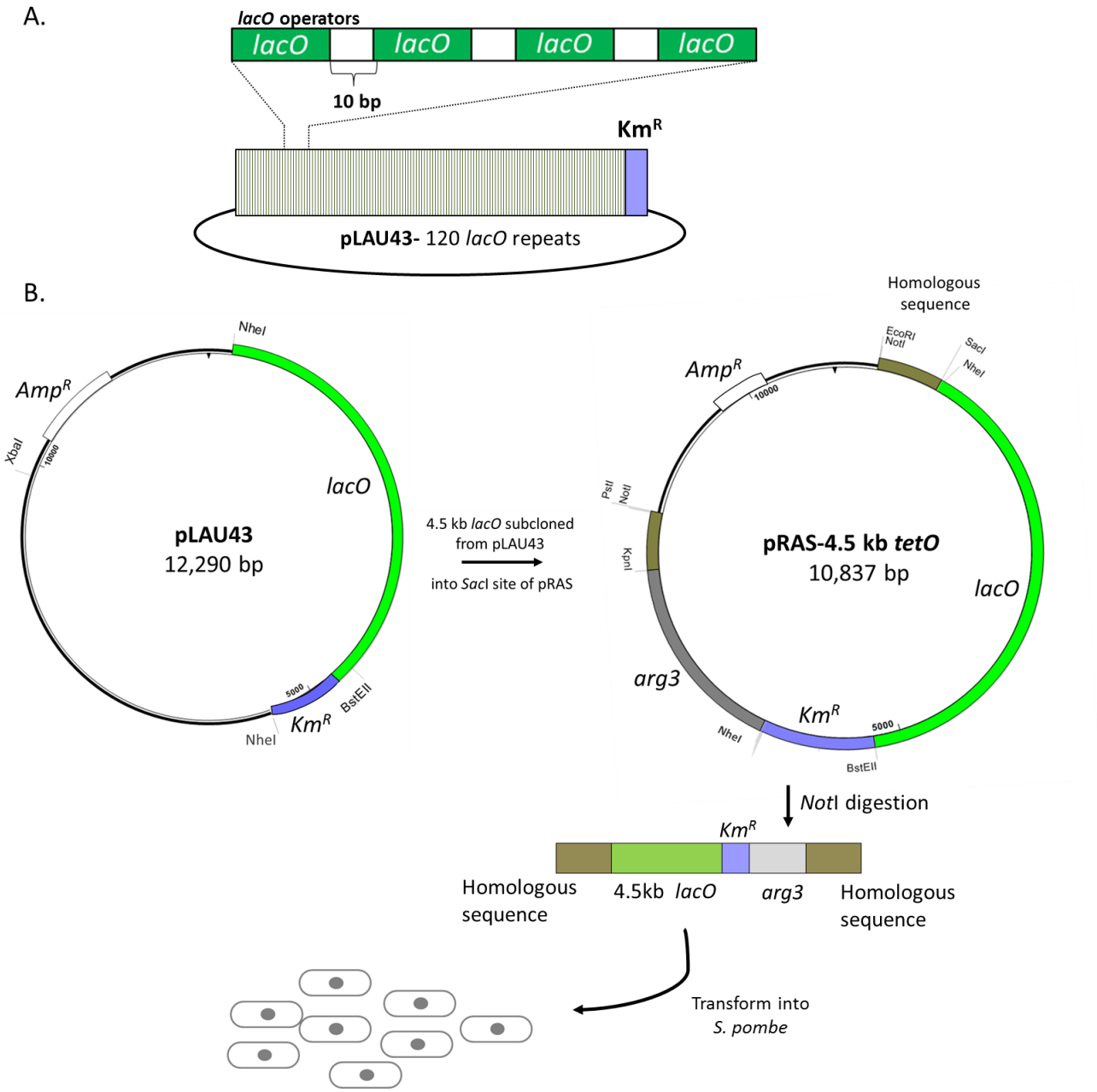

Figure 3-8. Schematics for the construct *lacO* repeats for transformation

(*A*) The plasmid, pLAU43 contains the 120x (4.5 kb) repeats of the *lacO* sequence, with 10 bp of different random sequence inserted between each and every *lacO* (21 bp) site. (*B*). The 4.5 kb *lacO* fragment containing the *kanamycin* resistance (*Km*^{R}) antibiotic resistance marker was produced from pLAU43 after digesting *Nhe*I. The resulting 4.5 kb *lacO* fragment and the *Sac*I site of the digested pRAS vector were modified by T4 DNA polymerase to convert the ends into blunt ends to allow the cloning of the fragment into pRAS. The resulting plasmid – pRAS-4.5kb lacO – was used to generate the final *lacO* fragment by digestion with *Not*I. This fragment was subsequently transformed into *S. pombe.*

2. Transformation of the tetO array into the mini-chromosome of S. pombe

To linearize the targeting fragment, pRHR-9 kb tetO was digested with *Not*I. The linear fragment for integration contained the 9 kb *tetO* repeats with *his3*$^{+}$ maker flanked by homologous region of upstream and downstream of *rad21* gene, and was subsequently transformed into the strain CJ41 (*ade6-704, arg3-D4, leu1-32, ura4-D18, chr16, ade6-m216, chk1::natMX6, bub1::loxP-kanMX6-loxM3*). The transforms were firstly selected on His^{-} plate/YNBA and subsequently replica plating upon other selection plates was used to identify the desired yeast strain which was predicted to have an Ade^{-} Arg^{-} Leu^{-} Ura^{-} His^{+} Nat^{R} Kan^{R} phenotype. The correct integration of the *tetO* fragment in the mini-chromosome was analysed by a RFLA and a PFGE. In the RFLA analysis, the genomic DNA of the candidates was firstly digested with *Cla*I. Subsequently a Southern blot assay was used to hybridise with the probe E, which detected the region outside the integrated sequence of the *tetO* cassette (Figure 3-9A). When the *tet*O fragment replaced the *rad21* locus, two bands were visible at the size of 4 kb and 11 kb (Figure 3-9B). Three candidates were chosen and tested by a PFGE combined with a Southern blot hybridization to confirm whether the *tetO* fragment had been integrated into Ch^{16} (Figure 3-9C). The probe B (targeting the ORF of the *Nat*^{R} gene) was used to show the position of Ch^{16} (Figure 3-9C, second panel). The probe his3 detected the ORF of *his3*$^{+}$ gene and the probe *Gm*^{R} that hybridised with a *gentamycin* resistance gene specifically indicated where the *tetO* cassette had been integrated (Figure 3-9C, third and fourth panels). The candidate 1 and 3 are incorrect colonies because the *tetO* cassette was located on chromosome III. However, candidate 2 was the desired strain revealing the signal of the probe his3 and probe Gm^{R} on the position of Ch^{16}. This strain was named CJ42 and it was used for further experiments. The strain CJ41, which did not contain the *tetO* fragment integration, showed that no signal could be detected using the probes his3 and Gm^{R}.

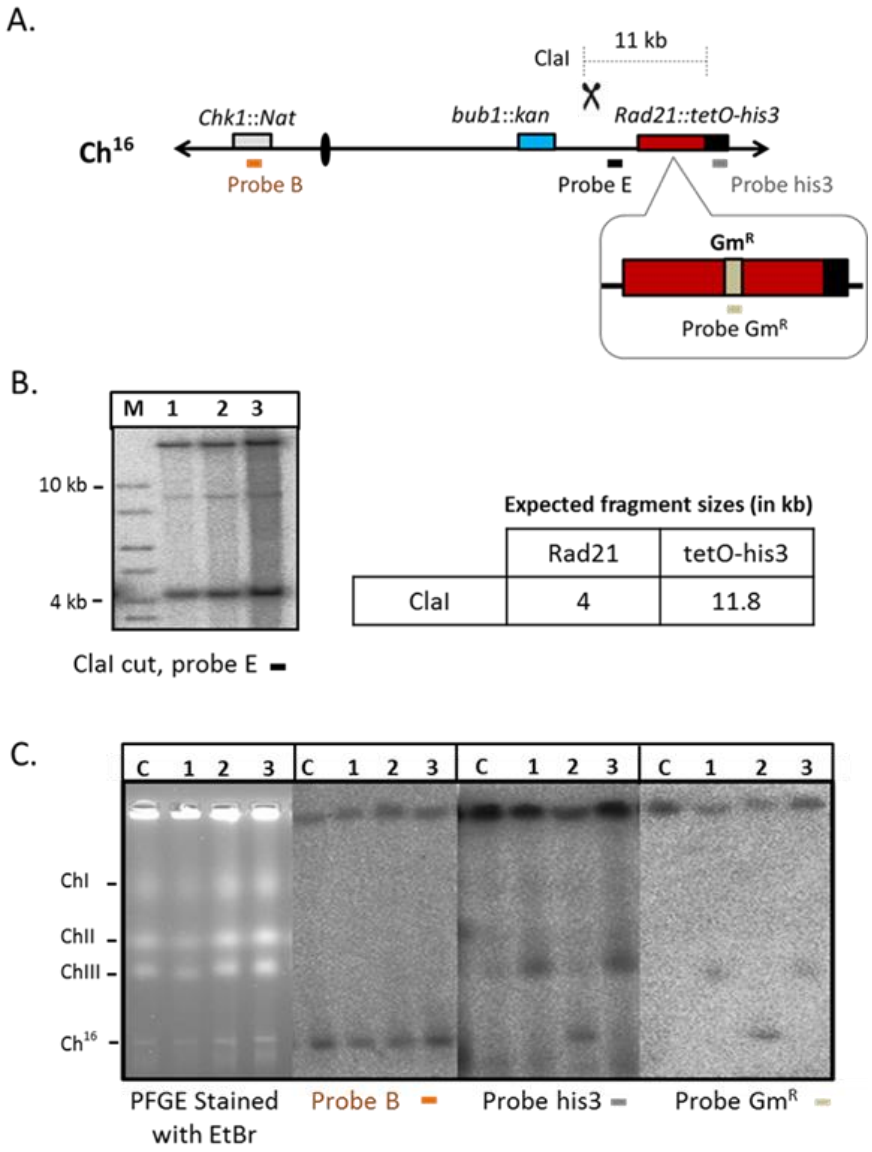

Figure 3-9. Integration of the 9 kb *tetO* fragment with *his3*$^{+}$ gene on Ch^{16} of *S. pombe*.

(A) Positions of the probes used in a Southern blot hybridization are indicated as filled blocks on Ch^{16}. (B) A RFLA combined with a Southern blot hybridization. The desired strains showed two bands at 4 kb and 11 kb detected by the probe E (designed to recognize the region outside of the *tetO* repeats integration) after digesting with *Cla*I. M: DNA ladder. (C) Pulsed Field Gel Electrophoresis. The gel staining EtBr indicates the position of chromosome I, II, III and Ch^{16} (left panel). In all colonies the probe B (probe flanking ORF of the *Nat*^{R} gene) was able to hybridise to Ch^{16}. The integration of the 9 kb *tetO* fragment on Ch^{16} was confirmed by probing with his3 (probe targeting the ORF of *his3*$^{+}$gene) and the probe *Gm*^{R}. C: Control, the strain CJ41 which was without the *tetO* fragment integration.

3. Transformation of the lacO fragment into the mini-chromosome of S. pombe

After digesting the pRAS-4.5 kb lacO with *Not*I, the linear fragment that contained the 4.5 kb *lacO* repeats with an $arg3^+$ maker flanked by homologous regions outside *ARS* (3040) was isolated and subsequently transformed into the strain CJ42 (*ade6-704, arg3-D4, leu1-32, ura4-D18, chr16, ade6-m216, chk1::natMX6, bub1::loxP-kanMX6-loxM3, rad21::9kbtetO-his3*$^+$). The transformants were firstly selected on the arg^- plate/YNBA (see Materials and Methods) and subsequently the other makers were checked by replica plating to other appropriate selectable plates. The chosen yeast strain was expected to have the phenotype Ade^- Arg^+ Leu^- Ura^- His^+ Nat^R Kan^R. To confirm the integration of the *lacO* cassette on the mini-chromosome, the potential colonies were examined by a RFLA and a PFGE. The chromosomal DNA of the candidates was digested by *Nhe*I and subsequently analysed by a Southern blot assay hybridizing with the probe F, which identified the region outside integrated sequence of the *lacO* cassette (Figure 3-10A). The strain without the *lacO* integrated into *ARS* (3040) locus only showed one DNA fragment at 4.7 kb by probing with the probe F. When the *lacO* fragment replaced *ARS* (3040) sequence two bands were shown at size 4.7 kb and 2.5 kb (Figure 3-10B). To check the *lacO* fragment integration on Ch^{16}, five colonies were tested using a PFGE combined with a Southern blot hybridization. The probe B (targeting the ORF of the Nat^R gene) was visible at Ch^{16} in all the tested strains (Figure 3-10C, second panel). Two probes were designed to specifically detect the *lacO* cassette: the probe arg3 detected the ORF of $arg3^+$ gene and the probe Km^R hybridised with a *kanamycin* resistance gene (Figure 3-10C, third and fourth panel). As the result shows, candidates 1, 2 and 5 are correct colonies because the signal by the probe arg3 and probe Km^R shows its hybridization on Ch^{16}. Candidates 3 and 4 however, were incorrect strains because a faint signal was detected on chromosome III by the probe arg3 and probe Km^R hybridization.

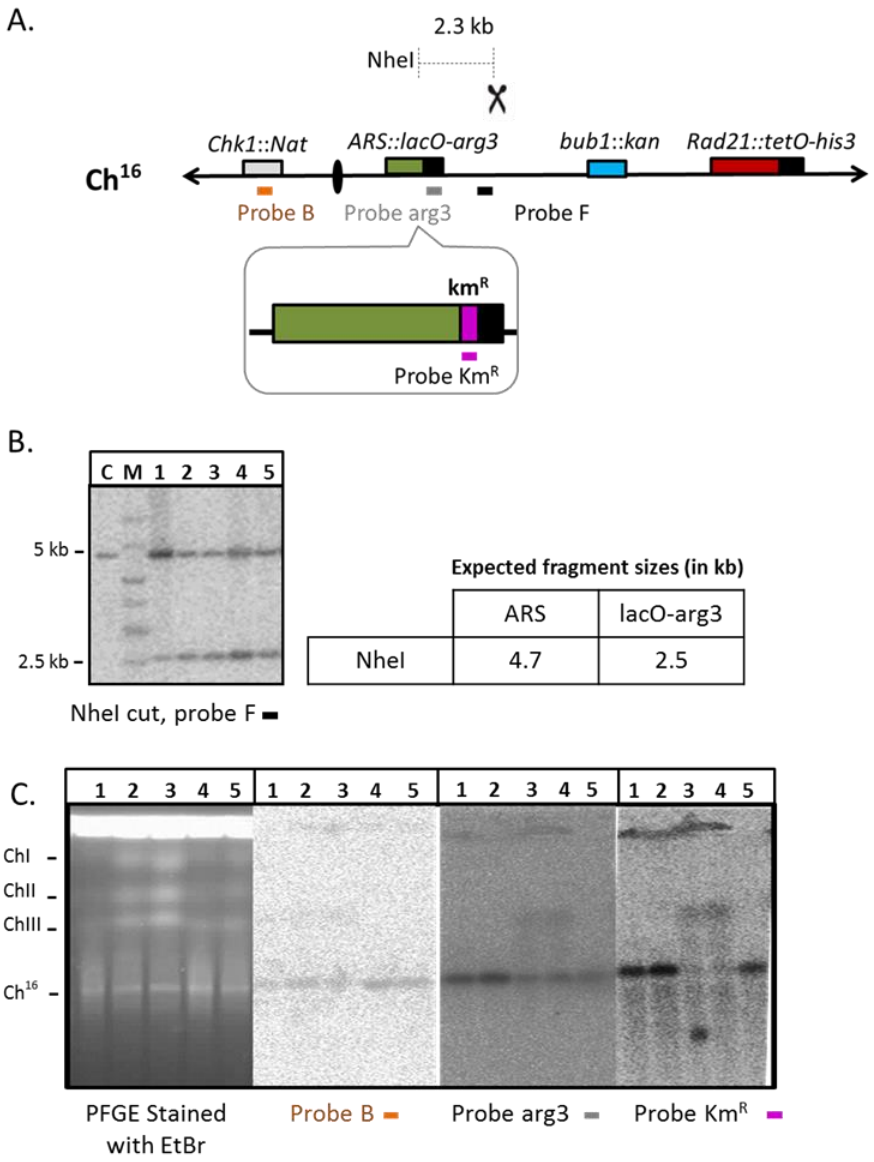

Figure 3-10.Integration of the 4.5 kb *lacO* fragment with *arg3*$^{+}$ gene on the Ch^{16} of *S. pombe*.

(A) Positions of the probes used in a Southern blot hybridization are shown as filled blocks on Ch^{16}. (B) RFLA in a Southern blot hybridization – the integration of the *lacO* fragment revealed two bands at 2.5 kb and 4.7 kb detected by the probe F (targeting the region outside of the *lacO* repeats integration) after digesting with *Nhe*I. C: Control, the strain without the *lacO* repeats integration showed only one band at 4.7 kb after digesting with *Nhe*I. M: DNA ladder. (C) Pulsed Field Gel Electrophoresis. The PFGE staining with EtBr indicates the position of chromosome I, II, III and Ch^{16} (left panel). In all colonies the position of Ch^{16} was detected by the probe B (probe targeting the ORF of the *Nat*^{R} gene). The integration of the *lacO* fragment into Ch^{16} was detected by the probe arg3 (probe flanking the ORF of the *arg3*$^{+}$gene) and probe Km^{R}.

3.2.2 Establishing strain construct II

3.2.2.1 Transformation of sup3-5 maker gene and nmt41 promoter into S. pombe

For the construction of strain II the *rtf1* promoter was replaced by *nmt41* promoter to regulate Rtf1 protein expression in the *S. pombe* strain that contained the *lacI-gfp* and *tetR-tdtomato* on Chromosome II. Two long pairs of primers were designed to amplify the cassettes that contained *sup3-5* gene and *nmt41* promoter flanking with different homology regions for the chosen chromosomal loci from the pGEM-NTAP (provided by Dr. Ellen Tsang): one is for replacement of the *rtf1* promoter with the *sup3-5-nmt41* promoter construct (Figure 3-11A) and another is for a full deletion of the *rtf1* gene by *sup3-5-nmt41* insertion (Figure 3-11B). Both of the fragments contained a *sup3-5* gene as a selection marker, which can suppress the *ade6-704* nonsense mutation. The *ade6-704* mutants produce red pigment when grown in limiting concentrations of adenine. If the *ade6-704* mutant cells contained a chromosomal copy of a *sup3-5* gene they could form white colony.

Following the transformation of both linear fragments into CJ40 (*ade6-704, his7*$^{+}$*<<Pdis1-GFP-lacI-NLS, arg3-D4, his3-D1, leu1, ura4-D18, Z::hyh*^{R} *<<Padh31-tetR-Tomato*) separately, cells from each transformation were plated on YNBA with 10 mg/ml adenine. The desired strains formed white colonies (ade^{+} phenotype). In these colonies the nonsense mutation of *ade6-704* allele was suppressed by the presence of the *sup3-5* tRNA. To check for integration at the correct locus, PCR was performed on total genomic DNA using one primer hybridizing to the region outside of the integration and the other pairing to the *nmt41* sequence. Amplified fragments were checked by sequencing. The results showed that in CJ53 (*rtf1:Pnmt41:rtf1*$^{+}$*:sup3.5, his7*$^{+}$*<<Pdis1-GFP-lacI-NLS, z::hph*^{R}*<<Padh31:tetR-Tomato , ade6-704, arg3-D4, his3-D1, leu1-32, ura4-D18*) *rtf1* promoter was

replaced by the *sup3-5* gene and *nmt41* promoter and in CJ56 (*rtf1:Pnmt41:rtf1Δ:sup3.5, his7*$^{+}$*<<Pdis1-GFP-lacI-NLS, z::hph*^{R}*<<Padh31:tetR-Tomato , ade6-704, arg3-D4, his3-D1, leu1-32, ura4-D18*) *rtf1* gene was deleted by replacing it with the *sup3-5-nmt41* sequence (Figure 3-11C, white squares).

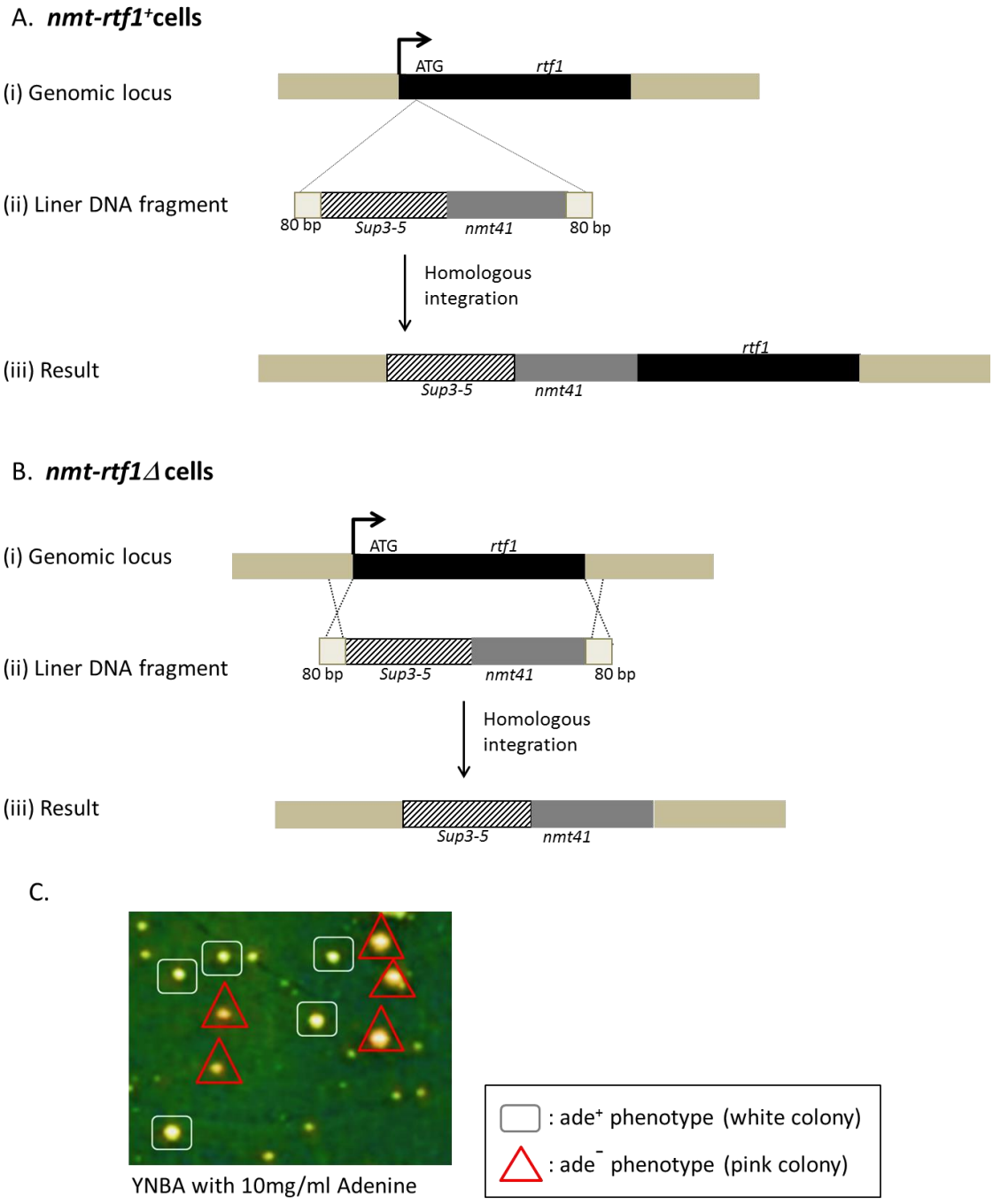

Figure 3-11. Transformation of a *sup3-5* maker gene and the *nmt41* promoter into *S. pombe*.

PCR was performed to amplify the cassettes that contained a *sup3-5* marker gene and the *nmt41* promoter from the pGEM-NTAP with different homologous sequences for the desired genomic loci. (*A*) Illustration of the *sup3-5-nmt41* promoter replacing *rtf1* promoter to regulate RTF1 protein expression. (*B*) A *sup3-5-nmt41* promoter replaced the intact *rtf1* gene including *rtf1* promoter. (*C*) Following successful integration of the cassettes into *S. pombe* cells showed ade^{+} phenotype (white blocks).

3.3 A fork-arrest system integration using Cre/lox site-specific recombinase-mediated cassette exchange (RMCE)

Following the crossing of strains I and II, the base strain (containing the Ch^{16}-NRKH) was obtained containing all the desired modified loci: 1. Nat^R gene replaced the *chk1* site, 2. The *tetO* and *lacO* repeats were inserted on either side of loxP-Kan^R-loxM3 cassette, which is located at the upstream part of *bub1* locus on Ch^{16}; 3. The *lacI-gfp* and *tetR-tdtomato* genes are on chromosome II; 4. The *nmt41* promoter replaced the *rtf1* promoter. Two strains were established: one that could normally express Rtf1 protein regulated by the *nmt41* promoter (CJ73, *rtf1:Pnmt41:rtf1*$^+$*:sup3.5, his7*$^+$*<<Pdis1- GFP -lacI-NLS, z::hphR<<Padh31:tetR-Tomato, ade6-704, leu1-32, ura4-D18, chr16, ade6-m216, chk1::natMX6, bub1::loxP-kanMX6-loxM3, rad21:: 9kb tetO-his3*$^+$*, ARS:: 4.5kb lacO-arg3*$^+$); the other had the *rtf1* gene deleted. (CJ69, *rtf1:Pnmt41:rtf1Δ:sup3.5, his7*$^+$*<<Pdis1-GFP-lacI-NLS, z::hyh*^{R}*<<Padh31:tetR -Tomato, ade6-704, leu1-32, ura4-D18, chr16, ade6-m216, chk1::natMX6, bub1::loxP-kanMX6-loxM3, rad21:: 9kb tetO-his3*$^+$*, ARS:: 4.5kb lacO-arg3*$^+$).

The final step was the integration of the fork-arrest system-*RuiuR* by using a Cre recombinase-mediated cassette exchange (RMCE) method [128]. One advantage of the RMCE method is that the process is relatively quick and enables easy incorporation at the chosen chromosomal locus. Also, the sequence of *RuiuR* is difficult to produce by PCR amplification due to the high homology and *RuiuR* and the donor plasmid cassettes were already available in our laboratory (provided by Dr. Ken'Ichi Mizuno). The donor plasmid contained loxP-*RuiuR*-loxM3 in pAW8 and was based on the plasmid pAL19. It contained the *S. pombe ars1*$^+$ element, and the *LEU2*$^+$ marker gene of *Saccharomyces cerevisiae* that can supplement *S. pombe*

leu1-32 mutants. The cassette located on the plasmid consists of the *RuiuR* sequence flanked by a loxP site at one end and a loxM3 site at the other. LoxP is a 34 bp element that consists of two 13 bp inverted repeats and an asymmetric 8 bp spacer sequence. The repeats act as the Cre recombinase recognition sites. LoxM3 is derived from a wild-type loxP with different 8 bp spacer sequences (Figure 3-12A). Thereby, heterospecific flanking lox sites are stable and unlikely to recombine with each other. The donor plasmid has also been designed to contain the gene for expression of the Cre recombinase that mediates the recombination exchange event (Figure 3-12B). The process of RMCE can be described as a three step process: first the creation of the base strain (containing the Ch^{16}-NRKH) in what the loxP-Kan^R-loxM3 cassette is integrated into the genome using standard homologous recombination techniques (see detail in section 3.2.1.2). Following this step a Cre-expression plasmid containing the *RuiuR* sequences flanked by loxP and loxM3 is introduced into the base strain CJ53 (containing the Ch^{16}-NRKH *nmt-rtf*$^+$) and CJ56 (containing the Ch^{16}-NRKH *nmt-rtfΔ*). Finally the expression of Cre recombinase results in cassette exchange between the chromosomal cassette and the donor plasmid cassette by readily occurring reciprocal recombination (Figure 3-12C). The Leu^- Ura^+ Kan^s phenotype of recombinants was selected. This phenotype indicated the successful recombination and also the loss of the Cre expressing plasmid (see Materials and Methods).

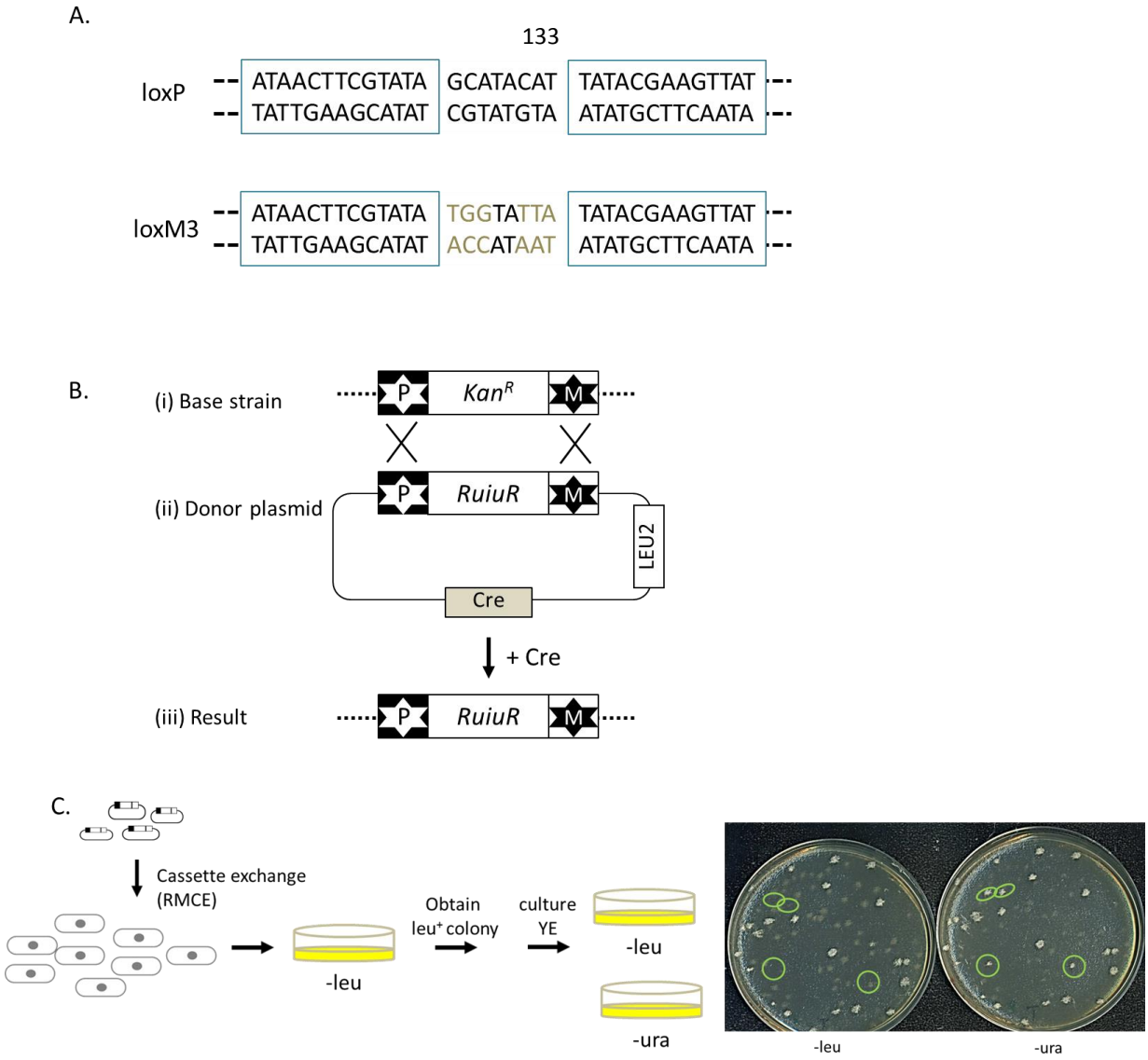

Figure 3-12. Fork-arrest system integration using the Cre/lox site-specific recombinase-mediated cassette exchange (RMCE).

(*A*) The sequences of the loxP and loxM3 sites. (*B*) Illustration of the Cre/lox site-specific recombinase-mediated cassette exchange (RMCE). The base *S. pombe* strain contained the loxP-*Kan*^{R}-loxM3 at the upstream part of the *bub1* gene locus and this was replaced by the loxP-*RuiuR*-loxM3 mediated by Cre recombinase. Cre: Cre recombinase. *LEU2*: a *LEU2*$^{+}$ marker gene of *S. cerevisiae*. (*C*) Schematic representation of the RMCE method. After transformation, cells were plated on the YBNA without leucine supplement. A leu^{+} colony was cultured in liquid YE overnight and subsequently spread on the YBNA without leucine or uracil supplement. The desired Leu^{-} Ura^{+} Kan^{S} of colonies are marked with green circles. This phenotype indicated that *RuiuR* successfully replaced the *Kan*^{R} gene and also lost its donor plasmid.

3.4 The mini-chromosome system can generate the dicentric and acentric chromosomes

To investigate the rearrangements of the chromosomes after fork arrest the *lacO* and *tetO* tandem arrays have been integrated to either side of the *RuiuR* loci on Ch^{16} (Figure 3-13A). The *lacO* repeats are encoded *cen*-proximal to RTS1. The GFP tagged LacI protein can bind to the *lacO* repeats. The *tetO* repeats are integrated on *tel*-proximal to RTS1. The TetR protein is tagged with the tdTomato fluorescent protein and can bind to the *tetO* repeats. To confirm the generation of the dicentric and acentric chromosomes after the induction of $rtf1^{+}$, a Southern blot assay was performed to visualise rearrangement products. The potential candidates were examined by a RFLA (Figure 3-13C) and a PFGE (Figure 3-14B). The chromosomal DNA of parent Ch^{16} and rearrangement products was visualised by a Southern blot hybridization using the probe ura4 (probe targeting the ORF of $ura4^{+}$ gene, see Figures 3-13 and 3-14). Following a PFGE, when a rearrangement caused the formation of the acentric and dicentric chromosomes, the probe Tel could bind to the acentric chromosomes, as well as to the initial mini-chromosome (Figure 3-14A and B, third panel) while the probe Cen can bind to the dicentric chromosomes as well as to the initial mini-chromosome (Figure 3-14A and B, right panel).

In the presence of thiamine (Rtf1 protein repressed, "pause off" growth) only the main 7.7 kb fragment from the initial Ch^{16}-NRUH was visible after digesting with *Xho*I (Figure 3-13C). In the absence of thiamine (Rtf1 present, "pause on" growth) a band appeared at 9.4 kb (predicted to arise from the dicentric chromosome) and one at 6.2 kb (predicted to arise form acentric chromosome) (Figure 3-13C, Ch^{16}-NRUH *nmt-*$rtf1^{+}$ cells, top panel). These bands were not seen when thiamine was present

(“pause off” growth), confirming that rearrangements were induced the presence of Rtf1. Candidate 1 of Ch^{16}-NRUH *nmt-rtf1*$^{+}$ cell did not reveal the expected bands when the pause was on. This may be due to a loading problem or because it was an incorrect strain. Candidates 2 and 3 of Ch^{16}-NRUH *nmt-rtf1*$^{+}$ cells presented the expected DNA fragments for the acentric and dicentric chromosomes when the pause was on, but not when it was off (Figure 3-13C, Ch^{16}-NRUH *nmt-rtf1*$^{+}$ cells, top panel). Candidate 2, named as CJ90 (*rtf1:Pnmt41:rtf1*$^{+}$*:sup3.5, his7*$^{+}$*<<Pdis1-GFP-lacI-NLS, z::hph*^{R}*<<Padh31:tetR-Tomato, ade6-704, leu1-32, chr16, ade6-m216, chk1::natMX6, bub1::loxP-RuiuR-loxM3, rad21:: 9kb tetO-his3*$^{+}$*, ARS:: 4.5kb lacO-arg3*$^{+}$) was used for the further experiments. By contrast Ch^{16}-NRUH *nmt-rtf1*deletion cells used as a control– CJ126 (*rtf1:Pnmt41:rtf1Δ:sup3.5, his7*$^{+}$*<<Pdis1-GFP-lacI-NLS, z::hph*^{R} *<< Padh31:tetR-Tomato, ade6-704, leu1-32, chr16, ade6-m216, chk1::natMX6, bub1::loxP-RuiuR-loxM3, rad21:: 9kb tetO-his3*$^{+}$*, ARS:: 4.5kb lacO-arg3*$^{+}$) did not produce rearrangement products when the pause was on (Figure 3-13C, Ch^{16}-NRUH *nmt-rtf1*$^{+}$ cells, bottom panel).

By the PFGE analysis, rearrangement products of the Ch^{16}-NRUH were detected by using the probe ura4 (Figure 3-14B, second panel). To confirm the presence of the acentric chromosome probe Tel was used (Figure 3-14B, third panel) while using the probe Cen enabled the detection of the dicentric chromosome. Both the probe Tel and Cen also hybridised to the parental Ch^{16}-NRUH (Figure 3-14B, right panel). Altogether, these results revealed that the fork-arrest system established on the Ch^{16}-NRUH could generate rearranged chromosomes and served as an excellent model system to study these processes. To test whether the fork-arrest induced-chromosomal rearrangements on the non-essential Ch^{16}-NRUH leads to loss

of viability a spot test assay was performed in presence (“pause off” growth) or absence (“pause on” growth) of thiamine (Figure 3-14C). Ch^{16}-NRUH *nmt-rtf1*$^{+}$ cells showed slight viability loss when the pause was on compared with the wild-type cells. The cells containing Ch^{16}-NRUH in *nmt-rtf1*Δ background did not affect the cell growth under the same experimental conditions. The reason for the slight cell viability loss is unclear. It may be caused by the spindle pole checkpoint activation during the segregation of the dicentric chromosomes. To discover the exact causes further experiments are required. Fortunately, this did not affect the observation of rearranged chromosomes *in vivo* and thus we used this modified mini-chromosome system during our further investigations.

Figure 3-13. The modified mini-chromosome system can generate the dicentric and acentric chromosomes.

(*A*) Schematic representation of the original construct and of expected chromosomal rearrangements on the Ch^{16}-NRUH system. Positions and the interval distances between each integrated marker and the size of centromere are indicated under the parental Ch^{16}-NRUH. The *Nat^{R}* gene replaced the *chk1* genes; the *lacO* repeats with an *arg3^{+}* marker replaced *ars* (3040); the *tetO* repeats with a *his3^{+}* marker replaced the *rad21* gene; the fork-arrest system replaced the upstream part of the *bub1* gene; the *ade6-m216* was at the original locus. (*B*) Schematics of the *RuiuR* and flanking region of the initial and the rearranged (dicentric and acentric) chromosomes. Predicted size of the band visualised by the probe Ura4 (probe recognising the ORF of the *ura4^{+}* gene) following *Xho*I digestion is shown. (*C*) Restriction fragment length analysis (RFLA) following *Xho*I digestion and probing with the probe Ura4. When the pause was on Ch^{16}-NRUH *nmt-rtf1^{+}* cells generated the dicentric and acentric chromosomes (Top panel). The chromosomal arrangement event did not occur in Ch^{16}-NRUH *nmt-rtf1*Δ cells when the pause was on (Bottom panel). Star (*) indicates bands of interest. M: DNA ladder.

A.

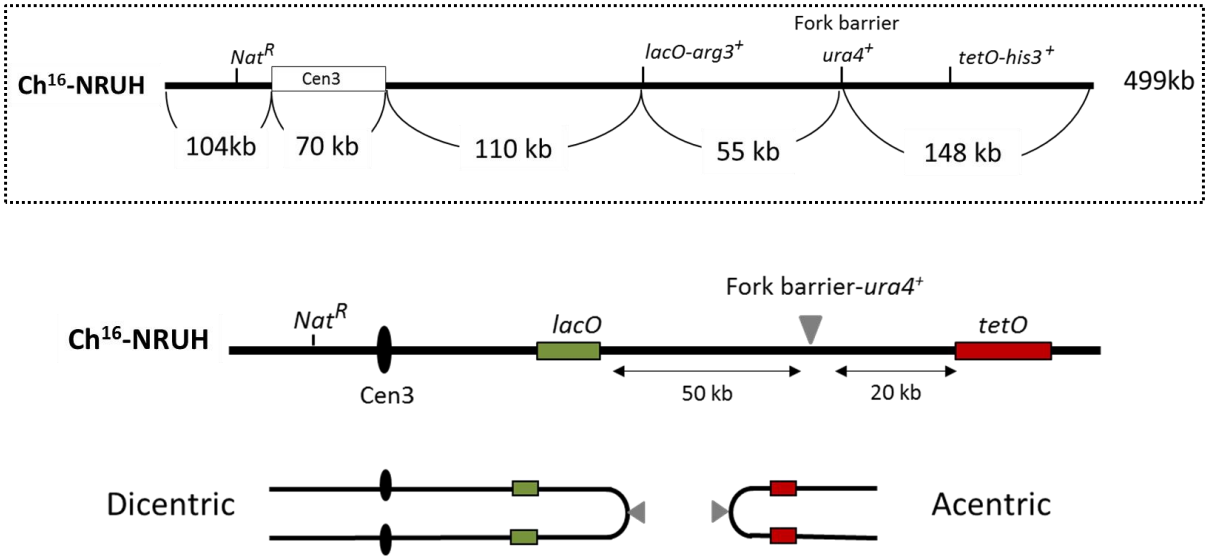

B.

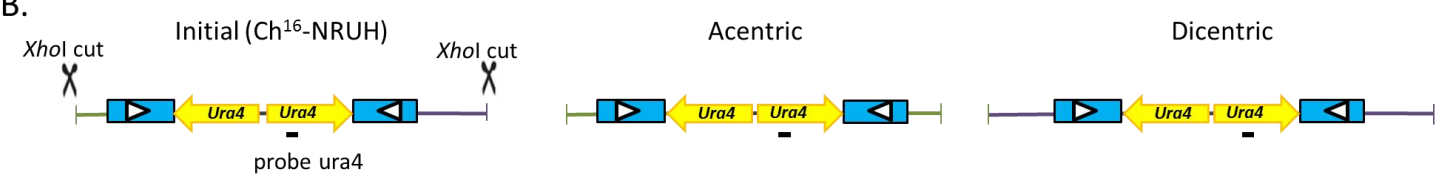

C.

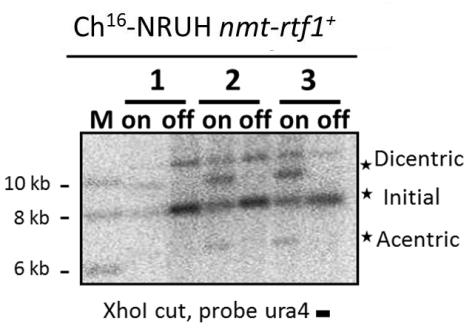

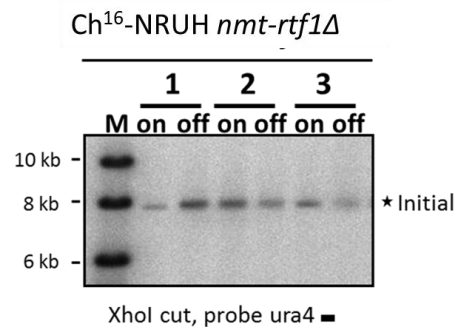

Expected fragment sizes (in kb)

	Initial	Acentric	Dicentric
XhoI	7.6	6	9.2

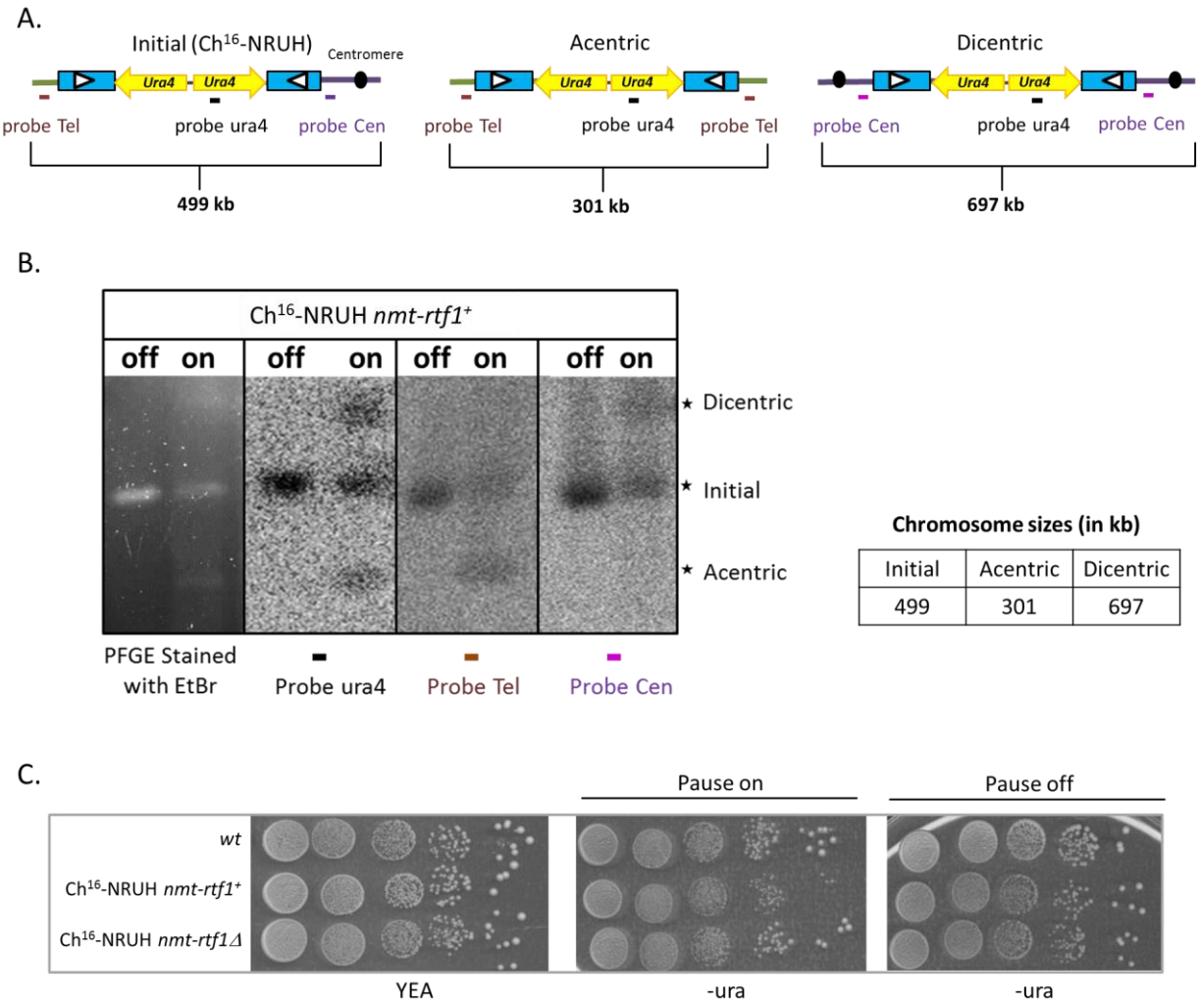

Figure 3-14. The modified mini-chromosome system can generate the dicentric and acentric chromosomes.

(*A*) Positions of the probes for the original construct and expected chromosomal rearrangement products. Schematics of the *RuiuR* and flanking region for the initial and the rearranged (dicentric and acentric) chromosomes. Predicted size of bands visualised by the probe Ura4, Cen and Tel are shown. (*B*) Pulsed Field gel electrophoresis (Left panel) combined with a Southern blot hybridization by the probe Ura4, Cen and Tel confirmed the presence of rearrangement products. Star (*) indicates bands of interest. (*C*) A spot test for cell viability. When the pause was on, the Ch^{16}-NRUH *nmt-rtf1*$^{+}$ cells showed a slight viability loss compared to the wild-type cells and Ch^{16}-NRUH *nmt-rtf1*Δ cells.

3.5 Discussion

To investigate fork-arrest induced-chromosomal rearrangement in a single cell a mini-chromosome model was established in this project. Our aim was to discover the fate of arranged chromosomal intermediates. To analyse the properties of the chromosomes microscopically, the *lacO*/LacI-GFP and *tetO*/TetR-tdTomato systems were introduced to either side of a fork stalling locus. In this chapter, the establishment of the experimental yeast model is presented. The final construct contained genes for different purposes: 1. A selectable marker for maintaining the intact Ch^{16}-a *nourseothricin* (*Nat*) resistance gene, 2. Fluorescence protein chromosomal binding loci-tetracycline operator (*tetO*) repeats and 3. The lactose operator (*lacO*) repeats, 4. A fork-arrest system-*RuiuR* sequence on Ch^{16}; 5. The *lacI-gfp* and 6. *tetR-tdTomato* fusion genes were located on the chromosome II; 7. Regulation of the replication fork stalling using replacement of *rtf1* promoter with *nmt41* promoter on chromosome I. Note that all the chromosomal integrations have been checked by a RFLA and a PFGE, confirming by the sequencing.

Altogether, this experimental yeast strain has been confirmed to generate the acentric and dicentric chromosomes when chromosomal rearrangement occurs on Ch^{16} upon activation of the fork stalling system. Although this lead to a slight cell viability loss, the observation of the acentric and dicentric chromosomes shows that our system is an excellent model to study chromosomal rearrangements *in vivo.*

CHAPTER 4

DIRECT VISUALISATION OF CHROMOSOMAL REARRANGEMENTS *IN VIVO*

4.1 Introduction

To directly visualise the chromosomal rearrangement events in *vivo*, the tetracycline operator (*tetO*) and lactose operator (*lacO*) arrays were integrated onto the either side of the fork arrest loci on the mini-chromosome, and to fluorescently mark these chromosomal regions. By the continuous expression of the LacI-GFP (green fluorescent protein) and the TetR-tdTomato (tomato red fluorescent protein), which can bind to the *lacO* and the *tetO* repeat respectively, the behaviour of the chromosome can be monitored. The images were obtained using a DeltaVision deconvolution light microscope system (refer to the Materials and Methods). The construction of the experimental yeast model was described earlier in Chapter 3, i.e.: the *tetO* and *lacO* arrays were established, a fork-arrest system - *RuiuR* - on the non-essential mini-chromosome (Ch^{16}) was constructed, and an inducible RTF1 expression construct to regulate fork stalling was integrated onto the chromosome I. The *lacI-gfp* and *tetR-tomato* fusion genes located on chromosome II were also introduced. In this chapter, the microscopic results using the modified mini-chromosome system are reported and discussed (Figure 4-1A).

4.2 Visualisation of the formation of the dicentric and acentric palindromic chromosomes and their fate

From the RFLA and a PFGE experiments described in Figures 3.13 and 3.14, Ch^{16}-NRUH *nmt-rtf1*$^{+}$ cells (strain CJ90, see Table 2 in Chapter 2 and Figure 4-1), as predicted, generated the dicentric and acentric chromosomes in the absent of thiamine ("pause on" growth). This raises interesting questions as to how do cells respond when faced with these abnormally structured chromosomes and at the end, what their fates are *in vivo*? To investigate the chromosomal behaviour after the rearrangement, the *lacO* and *tetO* tandem repeats have been introduced on either side of the *RuiuR* loci on the mini-chromosome to allow visualisation of the un-rearranged and rearranged chromosomes. Following the generation of a dicentric palindromic chromosome, the two GFP dots of the *lacO*/LacI are predicted to be physically linked in close proximity. For an acentric palindromic chromosome, two tdTomato dots of the *tetO*/TetR were similarly expected in close proximity.

The regulation of transcription by thiamine withdrawal using the *nmt41* promoter is slow. It takes about 14 to 16 hours for the cells to respond by inducing the transcript (Figure 4-1B). Thus, the Ch^{16}-NRUH *nmt-rtf1*$^{+}$ cells were grown in minimal media in the presence ("pause off" growth) or absence ("pause on" growth) of thiamine (30 ℃) for 16 hours and subsequently synchronized using lactose gradients (see Materials and Methods). The cells were collected from the top of the gradient, as these cells (the smallest in the population) have been previously shown to be in the G_2 phase. Isolated cells were then cultured for four hours in minimal media maintaining the same conditions, i.e.; either with ("pause off" growth) or without thiamine supplement ("pause on" growth). For the visualisation of fixed fission yeast cells, aliquots were

collected into methanol/acetone at regular time intervals for subsequent visualisation using a DeltaVision deconvolution light microscope Core system. For live cell imaging, isolated G_2 cells were grown on Lab-Tek chambers for around one hour and subsequently filmed the cells using a DeltaVision Personal DV deconvolution light microscope system.

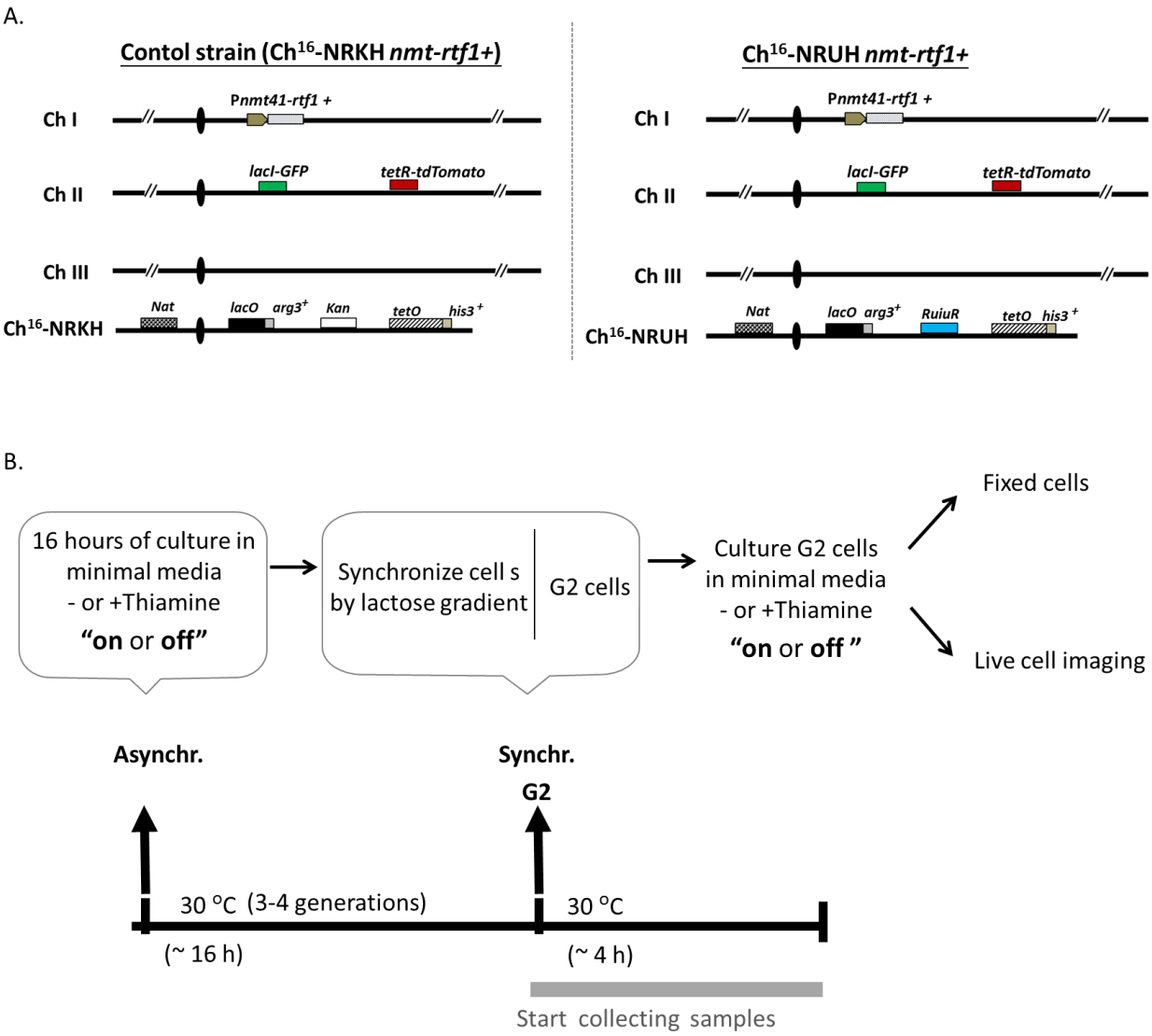

Figure 4-1. System to observe the behaviour of the mini-chromosome during mitotic cell cycle.

(*A*) Schematic of the system to monitor the behaviour of Ch^{16} in *vivo*. The control strain (Ch^{16}-NRKH *nmt-rtf1*$^{+}$) contains a *kan* resistant gene instead of the *RuiuR* sequence (strain CJ73, see Table 2 in Chapter 2). Hence, it was proposed that the inducible fork-arrest event occurred only in the Ch^{16}-NRUH *nmt-rtf1*$^{+}$ cells (the strain CJ90, see Table 2 in Chapter 2). (*B*) Procedure for growing cells to obtain G_2 cells by lactose gradient synchronization (pause on or off growth) followed by the growth of these G_2 cells in minimal medium.

4.2.1 Fixed *S. pombe* cells

4.2.1.1 The behaviour of the dicentric and acentric chromosomes during different stages of mitotic cell cycle during the "pause off" growth

In the initial experiments to study the behaviour and movement of the dicentric and acentric chromosomes, I used the fixed cells to capture a snapshot of images for the GFP and tdTomato foci in Ch^{16}-NRUH *nmt-rtf1*$^{+}$ cells. First, I followed the mitotic cell cycle and chromosome biology in the presence of thiamine ("pause off" growth). The mini-chromosome was expected to replicate normally without any chromosomal rearrangement event occurring. The GFP and tdTomato foci were thus expected to be co-localised on the same mini-chromosome copy, even during the period of nuclear division, as shown in the cartoon (Figure 4-2, middle and right panels). The sequence distance between the *lacO* and *tetO* arrays was ~70 kb. This was sufficient to spatially distinguish the GFP and tdTomato dots on the same copy of the mini-chromosome. When cells undergo the long G_2 phase typical of fission yeast, the cohesion between two sister chromatids is disrupted [102, 119]. This could be visualised by the presence of two distinct foci (see cartoon, Figure 4-2 ii). The two separate sister chromatids could thus potentially be recognized by the co-localization of two juxtaposed GFP and two juxtaposed tdTomato foci. When cells enter the M phase, the sister mini-chromosomes are attached by microtubules generated from the spindle poles and pulled towards to the two ends of the cell (Figure 4-2 iii-iv). There are three broad stages in the M phase: metaphase, anaphase and telophase (Figure 4-3). At the metaphase, the sister chromatids are attached to each other at the centromere. The pair of centromeres are bi-orientated (i.e. each is attached to spindle microtubules from the opposite spindle body) and thus the attached centromeres align between the spindle poles on the metaphase plate [122, 130, 131].

The *LacO* array – where the LacI/GFP can bind – is positioned close to the centromere of Ch^{16} (~110 kb far away from a centromere) and thus indicated the position of the *cen*-proximal right arm of Ch^{16}. The *tetO* array - bound by the TetR/tdTomato - is located close to the telomere of Ch^{16} (~128 kb far away from telomere), marking the *tel*-proximal right arm of Ch^{16}. The GFP and tdTomato dots on each copy of the sister chromatids are still close to each other (see example in Figure 4-3, metaphase). The two pairs may, however, not overlap as cohesion is not maintained between the arms. At the anaphase, the cohesion between the centromeres is cleaved and the two centromeres start to separate, moving in opposite directions (Figure 4-3, anaphase). In the anaphase, the nucleus tends to divide into two masses (bi-nuclear). The distance between the sister chromatids becomes obvious. The GFP and tdTomato dots on one chromatid of the mini-chromosome moved together. When a cell is in the telophase, sister chromatids are completely separated and cells achieve complete nuclear division (Figure 4-3, telophase). During nuclear division at telophase, the GFP and tdTomato foci of a single chromatid remain co-localised in the individual daughter nucleus. Subsequently, the septum was gradually formed in the middle of the cell and the two daughter cells contain one copy of the mini-chromosome. Finally, each nucleus thus retains one GFP dot and one tdTomato dot.

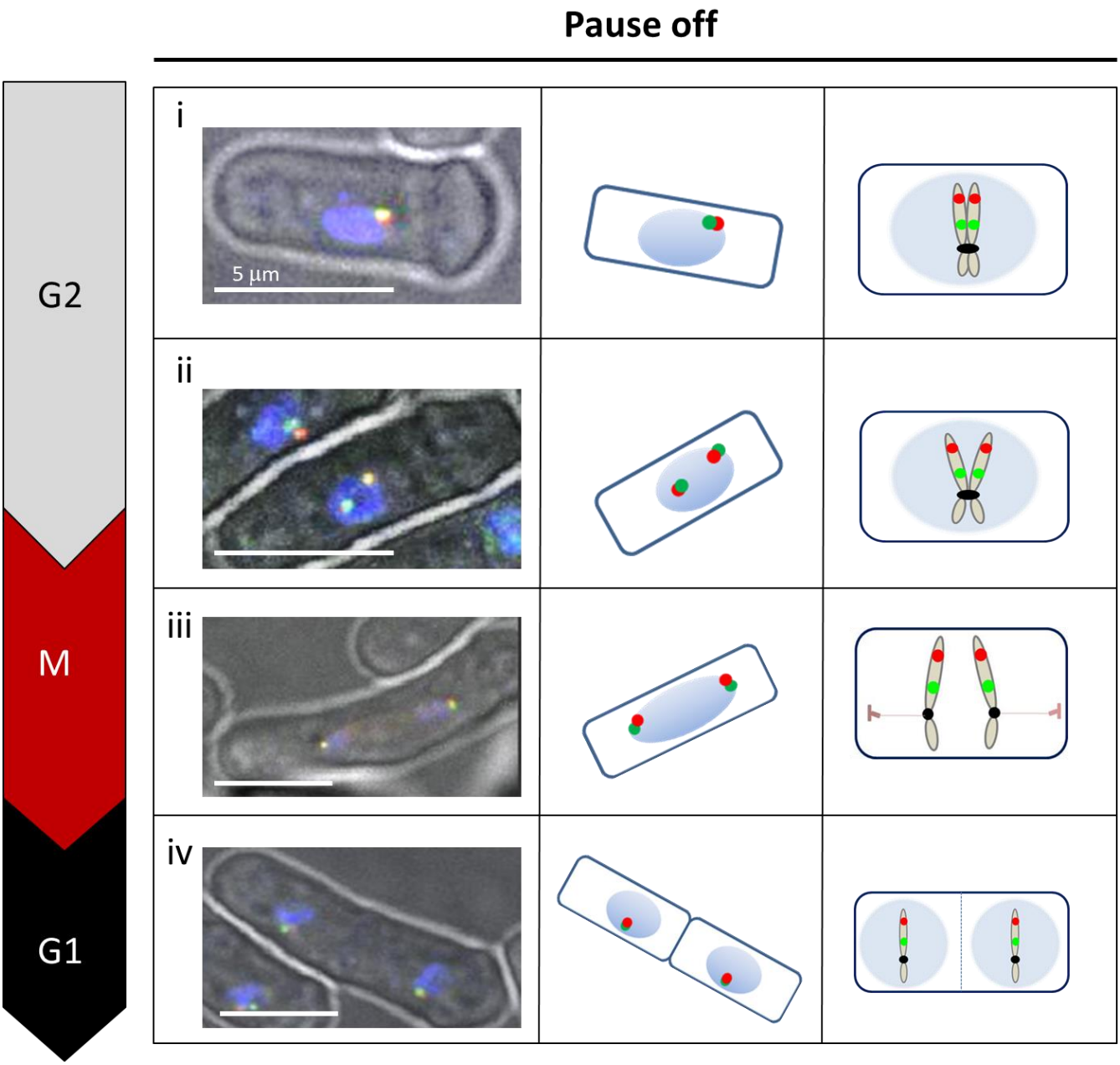

Figure 4-2. Observations on the mini-chromosome through the mitotic cell cycle during the "pause off" growth.

Left panel: Images i-iv acquired from fixed synchronized Ch^{16}-NRUH *nmt-rtf1*$^{+}$ cells through G_2 to the next G_1 phase. The GFP and tdTomato foci show the *lacO* and the *tetO* arrays on the mini-chromosome. The middle panels show schematic illustration of the images. The right panels are schematics of the anticipated chromosome conformation. Each nucleus revealed the co-localization of the GFP and tdTomato dots –, as was anticipated – during the "pause off" growth. The bar represents 5µm.

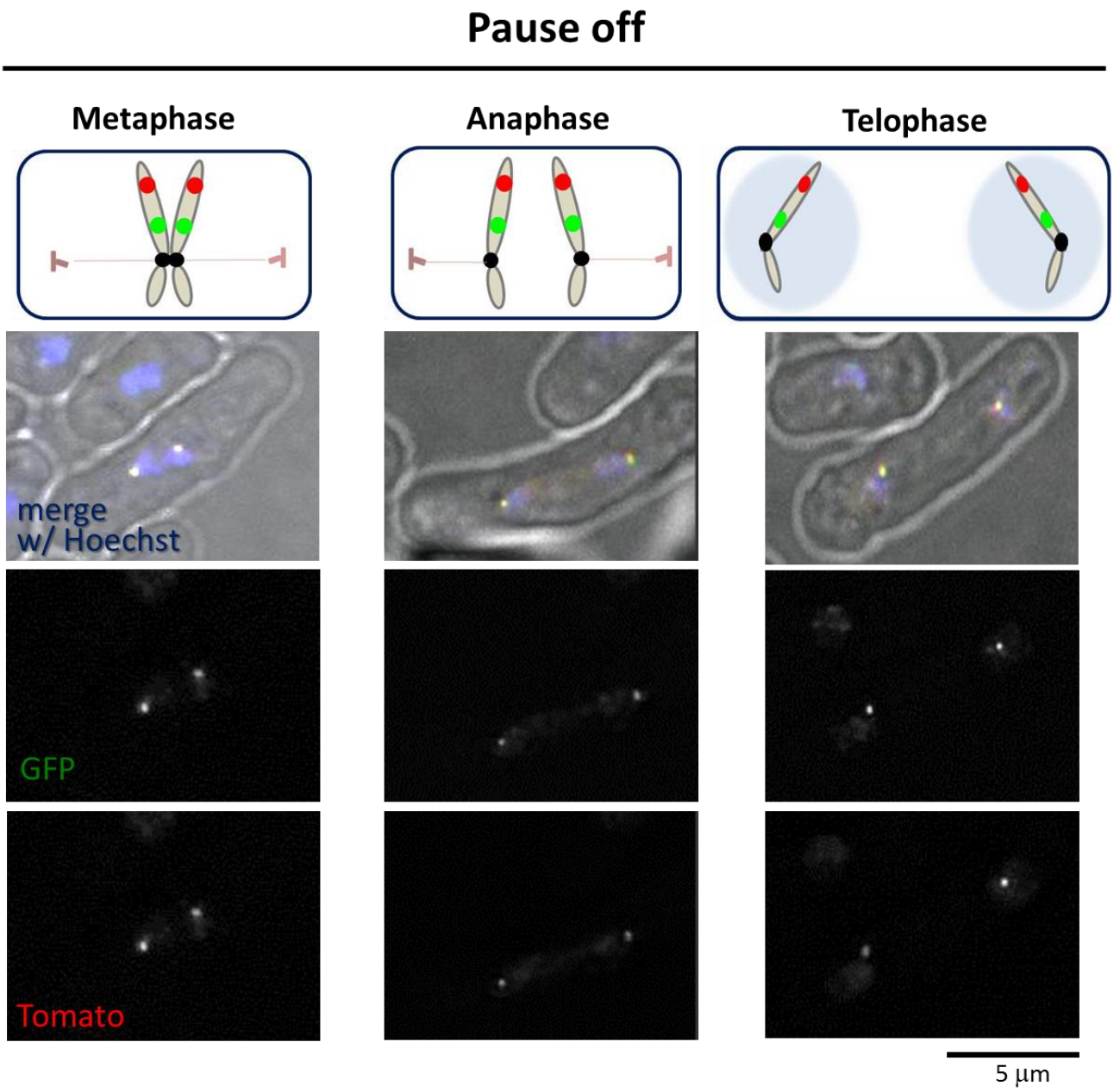

Figure 4-3. Detailed analysis of Ch[16]-NRUH *nmt-rtf1*$^{+}$ cells during the M phase visualised with the merged and split into the GFP and tdTomato channels through the mitotic cell cycle during the "pause off" growth. The GFP and tdTomato dots were co-localised on each copy of the sister mini-chromosome during the metaphase, anaphase and telophase in the present of thiamine ("pause off" growth). The merged images also show Hoechest dye staining of the DNA to visualise the nucleus. The bar represents 5µm.

4.2.1.2 The behaviour of the dicentric and acentric chromosomes during the different stages of the mitotic cell cycle during the "pause on" growth

In the absence of thiamine ("pause on" growth), the Ch^{16}-NRUH generates the acentric and dicentric chromosomes at a high frequency. It is estimated that this phenomenon occurs in approximately 1 of 10 replication events. When a rearrangement caused the formation of the acentric and dicentric chromosomes, the TetR-tdTomato fluorescent protein binds to the acentric chromosome, as well as to the initial mini-chromosome. Conversely, the LacI-GFP protein binds to the dicentric chromosome as well as to the initial mini-chromosome. Thus, when the cell is divided with the "pause on" growth, a proportion of the cells we can expect to see chromosomal rearrangements represented by the GFP and tdTomato foci localizing on the rearranged dicentric and acentric chromosomes respectively. They would not to be situated on the same copy of the mini-chromosome.

The event that generates the acentric and dicentric chromosomes can be described as follows: when replication fork arrest at the nearby *RTS1* barriers ("pause on" growth) causing chromosomal rearrangements at the S phase, the two arms of the newly formed acentric and dicentric chromosomes are attached by cohesion. However, the two aberrant entities (the acentric and dicentric chromosomes) are not necessarily attached to each other. We can expect the GFP and tdTomato foci on the rearranged chromosomes to show a different distribution within a single cell when compared to what was shown in cells within which chromosomes were not rearranged. However, observation of these rearranged chromosomes was only possible when the lacI-GFP and TetR-tdTomato foci were separated from each other sufficiently. This is illustrated in a cartoon in Figure 4.7 (middle and right panels). Interestingly, we

initially expected that the dicentric and acentric chromosome formation were coupled. In such issue, we will not be able to see a copy of unaltered Ch^{16}-NRUH. However, because we observed that a dicentric chromosome presented in a daughter nucleus companied with a copy of a parental Ch^{16}-NRUH (Figures 4-7 and 4-8), it is proposed that acentric and dicentric chromosomes may not be formed in the same event (Figure 4-9 and Chapter 6).

The observation of an acentric chromosome

Although a Southern blot assay and a PFGE confirmed the generation of the acentric chromosomes (Figure 3-14), there were certain limitations that were problematic for the direct visualisation of an acentric chromosome. The clearly distinguishable images, which were proposed to show the two, obviously closely associated tdTomato dots on an acentric chromosome within the nucleus in the fixed cells, were not captured. However, in the live cell imaging, a transit snapshot of the cells showing a tdTomato dot that was well separated from the GFP foci was observed. It is estimated that this phenomenon occurs in approximately 1 of 500 cells (Figure 4-4 A, white arrow). It was originally expected that the two tdTomato foci would be located on an acentric chromosome. The distance between the two tdTomato foci of an acentric chromosome is ~50 kb. This may, however, not be sufficient to distinguish the two tdTomato dots located on the acentric chromosome. Therefore, it is suggested that a tdTomato focus without an associated GFP focus may indicate the presence of an acentric chromosome (Figure 4-4 A, white arrow).

Moreover, in the M-phase and the G_1 phase, we observed that some cells did not contain any tdTomato foci within their nuclei (Figure 4-4 B). An increasing number of cells exhibited the disappearance of the tdTomato focus forming the nucleus as the

cell cycle progressed (Figures 4-4B, white arrow, and 4-10D). An acentric chromosome lacks centromeres and thus has no attachment to the microtubules. Consequently, our results seem to suggest that an acentric chromosome may disappear as quickly it forms, leaving the GFP foci within the nucleus (Figure 4-4B, white arrow).

A. Live cell imaging

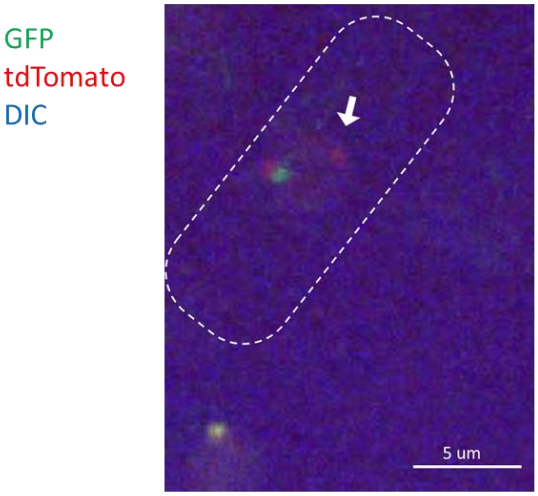

B. The cells only contain GFP dots due to the disappearance of an acentric chromosome within the nucleus.

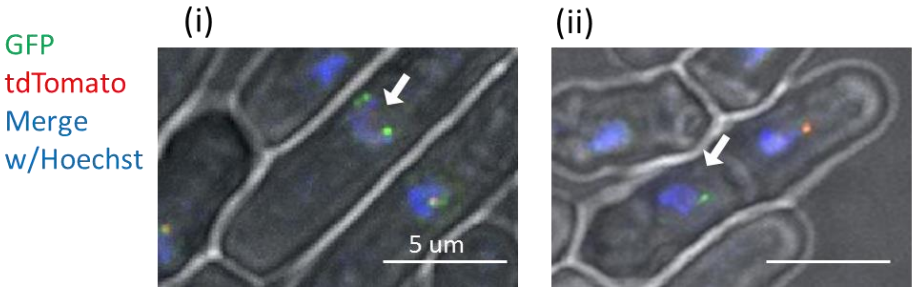

Figure 4-4. The observation of an acentric chromosome.

The observation of Ch[16]-NRUH *nmt-rtf1*$^{+}$ cells was obtained during the "pause on" growth. There are some problematic limitations for direct imagining of an acentric chromosome. (A) A tdTomato focus without an associated GFP focus may indicate the position of an acentric chromosome (white arrow). (B) An increasing number of cells that exhibited the disappearance of tdTomato focus form the nucleus as the cell cycle progressed. Therefore, some cells only contain the GFP foci within the nucleus (white arrow). The bar represents 5μm.

The observation of a dicentric chromosome

A dicentric chromosome can be visualised in the late G_2 phase or the early metaphase, in which some cells containing two closely associated GFP dots are well separated from the tdTomato foci (Figure 4-7 i). This phenomenon was consistent with our expectation, namely that the separated tdTomato and GFP foci are localised on the acentric and dicentric chromosomes, respectively, and are not juxtaposed on a single mini-chromosome. The dicentric chromosomes were visible at the metaphase in the form of two juxtaposed GFP dots in the "pause on" growth cells, while in the "pause off" growth cells that contained the unaltered mini-chromosome, the GFP signals were clearly separated (Figures 4-7 i and 4-8, white arrows).

During cell segregation, the dynamic properties of the spindle microtubules attached to the kinetochores can drive chromosome congressing, aligning them at the cell equator between the daughter cells, permitting the segregation of the sister chromatids to the opposite poles. Due to the unusual configuration of a dicentric chromosome, cells that contain the dicentric chromosomes are expected to encounter problems during the chromosomal segregation event. We predicted that the microtubules emanating from the mitotic spindle poles would bind to the two centromeres of a dicentric chromosome and would attempt to separate them during the M-phase. Thus, some cells will undergo chromosomal segregation problems. Moreover, we also observed that a dicentric chromosome presented in the daughter nucleus, companying with a copy of unchanged Ch^{16}-NRUH. This suggests that the acentric and dicentric chromosomes may not be generated during the same event. More details will be shown and will be discussed in the section below.

It was observed that some cells that contain two juxtaposed GFP dots were well

separated from the tdTomato foci during the M-phase. Because the induction of the *rtf1*$^{+}$ is not synchronous with the *nmt41* promoter, it is unclear whether the cells containing the two juxtaposed GFP dots occurred in the observed mitosis or in the preceding mitosis. We propose that there are two potential models for the situation that was observed in the cells containing two juxtaposed GFP dots:

(1) A random breakage may occur on a dicentric chromosome during the M-phase (Figure 4-5). At the anaphase, the dicentric chromosome may break at some point (Figure 4-5 a and b). The breakage may be caused by the pulling forces of the mitotic spindle. Of the two daughter cells, one will carry a deletion, encompassing one Cen3 without the GFP visualisation, while the other will contain an inverted duplication of the *lacO* repeats-*arg3*$^{+}$marker, containing one Cen3 and two GFP loci (Figure 4-5 c). Notably, the breakage event may also occur between the two GFP loci, so that a dicentric chromosome can be split into two broken fragments, each fragment containing one Cen3 and one GFP dot (Figure 4-5 d). However, if this were the case, we would not be able to see the two juxtaposed GFP dots within the nucleus. The broken-ended chromosomes could then be observed randomly in the daughter cells, depending on where they were initially formed. The stabilisation of broken-ended chromosomes can be carried out either by the subsequent BFB cycles or by telomere addition.

(2) Alternatively, a dicentric chromosome may be caught by one side of the spindle pole and initially move towards one of the nuclei (Figure 4-6). An intact dicentric chromosome may be maintained by further rearrangements, such as the deletion of one centromere, as has recently been found in human myeloid malignancy [35], or occurring through epigenetic centromere inactivation [36]. Therefore, we expect that the intact dicentric chromosome can be successfully segregated after further

rearrangements. A dicentric chromosome can exist in a cell and can be duplicated in the next cell cycle (Figure 4-6, d-f). However, we did not eliminate the possibility of the re-activation of centromeres on a dicentric chromosome. Again, the re-activation of the centromeres of a dicentric chromosome may undergo a BFB cycle until stabilised by further rearrangements, such as the telomere addition.

At the anaphase, ~2% cells with two GFP foci in only one nucleus of the daughter cells without the tdTomato foci co-localisation were observed (Figures 4-7 ii and 4-8, anaphase). According to the two potential models mentioned above, this phenomenon might result from chromosome breaks that occur between Cen3 and one of the GFP foci, due to the pulling force of the bi-polar spindle (Figure 4-4). In such cases, one part of the broken chromosome, encompassing one Cen3, would not be visualised, while the other broken chromosome would be visualised as a cluster of two GFP foci, containing one Cen3 and two GFP loci. This is consistent with the results described in Chapter 5, where we indeed obtained the truncated Ch^{16} produced from a dicentric chromosome. We will hereafter refer to a breakage event as a mechanism stabilising a dicentric chromosome, as seen in Chapter 5. In addition, two juxtaposed GFP dots may show the position of an intact dicentric chromosome, as suggested by model (2) described above (Figure 4-6). Consistent with the results shown in Chapter 5, we found that some cells could encompass the stable dicentric chromosomes, although it is still unclear as to how a dicentric chromosome can exist and be segregated successfully *in vivo*. Recently, our group has been working on the sequencing of these rearranged products in an attempt to gain more insight into the fate of a dicentric chromosome.

In the telophase, our transit snapshot of the cells showed two juxtaposed GFP foci in

the middle position. This illustrates the stretch of a dicentric chromosome between two separated nuclei, as observed in Figures 4.7 iii-v and 4.8 (white arrow). We assumed that a dicentric chromosome could undergo a breakage or a stabilisation by means of the mechanisms described above. Interestingly, at the next G_1 phase, ~1% cells showed a dicentric chromosome bridge at the septum of the cell (Figure 4-4 iv), which may generate a breakage afterwards (Figure 4-4 v).

Finally, approximately 5 to 10% cells contained more than one (>1) GFP focus that was well separated from the tdTomato foci within the nucleus (Figures 4-4B and 4-10D). We propose that the observation of >1 GFP focus within the nucleus was a truncated form of Ch^{16}-NRUH, produced by the dicentric chromosome fragments. This is consistent with the results presented in Chapter 5, where we found that the random breakage of the dicentric chromosomes occurred in these cells. Considering how >GFP foci might accumulate in one nucleus (Figure 4-10D), if the two centromeres of an unstable dicentric chromosome migrate towards the opposite poles at the anaphase, the pulling forces of the mitotic spindle increase the probability of disrupting the chromatin structure, generating broken chromosomes. The broken-ended chromosomes can then be inherited randomly by one of the two daughter cells, depending on when they were initially formed. However, because the Rtf1 expression is induced non-synchronously with the *nmt41* promoter, it is unknown whether the breakage of the observed chromosome occurred in the observed mitosis or in the preceding mitosis.

The production of the acentric and dicentric chromosomes may not occur in the same event

The microscopic observations demonstrated that the acentric chromosomes were dislocated from the nucleus; an intact dicentric chromosome, containing two Cen3 and two GFP loci, or a broken-ended dicentric chromosome containing one Cen3 and two GFP loci underwent imbalanced segregation into one of the daughter cells. Interestingly, we observed that a dicentric chromosome presented in a daughter nucleus, companying with a copy of the unchanged Ch^{16}. (Figures 4-6 and 4-11). Thus, this suggested that the production of the acentric and dicentric chromosomes might occur in separate events - if the dicentric and acentric chromosome formation were coupled, we would not be able to obtain a copy of the unaltered Ch^{16}-NRUH.

We wondered how the acentric and dicentric chromosomes were generated in separate events. In our U-turn model (Figure 1-13), the inverted repeats and their close 14bp spacing could permit an unusual replication product to be formed by the replication fork regression (Figure 4-9B). When the newly-synthesised 3’ end of the leading strand of a replication fork becomes detached from the leading strand template (Figure 4-9B i), the detached end can anneal to its complementary lagging strand (Figure 4-9B ii). This 3’ end primes and synthesises with the lagging template (Figure 4-9B iii) and converts the ligated fragments to the adjacent Okazaki fragment, forming a continuous DNA strand at the replication fork, known as a ‘‘closed Y’’ fork (Figure 4-9A ii). An approaching fork from an adjacent origin close to the closed fork would be resolved through a combination of both topological and enzymatic forces (Figure 4-9A ii-iv). As a result, the linear dicentric chromosome at both ends may be released and the approaching fork could complete the replication of the parent Ch^{16}-NRUH (generating the parent Ch^{16}-NRUH) (Figure 4-9A iv). This is because the

linear dicentric chromosome contains the origin and can be converted into a duplicate molecule by replication in the next S-phase (generating the dicentric chromosome). Alternatively, a linear dicentric chromosome at both ends may be cleaved by an unknown enzyme and the approaching fork could complete the replication, only generating the parent Ch^{16}-NRUH, without a dicentric chromosome formation (Figure 4-9A iv). This model still requires further experimentation in order to obtain the relevant information to prove the concept. Our group is currently working on changing the promoter for the induction of the Rtf1 protein. We expect that we can simultaneously regulate the Rtf1 expression and analyse the chromosomally rearranged intermediates via 2D gel, so as to obtain more supporting evidence for this model.

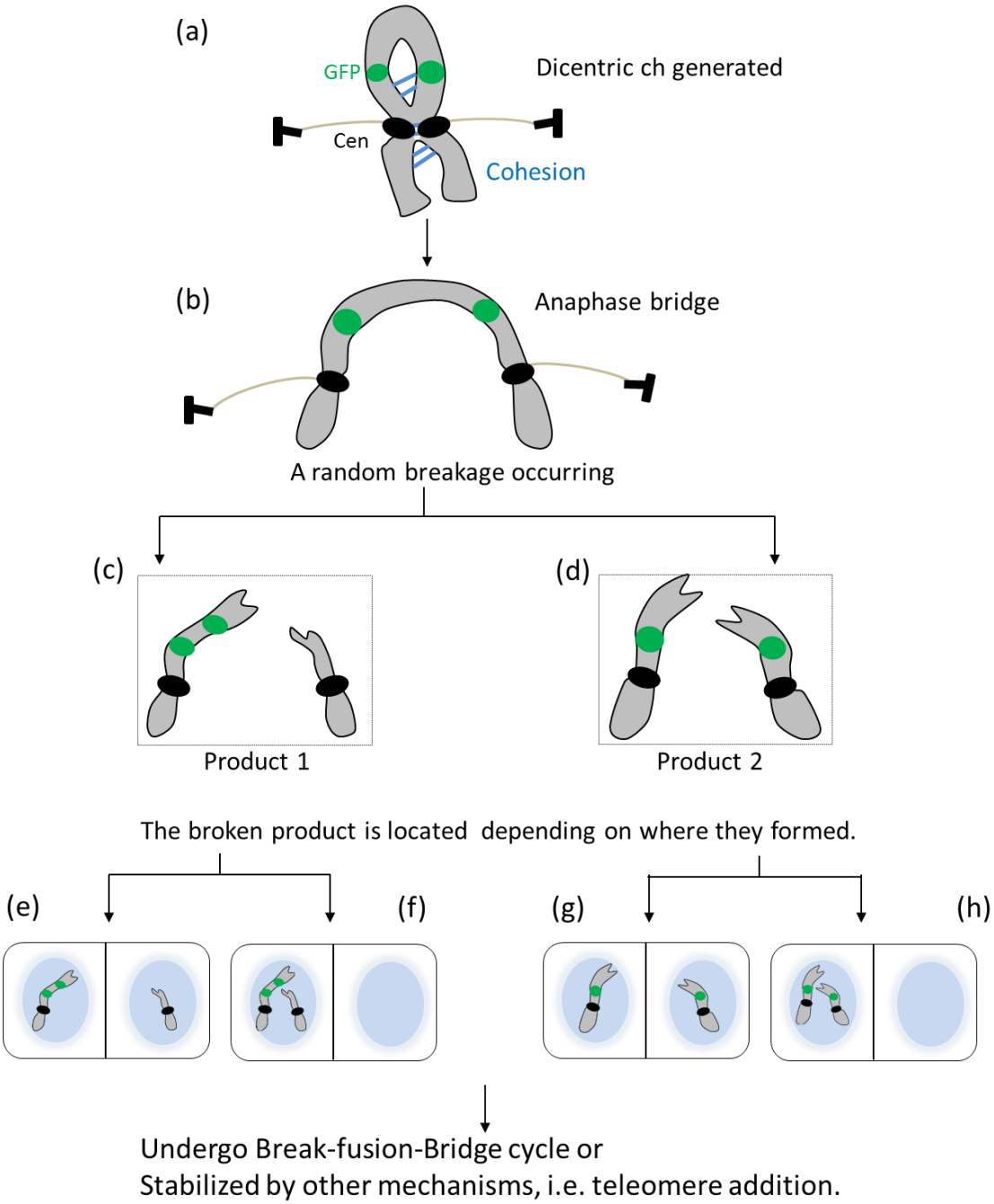

Figure 4-5. A random breakage occurs on a dicentric chromosome during the M phase.

(a-d) At the anaphase, the dicentric chromosome can form an anaphase bridge caused by the pulling forces of the opposite mitotic spindle poles. A random breakage occurs on a dicentric chromosome. (c-h) The broken-end chromosomes can be visualised randomly in the daughter cells, depending on where they were initially formed. The stabilisation of broken-end chromosomes are achieved by either subsequent BFB cycles or telomere addition.

Figure 4-6. An intact dicentric chromosome may be maintained and exist in the next cell cycle. (a and b) A dicentric chromosome may be bound to one side of spindle pole and initial moves toward in one of nucleus. (c-e) In the first mitotic cell cycle, the stabilisation of an intact dicentric chromosome may be retained by further rearrangements, i.e. deletion or inactivation of one of the centromeres. Thereby, we expect that the intact dicentric chromosome can be segregated successfully then be duplicated in the next cell cycle. (f) In the next cell cycle, the dicentric chromosome may steadily exist in a cell or the re-activation of centromeres on a dicentric chromosome. The re-activation of centromeres of a dicentric chromosome may undergo the BFB cycle till stabilisation of telomere addition.

Fist
mitotic cell cycle

(a)

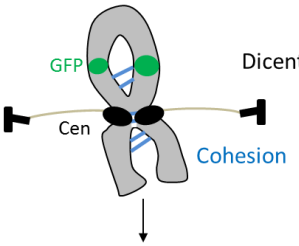

Dicentric ch generated

(b)

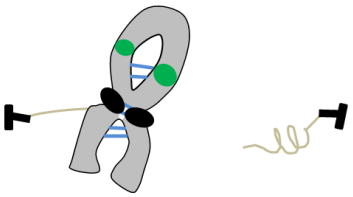

One spindle pore lost connection
to Dicentric ch

(c)

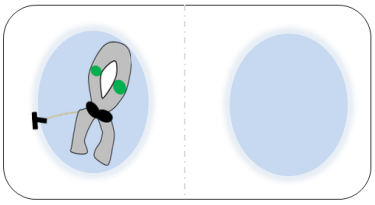

Dicentric ch may be stabilized by following mechanisms,
e.g. deletion or inactivated one of centromeres

Intact dicentric ch can be maintained
to next mitotic cell cycle

Secondary
mitotic cell cycle

(d)

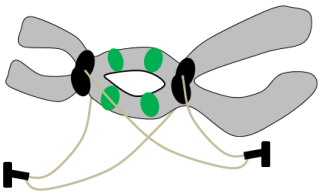

(e)

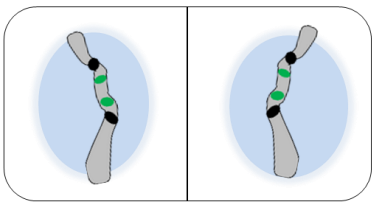

(f)

The dicentric ch may cause anaphase bridge

Undergo Break-fusion-Bridge cycle
or
Stabilized by other mechanisms, i.e. teleomere addition.

Figure 4-7. Observations of the mini-chromosome during mitotic cell cycle during the "pause on" growth.

Left panel: i-v - Images acquired from synchronized Ch^{16}-NRUH *nmt-rtf1*$^{+}$ fixed cells from the G_2 to next G_1 phase. The middle panels are schematic illustrations of the cells. The right panels show rearranged chromosome generation. The GFP foci and tdTomato foci show co-localization on the initial mini-chromosome. Two close GFP foci without tdTomato foci overlap when a dicentric chromosome is formed. Random breakage may occur on a dicentric chromosome. If a breakage occurs between Cen3 and one GFP focus, two GFP foci of broken dicentric chromosomes were proposed to migrate towards one of the daughter cells (Images ii). A stretched dicentric chromosome formed a bridge in the middle of cell found in the telophase (Images iii). As cells further progress through the cell cycle, the abnormal distribution of the dicentric chromosomes may occur (Images iv-v) due to miss-segregation problems during the M phase. The bar represents 5μm.

Pause on

G2

M

G1

		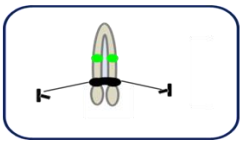
i 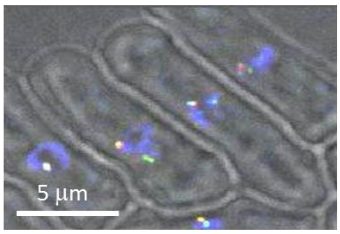	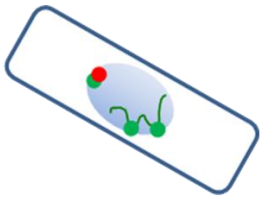	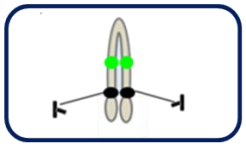
ii 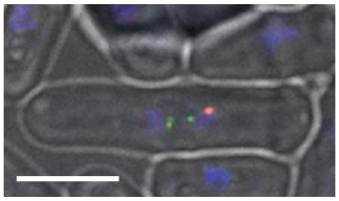		a. 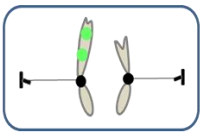 b. 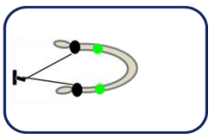
iii 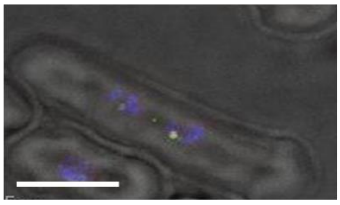	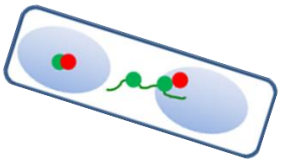	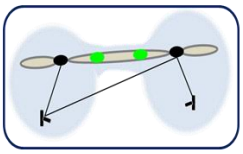
iv 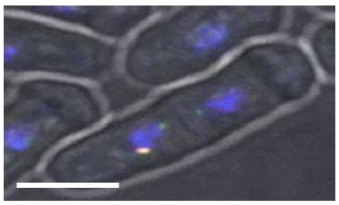	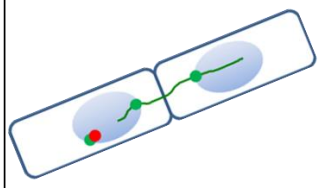	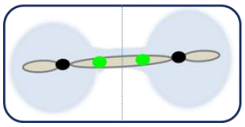
v 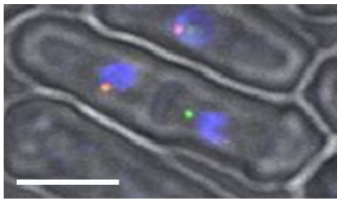	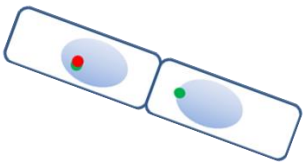	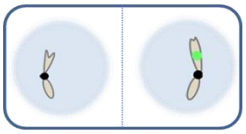

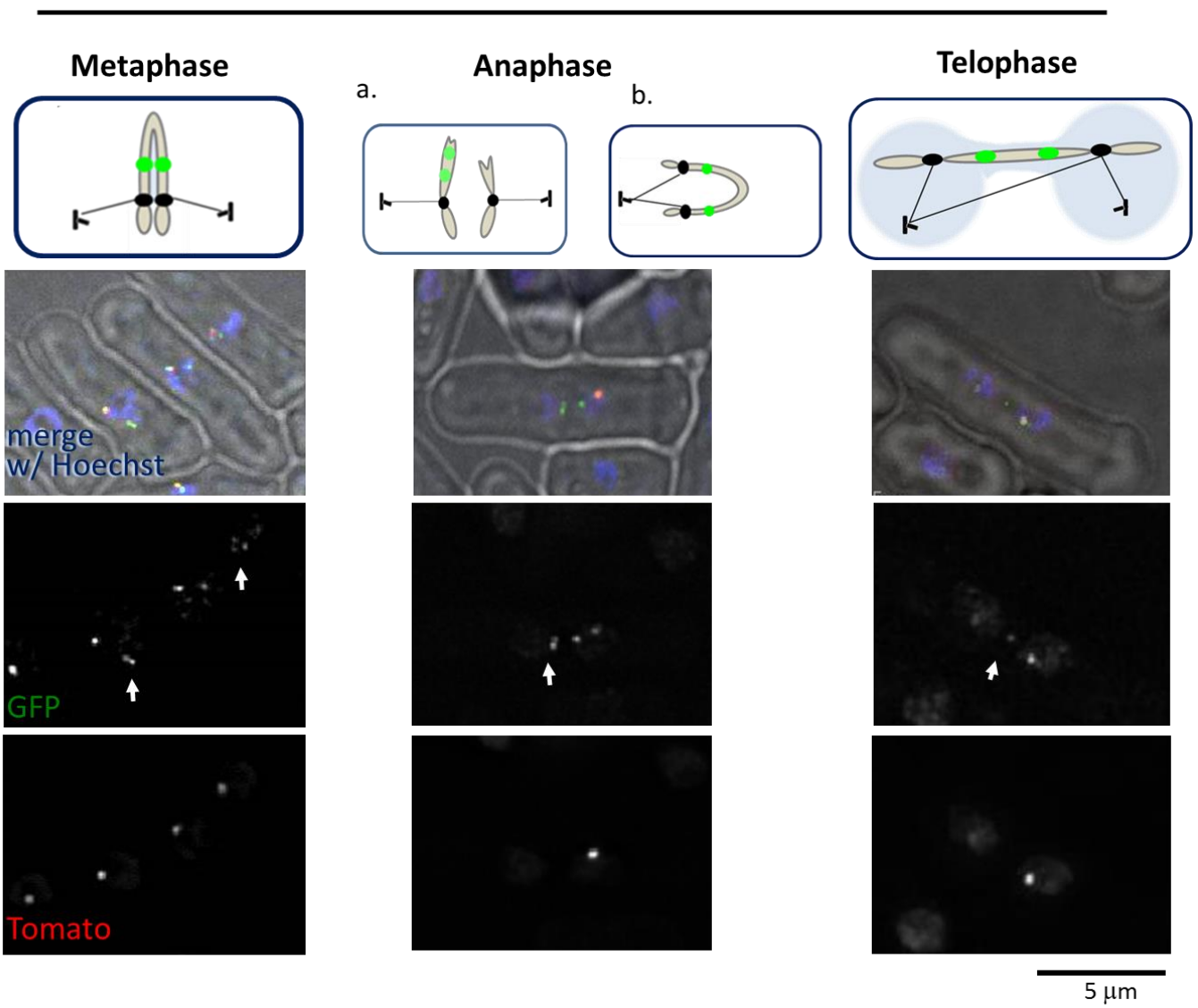

Figure 4-8. Detailed analysis of synchronized Ch[16]-NRUH *nmt-rtf1*$^{+}$ fixed cells at the M phase during the "pause on" growth.

White arrows indicate the position of the dicentric chromosomes. The dicentric chromosomes are distinguishable by two close GFP foci without the appearance of tdTomato foci at the metaphase entry. A dicentric chromosome is proposed to undergo a random breakage event and may be observed as a broken dicentric chromosome with two GFP foci, as cartoon (a) in the anaphase. A stable dicentric chromosome may also exist in the anaphase through further rearrangement, as cartoon (b) in the anaphase. In some cases, a dicentric chromosome is stretched in the middle of a telophase cell, generating a chromatic bridge across the two nuclei. The merged images show Hoechest dye staining of DNA to visualise the nucleus. Bar: 5µm.

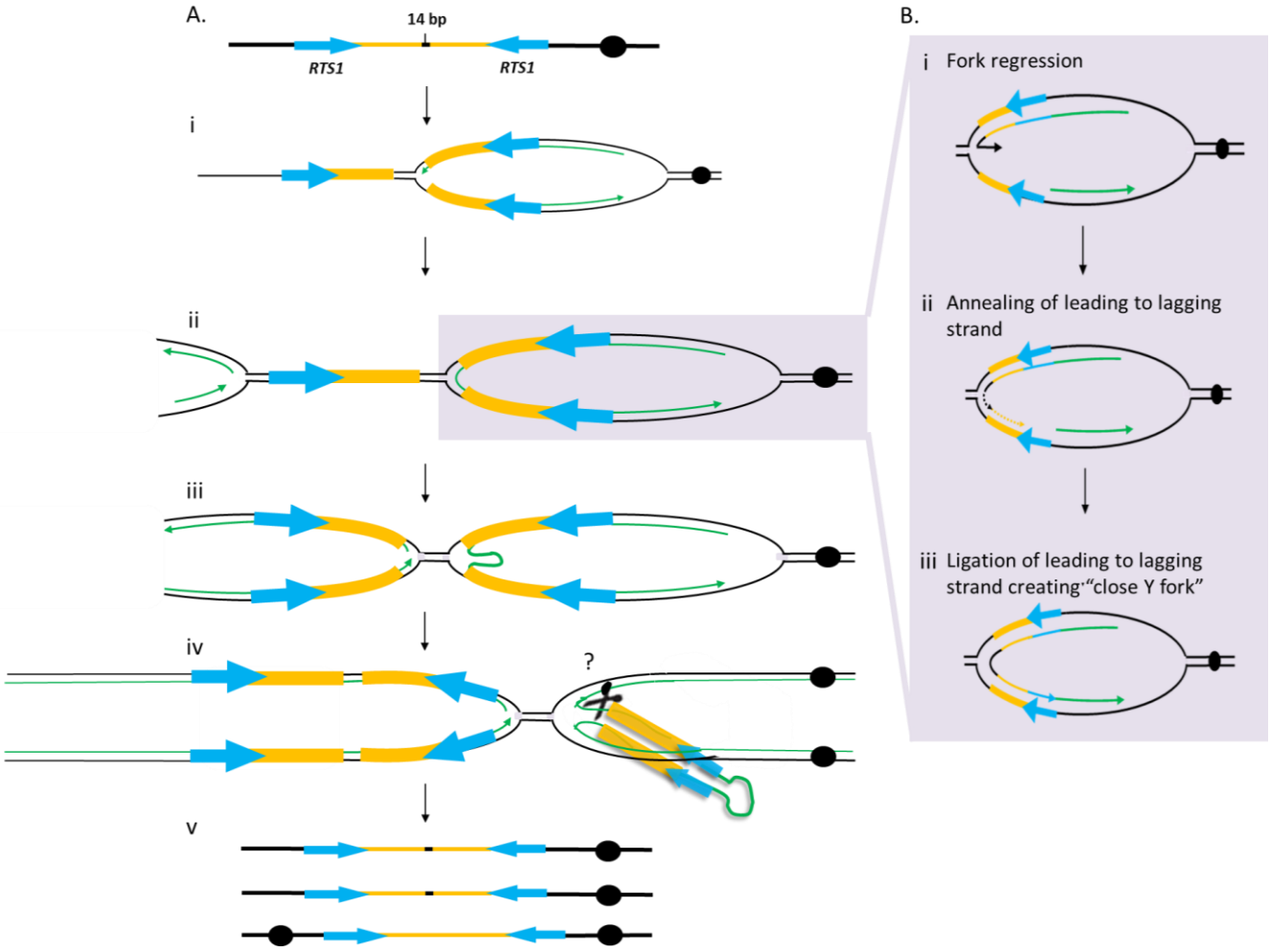

Figure 4-9. The model for the dicentric chromosome with Ch[16]-NRUH after replication fork stalling.

(A) An overview of the release of a dicentric chromosome and parent Ch[16]-NRUH that rise from unusual replication progression. Failure of fork restart leads to a "closed" Y structure intermediate. An approaching fork from an adjacent origin at the closed fork would resolve through a combination of both topological and enzymatic forces. As a result, the dicentric chromosome and parent Ch[16]-NRUH will be formed. Additionally, the hairpin-loop form of the dicentric chromosome may be digested by unknown enzyme, only generating parent Ch[16]-NRUH. (B) Details of the mechanism that leads to a "closed" Y structure intermediate. During fork regression, the newly-synthesised 3'-end strand from the leading strand detaches, annealing to the lagging strand template within a close homologous sequence to form a "closed" Y structure.

4.2.1.3 Quantification of the observations from the synchronised Ch^{16}-NRUH nmt-rtf1^{+} fixed cells

To quantify the observations from the synchronized Ch^{16}-NRUH *nmt-rtf1*$^{+}$ fixed cells (CJ90, Figure 4-1A), I categorised the properties of chromosome segregation and compared them with those of the control strain, where the *RuiuR* locus is replaced by a *Kan* resistant gene in the *nmt-rtf1*$^{+}$ background. I assigned each cell to one of three categories. In the first category, cells can resume replication via a correct HR protein-dependent repair mechanism and can then complete replication. This leads to an unchanged Ch^{16,} and thus no chromosomes rearrangements occur. ~82% Ch^{16}-NRUH *nmt-rtf1*$^{+}$ cells showed the GFP and tdTomato dots co-localised on each copy of Ch^{16} (Figure 4-10D; the black block shows the cells that underwent normal cell segregation). For the control strain that lacked the *RuiuR* system (CJ73, Figure 4-1A), we predicted that the cells would complete replication, and thus no acentric or dicentric chromosomes would be generated by the expression of the Rtf1 protein. Consistent with our expectation, all control cells showed that the GFP and tdTomato foci existed on unchanged Ch^{16} when using the same experimental conditions that were used in the Ch^{16}-NRUH *nmt-rtf1*$^{+}$ cells. All the control cells revealed normal chromosomal segregation over the entire period of the fixed section procedure (Figure 4-10C, black block).

The second category incorporated a situation in which the cells restarted the replication process and exhibited inappropriate replication due to the HR using an incorrect template. Thus, we expected to see HR-dependent rearrangements in the *RTS1* repeats, forming the acentric and dicentric chromosomes. Consequently, unusual chromosomal segregation events were included in this category (Figures 4-10B and D, grey block). An acentric chromosome, marked by two tdTomato dots,

was expected to present random nuclear distribution and to eventually become disassociated from the chromatid mass. However, although a Southern blot assay and a PFGE confirmed the generation of the acentric chromosomes (Figure 3-14), direct visualisation of an acentric chromosome proved to be problematic, as discussed in Chapter 6. In addition, the acentric chromosome appeared to be rapidly dislocated within the nucleus, creating further difficulties in following the fate of these structures. Due to the aforementioned problems with regard to following the acentric chromosomes, the cells were mainly characterised by the obvious generation of the dicentric chromosomes. This may result in the underestimation of the chromosomal rearrangement events.

Furthermore, in the second category, ~12% of cells showed unusual segregations of each of the analysed samples of the cells containing the *RuiuR* system (Figure 4-10D, in which the grey block shows cells that presented unusual segregations). The cells in the second category demonstrated the following phenomena:

1. Snapshots of the cells were labelled with two close GFP spots. This indicated the presence of either an intact (containing two Cen3 and two GFP dots) or a broken-ended dicentric chromosome (containing one Cen3 and two GFP dots) (Figure 4-8, metaphase). An intact or a broken-end dicentric chromosome moved towards one of the two daughter cells (Figure 4-8, anaphase).
2. A lagging dicentric chromosomal bridge, containing two Cen3 and two GFP dots, persisted across the two nuclei (Figure 4-8, telophase). Notably, no unusual segregation event was found in the control strain, which is consistent with our expectation that no rearrangement event occurred in the absence of the *RuiuR* system.

Approximately 5 to 10 % cells (white block) retained an unusual number of GFP dots

in one of the daughter nuclei (>1 GFP foci) (Figure 4-4B). These may represent partial fragments of the dicentric chromosomes derived from secondary rearrangement events, such as a random breakage, which remained within the nucleus from a previous cell cycle. Note that, again, that the induction of the *rtf1*$^{+}$ is not synchronous with the nmt41 promoter. These structures were not observed in the control strain. Taken together, these results show that the occurrences of inappropriate segregation and an unusual number of GFP dots were caused by the Rtf1-RTS1 fork-stalling system.

Figure 4-10. Quantification of chromosome segregation in synchronized control and Ch^{16}-NRUH fixed cells during the "pause on" growth.

Cells were categorized according to the chromosomal behaviour during the M phase segregation (n=number of cells). The control strain (CJ73, described in Figure 4-1) is where the *RuiuR* locus is replaced by a *Kan^{R}* gene in *nmt-rtf1^{+}* background. (*A*) Schematic summary of the microscopic observations as cells undergo normal segregation. The GFP and tdTomato dots are expected to co-localise and separate equally on each of the sister chromatids. (*B*) Schematic summary of the microscopic observations as cells undergo unusual segregation. A portion of cells containing the acentric and dicentric chromosomes shows unusual chromosome segregation. (*C*) and (*D*) Quantification of aberrant chromosome segregation in control strain and Ch^{16}-NRUH *nmt-rtf1^{+}* fixed cells during the "pause on" growth.

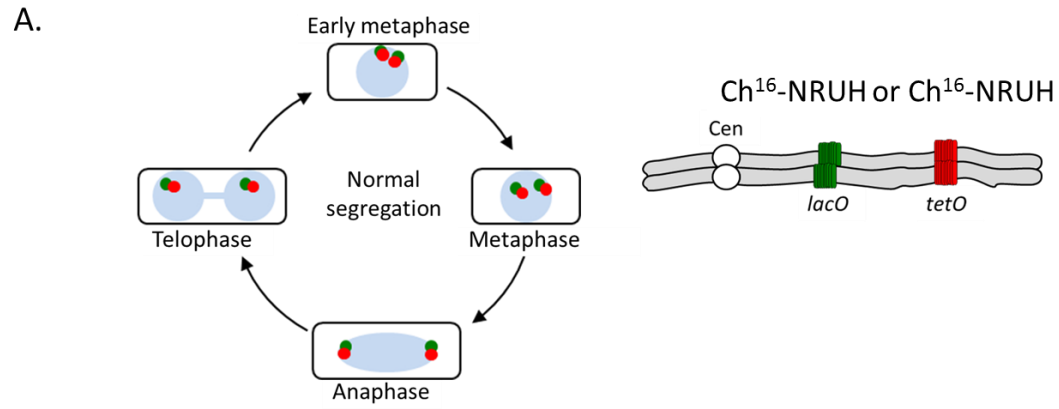
A.
Early metaphase
Normal segregation
Metaphase
Anaphase
Telophase
Ch16-NRUH or Ch16-NRUH
Cen
lacO
tetO

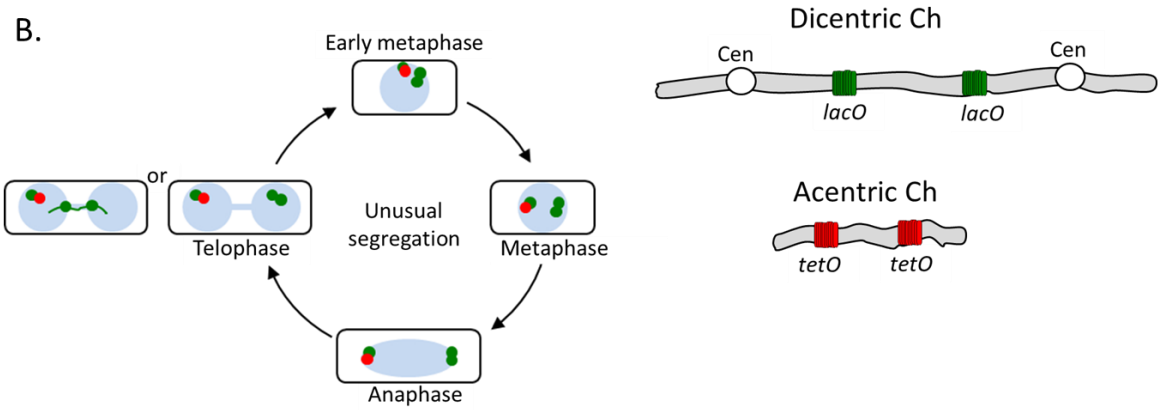
B.
Early metaphase
Unusual segregation
Metaphase
Anaphase
Telophase
or
Dicentric Ch
Cen
Cen
lacO
lacO
Acentric Ch
tetO
tetO

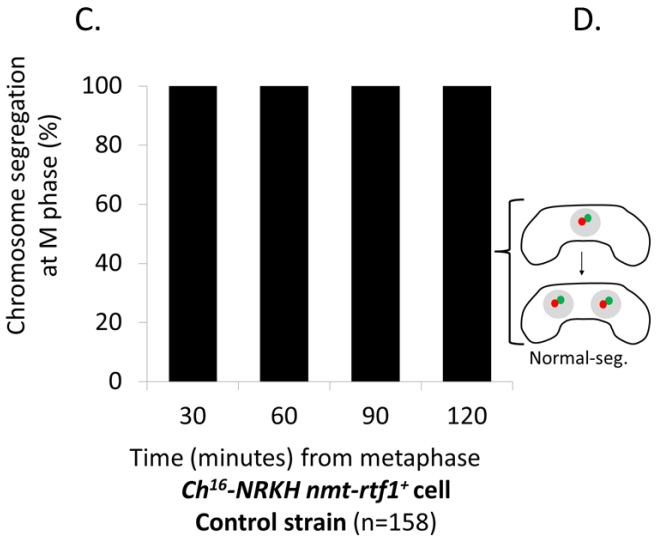
C.
Chromosome segregation at M phase (%)
100
80
60
40
20
0
30
60
90
120
Normal-seg.
Time (minutes) from metaphase
Ch16-NRKH nmt-rtf1+ cell
Control strain (n=158)

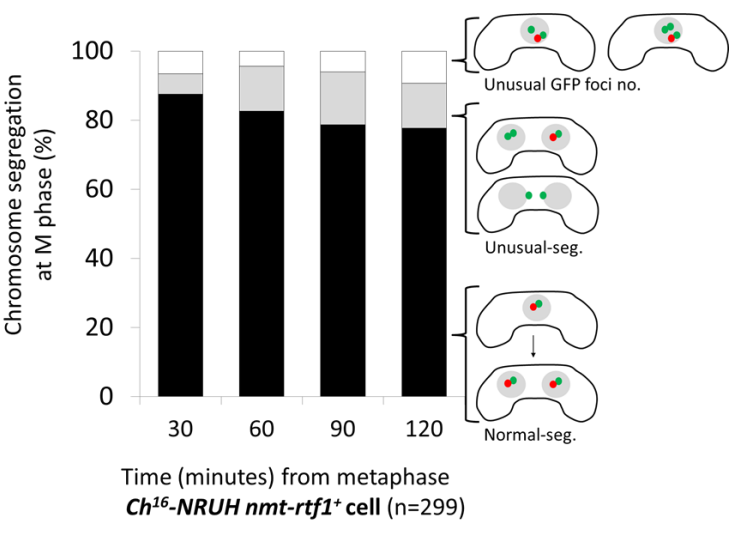
D.
Chromosome segregation at M phase (%)
100
80
60
40
20
0
30
60
90
120
Unusual GFP foci no.
Unusual-seg.
Normal-seg.
Time (minutes) from metaphase
Ch16-NRUH nmt-rtf1+ cell (n=299)

4.2.2 Live cell imaging of the Ch^{16}-NRUH *nmt-rtf1*$^{+}$ cells

To determine the behaviour and fate of a dicentric chromosome, I attempted to analyse chromosome segregations in living cells. The Ch^{16}-NRUH *nmt-rtf1*$^{+}$ (strain CJ90) or control cells (the strain CJ73, containing Ch^{16}-NRKH *nmt-rtf1*$^{+}$) containing the *lacO* and *tetO* repeats were grown in minimal media for 16 hour induction without thiamine supplement ("pause on" growth, 30 ℃) and the G_2 phase cells were isolated on lactose gradient. (Figure 4-1B, "pause on" growth). G_2 cells were plated in 4-well Lab-Tek chamber slide at a density of 4 x 10^5 cells/well and inoculated continuously (30 ℃) in minimal media without thiamine supplement (see Materials and Methods). In accordance with the data obtained from the fixed cells, there were very few distinguishing features between the rearranged chromosomes and the initial Ch^{16} at the G_2 phase because the sister chromatids were still closely attached by cohesion. Moreover, one of the challenges of fluorescence imaging is minimizing the harmful effects of excitation light exposure on cells that is equivalent to sun-burning of the cells and can cause damage leading to cell death.

Considering these two issues, time-lapse images of living cells were filmed from the time of metaphase onset, decreasing the exposure time of excitation light. Thus, aliquots of G_2 cells from lactose gradient synchronization were cultured continuously in Lab-Tek chamber for one hour — this can also enhance cell adhesion to chamber surface and to stabilise microscope focus. The chamber was then transferred to the work platform of the microscope. The images of living cells were recorded using a DeltaVision Personal DV deconvolution light microscope system connected to an external temperature controller (which maintained the temperature constant at 30 ℃).

4.2.2.1 The fate of a dicentric chromosome in a living cell during the mitotic cell cycle of Ch^{16}-NRUH nmt-rtf1^{+} cells during the "pause on" growth

At the beginning of the film, the cells had already finished the S phase and had completed the DNA replication. A portion (18% to 20%) of Ch^{16}-NRUH *nmt-rtf1*$^{+}$ cells underwent chromosomal rearrangements, and thus Ch^{16}-NRUH was split into the acentric and dicentric chromosomes. Two LacI-GFP dots from a dicentric chromosome were visible and were clearly separated from the TetR-tdTomato foci in a single nucleus (Figure 4-11, frames 1-8). Two GFP dots located on the dicentric chromosomes will move together during nuclear division at the onset of the dicentric chromosome formation. For the non-rearranged Ch^{16}-NRUH, the two distinct GFP foci should become visible at the late G_2 phase or the early metaphase, and should be separated from each of the chromatids during mitosis/nuclear division.

This is what we saw: where they represented the position of the dicentric chromosomes, the LacI-GFP spots clustered and moved in the same direction (Figure 4-11, frame 9), while the un-rearranged chromosomes diverted to separate spindle poles. During the anaphase, a cell usually imposes chromosome segregation and begins nuclear division. The dynamic movement of the mitotic spindle microtubules is central to the processes that enable accurate chromosome segregation. Once a dicentric chromosome is formed, microtubules are expected to attach normally to the two centromeres of the dicentric chromosome in a bi-orientated manner. However, normal separation will be difficult, due to the aberrant conformation of the dicentric chromosome. We expected that the unusual distribution of a dicentric chromosome in a cell might reflect the association between the dicentric chromosomes and the spindle poles during chromosomal segregation. Our time-lapse films, represented as sequential, still frames in Figure 4.11, showed that during the progress of nuclear

division, the dicentric chromosomes showed extremely active movement, presumably caused by the pulling force of the mitotic spindle microtubules. First, two GFP foci on the dicentric chromosome were pulled from one pole towards the opposite pole. However, they changed direction and moved dramatically back towards the original nucleus (Figure 4-11, frames 10-20). The film also showed some moments in which the two GFP foci moved slowly or ceased to move altogether, remaining in a central position in the cells. It is postulated that this phenomenon is a result of the tension that appears across the centromeres of a dicentric chromosome for a transient interval (Figure 4-11, frames 10, 15 and 16), derived from the increased pulling force of the bipolar spindle pole elongation. Taken together, this analysis of the dynamic movements of the GFP foci revealed asymmetrically distributed chromosomes between the two separating nuclei, occasionally presenting a transient chromatin stretching configuration. We anticipate that the dynamics of the microtubules provide the influence that directs chromosome motion in the living cell (see details in section 4.2.2.2.).

By the end of the film, before the formation of a centrally placed division septum, the dual GFP spots representing the dicentric chromosome underwent imbalanced separation and were packed into one of the two daughter cells, leaving the other daughter cell without any GFP foci (Figure 4-11, frames 21-25). This form of imbalanced segregation was seen in the majority of Ch^{16}-NRUH *nmt-rtf1*$^{+}$ cells during the "pause on" growth stage (Figures 4-11, 4-12 and 4-14B). Under the same experimental conditions, the control cells did not reveal abnormal chromosomal segregation when the pause was on (Figures 4-12A and 4-14B). These data indicated how cells respond to errors in the genetic architecture of chromosomes, while attempting to generate chromosome segregation with unparalleled accuracy.

Interestingly, we observed that the main outcome for a dicentric chromosome was to present in a daughter nucleus, companying with a copy of unchanged Ch^{16}-NRUH (Figure 4-11). This would suggest that the production of the acentric and the dicentric chromosomes might be not generated during the same event, as described in section 4.2.1.2 and in Chapter 6. We speculated that the acentric and dicentric chromosomes might be able to be generated in separate events. Figure 4-9 illustrates the potential model that generates dicentric chromosomes and parent Ch^{16}-NRUH arising from aberrant replication progression. Notably, this model may also occur when an acentric chromosome is generated, if the aberrant replication progression occurred in the *tel*-proximal Ch^{16}-NRUH.

The other interesting point is why the dicentric chromosomes always accompany a copy of unchanged Ch^{16}-NRUH in a daughter nucleus. As Figure 4-14 shows, this is the fate of the majority (92%) of the dicentric chromosomes in imbalanced segregation. In human cancer, DMs (double-minute chromosomes that are usually acentric chromatin bodies) attach to the periphery of a normal chromosome connected via unknown bridge molecules [35-37]. We propose that the dicentric chromosome may also have various associated connections with the parent Ch^{16}-NRUH; thus, the dicentric chromosomes always present in a daughter cell with a copy of the unchanged Ch^{16}-NRUH. However, further experimentation is needed in order to verify this.

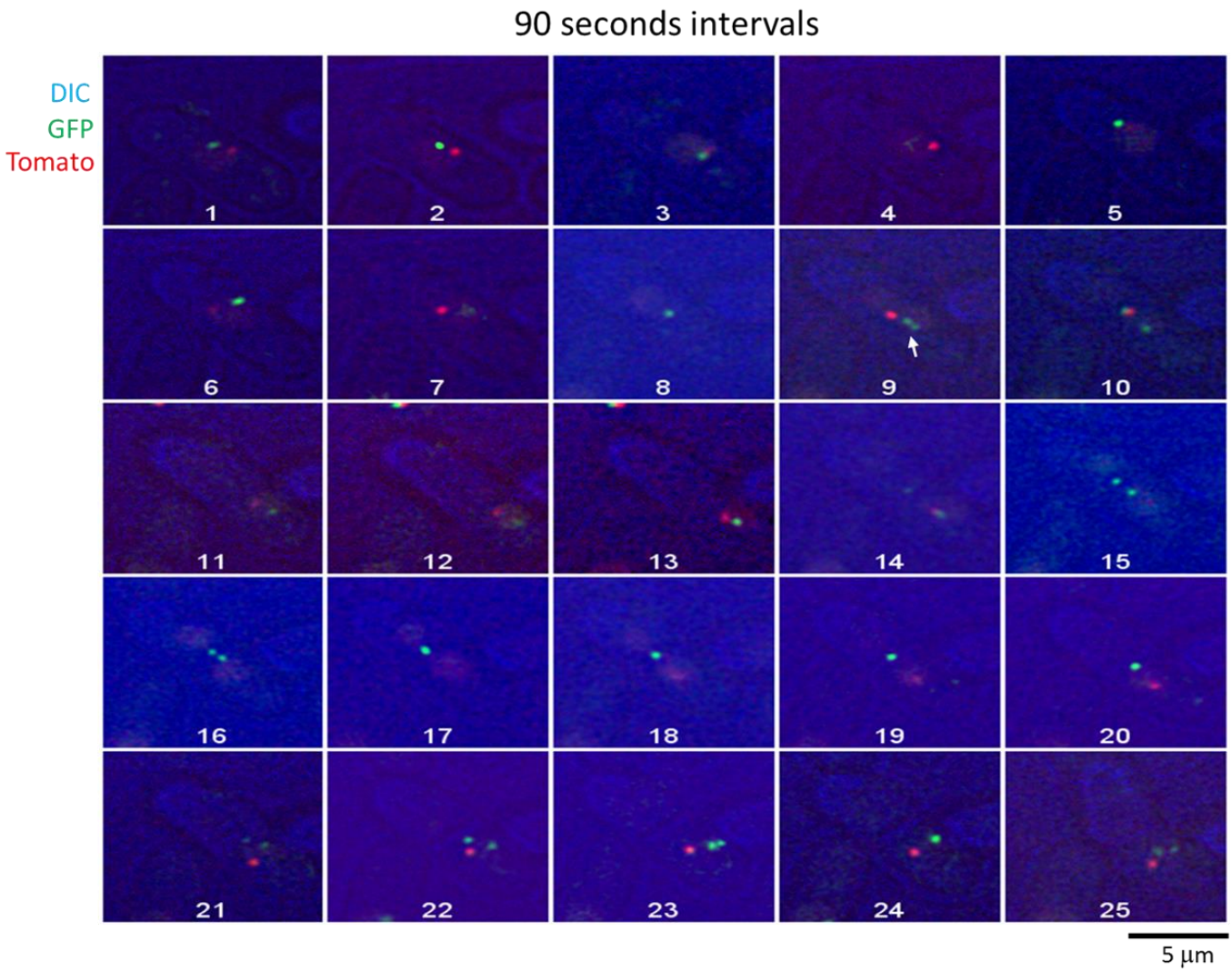

Figure 4-11. Time-lapse images of the dicentric chromosome behaviour in a living Ch^{16}-NRUH *nmt-rtf1*$^{+}$ cell.

A sequence of images of a cell progressing from the metaphase with a dicentric chromosome was recorded from the early metaphase to the next G_1 phase. A dicentric chromosome with two GFP foci was distinguishable at the frame 9 (white arrow) and moved actively between the opposite poles. The stretched transient dicentric chromosome can be clearly seen across the two daughter nuclei at frames 10, 15 and 16. Finally, a dicentric chromosome segregated towards one of the daughter nuclei (frame 21 to 25). These stacks of images were filmed in 90 seconds intervals. Bar: 5µm.

Figure 4-12. The behaviour of the dicentric chromosomes in a living control cell and Ch^{16}-NRUH *nmt-rtf1*$^{+}$ metaphase cell.

Time-lapse sequence of film images of the dynamic segregation of the dicentric chromosomes from semi-separate to two separated daughter nuclei. (*A*) The mini-chromosome without rearrangement event – the GFP and tdTomato dots are located on the same chromosome during nuclear division. (B) The images of individual cells with rearranged chromosome – picture 1 to 4 shows the generation of a dicentric chromosome which moved first towards one pole and changed direction rapidly stalled at the middle of the two separating daughter cells forming a bridge and which eventually were incorporated into one of the daughter nucleus.

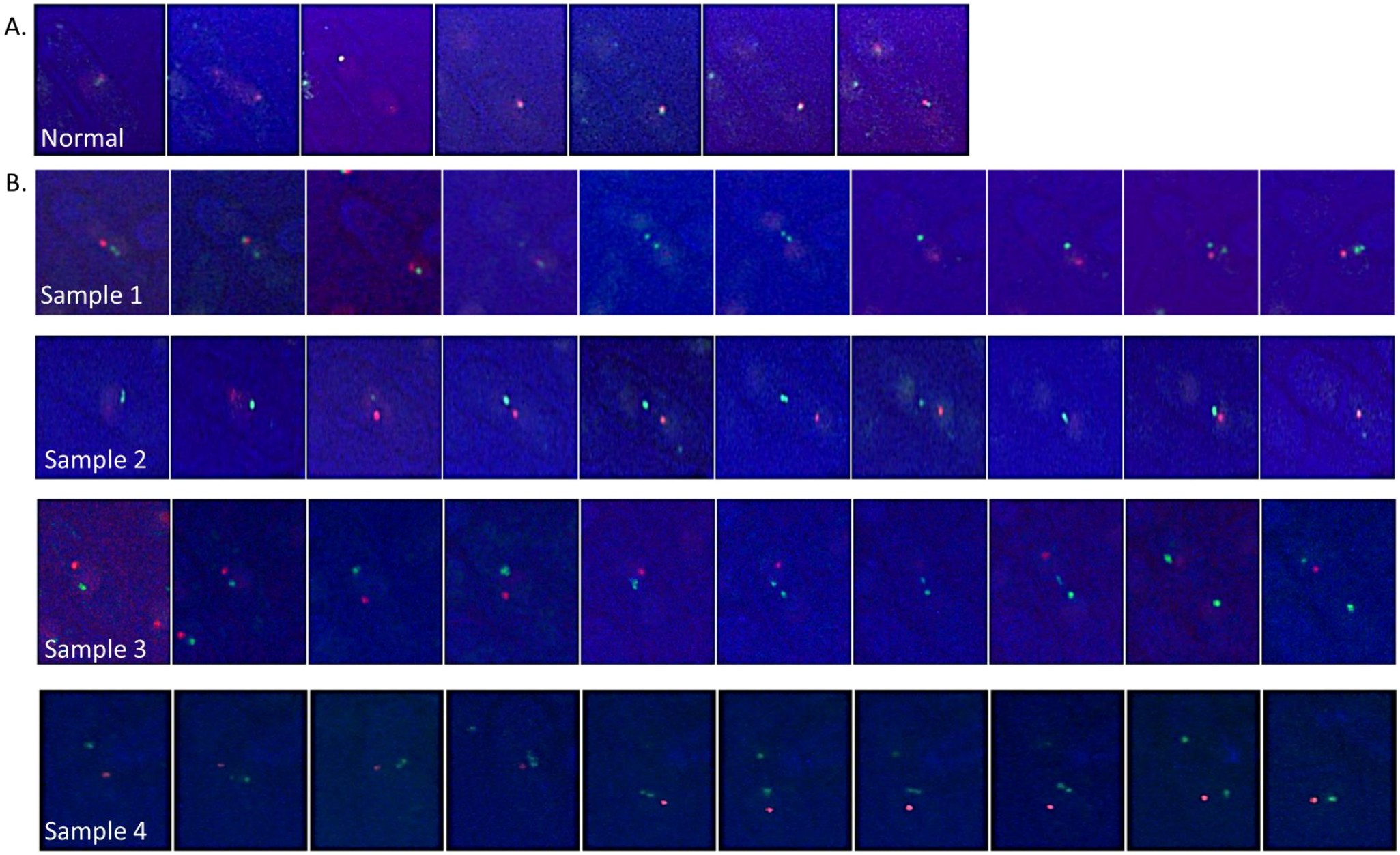
A.
Normal
B.
Sample 1
Sample 2
Sample 3
Sample 4

4.2.2.2 A detailed illustration of the organisation of a dicentric chromosome in the mitotic cells of Ch^{16}-NRUH nmt-rtf1^{+} cells during the "pause on" growth

Two co-localised GFP foci were considered to reveal the position of a dicentric chromosome in Ch^{16}-NRUH *nmt-rtf1*$^{+}$ cells. During chromosomal segregation, the spindle poles underwent a dynamic progression and mitotic spindle microtubules attached to the centromeres of a dicentric chromosome. Thereby, during spindle pole elongation, the movements of a dicentric chromosome are highly dynamic and mobile. The film that was shown in Figure 4.11 provided a detailed illustration of the behaviour that a dicentric chromosome might display during cell division. To begin with, two close GFP foci were presented at the point at which it is proposed that these represent dicentric chromosome architecture within an isolated nucleus in the anaphase (Figure 4-13, cell 1 and cartoon 1). During cell segregation, spindle microtubules attached to kinetochores and aligned with the dicentric chromosome at the cell equator. This arrangement pulled the dicentric chromosomes to the opposite poles (Figure 4-13, cell 2-4 and cartoon 2-4). The opposite spindle poles gradually pulled each centromere of the dicentric chromosome in this bi-oriented manner. The dicentric chromosome then showed an apparently transient, stretched configuration between the two nuclei (Figure 4-13, cell 4 and cartoon 4). When investigation of the septum was well underway and the nuclei were just completing division, the dicentric chromosome was still stretched across the two nuclei for a transient moment (Figure 4-13, cell 5 and cartoon 5). Finally, the dicentric chromosome moved into one of the daughter cells (Figure 4-13, cell 6 and cartoon 6).

We propose that there were two possible events present in cell 6 in Figure 4.13: 1. The cells contained a broken chromosome, caused by a breakage occurring on a dicentric chromosome. Consequently, part of the dicentric chromosome becomes segregated

into one of the two daughter cells if the breakage is between the Cen3 and the GFP site, as the GFP loci are close together. This is revealed as an imbalanced segregation of the foci. In Chapter 5, we collected evidence that a breakage event occurred on a dicentric chromosome.

2. Cell 6 in Figure 4.13 might also represent a situation in which an intact dicentric chromosome can be maintained in a single cell without a breakage event occurring. A dicentric chromosome can be bound to one side of the spindle pole, while the other spindle pole is disattached from a dicentric chromosome. An intact dicentric chromosome initially moves towards one of the nuclei. The stabilisation of an intact dicentric chromosome may be caused by further rearrangements, such as the deletion or inactivation of one of the centromeres. This intact dicentric chromosome can be successfully maintained and segregated, duplicating in the next cell cycle (Figure 4-13, cartoon illustrations in the right-hand box). Consistent with the results shown in Chapter 5, we indeed observed that some cells could contain a stable dicentric chromosome.

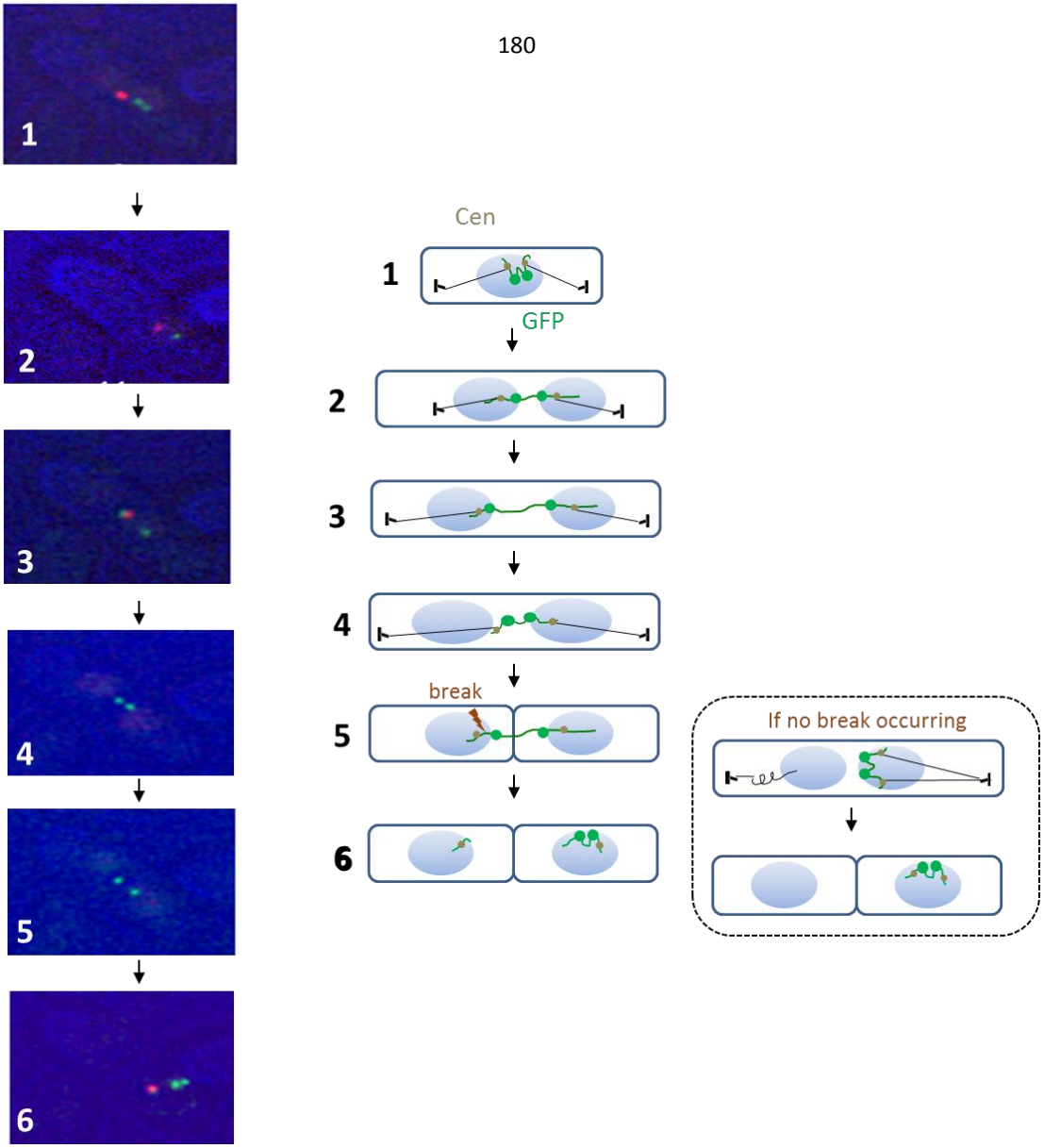

Figure 4-13. A dicentric chromosome organisation from the metaphase to the next G_1 phase.

The dicentric chromosome is labelled at two copies of *lacO* array with lacI-GFP (green). The *lacO* repeats are integrated near the centromeres. A dicentric chromosome was evidenced from two close GFP foci in the anaphase (cell 1). The passive movement of this dicentric chromosome due to spindle microtubules separation will lead to formation of a stretched intermediate (cell 2-4). The dicentric chromosome still stretched across the two daughter nuclei for a transit moment when the septum was formed (cell 5). If there was a breakage occurring on a dicentric chromosome, the broken part which contains two GFP foci was shown an imbalanced segregation occurring between lineages (cell 6). But it still has the possibility of intact dicentric chromosome exists in a cell when no breakage event occurring (as cartoon illustrated in right box).

4.2.2.3 Quantitation of time-lapse images from Ch^{16}-NRUH nmt-rtf1^{+} living cells

Time-lapse microscopy in real time performed on Ch^{16}-NRUH *nmt-rtf1*$^{+}$ cells enables us to determine what the fate of a dicentric chromosome is. By tracking the distribution changes between fluorescently marked chromosome loci at high temporal and spatial resolution, I defined two phenomena to describe the dynamic behaviour of chromosomal segregation: The first phenomenon is that, when the mini-chromosome is replicated normally without conformational rearrangements, the hereditary material is well prepared for its normal segregation during cell divisions. The GFP and tdTomato foci are expected to be co-localised on each of the sister mini-chromosomes during the period of nuclear division (Figure 4-14 A). When the sister chromatids are completely separated and the cells undergo nuclear division, the GFP and tdTomato foci of a single chromatid remain co-localised and travel together into the individual daughter nuclei. When the septum is formed in the centre of the cell, each of the two daughter cells contains one copy of the mini-chromosome. Each nucleus maintains one GFP and one tdTomato focus (Figure 4-14 A).

In the second phenomenon, if chromosomal rearrangements occur, this will generate the acentric and dicentric chromosomes (Figure 4-14B). It is proposed that the GFP and tdTomato foci are delocalised relative to one another. The acentric chromosome appears to dislocate rapidly within a nucleus. It is difficult to follow the fate of the acentric chromosome (see discussion in Chapter 6). Thus, the second phenomenon mainly characterised cells in which the obvious generation of the dicentric chromosomes could be seen. The dicentric chromosomes were clearly revealed by two closely clustered GFP foci, which subsequently underwent imbalanced segregation into one of the daughter nuclei. According to the motion path of two GFP dots on a dicentric chromosome, along with nuclear division (Figure 4-14 C), 64% of

Ch^{16}-NRUH *nmt-rtf1*$^{+}$ cells (N >142 cells; N=cell number) showed normal segregation (phenomenon 1) and 18% of Ch^{16}-NRUH *nmt-rtf1*$^{+}$ cells revealed a dicentric chromosome moving dynamically within the nucleus. The cells migrated towards one of two lineages via imbalanced segregation, which was the primary fate of the dicentric chromosome (phenomenon 2). Within this second population, about 92% of the cells showed that a dicentric chromosome entered a daughter nucleus in the company of a copy of a parental Ch^{16} (Figure 4-14B). The * in Figure 4.14 indicates the mode of the main fate of a dicentric chromosome. Originally, we would have expected to see the dicentric and acentric chromosomes in the same cell with no parental chromosomes remaining, if they were formed during the same event. Hence, this suggests that the production of a dicentric chromosome might be not coupled to the production of an acentric chromosome (see the discussion in Chapter 6). In the remaining 8% of the cells, there was one GFP spot located within a nucleus without the co-localisation of either the parental Ch^{16} or an acentric chromosome. This may imply the occurrence of a secondary event, such as a random breakage on a dicentric chromosome, with part of a broken-dicentric chromosome containing one of the GFP foci being present in a daughter nucleus (Figure 4-12, sample cells 3 and 4).

Finally, I noted that ~18 % of Ch^{16}-NRUH *nmt-rtf1*$^{+}$ cells and ~4 % of the control cells (containing Ch^{16}-NRKH *nmt-rtf1*$^{+}$) displayed late segregation or were growing slowly, while one GFP and one tdTomato focus were visible in the nucleus. Most of these cells ultimately underwent normal segregation. However, the time required for this was delayed around three hours when compared to the occurrence of the first normal cell segregation. The exact reasons for these phenomena remain unknown: they may be caused by various problems, such as damage from the harmful effects of the excitation light exposure, or by some unknown, internal genetic problems.

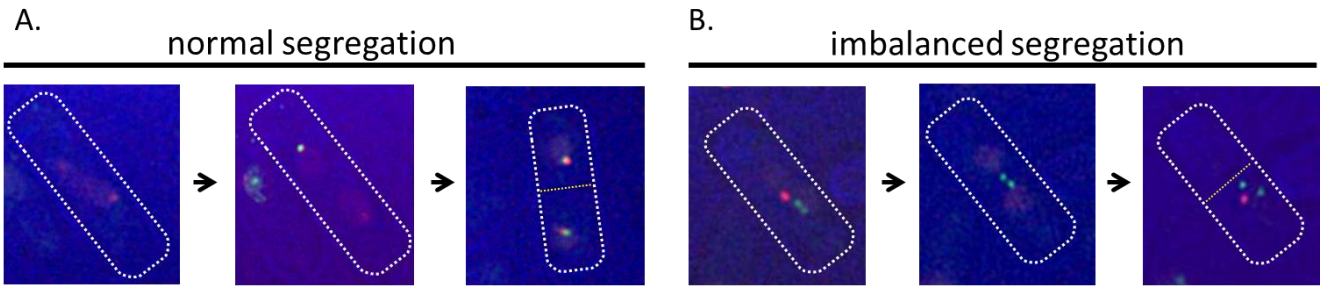

C.

		Ch[16]-NRUH *nmt-rtf1*[+]		Control strain	
		n	%	n	%
Normal segregation	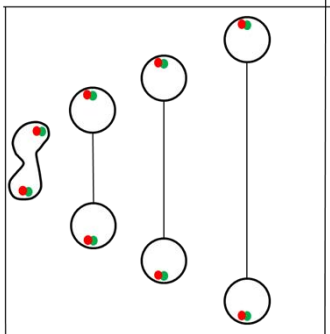	90/142	64%	122/127	96%
*Imbalanced segregation	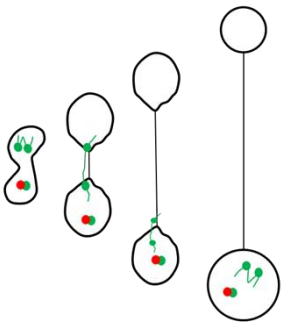	26/142	18%	0/127	0%
No division cells		26/142	18%	5/127	3.9%

n= cells no.

Figure 4-14. Quantitation of time-lapse images from the living cells.

The white line represents the membrane of a cell. The yellow line indicates the presence of a septum. (*A*) Normal segregation is indicated by the co-segregation of the GFP and tdTomato foci during nuclear division. (*B*) Imbalanced segregation reveals a movement where both of the two GFP foci located on a dicentric chromosome are inherited into one of daughter nuclei. (*C*) Quantitation of data from live cell microscopy on control (containing Ch[16]-NRKH *nmt-rtf1*[+]) and Ch[16]-NRUH *nmt-rtf1*[+] cells (n=number of cells); * shows the majority (92%) for the fate of a dicentric chromosome in imbalanced segregation.

4.3 Discussion

As described in Chapter 3, the *RuiuR* system was integrated upon Ch^{16} in the *nmt-rtf1*$^{+}$ genetic background, and this system confirmed the formation of the acentric and dicentric chromosomes as proven by the molecular analyses, RFLA and PFGE. In this chapter, we show the subsequent studies for a direct visualisation of the rearranged chromosomes *in vivo* using two fluorescently marked loci on either side of the *RuiuR* sequence. The behaviour of the acentric and dicentric chromosomes was identified from the observations of the fixed and living Ch^{16}-NRUH *nmt-rtf1*$^{+}$ cells. The acentric chromosome appears to be lost rapidly by the nucleus. Some cells that contained a dicentric chromosome were found to form a stretched chromosomal bridge between the two segregating nuclei during the M-phase. Two GFP spots showed imbalanced segregation into one of the daughter cells. This may be caused by one of two events, as follows:

1. A breakage could occur between Cen3 and one of GFP focus. This results in part of the broken chromosome, which contains two GFP foci, being formed and subsequently undergoing imbalanced segregation into one of the two daughter cells.
2. An intact dicentric chromosome exists in a cell via further rearrangements, such as deletion or inactivation of one of the centromeres. Moreover, some cells containing a dicentric chromosome moved into a daughter nucleus, accompanied by a copy of the parental Ch^{16}. This may raise the issue of the production of the acentric and dicentric chromosomes possibly being formed by separate events (see Chapter 6 for details).

Overall, these results provide information regarding the progression of abnormal chromosomal architectures in a single cell. This contributes to our knowledge and understanding of how cells respond to the presence of unstable chromosomal

intermediates *in vivo*, as well as providing direct physical evidence of the conformational rearrangement events.

CHAPTER 5

THE FATES OF REARRANGED CHROMOSOMES

5.1 Introduction

From the observations of the mini-chromosome rearrangements using DeltaVision deconvolution light microscope (Chapter 4), the results demonstrated that an acentric chromosome showed disappeared from the chromosomal mass; a dicentric chromosome was detected to undergo imbalanced segregation into one of the daughter cells and some cells captured in the images visualised lagging of a dicentric chromosome between daughter cells for a transient moment. Intriguingly, because we observed that a dicentric chromosome presented in a daughter nucleus, companying with a copy of a parental Ch^{16}-NRUH, it suggests that production of the acentric and dicentric chromosomes may be not formed during the same event (we had originally expected that if the dicentric and acentric chromosome formation were coupled. If so, we will not see a copy of unaltered Ch^{16}-NRUH).

The next issue we wanted to investigate was “What is the fate of the dicentric and acentric chromosomes?”, “How do cells overcome this abnormal dicentric chromosome structure?” and “Will the dicentric chromosome undergo a random breakage afterward?” The dicentric chromosomes have been viewed as signatures of the genomic instability associated with cancer. Their stability has been attributed to a number of different secondary events (Figure 5-1), creating more stable derivatives such as intercentromeric deletion, centromere inactivation, inversion, amplification, double minute, and ring chromosomes. In humans, the dicentric chromosomes are

usually prone to further rearrangements in order to segregate successfully in mitosis and meiosis. For example, deletion of one of the centromeres has been recently recognized to be a significant occurrence in myeloid malignancy [35]. Stabilisation of chromosomes with multiple centromeres is also found to occur through epigenetic centromere inactivation, which is initiated by kinetochore disassembly, generating a functionally monocentric chromosome [36].

The dicentric chromosomes have not been found to occur naturally in the fission yeast *S. pombe*. Studies with the artificial dicentric chromosome in *S. pombe* reveal that the majority (99 %) of cells with a dicentric chromosome were arrested in growth or died. Interestingly, those defects did not mainly result from chromosome miss-segregation or a breakage because the observations obtained from cell cycle showed that these cells arrested indefinitely in the interphase. Notably, a small proportion (~1 %) of the dicentric chromosomes was stably retained. Within this population, two categories were identified: in some cells the dicentric chromosomes were resolved by a breakage event that caused the chromosomes to split into monocentric derivatives, while in other cells the dicentric chromosomes were stabilised by the mechanisms resulting in physical deletion or inactivation of one of the two chromosomes in which the central core regions of these inactive centromeres lack of component of functional kinetochore, such as Cnp1/CENP-A/CenH3 [36-38].

In our study, we attempted to explore the dicentric chromosome behaviour in *S. pombe* and the potential mechanisms by which they are stabilised. Here, I present possible models that predict the fate of a dicentric chromosome (Figure 5-1). A. Cells may lose their viability due to genomic insatiability caused by the effect of a dicentric chromosome. B. They may to undergo random breakage, leading to a secondarily

monocentric chromosome generation. The breakage event can be caused by two mechanisms (Figure 5-1): one can occur during the anaphase, when both centromeres of the dicentric chromosome are bound to opposite spindle poles and attempt to pull towards either sides of the cell, leading to a breakage. Alternatively, the breakage may arise from cleavage furrow ingression during cytokinesis when a dicentric chromosome expanses among two new-born cells [5, 24]. C. The centromere may be inactivated, for example by epigenetic mechanisms (Figure 5-1). D. The centromere may be deleted entirely at the sequence level (Figure 5-1). More detailed genetic analysis was used to provide insight into the fate of the dicentric chromosomes as outlined below.

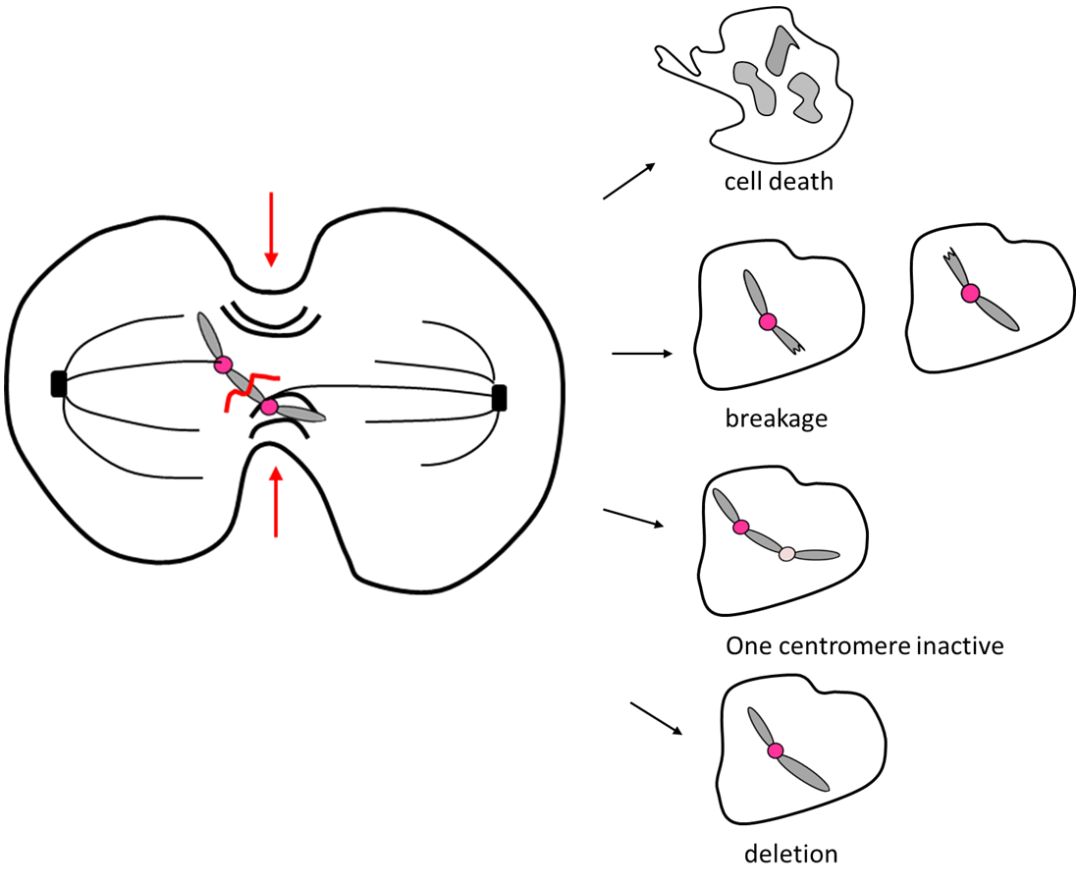

Figure 5-1. Schematics of the fate of rearranged chromosomes.

Cells may die because the miss-segregation of a dicentric chromosome during cell division. A random breakage may occur in the dicentric chromosome. There are two mechanisms that can cause a breakage in a dicentric chromosome. One occurs from the pulling force of the opposite spindle poles (black square). Another arises from cleavage furrow ingression during cytokinesis (red arrows show the orientation of the furrow progression). A dicentric chromosome may also be stabilised by inactivation or deletion of one centromere.

5.2 The fate of a dicentric chromosome

To genetically monitor the fate of rearranged chromosomes, on the right arm of the mini-chromosome, the *lac*O repeats were integrated with an *arg3*$^{+}$ gene maker *cen*-proximal to the *RTS1* sequence; the *tet*O repeats were integrated with a *his3*$^{+}$ gene maker *tel*-proximal to the *RTS1* sequence. A *Nat*^{R} marker gene was inserted on the left arm of the Ch^{16} to establish the integrity of mini-chromosome (Figure 5-2 A and B). The cells containing the parental Ch^{16}-NRUH were the Nat^{R} Arg^{+} Ura^{+} His^{+} phenotype. If the full-length Ch^{16}-NRUH was lost, the Nat^{s} Arg^{-} Ura^{-} His^{-} phenotype of the clone was generated. Nat^{s} Arg^{-} Ura^{+} His^{+} cells were proposed to represent the gain of an acentric chromosome. A strain containing a dicentric chromosome was expected to show the Nat^{R} Arg^{+} Ura^{+} His^{-} phenotype (Figures 5-2 B and C).

The dicentric chromosome may be broken by the mechanical force caused during chromosome segregation or cytokinesis, leading to broken chromosomes. The broken chromosomes contain partially deleted or duplicated regions and exist randomly in the daughter nuclei, depending on where they originally formed. Hence, if a random breakage occurred on a dicentric chromosome during cell division, this may result in the Nat^{R} Arg^{+} Ura^{+} His^{-} phenotype (the phenotype I of the clone), which is postulated to be a truncated Ch^{16}-NRUH (Figure 5-2 C, right panel). Notably, the cells containing a primary dicentric chromosome also show the Nat^{R} Arg^{+} Ura^{+} His^{-} phenotype (the phenotype I of clone). The other truncated Ch^{16}-NRUH was the Nat^{R} Arg^{+} Ura^{-} His^{-} phenotype (the phenotype II of the clone) (Figure 5-2 C, right panel).

The Ch^{16}-NRUH *nmt-rtf1*$^{+}$cells were cultured in minimal media in the absence of thiamine (“pause on” growth) for 24 hours, 30 ℃ to induce chromosomal

rearrangement. The dicentric and acentric chromosomes were generated after induced fork arrest. A dicentric chromosome is proposed to undergo a random breakage event, producing the truncated chromosomes. To confirm the type of rearranged products, an aliquot of the cells was released from the inducing conditions onto non-selectable plates (300 cells were spread per each plate) supplemented with thiamine ("pause off" growth) to form colonies for checking the auxotrophic makers by replica plating on selective media (see Materials and Methods). In parallel, a second aliquot of cells was continuously grown in minimal media in the absence of thiamine ("pause on" growth, 30 ℃) for a further 24 hours before being plated onto non-selective plates plus thiamine supplement. Colonies were allowed to form from both the 24 and 48 hour induction samples and the auxotrophic makers were checked by replica plating onto four different types of selectable plates containing different nutritional supplements, arginine, leucine, uracil and histidine (Figure 5-3A). All selectable plates were supplemented with thiamine supplement ("pause off" growth).

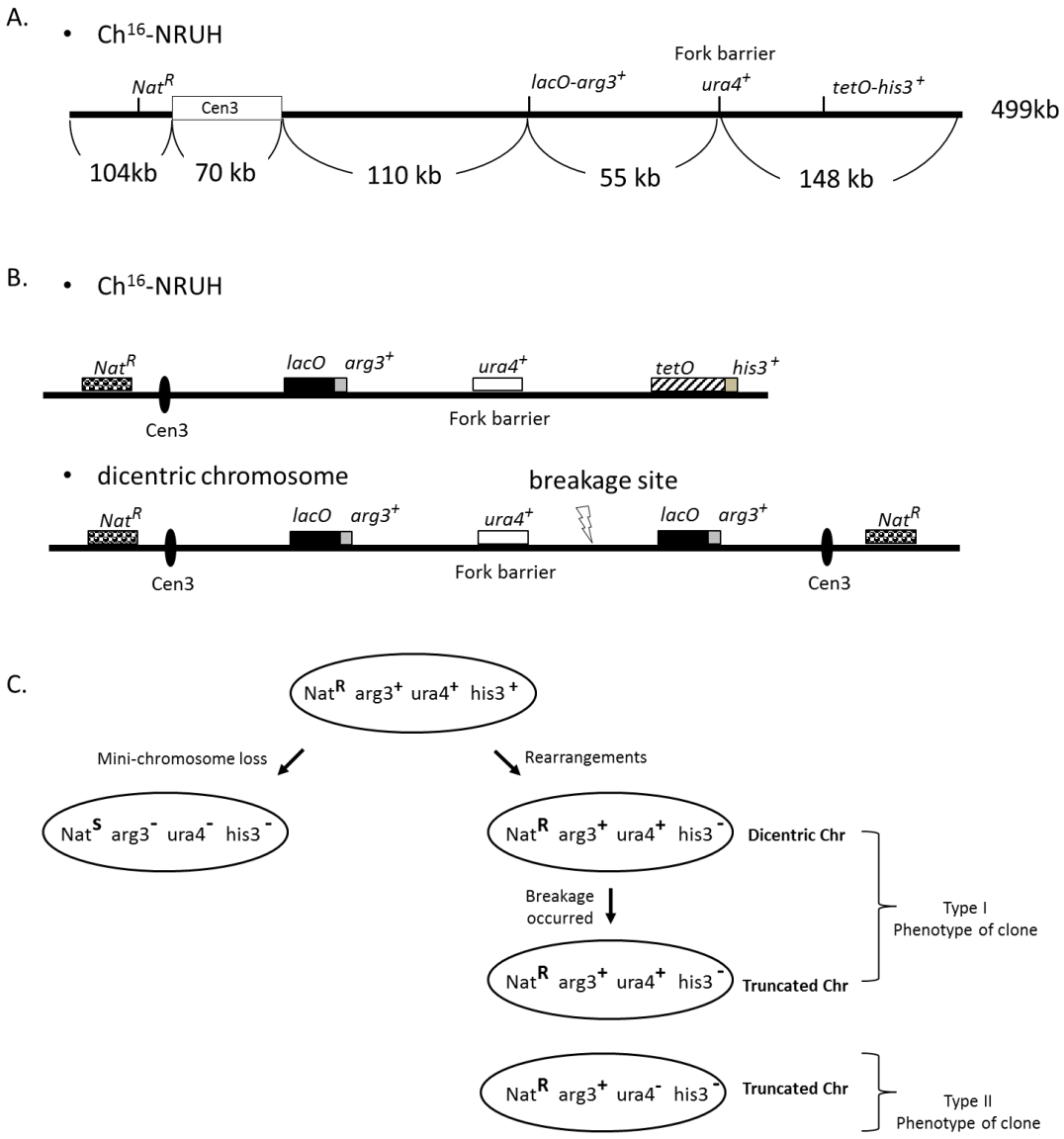

Figure 5-2. System to monitor the dicentric palindromic chromosomes stability.

(*A*) Positions and interval distances of the four integrated markers and molecular size of centromere 3 are indicated at the Ch^{16}-NRUH. (*B*) After chromosomal rearrangements occurred, a dicentric chromosome is generated. The dicentric chromosome is proposed to subsequently undergo a breakage event. The positions of selective markers were shown. (*C*) The yeast strain harbouring initial Ch^{16}-NRUH (*Nat^R*, *arg3$^+$*, *ura4$^+$*, *his3$^+$*) can form rearranged palindrome chromosomes that are associated with the specific marker loss: Nat^R Arg3$^+$ Ura4$^+$ His3$^-$ cells contain dicentric chromosome (left arrow). Following a breakage event, a truncated Ch^{16}-NRUH derived from a dicentric chromosome would give clones showing the phenotype I or II of clone. The loss of the full mini-chromosome leads to the Nat^s Arg3$^-$ Ura4$^-$ His3$^-$ phenotype (right arrow)

5.2.1 Random breakage of a dicentric chromosome occurs

To determine how genomic products generated after the fork-arrest induced chromosomal rearrangement, the clone selection assay was used to identify phenotypes of the colonies. After inducing the rearrangement event ("pause on" growth), Ch^{16}-NRUH *nmt-rtf1*$^{+}$cells were grown on non-selectable plates with thiamine supplement ("pause off" growth). When colonies formed, replica plating was used to check for the presence of various markers on selective plates containing thiamine supplement ("pause off" growth).

A random breakage occurred on a dicentric chromosome

The colonies showed different phenotypes (Figure 5-3). 0.62% Nat^{R} Arg^{+} Ura^{+} His^{-} colonies (type I phenotype of the clone) were obtained after 24 hours induction and this percentage increased three-fold after 48 hours of induction. ~ 2% Nat^{R} Arg^{+} Ura^{-} His^{-} colonies (type II phenotype of the clone) were found after 24 and 48 hours of induction. These results indicate that truncated mini-chromosomes may be generated by a dicentric chromosome breakage event. Furthermore, although the acentric chromosomes have previously been detected by a PFGE, combined with a Southern blot hybridisation (see the data in Chapter 3), Nat^{s} Arg^{-} Ura^{+} His^{+} strains, which contain only an acentric chromosome, were not obtained in this experiment. This is consistent with our microscopy, which indicated that the acentric chromosomes might be removed rapidly from the nucleus after their formation. A further discussion of this will follow in Chapter 6.

22~35% of the colonies were Nat^{s} Arg^{-} Ura^{-} His^{-}, showing the Ch^{16}-NRUH loss after 24 and 48 hours of induction. In addition, and somewhat unexpectedly, 10% of the

colonies were Nat^R Arg^- Ura^- His^-, suggesting that an isochromosome may be formed by the rearrangement of Cen3 in these cells. Cen3 consists of a central core (*cnt3*) sequence and three pairs of inverted repeats, including *imr3*, *otr3* and *irc3*. A recent study identified the generation of an isochromosome caused by the rearrangement of the homologous sequences of Cen3. By contrast, without the occurrence of a rearrangement event ("pause off" growth), neither the type I nor the type II phenotype of colonies were observed after 24 and 48 hours of incubation (Figures 5-3 B and C). This indicated that the generation of the dicentric chromosomes and the subsequent derivatives resulted from the RTS1-Rtf1 activity. Altogether, these data imply that when an unstable dicentric chromosome is formed, the instability can be resolved by a subsequent random breakage event.

Where did the breakage occur on a dicentric chromosome?

According to the results shown in Chapter 4, we propose that there may be a breakage site located between Cen3 and the *lacO-arg3*$^+$ array. Hence, we observed that two closed-GFP foci entered one of the daughter cells. However, in this chapter, we gained the Nat^R Arg^+ Ura^+ His^-/type I phenotype and the Nat^R Arg^+ Ura^- His^-/type II phenotype of colonies. This result indicated that a breakage occurred between the *lacO-arg3*$^+$ array and the fork-arrest system. However, we also obtained an isochromosome that has a duplication of the left arm Ch^{16}. This production of isochromosome may initiate from a break close to Cen3. A breakage event can be caused when both the centromeres of the dicentric chromosome are bound to opposite spindle poles and the pulling force is directed towards either side of the cell, leading to a breakage during the anaphase. The breakage may occur on a dicentric chromosome stretch in two newly born cells during cytokinesis [5, 24]. Hence, we propose that a breakage event can happen at a random site on a dicentric

chromosome.

5.2.2 Detection of truncated chromosome products

To define the kind of chromosomal rearrangement products generated in the mini-chromosome system, a PFGE performed under the condition where 50–800 kb DNA fragments can separate. The initial mini-chromosome was ~500 kb and we expected that the dicentric chromosome was 700–800 kb, while an acentric chromosome was 300–400 kb (Figure 5-4). The chromosomes of the colonies obtained from the colony selection assay described above were resolved by PFGE. The DNA fragments were then hybridised with specific probes using a Southern blot assay, as shown in Figure 5.4A. The names of the probes indicate the ORFs that overlap the probes shown on Ch^{16}. The probes Cen and Tel detected the nearby regions on either side of *RuiuR*. The initial Ch^{16}-NRUH is postulated to be characterised by a possible reaction with the probes Nat, Arg, Ura4, Cen and Tel; a dicentric chromosome would be detected by these probes; an acentric chromosome would be indicated by these probes Nat, Ura4 and Tel.

Identification of different colony phenotypes

In the PFGE stained with EtBr, two chromosomes of different lengths were visible in each Nat^R Arg^+ Ura^+ His^-/type I phenotype of colonies (Figure 5-4 B, lane 1-5). These two chromosomes of differing lengths in type I of the colonies were detected by the probe Nat. None of the chromosomes was recognised by the probe Tel (specific to the region on the *tel*-proximal of the RTS1 sequence of the parent Ch^{16} and an acentric chromosome), indicating that they were created from a dicentric chromosome. We originally expected that a greater molecular size of a chromosomal fragment would indicate the presence of a dicentric chromosome (Figure 5-4 C, type I clone, lane 1-5).

The smaller molecular size of the chromosomal fragment was less than that of the parental Ch^{16}-NRUH. We originally anticipated that the lower band would represent a truncated Ch^{16}-NRUH (Figure 5-4 C, type I clone, lane 1-5). However, we found unexpected experimental results, which the following context and section will explain in greater detail.

The greater molecular size of the chromosomal fragment shown in each type I of the colonies was longer than that of the parental Ch^{16}-NRUH and was similar in size to a dicentric chromosome (Figure 5-4 B, type I clones, lane 1-5), when compared to the dicentric chromosome shown in the Ch^{16}-NRUH *nmt-rtf1*$^{+}$cells (Figure 5-4 B, left lane, labelled Ch^{16}-NRUH). The higher band was hybridised with the probes Nat, Arg, Ura4. This greater molecular size of the chromosomal fragment may indicate two types of product, as follows:

1. A primary, or newly created dicentric chromosome, tends to undergo the BFB cycle, therefore generating a truncated derivative. A newly created dicentric chromosome is produced from a primary dicentric chromosome that has undergone a breakage and re-joining event, as explained in more detail below. Hence, we expected that a newly created dicentric chromosome may have partial amplification or deletion of the region located between the two centromeres. It is difficult to define how the length of the region was amplified or deleted on a newly created dicentric chromosome under the conditions we used in the PFGE. We are currently working on the analysis of sequences for the rearrangement products. 2. A primary, or newly created dicentric chromosome, can exist stably in a cell. Therefore, these stable dicentric chromosomes were proposed to be stabilised by further rearrangements, such as the deletion or inactivation of one centromere (Figure 5-5).

It was, however, difficult to define whether a dicentric chromosome had undergone such further rearrangements. The cells encompassing a dicentric chromosome with the inactivation of one centromere showed the Nat^R Arg^+ Ura^+ His^- phenotype (type I phenotype) and have a similar molecular size in the PFGE, compared to a dicentric chromosome shown in the Ch^{16}-NRUH *nmt-rtf1*$^+$cells (Figure 5-4 B, left lane, labelled Ch^{16}-NRUH). Instead, the cells containing a dicentric chromosome with the deletion of one centromere (the molecular size of Cen3 is ~110 kb) may have a smaller molecular size than that of a primary dicentric chromosome. However, if there is insufficient resolution under the PFGE conditions we used, it would be difficult to define the different molecular sizes of chromosomal fragments. Although we need to conduct further experiments to investigate this explanation, in the following section we will show that some cells contained stable dicentric chromosomes over a period of 15 days. This seems to suggest that the stabilisation of a dicentric chromosome was maintained by further rearrangements. We will present the results in the next section.

The reduced molecular size of the chromosomal fragment shown in each type I of the colonies was smaller than that of the parental Ch^{16}-NRUH (Figure 5-4 B, type I clones, lane 1-5), but was greater than that of an acentric chromosome (Figure 5-4 B, left lane, labelled Ch^{16}-NRUH). We originally thought that the lower band was a truncated chromosome. However, it was only detected by the probe Nat and was not detected by the probes Arg, Ura4 or Cen. This suggested that the lower band represented the formation of an isochromosome, where the original right arm has been replaced by a copy of the left arm, creating an additional copy of the *Nat*^{R} gene around Cen3 (Figure 5-4 C, an isochromosome). To test this possibility, the probe X was used to hybridise with the region near the centromere (~20 kb away from Cen3) on the right arm of Ch^{16}, as shown in Figure 5.4B. The smaller chromosomal

fragments found in the type I phenotype of colonies (Figure 5-4 B, type I clones, lane 1-5) may well indicate the presence of an isochromosome, presumably produced by rearrangement within Cen3 repeats. However, further experimentation is needed to prove this explanation.

Moreover, the Nat^R Arg^+ Ura^- His^-/ type II phenotype of colonies was also obtained, and these colonies were postulated to contain a truncated derivative (Figure 5-4 B, type II phenotype of clone, lane 6-10). They revealed that the chromosomal fragment was smaller than was the parental Ch^{16}-NRUH, but was larger than an acentric chromosome in the PFGE stained with EtBr. This band was detected by the probes Nat, Arg and Cen, but was not detected by the probes Ura (except lane 6) or Tel. The chromosome fragment shown in Figure 5.4 B (lane 6) was detected by the probe Ura, although it exhibited the Nat^R Arg^+ Ura^- His^- phenotype. We expected that it might contain a mutation of the *ura4* gene, such as a single base-substitution or partial deletion, which would prevent its growth on media without uracil. Altogether, these results support the model that unstable dicentric chromosomes are prone to becoming a truncated form of the mini-chromosomes caused via random breakage occurring during the cell division.

The fate of a dicentric chromosome

To sum up the results of this experiment, there are four potential models for the fate of a dicentric chromosome (Figure 5-5), as follows:

1. A breakage occurs on a dicentric chromosome. The broken fragment was postulated to undergo a repeat of breakage and rejoining (the BFB cycle) until stabilised by further mechanisms, such as the addition of telomeres on a truncated chromosome or the inactivation or deletion of one centromere on a dicentric chromosome (Figure 5-5

a).

2. The inactivation of one centromere occurs on a dicentric chromosome (Figure 5-5 b). In this situation, these colonies will show the Nat^R Arg^+ Ura^+ His^- phenotype (type I phenotype). A dicentric chromosome with an inactivated centromere can exist normally *in vivo* [35-37] and can exhibit a similar molecular size to a dicentric chromosome in PFGE.

3. The deletion of one centromere takes place on a dicentric chromosome (Figure 5-5 c). We are not certain how much of the length of the sequence was deleted (the molecular size of Cen3 is ~110 kb). It may be difficult to define them by the chromosomal molecular size compared with a primary dicentric chromosome in the PFGE.

4. The isochromosome that arose from the original right arm was replaced by a copy of the left arm (Figure 5-5 d), creating an additional copy of the *Nat*^{R} gene around Cen3 (Figure 5-4 B, the smaller chromosomal fragment is shown in the type I phenotype of the clone, lane 1-5). This isochromosome can be produced from the over-resection of the DNA repair progression after fork-stalling induction.

Thus, a dicentric chromosome may undergo a random breakage and produce monocentric derivatives. We demonstrated that a breakage event occurred on a dicentric chromosome. We expected that the broken fragment was prone to repeating the BFB cycle until being stabilised by further mechanisms. The stabilisation of mechanisms can occur on a monocentric derivative with the telomere addition (Figure 5-5 e). Hence, we found that some cells contained a stable, truncated Ch^{16}-NRUH (containing one *lacO* repeats-*arg3*$^+$marker and one Cen3, but without the fork-arrest system), as shown in the Nat^R Arg^+ Ura^- His^- phenotype of clones (type II phenotype), (Figure 5-4 Type II clone, lane 6-10 and 5-5 a).

We expected that some cells would contain the other truncated Ch^{16}-NRUH, which encompasses one *lacO* repeats-*arg3*$^{+}$marker, the fork-arrest system and one Cen3, showing the Nat^{R} Arg^{+} Ura^{+} His^{-} phenotype (type I phenotype). However, we did not observe the truncated Ch^{16}-NRUH in the Nat^{R} Arg^{+} Ura^{+} His^{-} phenotype of clones (Figure 5-4 Type I clone, lanes 1-5 and 5-5 a). The reason for this is still unclear. We propose that the truncated Ch^{16}-NRUH, containing one *lacO* repeats-*arg3*$^{+}$marker, the fork-arrest system and one Cen3, may tend to repeat the BFB cycle, forming a new dicentric chromosome (Figure 5-5 e). The newly formed dicentric chromosome may be retained by a secondary rearrangement, such as the inactivation or deletion of one centromere. Hence, we observed that a dicentric chromosome existed stably in the Nat^{R} Arg^{+} Ura^{+} His^{-} phenotype of clones (Figure 5-4 B, type I clones, lane 1-5). In the following section, we will indicate that some cells, which contained a dicentric chromosome, maintained steadily for over 15 days. Notably, the original dicentric chromosome may also exist stably in the Nat^{R} Arg^{+} Ura^{+} His^{-} phenotype of clones if it has undergone the inactivation or deletion of one centromere event. The newly formed dicentric chromosome may contain the partial amplification or deletion of the region between the two centromeres, although it is difficult to define how much of the length of the region was amplified or deleted under the condition in the PFGE that we used. We are currently working on the analysis of the sequence of the rearrangement products.

Finally, the truncated Ch^{16}-NRUH can become an isochromosome produced by the over-resection of the DNA repair progression. Therefore, according to our results, an isochromosome (containing a duplication of the left arm of Ch^{16}-NRUH) was found in the Nat^{R} Arg^{+} Ura^{+} His^{-} (Figure 5-4 B, type I clones, lane 1-5). We also obtained the Nat^{R} Arg^{-} Ura^{-} His^{-} phenotype of clones that contain isochromosomes (Figure 5-3 C).

This suggests that this isochromosome was produced as a byproduct of the dicentric chromosome instability.

Figure 5-3. A random breakage is associated with a dicentric chromosome.

To determine the fate of a dicentric chromosome after chromosomal rearrangements occurred, genetic markers were introduced on the Ch^{16}-NRUH, the *Nat*^{R} gene was introduced on the left arm proximal to Cen3, whereas the *lac*O repeats with an *arg3*$^{+}$ gene maker and the *tet*O repeats with a *his3*$^{+}$ gene maker were incorporated on either side of the (*RuiuR*) on the right arm. (*A*) Illustration of the progression of a colony selection assay. After chromosomal rearrangements occurred, colonies with the type I (Nat^{R} Arg^{+} Ura^{+} $His^{–}$) or type II (Nat^{R} Arg^{+} $Ura^{–}$ $His^{–}$) phenotype were selected from a colony selection assay. These phenotypes indicated the loss of the markers in the rearranged mini-chromosome clones. A Nat^{s} $Arg^{–}$ $Ura^{–}$ $His^{–}$ phenotype were considered to mark the loss of Ch^{16}-NRUH. A Nat^{R} $Arg^{–}$ $Ura^{–}$ $His^{–}$ phenotype suggested the formation of isochromosome. When colonies formed on non-selective plates with thiamine supplement, they were replicated on selective plates with thiamine supplement to check the presence of the markers. (*B*) Quantification of a colony selection assay calculated from (*C*).

A.

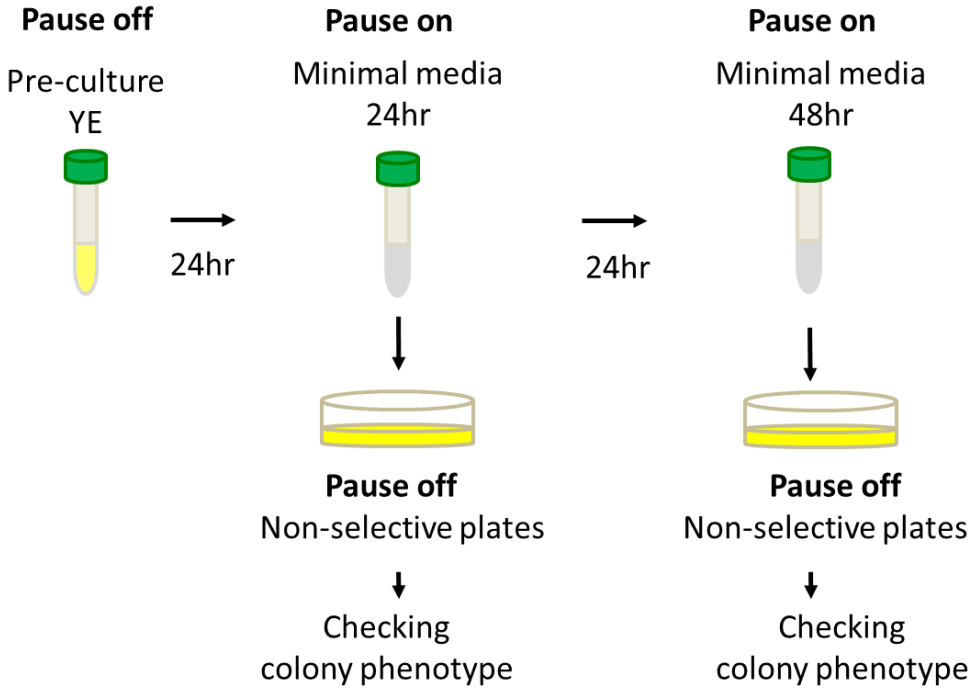

B.

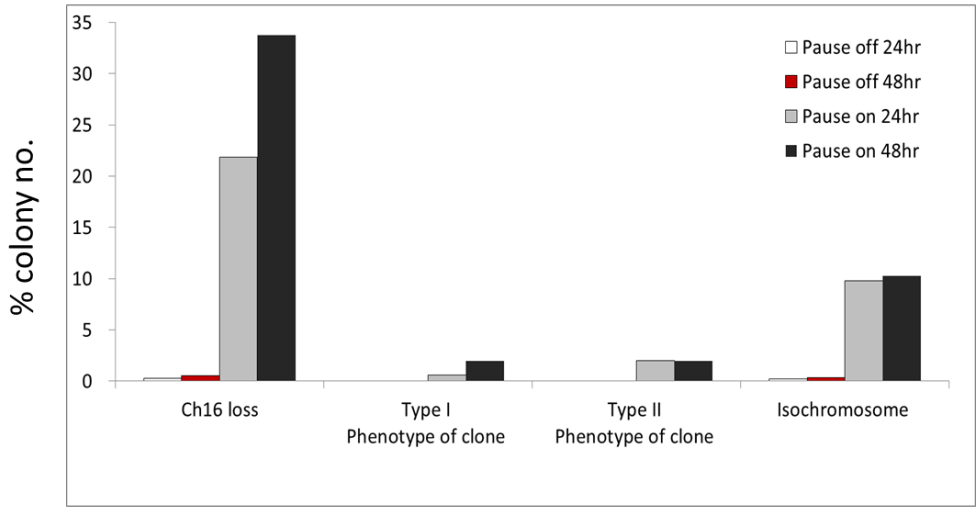

C.

	Ch^{16} loss		**Type I Phenotype of clone**		**Type II Phenotype of clone**		**Isochromosome**	
Phenotype	NAT^{S} arg3^{-} ura4^{-} his3^{-}		NAT^{R} arg3^{+}ura4^{+} his3^{-}		NAT^{R} arg3^{+}ura4^{-} his3^{-}		NAT^{R} arg3^{-}ura4^{-} his3^{-}	
	n	%	n	%	n	%	n	%
Pause off 24hr	1/305	0.32	0/305	0	0/305	0	1/305	0.32
Pause off 48hr	3/568	0.53	0/568	0	0/568	0	2/568	0.34
Pause on 24hr	176/806	21.8	5/806	0.6	16/806	2	78/806	9.6
Pause on 48hr	156/462	33.8	9/462	1.9	8/462	1.9	47/462	10.2

Figure 5-4. Analysis of chromosomes by a PFGE followed by a Southern blot assay.

(*A*) Positions of the probes (black and red blocks) used in a Southern blot hybridization are designated under Ch^{16}-NRUH. (*B*) Chromosomal DNA was separated by a PFGE staining with EtBr (left panels). Positions of Ch^{16}-NRUH, the dicentric chromosome (**D**) and the acentric chromosome (**A**) are indicated respectively on the left of the EtBr panel in Ch^{16}-NRUH *nmt-rtf1*$^{+}$cells (**Ch16-NRUH**). The type I phenotype clones (Nat^{R} Arg^{+} Ura^{+} His^{-}) were originally expected to show a truncated Ch^{16}-NRUH. The higher band proposed to show the position of a dicentric chromosome which may be stabilised by further rearrangements, i.e. inactivation or deletion of one centromere. However, the lower band in each type I phenotype clones can not be detected using the probe X. Thus, this lower band proposed to show the position of an isochromosome. The type II phenotype clones (Nat^{R} Arg^{+} Ura^{-} His^{-}) that were proposed to have another type of truncated-formed Ch^{16}-NRUH (*C*) Positions of the probes (black and red blocks) used in a Southern blot hybridization for each type of chromosomal rearrangement products.

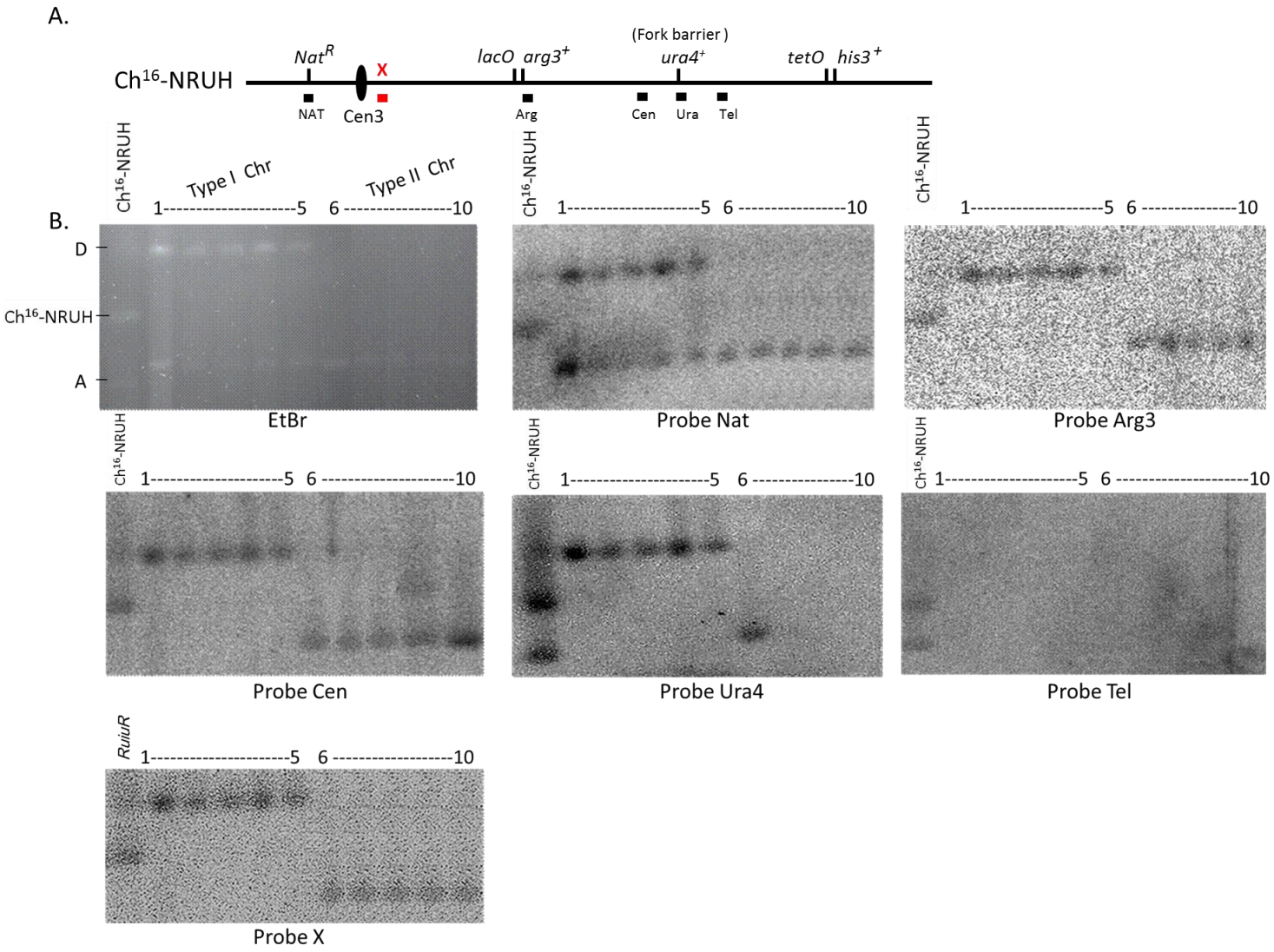
A.
Ch16-NRUH
NatR
X
lacO arg3+
(Fork barrier)
ura4+
tetO his3+
NAT
Cen3
Arg
Cen
Ura
Tel
B.
Type I Chr
Type II Chr
1----------5 6----------10
D
Ch16-NRUH
A
EtBr
Probe Nat
Probe Arg3
Probe Cen
Probe Ura4
Probe Tel
RuuR
Probe X

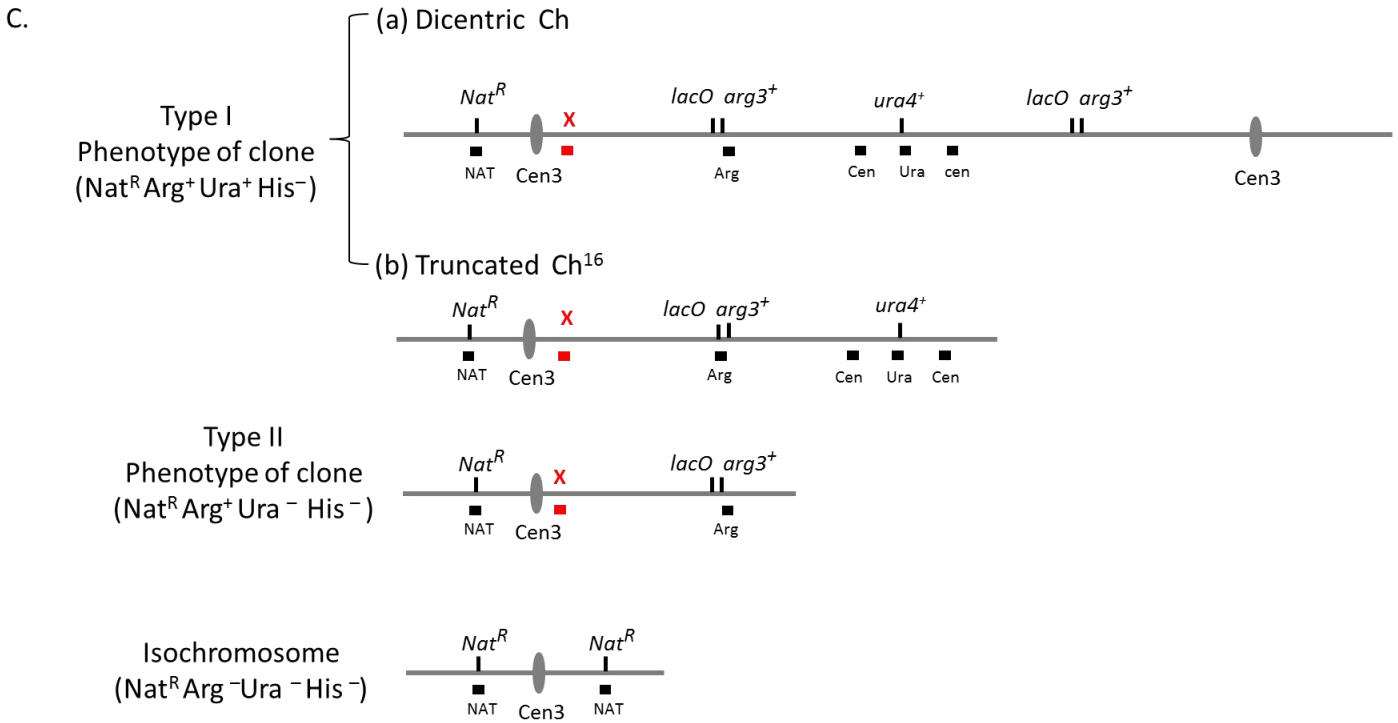
C.
Type I
Phenotype of clone
(NatR Arg+ Ura+ His−)
(a) Dicentric Ch
NatR
X
lacO arg3+
ura4+
lacO arg3+
NAT
Cen3
Arg
Cen
Ura
cen
Cen3
(b) Truncated Ch16
NatR
X
lacO arg3+
ura4+
NAT
Cen3
Arg
Cen
Ura
Cen
Type II
Phenotype of clone
(NatR Arg+ Ura − His −)
NatR
X
lacO arg3+
NAT
Cen3
Arg
Isochromosome
(NatR Arg −Ura − His −)
NatR
NatR
NAT
Cen3
NAT

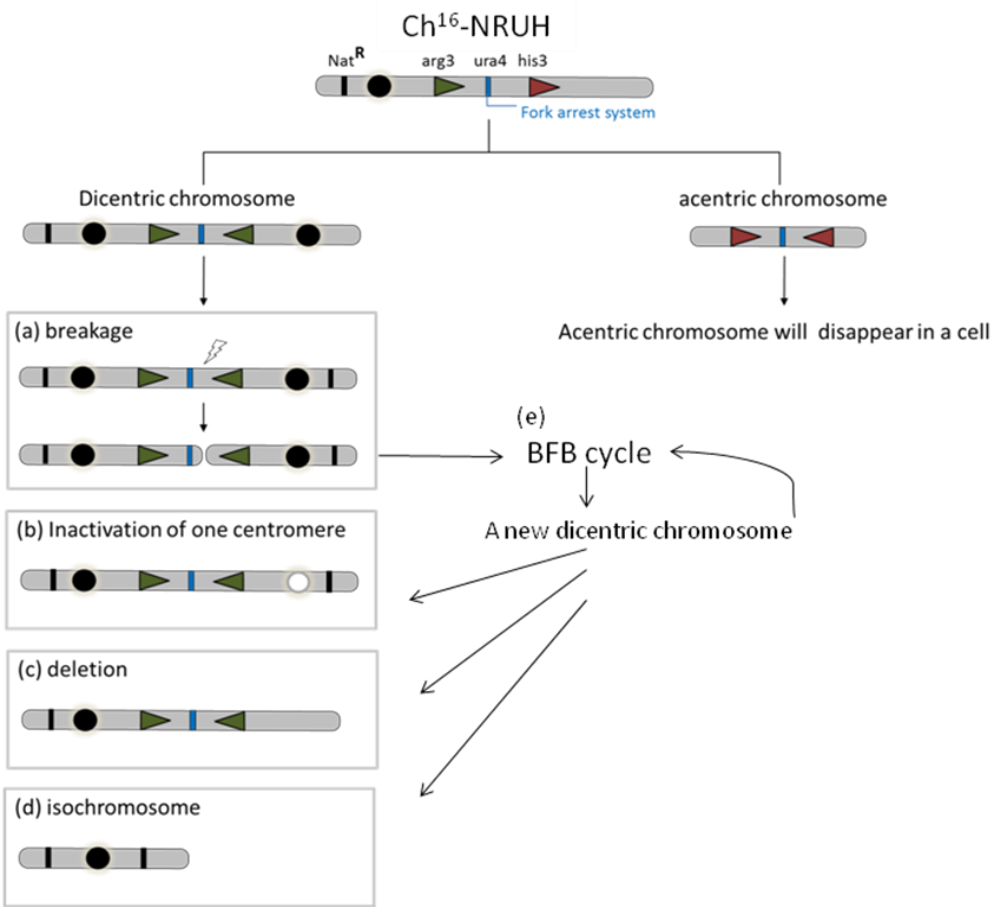

Figure 5-5. The fate of the acentric and dicentric chromosomes.

After inducing replication fork stalling nearby the fork-arrest system, the acentric and dicentric chromosomes will be generated. In our finding, an acentric chromosome disappeared within a cell. A dicentric chromosome may undergo further rearrangements and gain four products: (a) A random breakage may occur on the dicentric chromosome. It may cause the generation of two different monocentric derivatives. (b) A dicentric chromosome may also be stabilised by inactivation or (c) deletion of one centromere. (d) The isochromosome which contains duplications of original right arm was generated, forming an additional copy of the *Nat*^{R} gene around Cen3. (e) The broken chromosome may undergo the BFB cycle and form a new-created dicentric chromosome. A new-created dicentric chromosome may be stabilised by further rearrangements, i.e. the models (a-d).

5.2.3 Identification of the fate of the dicentric chromosomes and secondary rearrangements

As per the results described above, a breakage event occurred on a dicentric chromosome. We found that some cells contained the stable, truncated Ch^{16}-NRUH and showed that the Nat^R Arg^+ Ura^- His^- phenotype was produced by a dicentric chromosome (Figure 5-4B, type II clones, lane 6-10). We suggest that a truncated Ch^{16}-NRUH may be stabilised by further rearrangements, such as the telomere addition (Figure 5-5 e). A truncated Ch^{16}-NRUH may also undergo chromosomal fusion, generating a new dicentric chromosome, the details of which are presented in the following section. In addition, we obtained the Nat^R Arg^- Ura^- His^- phenotype of clones that included the isochromosomes containing the duplication of the left arm of Ch^{16}-NRUH (Figure 5-3 C). It was postulated that an isochromosome was produced as a byproduct of the dicentric chromosome instability.

We anticipated that the truncated Ch^{16}-NRUH might repeat the BFB cycle during cell division, forming a new dicentric chromosome (Figure 5-5 e). This newly formed dicentric chromosome can repeat a breakage event and can undergo the BFB cycle until it is stabilised by the telomere addition. A dicentric chromosome is extremely unstable *in vivo* [5, 24, 35-38]. Consequently, we should observe some cells containing the truncated Ch^{16}-NRUH instead of a dicentric chromosome in a cell. However, we observed that a dicentric chromosome existed in the Nat^R Arg^+ Ura^+ His^- phenotype of clones (Figure 5-4 B, type I clones, lane 1-5). This dicentric chromosome may indicate either a primary or a newly formed dicentric chromosome stabilised by secondary rearrangements, such as the inactivation or deletion of one centromere. We were limited in defining these two chromosomes. This may cause by the conditions in the PFGE that we used. Our group is working on the analysis of

sequence for the rearrangement products. Moreover, we wonder whether a dicentric chromosome can stably exist in a cell for a long time. We will discuss this in more detail in the following context.

To explore this hypothesis, five independent Nat^R Arg^+ Ura^+ His^- of clones, which were obtained from the experiment described in section 5.2.2, were proposed to contain three types of rearrangement products, namely:

1. A primary dicentric chromosome
2. A newly created dicentric chromosome
3. An isochromosome.

Five Nat^R Arg^+ Ura^+ His^- clones were grown in complete media in the presence of thiamine ("pause off" growth) (30 °C) for a total of 15 days (Figure 5-6 A). To check the type of rearranged products, an aliquot of cells (300 cells per plate) were spread on non-selectable plates with thiamine supplement ("pause off" growth) at 24 hour intervals. After colony formation replica plating was used to confirm the phenotype on selective plates with thiamine supplement ("pause off" growth) (see Materials and Methods). In parallel, a second aliquot of the cells were cultured in complete media in the presence of thiamine supplement ("pause off" growth) (30 ℃) for another 24 hours. This procedure was repeated under the same experimental conditions for a period of 15 days (see Materiel and Methods).

Identification of different colony phenotypes over 15 days

Quantification of different colony phenotypes over 15 days revealed that a dicentric chromosome had either undergone further rearrangement or was apparently maintained in a cell (Figure 5-6 B). First, the Nat^R Arg^+ Ura^+ His^- colonies (type I phenotype) were obtained. The number of the Nat^R Arg^+ Ura^+ His^- colonies remained

constant at ~0.6 % for a total of 15 days. To determine the kind of chromosome present in the type I phenotype of colonies, a PFGE was performed and was characterised by a Southern hybridisation with specific probes (Figure 5-7). Two different molecular sizes of DNA fragments were found in each type I phenotype of the clone. These Nat^{R} Arg^{+} Ura^{+} His^{-} type of clones were obtained from plates that were spread with liquid culture and which had produced cells from the day 1, 2, 3, 5, 7, 9, 11, 13 and 15 (Figure 5-7 B, lane 1-9).

The larger molecular sized DNA fragments were detected by the probes X, Arg and Ura, but were not detected by the probe Tel. This showed a similar molecular size as that of the dicentric chromosome shown in the Ch^{16}-NRUH *nmt-rtf1*$^{+}$cells (Figure 5-7 B, left lane, labelled Ch^{16}-NRUH). Hence, the greater molecular size of the DNA fragment was proposed to indicate the presence of a dicentric chromosome. The greater molecular size of a DNA fragment may also show the presence of a newly created dicentric chromosome produced from a primary dicentric chromosome that had undergone a breakage and re-joining event. Hence, a newly created dicentric chromosome may have partial amplification or deletion of the region positioned between the two centromeres. It was difficult to differentiate a primary and a newly formed dicentric chromosome according to the molecular size. This was because we were not certain of the extent to which the length changed on a newly formed dicentric chromosome. In addition, the insufficient resolution of the condition in the PFGE that we used may have caused the indeterminate distinction between a primary and a newly formed dicentric chromosome. Another interesting issue that we observed was that a dicentric chromosome was found in the Nat^{R} Arg^{+} Ura^{+} His^{-} of clones for over 15 days. Therefore, our results suggest that a dicentric chromosome might exist stably in a cell that has been stabilised by secondary rearrangements, such as the

inactivation or deletion of one centromere. However, we need to conduct further experiments in order to prove this theory.

The lower molecular size of the DNA fragments obtained from the Nat^R Arg^+ Ura^+ His^- phenotype of clones contained the isochromosomes that contained the duplication of the left arm of Ch^{16}-NRUH. The lower chromosomal fragments were smaller than those of Ch^{16}-NRUH and were found to have lost the markers located on the right arm of Ch^{16}-NRUH (Figure 5-7B). None of the lower chromosomes of the Nat^R Arg^+ Ura^+ His^- clones were detected by the probes X, Arg and Ura (specific to the Ch^{16}-NRUH right arm), indicating that they represented isochromosomes containing two copies of the Ch^{16}-NRUH's left arm. An isochromosome was proposed to be produced by the instability of the dicentric chromosome.

Moreover, the generation of the Nat^R Arg^+ Ura^- His^- colonies – cells encompassing type II truncated Ch^{16}-NRUH – showed a constant ratio of 2~2.5% for 15 days (Figure 5-6B). In PFGE staining with EtBr, the chromosomes of the Nat^R Arg^+ Ura^- His^- colonies exhibited a DNA fragment smaller than that of the parental Ch^{16}-NRUH (Figure 5-8B, lane 1-5). The chromosome in lane 5 showed indistinct patterns, because a lesser amount of chromosomal DNA was embedded in the agarose plugs. Five Nat^R Arg^+ Ura^- His^- clones were gained from plates that were spread with liquid culture and which produced cells from the day 1, 3, 5, 10 and 15. All of them were detected using the probe Nat and the probe X in a Southern blot hybridisation. The probe Ura could not detect the chromosomes from the type II phenotype colonies, indicating that they were truncated Ch^{16}-NRUH produced from the dicentric chromosomes.

In addition, ~10 % of the colonies were the Nat^R Arg^- Ura^- His^-phenotype, indicating that the cells contained an isochromosome produced via the replacement of the original right arm by a copy of the left arm, leading to an additional copy of the *Nat^R* gene, which formed around Cen3. A smaller chromosomal fragment was observed in Nat^R Arg^- Ura^- His^- colonies using the PFGE, which could hybridise with the probe Nat, but which could not be detected by the probe X in a Southern blot assay (Figure 5-8B, lane 6-9). These four Nat^R Arg^- Ura^- His^- of clones were obtained from plates that had been spread with liquid culture and which produced cells from the day 1, 5, 10 and 15.

Finally, ~50% of the colonies were Nat^s Arg^- Ura^- His^- as a result of the Ch^{16}-NRUH loss (Figure 5-6 B). These results imply that, when a monocentric derivative of the Nat^R Arg^+ Ura^- His^- clones was produced from the primary dicentric chromosome, a subsequent rearrangement event can occur in order to generate a more stable genetic product in the form of a monocentric isochromosome.

The fate of the dicentric chromosome and secondary rearrangements

We originally predicted that the truncated Ch^{16}-NRUH might go through the BFB cycle during cell division, forming a new dicentric chromosome (Figure 5-5 e). The truncated Ch^{16}-NRUH can either undergo the BFB cycle or be stabilised by further pathways, such as the telomere addition. Consequently, we should detect some cells containing the stable truncated Ch^{16}-NRUH instead of a dicentric chromosome in a cell. However, we observed that a dicentric chromosome was retained in the Nat^R Arg^+ Ura^+ His^- phenotype of clones over 15 days (Figure 5-7). This showed that a dicentric chromosome could exist stably in a cell for a long time. We suggest that the stabilisation of a dicentric chromosome may take place by secondary rearrangements,

such as the inactivation or deletion of one centromere. This requires further experiments in order to prove the theory.

Figure 5-6. The fates of the dicentric chromosomes and secondary rearrangements

(*A*) Illustration for the progression of the experiment. After the chromosomal rearrangement event occurred, colonies with the Type I (Nat^R Arg^+ Ura^+ His^-) or Type II (Nat^R Arg^+ Ura^- His^-) phenotype were generated. The five Nat^R Arg^+ Ura^+ His^- phenotype colonies cultured in YE media ("pause off" growth) for 1 day at 30 ℃ and aliquots of cells were spread on non-selective plates. When colonies formed, replica plating was used to check for the loss of markers. A separate aliquot was grow for a further 24 hours and this action repeated for a total of 15 days. (*B*) Quantification of a colony selection assay calculated over 15 days for the five separated the Nat^R Arg^+ Ura^+ His^- phenotype cultures.

A.

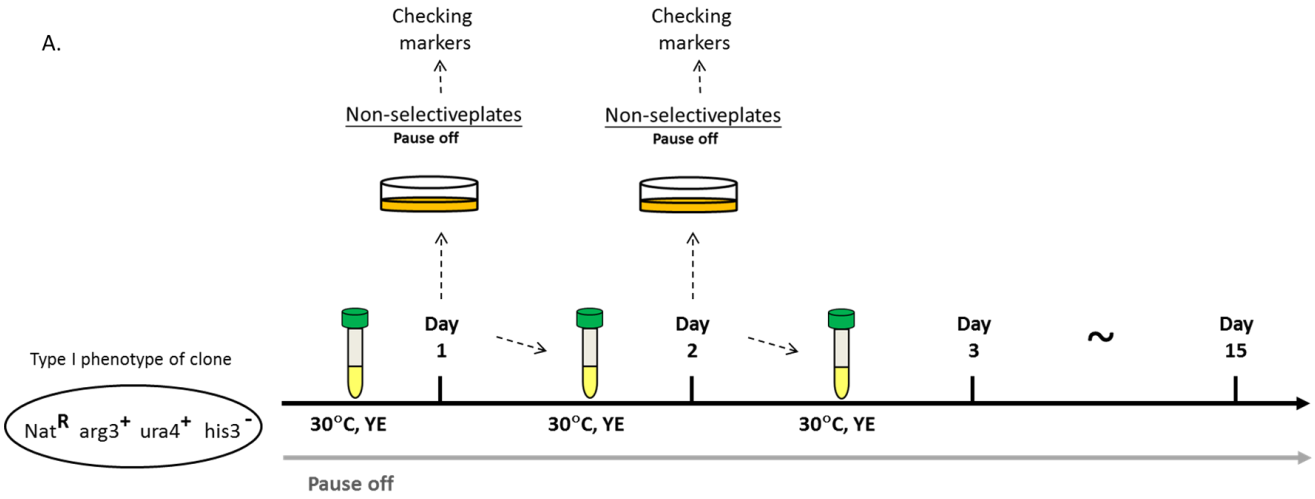
Checking markers
Non-selectiveplates
Pause off
Checking markers
Non-selectiveplates
Pause off
Type I phenotype of clone
Nat^R arg3^+ ura4^+ his3^-
Day 1
Day 2
Day 3
~
Day 15
30°C, YE
30°C, YE
30°C, YE
Pause off

B.

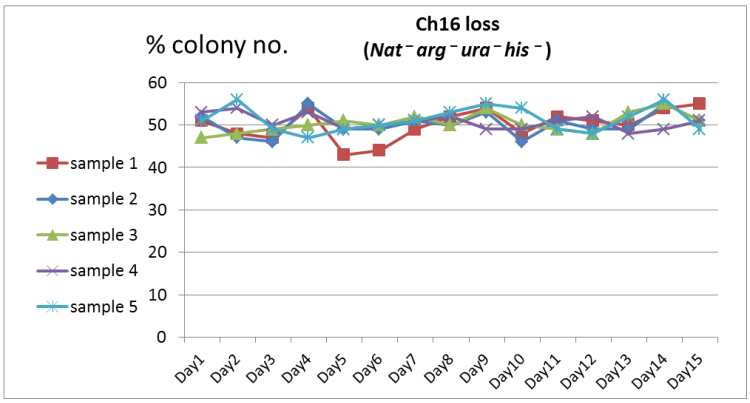
Ch16 loss
(Nat⁻ arg⁻ ura⁻ his⁻)
% colony no.
sample 1
sample 2
sample 3
sample 4
sample 5

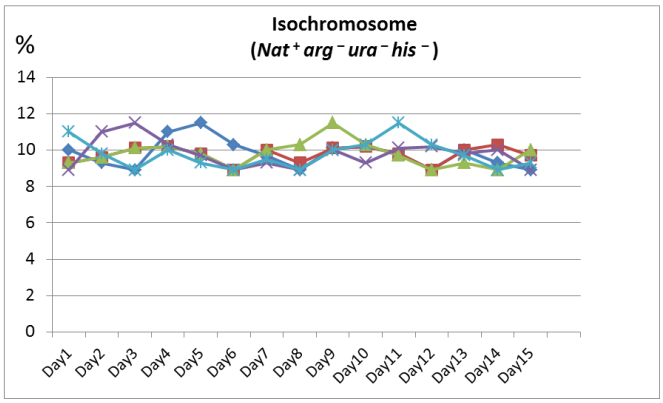
Isochromosome
(Nat⁺ arg⁻ ura⁻ his⁻)
%

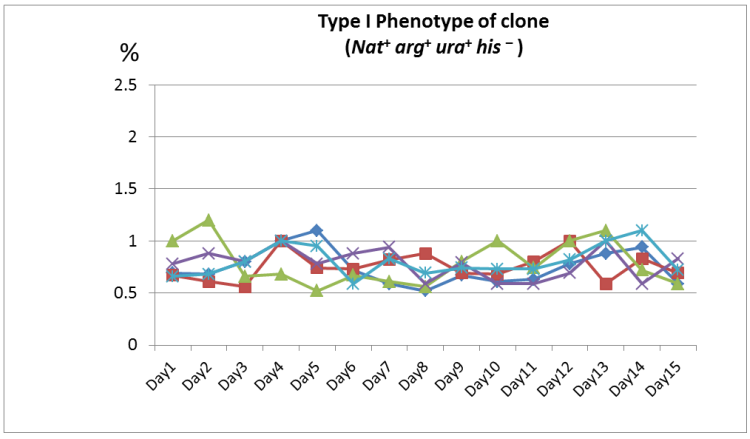
Type I Phenotype of clone
(Nat⁺ arg⁺ ura⁺ his⁻)
%

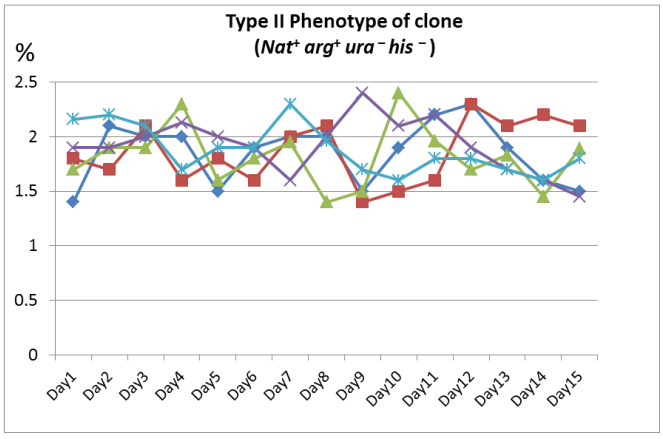
Type II Phenotype of clone
(Nat⁺ arg⁺ ura⁻ his⁻)
%

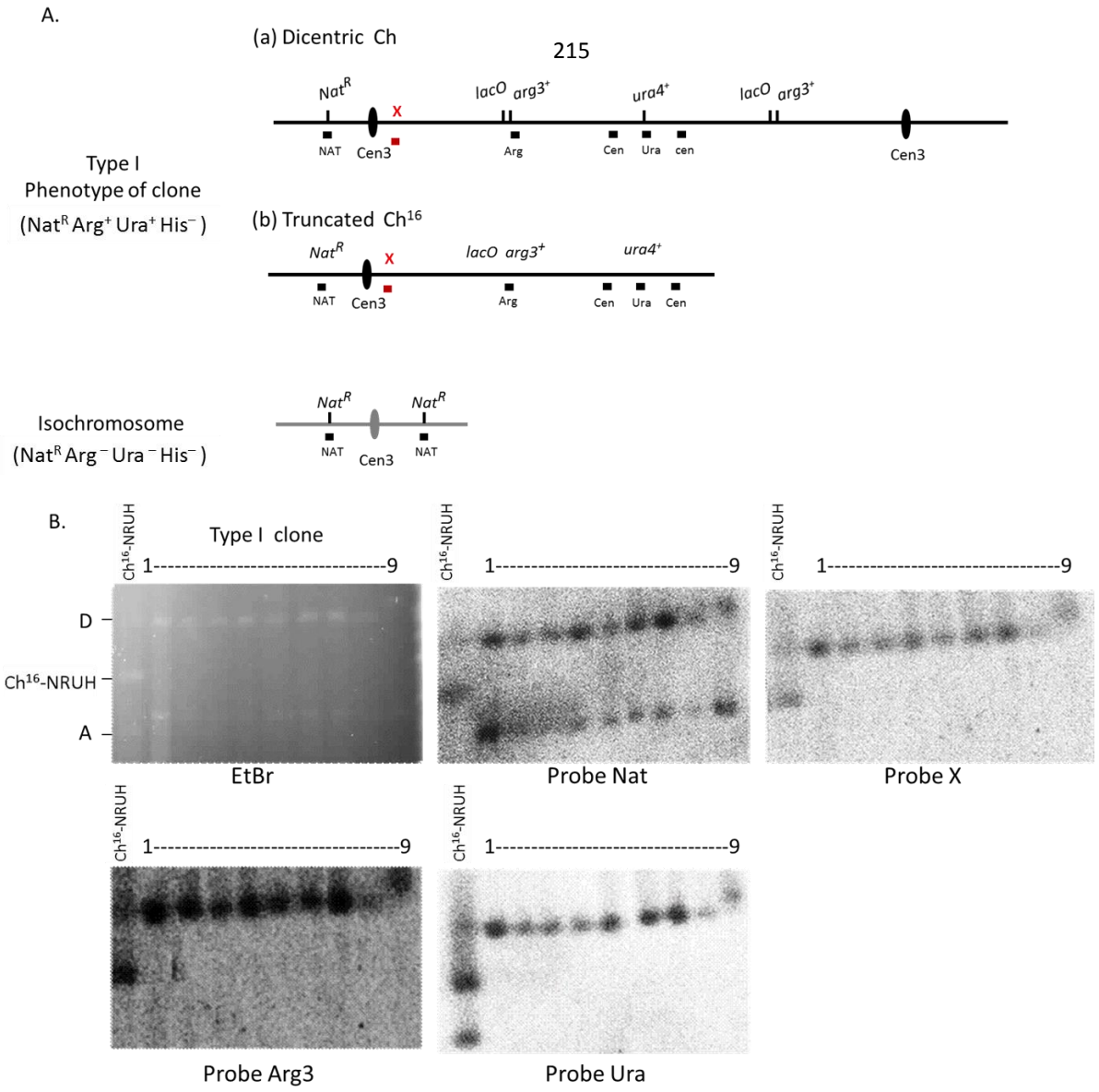

Figure 5-7. Analysis of chromosomes by a PFGE.

(*A*) Positions of the probes (black and red boxes) used in a Southern blot hybridization are indicated for the chromosomal rearrangement products. Clones with the Nat^R Arg^+ Ura^+ His^- phenotype were originally proposed to contain dicentric chromosomes and/or truncated Ch^{16}-NRUH that was derived from a dicentric chromosome. However, when the membrane was re-hybridised with the probe X, the smaller chromosomal fragment proved to be the isochromosome. (*B*) Analysis of chromosomal DNA was performed using a PFGE staining with EtBr (left panels). Positions of initial Ch^{16}-NRUH, dicentric chromosome (**D**) and acentric chromosome (**A**) are shown respectively in the Ch^{16}-NRUH *nmt-rtf1*$^+$cells (**Ch^{16}-NRUH**). In the PFGE combainted with a Southern blot assay the specific probes used are presented under each panel.

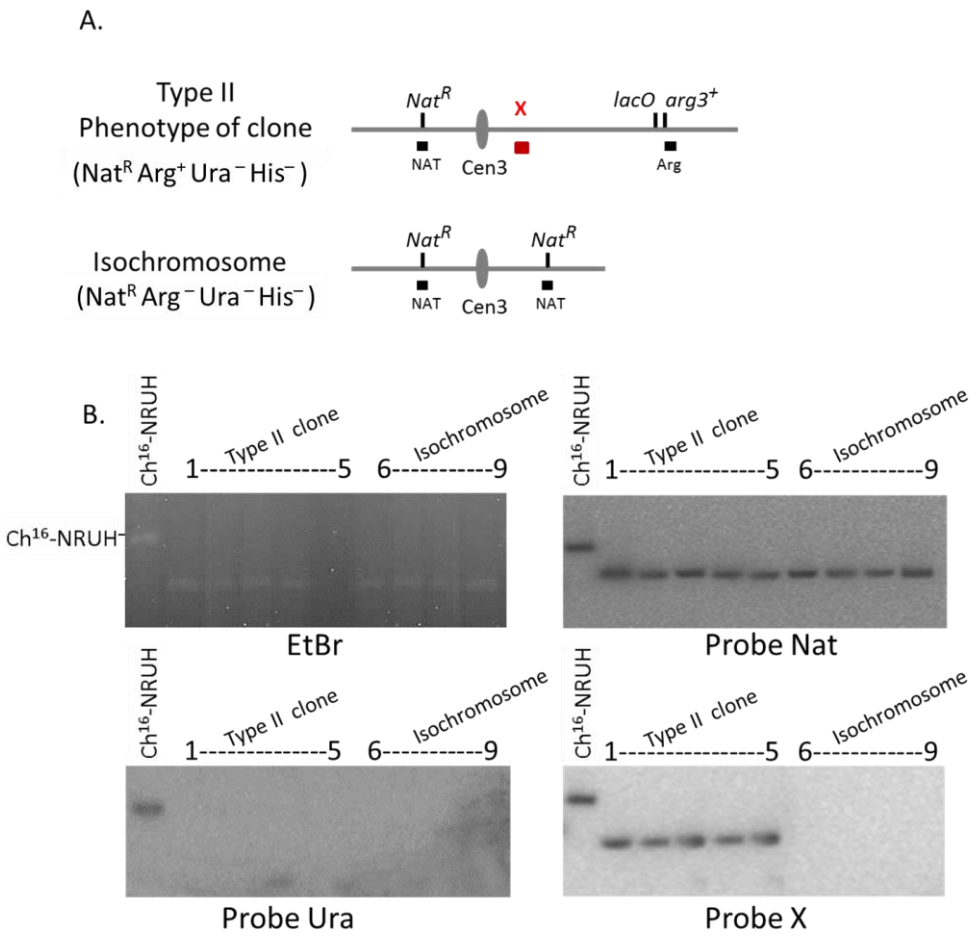

Figure 5-8. Analysis of chromosomes by a PFGE.

(*A*) Positions of the probes (black and red blocks) used in a Southern blot hybridization are indicated for the chromosomal rearrangement products. The Nat^R Arg^+ Ura^- His^- (lane 1–5) and the Nat^R Arg^- Ura^- His^- (lane 6–9) phenotype clones were expected to have either the truncated Ch^{16}-NRUH or the isochromosome, respectively. (*B*) Chromosomal DNA was resolved by the PFGE staining with EtBr (left panels). Positions of parental Ch^{16} were indicated on the left lane of the EtBr panel by the Ch^{16}-NRUH *nmt-rtf1*$^+$cells (**Ch^{16}-NRUH**). In a Southern blot hybridization, DNA was detected on a hybridization membrane sequentially using the specific probes presented under each panel.

5.3 Discussion

To determine the fates of the rearranged chromosomes arising in our mini-chromosome system, two auxotrophic markers were inserted on either side of a fork-arrest locus on the right arm of the Ch^{16}-NRUH. An *arg3*$^{+}$ gene maker was integrated *cen*-proximal to the *RTS1* sequence and a *his3*$^{+}$ gene maker was located *tel*-proximal to the *RTS1* sequence. In addition, a *Nat*^{R} marker gene was inserted on the left arm of the Ch^{16} in order to monitor the mini-chromosome stability. This construct allowed us to follow the fates of rearranged chromosomes using a clone selection assay.

The cells that contained a parental Ch^{16}-NRUH showed the Nat^{R} Arg^{+} Ura^{+} His^{+} phenotype. Conversely, if the Ch^{16}-NRUH was lost, the cells revealed the Nat^{S} Arg^{-} Ura^{-} His^{-} phenotype. A dicentric chromosome may undergo a random breakage and cause the production of monocentric derivatives. We observed that the Nat^{R} Arg^{+} Ura^{-} His^{-} phenotype of clones contained the truncated Ch^{16}-NRUH, which was produced from a primary dicentric chromosome. Interestingly, a dicentric chromosome might also be maintained by a secondary event, such as the inactivation or deletion of one of the centromeres. Therefore, we observed that a dicentric chromosome existed in some cells found in the Nat^{R} Arg^{+} Ura^{+} His^{-} phenotype of clones. From further experimentation, we determined that a dicentric chromosome could be steadily maintained *in vivo* for over 15 days. In addition, our analysis also revealed that the isochromosomes of the Nat^{R} Arg^{-} Ura^{-} His^{-} clones that contained the duplication of the left arm of the Ch^{16}-NRUH were produced as byproducts of the dicentric chromosome instability.

CHAPTER 6

GENERAL DISCUSSION, CONCLUSIONS AND FUTURE WORK

6.1 General Discussion

Aberrant chromosomal structures can act as substrates for ectopic chromosome rearrangements. Such rearrangements, including gene deletions, amplifications and inversions at specific regions may result in the loss or gain of genomic material and lead to the genomic instability related to cancer. For example, Lange *et al.* found that the formation of the dicentric chromosomes by the fusion of large inverted repeats on the human Y chromosome can lead to spermatogenic failure [135]. Turner syndrome is a sex chromosome related disorder where the genome of some patients contains an unstable dicentric Y chromosome [135]. It has been shown that Turner syndrome patients have a higher incidence of getting cancer [136].

Interestingly, genomic instability events in human genomic disorders have been proposed to be generated from common models: double-strand break (DSB) repair-dependent and replication-associated recombination, which is DSB repair-independent [49, 50]. In our group, we propose that restarting a stalled replication fork can occur via non-allelic homologous recombination (NAHR) and a U-turn model, (Figures 1-12 and 1-13) without a DSB intermediate. These mechanisms make an important contribution to the genome rearrangements [48, 52]. However, it is yet unclear how these pathways and their intermediates are involved in

the genomic instability, which may promote the development of tumors at an early stage.

A common issue that has been discussed for aberrant genomic architecture is oncogene amplification. For example, Pelizaeus-Merzbacher disease (PMD), a human genomic disorder, is characterized by the duplications of the dosage-sensitive proteolipid protein gene (PLP1) [55, 92]. PLP1 is an integral membrane protein and abundant component of myelin in oligodendrocytes in the central nervous system (CNS). An extra copy of PLP1 can cause oligodendrocyte cell death and abnormal CNS myelination [55, 92]. Analysis of the genome sequence of the PMD patients suggests that low-copy repeats (LCRs) surrounding the PLP1 gene may stimulate genomic rearrangements responsible for the majority of PMD cases. Unique recombination-specific re-junction fragments containing LCRs near the breakpoints have been identified at the PLP1 locus in PMD patients. It appears that LCRs flanking the PLP1 gene are likely hotspots for initializing the rearrangements, yielding duplicated genomic segments.

The human genome contains a high frequency of inverted repeats sharing high sequence homology [56]. For example, repetitive DNA sequences such as Alu elements (~10% of the genome) and LCRs（~5%), which are usually separated by other sequences [56]. These repeats are potential substrates for genomic rearrangements caused by recombination reactions, for example following replication perturbation. However, it is still unclear as to what extent repetitive DNA sequences can cause instability in mammalian genomes and how unstable genomic structures, like the acentric and dicentric chromosomes, are formed and behave during the subsequent cell divisions.

6.1.1 Chromosomal rearrangements and instability caused by recombination events in prokaryotic and eukaryotic model organisms

In certain human disorders, fusion events by a template exchange mechanism have been proposed as an explanation of the complex rearrangements. These fusions can occur between specific genomic sequences with sequence homology from a few kilobases (kb) to several megabases (Mb) in length [1-7]. Models involving recombination-based chromosomal rearrangements have also been proposed previously in other organisms.

Two studies in bacteria proposed that recombination-based chromosomal rearrangements are caused by a faulty template switch mechanism [18, 54]. *Bi et al.* found that plasmids carrying inverted repeats [54] undergo complex rearrangements. A second study identified DNA intermediates that also appeared to undergo inverted repeat fusions [18]. Chromosome rearrangements leading to the formation of acentric chromosomes due to the fusion of two nearby inverted repeats have been observed in fission yeast [42]. The strains contained high copies of the acentric chromosome, leading to the amplification of the *Sod2* gene (a resistance gene for lithium chloride). In budding yeast, it was determined that fusion of nearby inverted repeats by a replication-based mechanism was followed by the formation of the dicentric and acentric chromosomes [48]. While these studies show similarities of chromosome rearrangements initiated by homologous recombination (HR), the formation and metabolism of intermediates may differ.

6.1.2 A replication-based mechanism for the fusion of nearby, inverted repeats in fission yeast

The data from our laboratory provides evidence that replication fork stalling can induce recombination-caused chromosomal rearrangements in the fission yeast, *S. pombe*. In both prokaryotic and eukaryotic organisms, replication fork stalling at the barrier has been viewed as a common cause of chromosomal rearrangements [8, 29, 65, 100 and 119]. A growing body of studies implies that a consequence of replication stalling at the impediments could be related to genomic instability [15-23, 46]. We would particularly like to draw attention to the HR-dependent chromosomal rearrangements without the DSB intermediates. It is proposed that one of the common repair mechanisms at replication dysfunctional sites is initiated through a DSB. Following DSB formation, the replication fork can be incorrectly restarted on the basis of homology or microhomology [15, 17, 23 and 46]. However, several recent studies indicate that repetitive DNA sequences may undergo HR-dependent fusions following replication perturbations independently of DSB formation [18-20].

We focus on the investigation of inaccurately restarted forks without a DSB intermediate, which can contribute to genome rearrangements. Our assays exploited programmed replication barriers induced by the Rtf1-RTS1 fork-stalling system [19, 49-50, 57-58]. We proposed two models for the observed genome rearrangements; non-allelic homologous recombination (NAHR) and the U-turn model (Figures 1-12 and 1-13). Our observations strongly suggest that HR proteins are associated with the nascent strand behind the collapsed fork and can help strand invasion of the homologous sequences near to sites of replication fork collapse. A collapsed fork frequently selects the correct homologous sequence template in order to restart but, in some cases, an erroneous strand invasion occurs at an incorrect template via NAHR

[49]. Our results found that inverted repeats fuse, due to the invasion of the homologous RTS1 sequence during an HR-dependent fork restart. Alternatively, we also suggest a novel mechanism of chromosomal rearrangements, the U-turn model [50]. In the U-turn model, the collapsed replication fork initially travels with the correct template, but subsequently changes the orientation of DNA replication as it hits the centre of the palindrome. This leads to the formation of acentric and dicentric chromosomes. The main conclusion from our work is that the rearrangements in inverted *RTS1* systems are caused by an HR-restarted replication fork via the NAHR or U-turn mechanisms. Ectopic template exchange is dependent on HR, which leads to a Holliday junction intermediate, the resolution of which can form isochromosomes.

Intriguingly, this raises the question of what determines the outcome of the replication fork restart at the barriers and how that fate is decided. Further investigation of replication fork stalling and restarting, using our mini-chromosome system, can provide significant information regarding the connections between the DNA replication perturbation, the fork restart and the maintenance of genomic stability. By using the mini-chromosome system in this project, the microscopy data provided direct evidence for the rearranged chromosome formation and have given significant insight into their fates. Acentric chromosomes lack centromeres and show disassociation from the genomic mass rapidly after they have been formed. The dicentric chromosomes contain two centromeres and show aberrant segregation during cell division. They can suffer from random breakage during the anaphase, which generates broken-ended chromosomes. These mechanisms suggest a model for the manner in which rearranged chromosomes can undergo further rearrangements, which could lead to GCRs in cancerous cells and which could promote tumour

development at an early stage.

6.1.3 Does one event generate both an acentric and a dicentric chromosome in our system?

The outcome of the replication failure in our fission yeast system may reveal what happens at a replication arrest site with repetitive sequences in the vicinity. One very interesting question is whether one replication restart event forms both an acentric and a dicentric chromosome, or if the acentric and dicentric chromosomes are formed independently. Our microscopy data suggest that the dicentric chromosome is often segregated to cells with what appears to be a parental Ch^{16}-NRUH (Figures 4-7 and 4-11). We had expected that, if the formation of the dicentric and acentric chromosomes were coupled - formed from the same event in the cell - we would not be able see this. We have not directly established whether the acentric and dicentric chromosomes are generated in the same event or by separate events. The primary fate of a dicentric chromosome showed imbalanced segregation into the cells that also contained a parental chromosome (Figures 4-11 and 4-14). This might imply that a dicentric chromosome can generate without an acentric chromosome being formed.

6.1.4 Why are acentric chromosomes difficult to follow?

In our construct, the tetracycline operator (*tetO*) and the lactose operator (*lacO)* arrays were inserted into the mini-chromosome on either side of the fork arrest loci. Once rearrangements occurred, two *tetO* and two *lacO* arrays existed on an acentric and on a dicentric chromosome, respectively. The movement of the dicentric chromosomes was easy to monitor, because the two *lacO*/lacI-GFP foci (~110 kb distance between two GFP foci) on a dicentric chromosome were clearly distinguishable from an unaltered parental Ch^{16}-NRUH.

Although the analysis of a Southern blot assay proved the formation of acentric chromosomes in our mini-chromosome system (see Chapter 3 for details), it has been difficult to identify the position of an acentric chromosome *in vivo*. The failure to detect acentric chromosomes may be because of two reasons:

1. The genomic distance of ~50 kb between two *tetO*/tetR-tdTomato foci on an acentric chromosome may be insufficient for them to be observed separately, and they could appear to be one merged tdTomato dot (Figure 4-4). This makes it more difficult to determine when an acentric chromosome is present.
2. Because of the special configuration of acentric chromosomes (lacking a centromere), it was proposed that they showed random distribution without an association with the microtubules emanating from the mitotic spindle poles. An acentric chromosome might, therefore, be unstable during segregation and may tend to disappear rapidly, limiting the observation time for analysing its movements during nuclear segregation.

In our findings, there were a number of nuclei that contained two GFP foci without the co-localisation of the tdTomato foci. We also did not observe any nuclei that contained only the tdTomato foci (Figure 4-14). This may provide indirect evidence that acentric chromosomes disappear rapidly after their formation (Figure 4-4 B).

Acentric palindromic chromosomes were postulated to be precursors of extra-chromosomal elements, which may lead to gene amplification [42]. Thus, it would be interesting to investigate whether acentric chromosomes can form extra-chromosomal fragments, such as micronuclei, which have been found in some cancer cells [48-49]. From recent studies, the micronuclei are proposed to be incorporated into the normal chromosomes [24 and 36-37]. Consequently, our group is working on a new technology, Next-Generation Sequencing (NGS), which is a

fundamentally different approach to sequencing. We will test whether the acentric chromosomes can be found *in vivo* or whether the acentric chromosomes are incorporated into the regular chromosomes.

6.1.5 The fate of the dicentric chromosomes

The stabilisation of the dicentric chromosome may arise from a breakage event, generating a stable monocentric product. The images of fixed and live cells indicated that the dicentric chromosomes formed a stretched chromatin structure across the daughter cells and underwent imbalanced segregation, as seen in Chapter 4. In Chapter 5, the PFGE analysis confirmed the presence of a truncated form of the mini-chromosome derived from the dicentric chromosomes. Our results revealed evidence of random breakages occurring on the dicentric chromosomes. A breakage may be caused by the forces generated by the mitotic spindle during the anaphase, or it can occur during the progression of cytokinesis.

The stabilisation of a dicentric chromosome may also occur through multiple centromeres or the deletion of one centromere *in vivo*. According to the analysis by PFGE, combined with the Southern blot hybridisation (Figure 5-4), dicentric chromosomes were found in cells with the Nat^R Arg^+ Ura^+ His^- phenotype over 15 days. A dicentric chromosome is postulated to be an unstable, rearranged intermediate and tends to undergo secondary rearrangement events in order to form a stable product. This raises the following question: “Why can the dicentric chromosome be stable for such a long time in a cell?” From studies in humans, it is known that the dicentric chromosomes can lose one of their centromeres, as has been found in myeloid malignancy [35]. A dicentric chromosome can also be maintained with multiple centromeres through epigenetic centromere inactivation, such as kinetochore

disassembly [36]. Similar situations were also described in studies with artificial dicentric chromosomes in *S. pombe* [37-38]. Therefore, we suggest that a dicentric chromosome may exist in a cell stabilised by subsequent events, such as the deletion or inactivation of one of the centromeres. In order to understand how cells respond to these derivatives, we will need to conduct more experiments in order to confirm how the stabilisation of the dicentric chromosomes occurs in our system.

6.2 Conclusions

There are two main conclusions to report and discuss from my findings. The first aim of this project was to directly visualise chromosomal rearrangements *in vivo* using the DeltaVision deconvolution light microscopy system. Our previous studies using the Rtf1-RTS1 fork-stalling system have successfully demonstrated that nearby inverted repeats fuse to form the dicentric and acentric chromosomes when the replication fork was arrested and restarted at the RTS1 barrier [48-52]. The microscopy data presented here is showing for the first time that rearranged chromosome formation and their behaviour in a single cell. The physical properties of rearranged chromosomes were revealed: the acentric chromosomes, lacking centromeres, rapidly disassociated from the genomic mass as they formed and the dicentric chromosomes, containing two centromeres, showed aberrant segregation during cell division.

The second aim of this project was to investigate the outcome of the dicentric chromosome formation. The dicentric chromosomes have been shown to undergo a random breakage during mitosis and to generate more stable derivatives like the truncated Ch^{16}-NRUH and isochromosomes that were suspected to lack the right arm of Ch^{16}. We also found that some cells contained a stable dicentric chromosome for

over 15 days. This suggests that a dicentric chromosome may exist in a cell maintained by subsequent events, i.e. the deletion or inactivation of one of the centromeres. With these results we gained insight into how unstable rearranged chromosomal structures undergo further rearrangements, which may be relevant to the genetic instability observed in tumor development at an early stage.

6.3 Future Work

The very promising results obtained from this project have allowed us to demonstrate how chromosome rearrangements occur in live cells. To achieve our goal to understand the behaviour of rearranged chromosomes during cell segregation, the *lacO-arg3*$^{+}$ and *tetO-his3*$^{+}$ arrays were integrated on each arm of the mini-chromosome. This enabled us to observe chromosome rearrangements microscopically and genetically. And also to localise their positioning in the cell i.e. respective to spindle microtubules and to follow their fate with the specific marker loss. This study evaluated the physical properties of the rearranged molecules and guided our efforts in deducing the mechanisms that contribute to the segregation of aberrant chromosomal structures.

It would be important, however, to use this modified mini-chromosome in studies following the rearrangement derivatives to determine their fates in more detail. Useful insights on these processes are presented in this project with some very promising results, however, the further rearrangements of the dicentric chromosomes are still not fully explored. It requires amending of the experimental protocol to explore these processes in the future.

CHAPTER 7

REFERENCES

[1] Lupski, J. R. (1998) "Genomic disorders: structural features of the genome can lead to DNA rearrangements and human disease traits". *Trends Genet.* 14: 417–422.

[2] Stankiewicz P and Lupski JR. (2002) "Genome architecture, rearrangements and genomic disorders" *Trends Genet.*18:74-82.

[3] Feuk L, Carson AR, and Scherer SW. (2006) "Structural variation in the human genome." *Nat. Rev. Genet.* 7:85-97.

[4] Stankiewicz P and Lupski JR. (2010) "Structural Variation in the Human Genome and its Role in Disease" *Annu. Rev. Med.* 61:437–55.

[5] Zhang F, Carvalho CM, and Lupski JR. (2009) "Complex human chromosomal and genomic rearrangements" *Trends Genet.* 25:298-307.

[6] Albertson DG. (2006) "Gene amplification in cancer" *Trends Genet.* 22:447–455.

[7] Liu P, Carvalho CM, Hastings PJ, and Lupski JR. (2012) "Mechanisms for recurrent and complex human genomic rearrangements" *Curr. Opin. Genet.* 22:211–220.

[8] Slack A, Thornton PC, Magner DB, Rosenberg SM, and Hastings PJ. (2006) "On the mechanism of gene amplification induced under stress in *Escherichia coli*" *PLoS. Genet.* 2:385–398.

[9] Bester AC, Roniger M, Oren YS, Im MM, Sarni D, Chaoat M, Bensimon A, Zamir G, Shewach DS, and Kerem B. (2011) "Nucleotide Deficiency Promotes Genomic Instability in Early Stages of Cancer Development" *Cell* 145:435–446.

[10] Arlt MF, Wilson TE, and Glover TW. (2012) "Replication stress and mechanisms of CNV formation" *Curr. Opin. Genet. Dev.* 22:204–210.

[11] Admire A, Shanks L, Danzl N, Wang M, Weier U, Stevens W, Hunt E, and Weinert T. (2006). "Cycles of chromosome instability are associated with a fragile site and are increased by defects in DNA replication and checkpoint controls in yeast" *Genes Dev.* 20:159–173.

[12] Allen C, Ashley AK, Hromas R, and Nickoloff JA. (2011) "More forks on the road to replication stress recovery" *J. Mol. Cell Biol.* 3:4 –12.

[13] Hastings PJ, Lupski JR, Rosenberg SM, and Ira G. (2009) "Mechanisms of change in gene copy number" *Nat. Rev.Genet.* 10:551-564.

[14] Haber JE. (1999) "DNA recombination: the replication connection" *Trends Biochem. Sci.* 24:271–275.

[15] Haber, J. E. (2000) "Partners and pathways: repairing a double-strand break"

Trends Genet. 16:259–264.

[16] Aylon Y, Liefshitz B, and Kupiec M. (2004) "The CDK regulates repair of double-strand breaks by homologous recombination during the cell cycle" *EMBO J.* 23:4868–4875.

[17] Mondello C, Smirnova A, and Giulotto E. (2010) "Gene amplification, radiation sensitivity and DNA double-strand breaks" *Mutat. Res.* 704: 29–37.

[18] Ahmed A and Podemski L. (1998) "Observations on template switching during DNA replication through long inverted repeats" *Gene* 223: 187–194.

[19] Lambert S, Watson A, Sheedy DM, Martin B, and Carr AM. (2005) "Gross chromosomal rearrangements and elevated recombination at an inducible site-specific replication fork barrier" *Cell* 121:689–702.

[20] Carr AM, Paek AL, and Weinert T. (2011) "DNA replication: Failures and inverted fusions" *Semin. Cell Dev. Biol.* 22:866– 874.

[21] Kolodner RD, Putnam CD, and Myung K. (2002) "Maintenance of genome stability in *Saccharomyces cerevisiae*" *Science* 297:552-557.

[22] Mefford HC and Eichler EE. (2009) "Duplication hotspots, rare genomic disorders, and common disease" *Curr. Opin. Genet. Dev.* 19:196-204.

[23] Weinstock DM, Elliott B, and Jasin M. (2006) "A model of oncogenic

rearrangements: Differences between chromosomal translocation mechanisms and simple double-strand break repair" *Blood* 107:777–780.

[24] Crasta K, Ganem NJ, Dagher R, Lantermann AB, Ivanova EV, Pan Y, Nezi L, Protopopov A, Chowdhury D, and Pellman D. (2012) "DNA breaks and chromosome pulverization from errors in mitosis" *Nature* 482:53-60.

[25] Holbro T, Beerli RR, Maurer F, Koziczak M, Barbas CF, and Hynes NE. (2003) "The ErbB2/ErbB3 heterodimer functions as an oncogenic unit: ErbB2 requires ErbB3 to drive breast tumor cell proliferation " *Proc. Natl. Acad. Sci. U S A.* 100:8933-8.

[26] Osborne C, Wilson P, and Tripathy D. (2004) "Oncogenes and tumor suppressor genes in breast cancer: potential diagnostic and therapeutic applications" *Oncologist.* 9:361-377.

[27] Rufini A, Tucci P, Celardo I, and Melino G. (2013)"Senescence and aging: the critical roles of p53 Oncogene" 1-15.

[28] Mirkin EV and Mirkin SM. (2007) "Replication Fork Stalling at Natural Impediments" *Microbiol. Mol. Biol. Rev.* 71:13–35.

[29] San Filippo J, Sung P, and Klein H. (2008) "Mechanism of eukaryotic homologous recombination" *Annu. Rev. Biochem.* 77:229–257.

[30] Roberts SA, Sterling J, Thompson C, Harris S, Mav D, Shah R, Klimczak LJ,

Kryukov GV, Malc E, Mieczkowski PA, Resnick MA, and Gordenin DA. (2012) "Clustered mutations in yeast and in human cancers can arise from damaged long single-strand DNA regions" *Mol. Cell* 46:424-35.

[31] Egel R. (2004) "DNA replication: stalling a fork for imprinting and switching" *Curr. Biol.* 14:R915- R917.

[32] Durkin SG, and Glover TW. (2007) "Chromosome Fragile Sites" *Annu. Rev. Genet.* 41:169–192.

[33] Ragland RL, Glynn MW, Arlt MF, and Glover TW. (2008) "Stably Transfected Common Fragile Site Sequences Exhibit Instability at Ectopic Sites" *Genes Chromosomes Cancer.* 47:860–872.

[34] Corbin S, Neilly ME, Espinosa R 3rd, Davis EM, McKeithan TW, and Le Beau MM. (2002) " Identification of unstable sequences within the common fragile site at 3p14.2: implications for the mechanism of deletions within fragile histidine triad gene/common fragile site at 3p14.2 in tumors" *Cancer Res.* 62:3477-3484.

[35] Mackinnon RN, and Campbell LJ. (2011) "The role of dicentric chromosome formation and secondary centromere deletion in the evolution of myeloid malignancy" *Genet. Res. Int.* 2011:1-11.

[36] Sato H, Masuda F, Takayama Y, Takahashi K, and Saitoh S. (2012) "Epigenetic inactivation and subsequent heterochromatinization of a centromere stabilise dicentric chromosomes" *Curr. Biol.* 22:658-67.

[37] Stimpson KM, Matheny JE, and Sullivan BA. (2012) "Dicentric chromosomes: unique models to study centromere function and inactivation" *Chromosome Res.* 20:595-605.

[38] Watanabe T, Tanabe H, and Horiuchi T. (2011) "Gene amplification system based on double rolling-circle replication as a model for oncogene-type amplification" *Nucleic. Acids Res.* 39:e106.

[39] Haber JE and Thorburn PC. (1984) "Healing of broken linear dicentric chromosomes in yeast" *Genetics* 106:207–226.

[40] Colnaghi R, Carpenter G, Volker M, and O'Driscoll M. (2011) "The consequences of structural genomic alterations in humans: Genomic Disorders, genomic instability and cancer" *Semin. Cell Dev. Biol.* 22:875– 885.

[41] Janssen A, van der Burg M, Szuhai K, Kops GJ, and Medema RH. (2011) "Chromosome segregation errors as a cause of DNA damage and structural chromosome aberrations" *Science* 333:1895–1898.

[42] Albrecht EB, Hunyady AB, Stark GR, and Patterson TE. (2000) "Mechanisms of sod2 gene amplification in *Schizosaccharomyces pombe*" *Mol. Biol. Cell* 11:873–886.

[43] Kanda T, Otter M, and Wahl GM. (2001) "Mitotic segregation of viral and cellular acentric extrachromosomal molecules by chromosome tethering" *J. Cell Sci.* 114:49-58.

[44] Narayanan V, Mieczkowski PA, Kim HM, Petes TD, and Lobachev KS. (2006) "The pattern of gene amplification is determined by the chromosomal location of hairpin-capped breaks" *Cell* 125:1283–1296.

[45] Weinert T, Kaochar S, Jones H, Paek A, and Clark AJ. (2009) "The replication fork's five degrees of freedom, their failure and genome rearrangements" *Curr. Opin. Cell Biol.* 21:778–784.

[46] Hefferin, M. L. and Tomkinson, A. E. (2005) "Mechanism of DNA double-strand break repair by non-homologous end joining" *DNA Repair* 4:639–648.

[47] Tanaka H and Yao MC. (2009) "Palindromic gene amplification — an evolutionarily conserved role for DNA inverted repeats in the genome" *Nat. Rev. Cancer* 9:215-224

[48] Paek AL, Kaochar S, Jones H, Elezaby A, Shanks L, and Weinert T. (2009) "Fusion of nearby inverted repeats by a replication-based mechanism leads to formation of dicentric and acentric chromosomes that cause genome instability in budding yeast" *Genes Dev.* 23: 2861-2875.

[49] Mizuno K, Lambert S, Baldacci G, Murray JM, Carr AM. (2009) "Nearby inverted repeats fuse to generate acentric and dicentric palindromic chromosomes by a replication template exchange mechanism" *Genes Dev.* 23:2876–2886 .

[50] Lambert S, Mizuno K, Blaisonneau J, Martineau S, Chanet R, Fréon K, Murray

JM, Carr AM, and Baldacci G. (2010) "Homologous recombination restarts blocked replication forks at the expense of genome rearrangements by template exchange" *Mol. Cell* 39:346–359.

[51] Iraqui I, Chekkal Y, Jmari N, Pietrobon V, Fréon K, Costes A, and Lambert SA. (2012) "Recovery of arrested replication forks by homologous recombination is error-prone" *PLoS Genet.* 8:1-15.

[52] Mizuno K, Miyabe I, Schalbetter SA, Carr AM, and Murray JM. (2013) "Recombination-restarted replication makes inverted chromosome fusions at inverted repeats" *Nature* 493:246-249.

[53] Brewer BJ, Payen C, Raghuraman MK, and Dunham MJ. (2011) "Origin-Dependent Inverted-Repeat amplification: A Replication-Based model for generating palindromic amplicons" *PLoS Genet.* 7:e1002016.

[54] Bi X and Liu LF. (1996) "DNA rearrangement mediated by inverted repeats" *Proc Natl Acad Sci USA.* 93:819–823.

[55] Lee JA, Inoue K, Cheung SW, Shaw CA, Stankiewicz P, and Lupski JR. (2006) "Role of genomic architecture in PLP1 duplication causing Pelizaeus-Merzbacher disease" *Hum. Mol. Genet.* 15:2250–2265.

[56] Beach, D., Nurse, P., and Egel, R. (1982) "Molecular rearrangement of mating-type genes in fission yeast" *Nature* 296:682–683.

[57] Ahn, J. S., Osman, F., and Whitby, M. C. (2005) "Replication fork blockage by RTS1 at an ectopic site promotes recombination in fission yeast" *EMBO J.* 24:2011–2023.

[58] Lambert S and Carr AM. (2012) "Replication stress and genome rearrangements: lessons from yeast models" *Curr. Opin. Genet. Dev.* 23:1–8.

[59] Inagawa T, Yamada-Inagawa T, Eydmann T, Mian IS, Wang TS, and Dalgaard JZ. (2009) "*Schizosaccharomyces pombe* Rtf2 mediates site-specific replication termination by inhibiting replication restart" *Proc. Natl. Acad Sci. U S A.* 106:7927–7932.

[60] Lambert S and Carr AM. (2013) "Impediments to replication fork movement: stabilisation, reactivation and genome instability" *Chromosoma.* 122:33-45.

[61] Bierne, H., Ehrlich, S. D., and Michel, B. (1997) "Deletions at stalled replication forks occur by two different pathways" *EMBO J.* 16:3332–3340.

[62] Aves, S. J. (2009) "DNA replication initiation" *Methods Mol. Biol.* 521:3–17.

[63] Masai H, Matsumoto S, You Z, Yoshizawa-Sugata N, and Oda M. (2010) "Eukaryotic Chromosome DNA Replication: Where, When, and How?" *Rev. Biochem.* 79:89-130.

[64] Araki, H. (2011) "Initiation of chromosomal DNA replication in eukaryotic cells; contribution of yeast genetics to the elucidation"*Genes Genet. Syst.* 6:141–149.

[65] Calzada A, Hodgson B, Kanemaki M, Bueno A, and Labib K. (2005) "Molecular anatomy and regulation of a stable replisome at a paused eukaryotic DNA replication fork" *Genes Dev.* 19:1905–1919.

[66] H¨ubscher, U. (2009) "DNA replication fork proteins" *Methods Mol. Biol.* 521:19–33.

[67] Labib K and Hodgson B. (2007) "Replication fork barriers: pausing for a break or stalling for time?" *EMBO Rep.* 8:346–353.

[68] Bi, X. and Liu, L. F. (1994) "recA-independent and recA-dependent intramolecular plasmid recombination. Differential homology requirement and distance effect" *J. Mol. Biol.* 235:414–23.

[69] Bae, S. H., Bae, K. H., Kim, J. A., and Seo, Y. S. (2001) "RPA governs endonuclease switching during processing of okazaki fragments in eukaryotes" *Nature* 412:456–461.

[69] Kolodner RD, Putnam CD, and Myung K. (2002) "Maintenance of Genome Stability in *Saccharomyces cerevisiae*" *Science* 297:552-557.

[70] Lambert S and Carr AM. (2005) "Checkpoint responses to replication fork barriers" *Biochimie* 87:591–602.

[71] Lambert S, Froget B, and Carr AM. (2007) "Arrested replication fork processing:

Interplay between checkpoints and recombination" *DNA Repair (Amst)* 6:1042–1061.

[72] Branzei D and Foiani M. (2009) "The checkpoint response to replication stress" *DNA Repair (Amst)* 8: 1036–1046.

[73] Boye E, Skjølberg HC, and Grallert B. (2009) "Checkpoint regulation of DNA replication" *Methods Mol. Biol.* 521:55–70.

[74] Adams KE, Medhurst AL, Dart DA, and Lakin ND. (2006) "Recruitment of ATR to sites of ionising radiation-induced DNA damage requires ATM and components of the MRN protein complex" *Oncogene* 25:3894–3904.

[75] Beucher A, Birraux J, Tchouandong L, Barton O, Shibata A, Conrad S, Goodarzi AA, Krempler A, Jeggo PA, and Löbrich M. (2009) "ATM and artemis promote homologous recombination of radiation-induced DNA double-strand breaks in G_2" *EMBO J.* 28:3413–3427.

[76] Cortez D, Guntuku S, Qin J, and Elledge SJ. (2001) "ATR and ATRIP: partners in checkpoint signaling" *Science* 294:1713–1716.

[77] Cimprich, K. A. and Cortez, D. (2008) "ATR: an essential regulator of genome integrity" *Nat. Rev. Mol. Cell Biol.* 9:616–627.

[78] Bermudez VP, Lindsey-Boltz LA, Cesare AJ, Maniwa Y, Griffith JD, Hurwitz J, and Sancar A. (2003) "Loading of the human 9-1-1 checkpoint complex onto DNA by the check point clamp loader hRad17-replication factor c complex *in vitro*" *Proc. Natl. Acad Sci. U S A.* 100:1633–1638.

[79] Nojima K, Hochegger H, Saberi A, Fukushima T, Kikuchi K, Yoshimura M, Orelli BJ, Bishop DK, Hirano S, Ohzeki M, Ishiai M, Yamamoto K, Takata M, Arakawa H, Buerstedde JM, Yamazoe M, Kawamoto T, Araki K, Takahashi JA, Hashimoto N, Takeda S, and Sonoda E. (2005) "Multiple repair pathways mediate tolerance to chemotherapeutic cross-linking agents in vertebrate cells" *Cancer Res.* 65:11704-11711.

[80] Atkinson J and McGlynn P. (2009) "Replication fork reversal and the maintenance of genome stability" *Nucleic Acids Res.* 37:3475–3492.

[81] Budd ME and Campbell JL. (1997) "A yeast replicative helicase, Dna2 helicase, interacts with yeast FEN-1 nuclease in carrying out its essential function" *Mol. Cell Biol.* 17:2136–2142.

[82] Bae KH, Kim HS, Bae SH, Kang HY, Brill S, and Seo YS. (2003) "Bimodal interaction between replication-protein and Dna2 is critical for Dna2 function both *in vivo* and *in vitro*" *Nucleic Acids Res.* 31:3006–3015.

[83] Constantinou A, Chen XB, McGowan CH, and West SC. (2002) "Holliday junction resolution in human cells: two junction endonucleases with distinct substrate specificities" *EMBO J.* 21:5577–5585.

[84] Heyer WD. (2004) " Recombination: Holliday junction resolution and crossover formation " *Curr. Biol.* 14:56–58.

[85] Ip SC, Rass U, Blanco MG, Flynn HR, Skehel JM, and West SC. (2008) "Identification of Holliday junction resolvases from humans and yeast" *Nature* 456:357–361.

[86] Bachrati, C. Z. and Hickson, I. D. (2008) "RecQ helicases: guardian angels of the DNA replication fork" *Chromosoma* 117:219–233.

[87] Agmon N, Yovel M, Harari Y, Liefshitz B, and Kupiec M. (2011) "The role of Holliday junction resolvases in the repair of spontaneous and induced DNA damage" *Nucleic Acids Res.* 39:7009-7019.

[88] Ashton TM, Mankouri HW, Heidenblut A, McHugh PJ, and Hickson ID. (2011) "Pathways for Holliday junction processing during homologous recombination in *Saccharomyces cerevisiae*" *Mol. Cell. Biol.* 31:1921–1933.

[89] Kaykov, A. and Arcangioli, B. (2004) "A programmed strand-specific and modified nick in *S. pombe* constitutes a novel type of chromosomal imprint" *Curr. Biol.* 14:1924–1928.

[90] Ira, G., Malkova, A., Liberi, G., Foiani, M., and Haber, J. E. (2003) "Srs2 and Sgs1-Top3 suppress crossovers during double-strand break repair in yeast" *Cell* 115:401–411.

[91] Brewer BJ and Fangman WL. (1994) "Initiation preference at a yeast origin of replication" *Proc. Natl. Acad. Sci. U S A.* 91:3418-3422.

[92] Lee, J. A., Carvalho, C. M., and Lupski, J. R. (2007) "A DNA replication mechanism for generating nonrecurrent rearrangements associated with genomic disorders" *Cell* 131:1235–1247.

[93] Nobile C, Toffolatti L, Rizzi F, Simionati B, Nigro V, Cardazzo B, Patarnello T, and Valle G, Danieli GA. (2002) "Analysis of 22 deletion breakpoints in dystrophin intron 49" *Hum. Genet.* 110:418-421.

[94] Boddy MN, Gaillard PH, McDonald WH, Shanahan P, Yates JR 3rd, and Russell P. (2001) "Mus81-Eme1 are essential components of a Holliday junction resolvase" *Cell* 107:537–548.

[95] P. J. Hastings. (2010) "Mechanisms of Ectopic Gene Conversion" *Genes* 1:427-439.

[46] Hefferin, M. L. and Tomkinson, A. E. (2005) "Mechanism of DNA double-strand break repair by non-homologous end joining" *DNA Repair (Amst).* 4:639–648.

[96] Bzymek, M. and Lovett, S. T. (2001) "Evidence for two mechanisms of palindrome-stimulated deletion in *Escherichia coli*: single-strand annealing and replication slipped mispairing" *Genetics* 158:527–540.

[97] Caldecott, K.W. (2008) "Single-strand break repair and genetic disease" *Nat. Rev. Genet.* 9:619– 631.

[98] Llorente B, Smith CE, and Symington LS. (2008) " Break-induced replication:

what is it and what is it for?" *Cell Cycle* 7: 859-864.

[99] Cullen JK, Hussey SP, Walker C, Prudden J, Wee BY, Davé A, Findlay JS, Savory AP, and Humphrey TC. (2007) "Break-Induced Loss of Heterozygosity in Fission Yeast: Dual Roles for Homologous Recombination in Promoting Translocations and Preventing De Novo Telomere Addition" *Mol. Cell Biol.* 27: 7745–7757.

[100] Bzymek M, Saveson CJ, Feschenko VV, and Lovett ST. (1999) "Slipped misalignment mechanisms of deletion formation: *in vivo* susceptibility to nucleases" *J. Bacteriol.* 181:477–482.

[101] Zhang F, Khajavi M, Connolly AM, Towne CF, Batish SD, and Lupski JR. (2009) "The DNA replication FoSTeS/MMBIR mechanism can generate genomic, genic and exonic complex rearrangements in humans" *Nat. Genet.* 41:849-854.

[102] Bermejo R, Branzei D, and Foiani M. (2008) "Cohesion by topology: sister chromatids interlocked by DNA" *Genes Dev.* 22:2297 –2301.

[103] Li, G. (2008) "Mechanisms and functions of DNA mismatch repair" *Cell Res.* 18:85–98.

[104] Klungland, A. and Lindahl, T. (1997) "Second pathway for completion of human DNA base excision-repair: reconstitution with purified proteins and requirement for DNase IV (FEN1) " *EMBO J.* 16:3341–3348.

[105] Araújo SJ, Tirode F, Coin F, Pospiech H, Syväoja JE, Stucki M, Hübscher U,

Egly JM, and Wood RD. (2000) "Nucleotide excision repair of DNA with recombinant human proteins: definition of the minimal set of factors, active forms of TFIIH, and modulation by CAK" *Genes Dev.* 14:349–359.

[106] Bonilla CY, Melo JA, and Toczyski DP. (2008) "Colocalization of sensors is sufficient to activate the DNA damage checkpoint in the absence of damage" *Mol. Cell.* 30:267–276.

[107] Dujon B. (2006) "Yeasts illustrate the molecular mechanisms of eukaryotic genome evolution" *Trends Genet.* 22: 375–387.

[108] Wood V, Gwilliam R, Rajandream MA, Lyne M, Lyne R, Stewart A, Sgouros J, Peat N, Hayles J, Baker S, Basham D, Bowman S, Brooks K, Brown D, Brown S, Chillingworth T, Churcher C, Collins M, Connor R, Cronin A, Davis P, Feltwell T, Fraser A, Gentles S, Goble A, Hamlin N, Harris D, Hidalgo J, Hodgson G, Holroyd S, Hornsby T, Howarth S, Huckle EJ, Hunt S, Jagels K, James K, Jones L, Jones M, Leather S, McDonald S, McLean J, Mooney P, Moule S, Mungall K, Murphy L, Niblett D, Odell C, Oliver K, O'Neil S, Pearson D, Quail MA, Rabbinowitsch E, Rutherford K, Rutter S, Saunders D, Seeger K, Sharp S, Skelton J, Simmonds M, Squares R, Squares S, Stevens K, Taylor K, Taylor RG, Tivey A, Walsh S, Warren T, Whitehead S, Woodward J, Volckaert G, Aert R, Robben J, Grymonprez B, Weltjens I, Vanstreels E, Rieger M, Schäfer M, Müller-Auer S, Gabel C, Fuchs M, Düsterhöft A, Fritzc C, Holzer E, Moestl D, Hilbert H, Borzym K, Langer I, Beck A, Lehrach H, Reinhardt R, Pohl TM, Eger P, Zimmermann W, Wedler H, Wambutt R, Purnelle B, Goffeau A, Cadieu E, Dréano S, Gloux S, Lelaure V, Mottier S, Galibert F, Aves SJ, Xiang Z, Hunt C, Moore K, Hurst SM, Lucas M, Rochet M, Gaillardin C, Tallada VA,

Garzon A, Thode G, Daga RR, Cruzado L, Jimenez J, Sánchez M, del Rey F, Benito J, Domínguez A, Revuelta JL, Moreno S, Armstrong J, Forsburg SL, Cerutti L, Lowe T, McCombie WR, Paulsen I, Potashkin J, Shpakovski GV, Ussery D, Barrell BG, and Nurse P. (2002) " The genome sequence of *Schizosaccharomyces pombe*" *Nature* 415: 871–880.

[109] Kohli J, Hottinger H, Munz P, Strauss A, and Thuriaux P. (1977) "Genetic mapping in SCHIZOSACCHAROMYCES POMBE by mitotic and meiotic analysis and induced haploidization" *Genetics* 87:471–489.

[110] O Niwa, T Matsumoto, and M Yanagida (1986) "Construction of a mini-chromosome by deletion and its mitotic and meiotic behaviour in fission yeast" *Mol. Gen. Genet.* 203:397-405.

[111] O Niwa, T Matsumoto, Y Chikashige, and M Yanagida (1989) "Characterization of *Schizosaccharomyces pombe* minichromosome deletion derivatives and a functional allocation of their centromere" *EMBO J.* 8: 3045-3052.

[112] Hayashi M, Katou Y, Itoh T, Tazumi A, Yamada Y, Takahashi T, Nakagawa T, Shirahige K, and Masukata H. (2007)"Genome-wide localization of pre-RC sites and identification of replication origins in fission yeast" *EMBO J.* 26:1327–1339.

[113] Nakamura K, Okamoto A, Katou Y, Yadani C, Shitanda T, Kaweeteerawat C, Takahashi TS, Itoh T, Shirahige K, Masukata H, and Nakagawa T. (2008) "Rad51 suppresses gross chromosomal rearrangement at centromere in *Schizosaccharomyces pombe*" *EMBO J.* 27: 3036–3046.

[114] Szilard RK, Jacques PE, Laramée L, Cheng B, Galicia S, Bataille AR, Yeung M, Mendez M, Bergeron M, Robert F, and Durocher D. (2010) "Systematic identification of fragile sites via genome-wide location analysis of gamma-H2AX" *Nat. Struct. Mol. Biol.* 17:299-305.

[115] Dalgaard, Jacob Z., Godfrey, Emma L. and McFarlane, and Ramsay J. (2011) "Eukaryotic Replication Barriers: How, Why and Where Forks Stall" *DNA Replication-Current Advances* P269–P305

[116] Krings, G. and Bastia, D. (2004) "Swi1- and swi3-dependent and independent replication fork arrest at the ribosomal DNA of *Schizosaccharomyces pombe*" *Proc. Natl. Acad Sci. U S A.* 101:14085–14090.

[117] Petermann E, Orta ML, Issaeva N, Schultz N, and Helleday T. (2010) "Hydroxyurea-stalled replication forks become progressively inactivated and require two different RAD51-mediated pathways for restart and repair" *Mol. Cell* 37:492-502.

[118] Brewer BJ, Lockshon D, and Fangman WL. (1992) "The arrest of replication forks in the rDNA of yeast occurs independently of transcription" *Cell* 71:267–276.

[119] Sakuno T, Tada K, and Watanabe Y. (2009) "Kinetochore geometry defined by cohesion within the centromere" *Nature* 458:852-859.

[120] Petrova B, Dehler S, Kruitwagen T, Hériché JK, Miura K, and Haering CH.

(2013) "Quantitative Analysis of Chromosome Condensation in Fission Yeast" *Mol. Cell Biol.* 33:984–998.

[121] Birren BW, Hood L, and Lai E. (1989) "Pulsed field gel electrophoresis: studies of DNA migration made with the programmable, autonomously-controlled electrode electrophoresis system" *Electrophoresis.* 10:302-309.

[122] Tatebe H, Goshima G, Takeda K, Nakagawa T, Kinoshita K, and Yanagida M. (2001) "Fission yeast living mitosis visualised by GFP-tagged gene products" *Micron* 32:67–74.

[123] Lau IF, Filipe SR, Søballe B, Ø kstad OA, Barre FX, and Sherratt DJ. (2003) "Spatial and temporal organization of replicating *Escherichia coli* chromosomes" *Mol. Microbiol.* 49:731–743.

[124] Snaith HA, Anders A, Samejima I, and Sawin KE. (2010) "New and Old Reagents for Fluorescent Protein Tagging of Microtubules in Fission Yeast: Experimental and Critical Evaluation" *Methods Cell Biol.* 97:147-172.

[125] Shaner NC, Steinbach PA, and Tsien RY. (2005) "A guide to choosing fluorescent proteins" *Nat. Methods.* 2:905-909.

[126] Fuchs J, Lorenz A, and Loidl J. (2002) "Chromosome associations in budding yeast caused by integrated tandemly repeated transgenes" *J. Cell Sci.* 115:1213-1220.

[127] Watson AT, Garcia V, Bone N, Carr AM, and Armstrong J. (2008) "Gene

tagging and gene replacement using recombinase-mediated cassette exchange in *Schizosaccharomyces pombe*" *Gene* 407:63–74.

[128] Hentges P, Van Driessche B, Tafforeau L, Vandenhaute J, and Carr AM. (2005) "Three novel antibiotic marker cassettes for gene disruption and marker switching in *Schizosaccharomyces pombe*" *Yeast* 22:1013–1019.

[129] Bähler J, Wu JQ, Longtine MS, Shah NG, McKenzie A 3rd, Steever AB, Wach A, Philippsen P, and Pringle JR. (1998) "Heterologous Modules for Efficient and Versatile PCR-based Gene Targeting in *Schizosaccharomyces pombe*" *Yeast* 14: 943–951.

[130] Hagan IM, and Hyams JS. (1988) "The use of cell division cycle mutants to investigate the control of microtubule distribution in the fission yeast *Schizosaccharomyces pombe*" *J. Cell Sci.* 89:343-357.

[131] Yanagida M. (1998) "Fission yeast *cut* mutations revisited: control of anaphase" *Trends Cell Biol.* 8:144-149.

[132] Brock JA and Bloom K. (1994) "A chromosome breakage assay to monitor mitotic forces in budding yeast" *J. Cell Sci.* 107:891-902.

[133] Kahana JA, Schnapp BJ, and Silver PA. (1995) "Kinetics of spindle pole body separation in budding yeast" *Proc. Natl. Acad. Sci U S A.* 92:9707-9711.

[134] Thrower DA and Bloom K. (2011)"Dicentric Chromosome Stretching during

Anaphase Reveals Roles of Sir2/Ku in Chromatin Compaction in Budding Yeast" *Mol. Biol. Cell.* 12: 2800–2812.

[135] Lange J, Skaletsky H, van Daalen SK, Embry SL, Korver CM, Brown LG, Oates RD, Silber S, Repping S, and Page DC. (2009) "Isodicentric Y chromosomes and sex disorders as byproducts of homologous recombination that maintains palindromes" *Cell* 138:855-869.

[136] Schoemaker MJ, Swerdlow AJ, Higgins CD, Wright AF, Jacobs PA; UK Clinical Cytogenetics Group. (2008) "Cancer incidence in women with Turner syndrome in Great Britain: a national cohort study" *Lancet. Oncol.* 9:239-246.